

2019-001 \_\_\_\_\_ EPRI Advanced Reactor Strategic Program (EPRI-AR)

May 31, 2019

Document Control Desk  
U. S. Nuclear Regulatory Commission  
11555 Rockville Pike  
Rockville, MD 20852

Docket No. 99902021

Attention: Boyce Travis, NRO/DAR/ARPB

Subject: Transmittal of "Uranium Oxycarbide (UCO) Tristructural Isotropic (TRISO) Coated Particle Fuel Performance: Topical Report EPRI-AR-1(NP)"

Enclosed is one (1) paper copy of the report "Uranium Oxycarbide (UCO) Tristructural Isotropic (TRISO) Coated Particle Fuel Performance: Topical Report EPRI-AR-1(NP)," EPRI Technical Report 3002015750, May 2019. This report is being transmitted to the NRC for review and approval.

The U. S. Department of Energy initiated the Advanced Gas Reactor Fuel Development and Qualification (AGR) Program in 2002 to establish U.S. capability to fabricate high-quality UCO TRISO fuel and to demonstrate its performance. Results from the first two fuel irradiation tests in the program, designated AGR-1 and AGR-2, demonstrate UCO fuel performance during irradiation and post-irradiation high-temperature accident safety tests.

TRISO fuel is utilized by all known contemporary designs for thermal spectrum high temperature reactors (HTRs), *i.e.*, thermal gas-cooled high-temperature reactors and fluoride salt-cooled high-temperature reactors, under development in the United States and elsewhere. This report consolidates the technical bases for the functional performance of UCO-based TRISO-coated particles so these particles can be used by a variety of HTR developers in their designs. This report is the product of an EPRI-led collaboration with the U.S. Department of Energy, Idaho National Laboratory, and key industry stakeholders in the HTR developer and fuel supplier community comprising the HTR Technology Working Group.

Submittal of the topical report for NRC review and approval provides an opportunity to "lock-in" available UCO TRISO particle fuel performance data and analysis in a manner that increases the efficiency of the safety review process for design certification and license applications.

Together . . . Shaping the Future of Electricity

**CHARLOTTE OFFICE**

1300 West W.T. Harris Boulevard, Charlotte, NC 28262-8550 USA • 704.595.2000 • Fax 704.595.2860  
Customer Service 800.313.3774 • www.epri.com

DD 35  
TD 10  
NRR

EPRI-AR-2019-001  
2019-001

Topical Report EPRI-AR-1(NP)  
EPRI Advanced Reactor Strategic Program (EPRI-AR)

May 31, 2019  
Page 2

Based on previous communications and engagements, including the May 8, 2019, Category 1 pre-submittal meeting (ML19119A229), EPRI understands that the NRC review will be conducted on an off-fee basis using internal resources allocated for this purpose. The topical report is non-proprietary, publicly available and subject to copyright protection only. Therefore marking and withholding of information are not required.

If you have questions about this submittal, please contact EPRI project manager Cristian Marciulescu by phone at 704-595-2401, or by email at [cmarciulescu@epri.com](mailto:cmarciulescu@epri.com).

Sincerely,



David B. Scott, Ph.D., P.E.  
EPRI Advanced Nuclear Technology Program Manager

Enclosure: One paper copy of non-proprietary report, *Uranium Oxycarbide (UCO) Tristructural Isotropic (TRISO) Coated Particle Fuel Performance: Topical Report EPRI-AR-1(NP)*. EPRI, Palo Alto, CA: 2019. 3002015750.

c: A. Cabbage, NRO/DAR/ARPB  
J. Monninger, NRO/DAR  
John Segala, NRO/DAR/ARPB  
A. Sowder, EPRI  
C. Marciulescu, EPRI

# Uranium Oxycarbide (UCO) Tristructural Isotropic (TRISO) Coated Particle Fuel Performance

Topical Report EPRI-AR-1(NP)

2019 TECHNICAL REPORT

# Uranium Oxycarbide (UCO) Tristructural Isotropic (TRISO) Coated Particle Fuel Performance

Topical Report EPRI-AR-1(NP)

3002015750

Final Report, May 2019

EPRI Project Managers  
C. Marciulescu  
A. Sowder

All or a portion of the requirements of the EPRI Nuclear  
Quality Assurance Program apply to this product.

YES



## **DISCLAIMER OF WARRANTIES AND LIMITATION OF LIABILITIES**

THIS DOCUMENT WAS PREPARED BY THE ORGANIZATION NAMED BELOW AS AN ACCOUNT OF WORK SPONSORED OR COSPONSORED BY THE ELECTRIC POWER RESEARCH INSTITUTE, INC. (EPRI). NEITHER EPRI, ANY MEMBER OF EPRI, ANY COSPONSOR, THE ORGANIZATION BELOW, NOR ANY PERSON ACTING ON BEHALF OF ANY OF THEM:

(A) MAKES ANY WARRANTY OR REPRESENTATION WHATSOEVER, EXPRESS OR IMPLIED, (I) WITH RESPECT TO THE USE OF ANY INFORMATION, APPARATUS, METHOD, PROCESS, OR SIMILAR ITEM DISCLOSED IN THIS DOCUMENT, INCLUDING MERCHANTABILITY AND FITNESS FOR A PARTICULAR PURPOSE, OR (II) THAT SUCH USE DOES NOT INFRINGE ON OR INTERFERE WITH PRIVATELY OWNED RIGHTS, INCLUDING ANY PARTY'S INTELLECTUAL PROPERTY, OR (III) THAT THIS DOCUMENT IS SUITABLE TO ANY PARTICULAR USER'S CIRCUMSTANCE; OR

(B) ASSUMES RESPONSIBILITY FOR ANY DAMAGES OR OTHER LIABILITY WHATSOEVER (INCLUDING ANY CONSEQUENTIAL DAMAGES, EVEN IF EPRI OR ANY EPRI REPRESENTATIVE HAS BEEN ADVISED OF THE POSSIBILITY OF SUCH DAMAGES) RESULTING FROM YOUR SELECTION OR USE OF THIS DOCUMENT OR ANY INFORMATION, APPARATUS, METHOD, PROCESS, OR SIMILAR ITEM DISCLOSED IN THIS DOCUMENT.

REFERENCE HEREIN TO ANY SPECIFIC COMMERCIAL PRODUCT, PROCESS, OR SERVICE BY ITS TRADE NAME, TRADEMARK, MANUFACTURER, OR OTHERWISE, DOES NOT NECESSARILY CONSTITUTE OR IMPLY ITS ENDORSEMENT, RECOMMENDATION, OR FAVORING BY EPRI.

THE FOLLOWING ORGANIZATION, UNDER CONTRACT TO EPRI, PREPARED THIS REPORT:

**BWXT TECHNOLOGIES, INC.**

THE TECHNICAL CONTENTS OF THIS PRODUCT WERE **NOT** PREPARED IN ACCORDANCE WITH THE EPRI QUALITY PROGRAM MANUAL THAT FULFILLS THE REQUIREMENTS OF 10 CFR 50, APPENDIX B. THIS PRODUCT IS **NOT** SUBJECT TO THE REQUIREMENTS OF 10 CFR PART 21.

### **NOTE**

For further information about EPRI, call the EPRI Customer Assistance Center at 800.313.3774 or e-mail [askepri@epri.com](mailto:askepri@epri.com).

Electric Power Research Institute, EPRI, and TOGETHER...SHAPING THE FUTURE OF ELECTRICITY are registered service marks of the Electric Power Research Institute, Inc.

Copyright © 2019 Electric Power Research Institute, Inc. All rights reserved.

## ACKNOWLEDGMENTS

---

The following organization, under contract to the Electric Power Research Institute (EPRI), prepared this report:

BWXT Nuclear Energy, Inc.  
109 Ramsey Place  
Lynchburg, VA 24501

Principal Investigators  
S. Schilthelm  
B. McIntyre  
S. Sloan

Development and preparation of this report was sponsored by EPRI and funded in part by the U.S. Department of Energy, Office of Nuclear Energy, through U.S. Government contract no. DE-AC07-05ID14517.

Under this collaborative project, technical content presented in Sections 2 – 7 and Appendices A and B was compiled and prepared specifically for this report with the assistance of Idaho National Laboratory (INL), Battelle Energy Alliance, LLC (BEA), under contract DE-AC07-05ID14517 with the U.S. Department of Energy. This content is documented in INL/LTD-18-46060 Rev. 0, *Technical Bases for the Performance Demonstration of TRISO-coated UCO Fuel Particles* and has been derived from other INL/BEA reports and results. The U.S. government retains a non-exclusive, paid-up, irrevocable worldwide license to publish or reproduce the published form of INL/LTD-18-46060, or allow others to do so, for U.S. government purposes.

EPRI appreciates and acknowledges the substantial support from and contributions by INL technical subject matter experts: P. Demkowicz, M. Holbrook, J. Kinsey, D. Marshall, W. Moe, H. Gouger, and D. Petti.

EPRI also appreciates and acknowledges the support of the following organizations and individuals, working collaboratively under the industry-led High Temperature Reactor Technology Working Group, to support the planning, development, and review of this report:

- Framatome (F. Shahrokhi)
- Kairos Power (P. Hastings, J. Tomkins, B. Collin, D. Peebles, D. Gardner, and M. Hackett)
- StarCore Nuclear (L. Eskin)
- X-energy (G. Bell)

This report benefitted greatly from technical reviews and comments provided by John Beale (EPRI) and independent reviewers Richard Hobbins and Finis Southworth.

---

This publication is a corporate document that should be cited in the literature in the following manner:

*Uranium Oxycarbide (UCO) Tristructural Isotropic (TRISO) Coated Particle Fuel Performance: Topical Report EPRI-AR-1(NP)*. EPRI, Palo Alto, CA: 2019. 3002015750.

## ABSTRACT

---

Nuclear fuel, fuel forms, and operating conditions vary widely across the numerous advanced reactor designs under development. However, tristructural isotropic (TRISO) coated particle fuel is foundational for many high-temperature reactor (HTR) designs, including high-temperature gas-cooled reactors (HTGRs) and fluoride salt-cooled high-temperature reactors (FHRs). The U.S. Department of Energy initiated the Advanced Gas Reactor Fuel Development and Qualification (AGR) Program in 2002 to establish U.S. capability to fabricate high-quality uranium oxycarbide (UCO) TRISO fuel and demonstrate its performance. Results from the first two fuel irradiation tests in the program, designated AGR-1 and AGR-2, demonstrate UCO fuel performance during irradiation and in post-irradiation high-temperature accident safety tests. This report consolidates the technical bases for the functional performance of UCO-based TRISO-coated particles so these particles can be used by a variety of HTR developers in their designs. The U.S. Nuclear Regulatory Commission (NRC) will review this topical report, which focuses on contemporary data and analysis from the AGR program demonstrating UCO-based TRISO fuel performance. Three key conclusions are presented for NRC review and approval:

1. Testing of UCO TRISO-coated fuel particles in AGR-1 and AGR-2 constitutes a performance demonstration of these particle designs over a range of normal operating and off-normal accident conditions. Therefore, the testing provides a foundational basis for use of these particle designs in the fuel elements of TRISO-fueled HTR designs (that is, designs with pebble or prismatic fuel and helium or salt coolant).
2. The kernels and coatings of the UCO TRISO-coated fuel particles tested in AGR-1 and AGR-2 exhibited property variations and were fabricated under different conditions and at different scales, with remarkably similar excellent irradiation and accident safety performance. Variations in key characteristics of the kernels and coatings are reflected in measured particle layer properties from AGR-1 and AGR-2. UCO TRISO-coated fuel particles that satisfy the parameter envelope defined by these measured particle layer properties can be relied upon to provide satisfactory performance.
3. Aggregate AGR-1 and AGR-2 fission product release data and fuel failure fractions, as summarized in this report, can be used for licensing of reactors employing UCO TRISO-coated fuel particles that satisfy the parameter envelope defined by measured particle layer properties from AGR-1 and AGR-2.

### Keywords

Advanced nuclear fuel  
Advanced nuclear technology  
Advanced reactors  
High temperature reactor (HTR)  
Tristructural isotropic (TRISO)  
Uranium oxycarbide (UCO)





**Deliverable Number: 3002015750**

**Product Type: Technical Report**

**Product Title: Uranium Oxycarbide (UCO) Tristructural Isotropic (TRISO) Coated Particle Fuel Performance: Topical Report EPRI-AR-1(NP)**

---

**PRIMARY AUDIENCE:** Developers of high-temperature reactor (HTR) designs that use UCO-based TRISO-coated particle fuel and regulators involved in design certification or licensing of HTRs utilizing TRISO fuel

**SECONDARY AUDIENCE:** Future owner-operators and other stakeholders interested in the technical basis for TRISO fuel performance

### KEY RESEARCH QUESTION

Most contemporary gas- and molten salt-cooled HTR designs rely on the performance of TRISO fuel particles embedded in prismatic blocks or pebble fuel; application to other reactor designs is possible and likely. EPRI has taken part in a collaborative effort involving the U.S. Department of Energy (DOE), Idaho National Laboratory, HTR developers, fuel suppliers, and other industry stakeholders. As part of its involvement, EPRI has developed a topical report on UCO TRISO-coated particle fuel performance to document key data and results from the first two phases of testing in the U.S. DOE Advanced Gas Reactor Fuel Development and Qualification (AGR) Program.

### RESEARCH OVERVIEW

Modern TRISO particle fuel technology is the product of coated particle fuel development spanning many countries over a half-century period. DOE launched the AGR program in 2002 to establish the ability to manufacture high-quality TRISO fuel in the United States and to demonstrate its performance. The first two phases of fuel irradiation testing, designated AGR-1 and AGR-2, provide data demonstrating the adequate performance of TRISO fuel during irradiation and in post-irradiation high-temperature accident safety tests. While most of these data have been or will be published in the public domain, the data have not been assembled in a concise format for efficient regulatory review and referencing by advanced reactor developers—a situation this topical report is intended to address.

### KEY FINDINGS

- Testing of UCO TRISO-coated fuel particles in AGR-1 and AGR-2 constitutes a performance demonstration of these particle designs over a range of normal operating and off-normal accident conditions. Therefore, the testing provides a foundational basis for use of these particle designs in the fuel elements of TRISO-fueled HTR designs (that is, designs with pebble or prismatic fuel and helium or salt coolant).
- The kernels and coatings of the UCO TRISO-coated fuel particles tested in AGR-1 and AGR-2 exhibited property variations and were fabricated under different conditions and at different scales, with remarkably similar excellent irradiation and accident safety performance. Variations in key characteristics of the kernels and coatings are reflected in measured particle layer properties from AGR-1 and AGR-2. UCO TRISO-coated fuel particles that satisfy the parameter envelope defined by these measured particle layer properties can be relied upon to provide satisfactory performance.

- Aggregate AGR-1 and AGR-2 fission product release data and fuel failure fractions, as summarized in this report, can be used for licensing of reactors employing UCO TRISO-coated fuel particles that satisfy the parameter envelope defined by measured particle layer properties from AGR-1 and AGR-2.

### **WHY THIS MATTERS**

This report consolidates foundational fuel performance data and results from the AGR-1 and AGR-2 tests in a form suitable for review by the U.S. Nuclear Regulatory Commission (NRC) and resulting in a safety evaluation report that can be referenced by multiple applicants to address UCO TRISO fuel performance. Accordingly, this report provides an opportunity to “lock-in” existing fuel performance data and results in a manner that can increase the efficiency of the safety review process for design certification and license applications in the United States and internationally.

### **HOW TO APPLY RESULTS**

The results documented in this topical report provide a consolidated reference on the performance of UCO TRISO-coated fuel particles demonstrated in AGR-1 and AGR-2 testing. Following review and approval by the NRC, this topical report will support streamlining and increase regulatory certainty of HTR design certification and licensing efforts by providing early acceptance of foundational information on UCO TRISO fuel particle performance.

### **LEARNING AND ENGAGEMENT OPPORTUNITIES**

- EPRI has established an Advanced Reactor Technical Advisory Group (TAG) under the Advanced Nuclear Technology Program to provide a forum for exchanging information and obtaining input on the direction and nature of EPRI’s strategic focus on advanced reactor technology.
- EPRI continues to seek and welcome collaborative research and development (R&D) opportunities that support commercialization of advanced nuclear technology, including consolidation and publication of R&D results that facilitate reactor developer efforts to pursue design certification as well as licensing and associated regulatory review of those designs.

**EPRI CONTACTS:** Andrew Sowder, Technical Executive, [asowder@epri.com](mailto:asowder@epri.com); and Cristian Marciulescu, Principal Technical Leader, [cmarciulescu@epri.com](mailto:cmarciulescu@epri.com)

**PROGRAM:** Advanced Nuclear Technology, P41.08.01

**IMPLEMENTATION CATEGORY:** Reference

---

*Together...Shaping the Future of Electricity®*

**Electric Power Research Institute**

3420 Hillview Avenue, Palo Alto, California 94304-1338 • PO Box 10412, Palo Alto, California 94303-0813 USA

800.313.3774 • 650.855.2121 • [askepri@epri.com](mailto:askepri@epri.com) • [www.epri.com](http://www.epri.com)

© 2019 Electric Power Research Institute (EPRI), Inc. All rights reserved. Electric Power Research Institute, EPRI, and TOGETHER...SHAPING THE FUTURE OF ELECTRICITY are registered service marks of the Electric Power Research Institute, Inc.

## ACRONYMS

---

3-D	three-dimensional
ACRS	Advisory Committee on Reactor Safeguards
ADUN	acid-deficient uranyl nitrate (solution)
AGR	Advanced Gas Reactor (Fuel Development and Qualification Program)
AOO	anticipated operational occurrence
ARDC	advanced reactor design criteria
ART	Advanced Reactor Technologies
ATR	Advanced Test Reactor (United States)
AVR	Arbeitsgemeinschaft Versuchsreaktor (Germany)
B&W	Babcock and Wilcox, Inc.
BAF	Bacon Anisotropy Factor
BISO	bistructural isotropic
BWXT	BWX Technologies, Inc. (also known as, Babcock and Wilcox or B&W)
CCCTF	Core Conduction Cooldown Test Facility (ORNL)
DLBL	deconsolidation-leach-burn-leach
DOE	U.S. Department of Energy
DTF	designed to fail
EAB	exclusion area boundary
EFPD	effective full-power day
EPA	U.S. Environmental Protection Agency
EPRI	Electric Power Research Institute
FACS	Fuel Accident Condition Simulator (INL)
FHR	fluoride salt-cooled high-temperature reactor
FIMA	fissions per initial metal atom
FPMS	fission product monitoring system
FRJ 2 DIDO	Forschungszentrum Jülich Research Reactor (Germany)
FSV	Fort St. Vrain (United States)

---

GA	General Atomics
GDC	general design criteria
GT-MHR	gas turbine modular helium reactor
HEU	highly enriched uranium
HFIR	high-flux isotope reactor (United States)
HFR	High Flux Reactor (Netherlands)
HM	heavy-metal
HMTA	hexamethylenetetramine
HPGe	high-purity germanium
HTGR	high-temperature gas-cooled reactor
HTR	high-temperature reactor
HTR-10	10-MW High-Temperature Gas-Cooled Reactor (China)
HTR-MODUL	200 MWth High Temperature Gas-Cooled Reactor (Interatom/Siemens/Framatome)
HTR-PM	High-Temperature Reactor-Pebble-bed Modular (China)
HTTR	High-Temperature Test Reactor (Japan)
IAEA	International Atomic Energy Agency
INET	Institute of Nuclear and New Energy Technology (China)
INL	Idaho National Laboratory (United States)
IPyC	inner pyrolytic carbon
JAERI	Japan Atomic Energy Research Institute (now Japan Atomic Energy Agency JAEA)
KüFA	Kühlfinger-Apparatur (Cold Finger Apparatus)
LBE	licensing basis events
LEU	low-enriched uranium
LHTGR	large high-temperature gas-cooled reactor
LWR	light water reactor
MCNP	Monte Carlo N Particle
MHTGR	modular high-temperature gas-cooled reactor
MTR	materials test reactor
MTS	methyltrichlorosilane
NaI(Tl)	thallium-activated, sodium iodide (scintillation detector)
NEFT	northeast flux trap
NGNP	Next Generation Nuclear Plant
Non-LWR	non-light-water reactor

---

NP-MHTGR	New Production Modular High-Temperature Gas-Cooled Reactor
NPR	New Production Reactor
NRC	U.S. Nuclear Regulatory Commission
NTTF	Near-Term Task Force
NUREG	publication prepared by the NRC staff
OPyC	outer pyrolytic carbon
ORNL	Oak Ridge National Laboratory
PAG	Protective Action Guide
PBMR	Pebble-Bed Modular Reactor (South Africa)
PDC	principal design criteria
PIE	post-irradiation examination
PIRT	phenomena identification and ranking table
PSER	pre-application safety evaluation report
PyC	pyrolytic carbon (also pyrocarbon)
R&D	research and development
R/B	release-rate-to-birth-rate ratio
RG	regulatory guide
SARRDL	specified acceptable system radionuclide release design limits
SECY	NRC Commission papers
SFR	sodium-cooled fast reactor
SiC	silicon carbide
SSC	structures, systems and components
SST	stainless steel
STP	standard temperature and pressure
TAVA	time-average volume-average
TC	thermocouple
THTR	Thorium High-Temperature Reactor (Germany)
TRISO	tristructural isotropic
U.S.	United States
UC <sub>x</sub>	uranium carbide
UCO	uranium oxycarbide
UO <sub>2</sub>	uranium dioxide

# CONTENTS

---

<b>ABSTRACT</b> .....	<b>v</b>
<b>EXECUTIVE SUMMARY</b> .....	<b>vii</b>
<b>ACRONYMS</b> .....	<b>ix</b>
<b>1 INTRODUCTION</b> .....	<b>1-1</b>
1.1 Report Scope and Purpose .....	1-2
1.2 Report Content and Structure .....	1-3
1.3 Key Conclusions for NRC Review and Approval .....	1-4
<b>2 U.S. REGULATORY BASES</b> .....	<b>2-1</b>
2.1 Prior NRC HTGR TRISO-Related Interactions .....	2-1
2.2 Current NRC Regulatory Framework .....	2-2
<b>3 TRISO-COATED PARTICLE FUEL EXPERIENCE BASE</b> .....	<b>3-1</b>
3.1 Particle Development Experience .....	3-2
3.1.1 General Experience and Coated Particle Evolution .....	3-2
3.1.2 Experience Prior to U.S. AGR Program .....	3-5
3.1.2.1 Fabrication .....	3-5
3.1.2.2 Irradiation .....	3-5
3.1.2.3 Safety Testing .....	3-7
<b>4 FISSION PRODUCT RETENTION, PARTICLE DESIGN, AND PERFORMANCE BASES</b> .....	<b>4-1</b>
4.1 Fission Product Retention .....	4-1
4.2 Particle Design .....	4-2
4.2.1 Fuel Kernel .....	4-3
4.2.2 Buffer Layer .....	4-4
4.2.3 Inner Pyrolytic Carbon Layer .....	4-4

4.2.4	Silicon Carbide Layer.....	4-4
4.2.5	Outer Pyrolytic Carbon Layer.....	4-5
4.2.6	Coated Particle.....	4-5
4.3	Failure Mechanisms.....	4-9
4.3.1	Structural/Mechanical Mechanisms.....	4-11
4.3.1.1	PyC Performance.....	4-11
4.3.1.2	Irradiation Induced Failure of IPyC Leading to SiC Cracking.....	4-11
4.3.1.3	Pressure Vessel Failure.....	4-12
4.3.2	Thermochemical Mechanisms.....	4-12
4.3.2.1	Kernel Migration.....	4-12
4.3.2.2	Chemical Attack of SiC.....	4-13
4.3.2.3	Thermal Decomposition of the SiC Layer.....	4-14
4.3.2.4	Relationship between Fuel-Failure Mechanisms and Fuel-Particle Properties.....	4-14
4.4	Performance Bases.....	4-14

**5 ADVANCED GAS REACTOR FUEL DEVELOPMENT AND QUALIFICATION PROGRAM.....5-1**

5.1	Program Background and Objectives.....	5-1
5.2	Overview of AGR Program Irradiations.....	5-4
5.2.1	Early Fuel Experiment (AGR-1).....	5-5
5.2.2	Performance Test Fuel Experiment (AGR-2).....	5-5
5.2.3	Fission Product Transport Experiments (AGR-3/4).....	5-5
5.2.4	Fuel Qualification and Fuel Performance Margin Testing Experiments (AGR-5/6/7).....	5-6
5.3	Summary of AGR-1 and AGR-2 Fuel Fabrication.....	5-7
5.3.1	Kernel Production.....	5-7
5.3.1.1	AGR-1 Kernels.....	5-7
5.3.1.2	AGR-2 Kernels.....	5-8
5.3.1.3	Diversity in Kernel Production.....	5-8
5.3.2	TRISO Fuel Particles.....	5-9
5.3.2.1	TRISO Coating Deposition.....	5-10
5.3.2.2	AGR-1 Particles.....	5-10
5.3.2.3	AGR-2 Particles.....	5-11
5.3.2.4	Diversity in TRISO Particle Properties.....	5-11

5.3.3	Sorting of Kernels and Particles.....	5-13
5.3.3.1	Sieving.....	5-13
5.3.3.2	Tabling.....	5-13
5.3.3.3	Roller Micrometer Sorting .....	5-13
5.3.4	Fuel Compact Fabrication.....	5-14
5.3.5	Quality Controls and Statistical Methods for Characterizing Fuel.....	5-14
5.3.6	Key Specifications and Property Ranges Observed in AGR-1 and AGR-2 TRISO Coated Particles.....	5-14
<b>6</b>	<b>AGR-1 AND AGR-2 IRRADIATIONS.....</b>	<b>6-1</b>
6.1	Capsule Design and Operation .....	6-2
6.2	Fission Rate, Burnup, and Fast Fluence .....	6-7
6.3	Thermal Analysis.....	6-16
6.4	Thermocouple Measurement and Performance.....	6-25
6.5	Uncertainty Quantification of Calculated Temperatures.....	6-29
6.6	Broader Comparisons of Key Service Conditions .....	6-31
6.7	Fission Gas Release .....	6-37
6.8	Implications on Fuel Performance .....	6-40
<b>7</b>	<b>ASSESSMENT OF FUEL PERFORMANCE FROM POST-IRRADIATION EXAMINATION AND SAFETY TESTING .....</b>	<b>7-1</b>
7.1	Fission Product Release During Irradiation .....	7-1
7.1.1	Methods .....	7-1
7.1.2	Results .....	7-3
7.2	Irradiated Fuel Particle Microstructural Evolution.....	7-7
7.3	Safety Testing .....	7-8
7.3.1	Isothermal Safety Tests in Dry Helium.....	7-8
7.3.2	Cesium .....	7-13
7.3.3	Silver .....	7-14
7.3.4	Europium and Strontium.....	7-15
7.3.5	Krypton.....	7-17
7.3.6	Transient Temperature Accident Simulation Tests in Dry Helium .....	7-17
7.4	SiC Failure Mechanisms .....	7-19
7.5	Particle Failure Statistics.....	7-23
<b>8</b>	<b>SUMMARY/CONCLUSIONS .....</b>	<b>8-1</b>



<b>9 REFERENCES .....</b>	<b>9-1</b>
<b>A U.S. REGULATORY BASES .....</b>	<b>A-1</b>
A.1 NRC Regulations .....	A-1
A.2 NRC Policy Statements.....	A-3
A.2.1 Functional Containment Performance.....	A-3
A.2.2 Source Term.....	A-4
A.3 NRC Guidance/References.....	A-4
A.3.1 NUREG-1338, "Pre-application Safety Evaluation Report for the MHTGR" .....	A-4
A.3.2 NUREG-0111, "Evaluation of High Temperature Gas-Cooled Reactor Particle Coating Failure Models and Data".....	A-5
A.3.3 NUREG-0800, Standard Review Plan, Section 4.2, "Fuel System Design" .....	A-6
A.3.4 TRISO-Coated Particle Fuel Phenomenon Identification and Ranking Tables .....	A-6
A.3.5 Next Generation Nuclear Plant .....	A-7
A.4 U.S. HTGR Precedents.....	A-10
A.4.1 Peach Bottom.....	A-10
A.4.2 Fort St. Vrain.....	A-10
A.4.3 Others .....	A-10
A.5 References.....	A-10
<b>B INTERNATIONAL COATED-PARTICLE DEVELOPMENT EXPERIENCE.....</b>	<b>B-1</b>
B.1 General Experience and Coated Particle Evolution .....	B-1
B.2 LEU UO <sub>2</sub> Experience in Russia .....	B-3
B.3 LEU UO <sub>2</sub> Experience in China.....	B-4
B.4 LEU UO <sub>2</sub> Experience in Japan .....	B-6
B.5 German High-Quality LEU-UO <sub>2</sub> Pebble-Fuel Experience .....	B-7
B.5.1 Fabrication.....	B-8
B.5.2 Irradiation and Accident Safety Testing .....	B-10
B.6 References.....	B-15

# LIST OF FIGURES

Figure 2-1 TRISO fuel performance relative to licensing end point.....	2-5
Figure 3-1 Early coated-particle designs .....	3-3
Figure 3-2 <sup>85m</sup> Kr release results for ramp heating tests of candidate HTGR fuel types. ....	3-8
Figure 4-1 The international-consensus TRISO particle design.....	4-3
Figure 4-2 Behavior of coating layers in a fuel particle .....	4-7
Figure 4-3 Tangential SiC stress history for a normal particle .....	4-8
Figure 4-4 TRISO particle failure mechanisms.....	4-10
Figure 4-5 Localized fission-product attack of the SiC layer in an irradiated UCO particle from the HRB-16 experiment.....	4-13
Figure 4-6 Radar plot of key parameters for TRISO-coated fuel performance. Germany and Japan plots represent historic values; NGNP indicates the performance envelope anticipated by the U.S. fuel development program .....	4-17
Figure 5-1 Sectioned TRISO fuel particle .....	5-9
Figure 6-1 ATR core cross section.....	6-2
Figure 6-2 Axial schematic of the AGR-1 capsules .....	6-3
Figure 6-3 Three-dimensional cutaway rendering of single AGR-1 capsule .....	6-4
Figure 6-4 Horizontal cross section of an AGR-1 experiment capsule.....	6-5
Figure 6-5 AGR-1 and AGR-2 experiment gas flow path.....	6-6
Figure 6-6 AGR-1 capsule average power density versus irradiation time in EFPDs.....	6-8
Figure 6-7 AGR-2 capsule average power density versus irradiation time in EFPDs.....	6-9
Figure 6-8 Power per particle for AGR-1 and AGR-2 irradiations .....	6-11
Figure 6-9 AGR-1 burnup (%FIMA) and fast neutron fluence (E >0.18 MeV) versus EFPD by capsule.....	6-12
Figure 6-10 AGR-2 burnup (FIMA) and fast neutron fluence (E >0.18 MeV) versus EFPD by capsule .....	6-13
Figure 6-11 Fast neutron fluence (E >0.18 MeV) vs. burnup (%FIMA) for AGR-1 and AGR-2 compacts .....	6-14
Figure 6-12 Two-dimensional cross-section of Abaqus FEA model for AGR-2 irradiation .....	6-17
Figure 6-13 Sample temperature profile in AGR-1 Capsule 4 after ~250 EFPDs and AGR-2 Capsule 3 after 290 EFPDs .....	6-18
Figure 6-14 AGR-1 calculated daily minimum, maximum and volume average temperatures for capsules 1-3.....	6-19
Figure 6-15 AGR-1 calculated daily minimum, maximum, and volume average temperatures for capsules 4-6 .....	6-20

Figure 6-16 AGR-1 calculated time-average minimum, time-average maximum and time-average volume-average temperatures for capsules 1-3 .....	6-21
Figure 6-17 AGR-1 calculated time-average minimum, time-average maximum and time-average volume-average temperatures for capsules 4-6 .....	6-22
Figure 6-18 AGR-2 calculated daily minimum, maximum, and volume average temperatures .....	6-23
Figure 6-19 AGR-2 calculated time-average minimum, time-average maximum, and time-average volume-average temperatures .....	6-24
Figure 6-20 Difference between measured and calculated TC temperatures for AGR-1 versus EFPDs .....	6-27
Figure 6-21 Difference between measured and calculated TC temperatures for AGR-2 versus EFPDs .....	6-28
Figure 6-22 Instantaneous peak and average fuel temperature (FT) and associated uncertainty for AGR-1 Capsule 4 .....	6-30
Figure 6-23 Time-average (TA) peak and time-average volume-average fuel temperatures (FT) for AGR-1 Capsule 4 .....	6-31
Figure 6-24 3-D scatter plot of the irradiation characteristics of the 72 AGR-1 and 36 AGR-2 UCO compacts .....	6-32
Figure 6-25 AGR-1 and AGR-2 fuel compact TAVA temperatures as a function of burnup ....	6-32
Figure 6-26 Distribution of time at temperature experienced by TRISO fuel particles in AGR-1 .....	6-33
Figure 6-27 Distribution of AGR-2 time at temperature for Capsules 5 and 6 UCO fuel.....	6-34
Figure 6-28 Distribution of AGR-2 time at temperature for Capsule 2 UCO fuel .....	6-35
Figure 6-29 Comparison of fuel temperature distribution in AGR-1 and AGR-2 capsules with that expected from a 750°C outlet temperature HTGR .....	6-36
Figure 6-30 AGR-1 R/B ratios for $^{85m}\text{Kr}$ , $^{88}\text{Kr}$ , and $^{135}\text{Xe}$ versus time in EFPDs .....	6-38
Figure 6-31 AGR-2 R/B ratios for $^{85m}\text{Kr}$ , $^{88}\text{Kr}$ , and $^{138}\text{Xe}$ versus time in EFPDs .....	6-39
Figure 6-32 $^{85m}\text{Kr}$ fission gas release for AGR-1 and AGR-2 compared to historic performance in U.S. and German TRISO fuel irradiations .....	6-41
Figure 7-1 Range of AGR-1 fractional fission product inventories found in the matrix of examined compacts and on the irradiation capsule components .....	7-3
Figure 7-2 Range of AGR-2 fractional fission product inventories found in the matrix of examined compacts and on the irradiation capsule components .....	7-4
Figure 7-3 AGR-1 and AGR-2 capsule-average compact $^{110m}\text{Ag}$ release based on total inventory measured on capsule components as a function of the capsule time-average maximum temperature .....	7-6
Figure 7-4 Ratio of measured $^{110m}\text{Ag}$ inventory to calculated inventory in AGR-1 and AGR-2 fuel compacts plotted vs. time-average maximum temperature .....	7-6
Figure 7-5 Examples of various AGR-1 irradiated particle microstructures .....	7-9
Figure 7-6 Fission product release from heating of AGR-2 compact 5-2-2 at 1600°C .....	7-10
Figure 7-7 Fission product releases from AGR-1 compacts during isothermal safety tests.....	7-11
Figure 7-8 Fission product releases from AGR-2 compacts during isothermal safety tests.....	7-12

---

Figure 7-9 Optical and electron micrographs of a region of the SiC layer corroded by CO in an irradiated UO <sub>2</sub> particle heated to 1600°C .....	7-14
Figure 7-10 <sup>154</sup> Eu and <sup>90</sup> Sr release from AGR-1 compacts heated to 1800°C.....	7-15
Figure 7-11 <sup>154</sup> Eu and <sup>90</sup> Sr release from AGR-2 Capsule 5 and 6 compacts heated to 1800°C .....	7-17
Figure 7-12 Fission product release during an accident simulation test in dry helium using three AGR-1 compacts.....	7-19
Figure 7-13 (a) X-ray tomogram showing microstructure in as-irradiated AGR-1 Compact 5-2-3 particle that led to SiC failure and cesium release; (b) x-ray close-up of degraded pathway through SiC; and (c) SEM micrograph of degraded region with EDS identification of Pd and U in the SiC and Si outside the SiC .....	7-21
Figure 7-14 Corroded region of the SiC layer of an AGR-1 particle safety tested at 1700°C .....	7-22
Figure 7-15 SiC layer and full TRISO failure fractions for combined AGR-1 and AGR-2 UCO results during irradiation and during safety tests. ....	7-25
Figure B-1 German LEU TRISO irradiation conditions, AVR and MTRs. The NGNP pebble-bed performance envelope is included for comparison .....	B-11
Figure B-2 Fuel burnup and mean operating temperature for German LEU UO <sub>2</sub> TRISO particles in accelerated irradiation tests conducted in European MTRs and in AVR prior to 2000 .....	B-12
Figure B-3 Summaries of <sup>85</sup> Kr and <sup>137</sup> Cs release during German accident safety tests in helium.....	B-14

## LIST OF TABLES

Table 4-1 Representative fuel defect levels and in-service failures for historic HTGR designs.....	4-2
Table 4-2 Particle design attributes contributing to tensile stress in SiC.....	4-6
Table 4-3 Relationship between mechanisms of fuel failure properties of fuel particles.....	4-16
Table 5-1 Differences in kernel production parameters for AGR-1 and AGR-2.....	5-8
Table 5-2 AGR-1 and AGR-2 kernel properties.....	5-9
Table 5-3 TRISO particle characterization data.....	5-12
Table 5-4 Sorting methods employed for AGR-1 and AGR-2 materials.....	5-13
Table 5-5 Particle layer property 95% confidence values on means and dispersion limits.....	5-16
Table 6-1 AGR-1 and AGR-2 minimum, average, and peak compact burnup and fast fluence at the end of irradiation.....	6-15
Table 6-2 Comparison of AGR-1 capsule fast neutron fluence ( $E > 0.18$ MeV) determined from measurement of fluence wires and from physics calculations.....	6-16
Table 6-3 Comparison of measured and calculated burnup values for AGR-1 fuel compacts.....	6-16
Table 6-4 End-of-irradiation time-average temperatures for AGR-1 and AGR-2 capsules.....	6-25
Table 6-5 Temperatures (T) and uncertainty ( $\sigma_T$ ) for time-average fuel temperatures at the end of AGR-1.....	6-29
Table 7-1 Maximum $^{85}\text{Kr}$ release fractions for AGR UCO and $\text{UO}_2$ fuel after ~300 hours at 1600, 1700, and 1800°C.....	7-18
Table 7-2 SiC layer and full TRISO failure statistics for AGR-1 and AGR-2 UCO fuel during irradiation and during safety tests. AGR-2 data are preliminary, pending completion of PIE and safety testing.....	7-27
Table B-1 LEU $\text{UO}_2$ TRISO fuels manufactured and tested.....	B-8
Table B-2 Manufacturing detail for LEU $\text{UO}_2$ TRISO fuel types.....	B-9

# 1

## INTRODUCTION

---

Nuclear fuel qualification represents one of the longest-lead items for commercializing a new reactor technology. While fuel forms and operating conditions vary widely across the many advanced reactor designs under consideration and development, many high-temperature reactor (HTR) concepts use tristructural isotropic (TRISO) coated particles as the basis for their fuel designs, including high-temperature gas-cooled reactors (HTGRs) and fluoride salt-cooled high-temperature reactors (FHRs).

A wide variety of HTR designs that would use TRISO-coated particle fuel in a carbonaceous matrix can operate safely under realistic operating and accident scenarios provided the time-at-temperature of the particles remains below fission product release thresholds. Experimental evidence shows that if these thresholds are not exceeded, a level of fuel performance and fission product retention is achieved such that the radioactive source term emitted from the plant will be lower by orders of magnitude than other reactor types. In the United States, siting of the plant near population centers and co-location with industrial users of process heat requires compliance of releases at or near the site boundary with U.S. Environmental Protection Agency (EPA) Protective Action Guides (PAG) for offsite dose. This enables a graded approach to emergency planning and the potential elimination of the need for evacuation and sheltering beyond the site boundary. However, achieving this level of performance is predicated on the fabrication of coated-particle fuel that demonstrates excellent performance under anticipated operation and accident conditions.

The U.S. Department of Energy initiated the Advanced Gas Reactor Fuel Development and Qualification (AGR) Program in 2002 to establish the capability in the U.S. to fabricate high-quality TRISO fuel and to demonstrate fuel performance. The AGR program to date has focused on manufacturing and testing the fuel design for HTR concepts using the most recent gas turbine modular helium reactor fuel product specification as a starting point [1]. Irradiation, safety testing, and post-irradiation examination (PIE) plans support fuel development and qualification in an integrated manner. The AGR program consists of four testing campaigns; AGR-1, AGR-2, AGR-3/4 and AGR-5/6/7. The first two fuel irradiation tests in the program, designated AGR-1 and AGR-2, demonstrated uranium oxycarbide (UCO)<sup>1</sup> fuel performance during irradiation and during post-irradiation high-temperature accident safety tests. **This topical report covers the foundational fuel performance testing from the AGR-1 and AGR-2 tests and the irradiation, safety testing and PIE results to date.**

---

<sup>1</sup> Uranium oxycarbide as used here is a short-hand term to denote a mixture of uranium dioxide (UO<sub>2</sub>) and uranium carbide (UC<sub>x</sub>), the two phases present in the kernel.

## 1.1 Report Scope and Purpose

This report provides the technical bases (that is, particle design, irradiation, and accident testing results) that demonstrate the functional performance of UCO TRISO-coated particles so these particles can be used by a variety of high-temperature reactor developers in their designs. This report addresses UCO fuel performance only. Any information related to uranium dioxide (UO<sub>2</sub>) fuel is provided for context and comparison purposes only.<sup>2</sup>

This report is being prepared for submission to the U.S. Nuclear Regulatory Commission as topical report for formal review and issuance of a safety evaluation report (SER). Nuclear Regulatory Commission (NRC) NRR Office Instruction LIC-500, Topical Report Process [2], defines a topical report as a stand-alone report containing technical information about a nuclear power plant safety topic. Further, a topical report provides the technical basis for a licensing action.

Topical reports are reviewed by the NRC staff with the intent of maximizing their scope of applicability consistent with current standards for licensing actions, compliance with the applicable regulations, and reasonable assurance the health and safety of the public will not be adversely affected. Topical reports improve the efficiency of the licensing process by allowing the staff to review proposed methodologies, designs, operational requirements, or other safety-related subjects on a generic basis, so they may be implemented by reference by multiple U.S. licensees once determined to be acceptable for use and verified by the NRC staff. By reviewing this information as a topical report, the NRC will reduce the review time for the technical bases by allowing applicants to reference the topical report and associated safety evaluation, rather than submitting it for review and approval on each application.

The review of the information provided in this topical report is intended to support HTR developers and other stakeholders by:

- Providing early acceptance and resolution of technical information and foundational information for industry to move forward with a degree of design and regulatory certainty
- Identifying technology neutral open issues that might be resolved generically from subsequent AGR-3/4 or AGR-5/6/7 tests in subsequent topical reports or applications
- Identifying technology specific open issues that can be resolved in subsequent topical reports or applications
- Progressing fuel performance reviews in parallel with ongoing efforts on source term, functional containment performance, and the development/review of NEI-18-04 with respect to licensing basis events (LBE), structures, systems, and components (SSC) classification and defense in depth
- Providing data on fuel performance and fission product release that can be utilized as part of a computational code verification and validation effort

---

<sup>2</sup> While some limited work on UO<sub>2</sub> was included in AGR-2 as part of an international collaboration under the auspices of the Generation IV International Forum, the AGR program is focused on UCO TRISO-coated particle fuel. AGR UO<sub>2</sub> fuel performance is included in this report for context and background.

## 1.2 Report Content and Structure

The substantive content of this report is adapted from material prepared by INL as part of a collaborative project to develop and submit a topical report on UCO TRISO-coated particle fuel performance based on available results from the AGR-1 and AGR-2 campaigns [3].<sup>3</sup> The report content is organized and presented in the following manner:

- Section 2 provides an overview of the TRISO-related NRC Regulatory Bases, including a description of how this topical report fits into the overall TRISO-fueled plant licensing strategies.
- Section 3 summarizes the background information for the basis of TRISO-coated particle fuel technology resulting from decades of development of TRISO-coated fuel particles in the United States.
- Section 4 introduces the concept of fission product retention for reactor systems that use TRISO-coated particle fuel and presents the basis for the particle design and performance used in the AGR program and provides representative levels of fuel performance requirements necessary to implement such an approach.
- Section 5 provides a brief overview of the AGR program, including the different program elements and the four fuel irradiation campaigns around which the program is structured. Fabrication of the AGR fuel is described in Section 5.3.
- Section 6 provides the irradiation response of fuel particles in the AGR-1 and AGR-2 campaigns.
- Section 7 presents follow-on safety test performance and PIE data for AGR-1 and AGR-2.
- Section 8 provides a summary of the report, including the key conclusions drawn from this work in regard to U.S. UCO TRISO fuel performance.
- Appendix A provides an overview of the regulatory history for the U.S. related to TRISO fuel.
- Appendix B provides an overview of the international TRISO-coated particle fuel experience base.

---

<sup>3</sup> Under a collaborative project jointly funded by EPRI and DOE, the technical content presented in Sections 2–7 and Appendices A and B was compiled and prepared specifically for this report with the assistance of Idaho National Laboratory (INL), Battelle Energy Alliance, LLC (BEA), under contract DE-AC07-05ID14517 with the U.S. Department of Energy. This content is also documented in INL/LTD-18-46060 Rev. 0, *Technical Bases for the Performance Demonstration of TRISO-coated UCO Fuel Particles* [3] and has been derived from other INL/BEA reports and results.



### **1.3 Key Conclusions for NRC Review and Approval**

EPRI is requesting NRC review of AGR-1 and AGR-2 data and analyses documented in Sections 5-7 of this topical report<sup>4</sup> and is seeking NRC approval of the following three conclusions presented in Section 8:

1. Testing of UCO TRISO-coated fuel particles in AGR-1 and AGR-2 constitutes a performance demonstration of these particle designs over a range of normal operating and off-normal accident conditions. Therefore, the testing provides a foundational basis for use of these particle designs in the fuel elements of TRISO-fueled HTR designs (that is, designs with pebble or prismatic fuel and helium or salt coolant).
2. The kernels and coatings of the UCO TRISO-coated fuel particles tested in AGR-1 and AGR-2 exhibited property variations and were fabricated under different conditions and at different scales, with remarkably similar excellent irradiation and accident safety performance results. The ranges of those variations in key characteristics of the kernels and coatings are reflected in measured particle layer properties provided in Table 5-5 from AGR-1 and AGR-2. UCO TRISO-coated fuel particles that satisfy the parameter envelope defined by these measured particle layer properties in Table 5-5 can be relied on to provide satisfactory performance.
3. Aggregate AGR-1 and AGR-2 fission product release data and fuel failure fractions, as summarized in this report, can be used for licensing of reactors employing UCO TRISO-coated fuel particles that satisfy the parameter envelope defined by measured particle layer properties in Table 5-5 from AGR-1 and AGR-2.

---

<sup>4</sup> Sections 5-7 document AGR program results and analyses that represent the core scope of this topical report and support the conclusions of this report. Sections 1-4 and Appendices A and B are included as historical background and context only. The U.S. TRISO fuel qualification program and the conclusions of this topical report do not rely upon historical pre-AGR data.

# 2

## U.S. REGULATORY BASES

---

### 2.1 Prior NRC HTGR TRISO-Related Interactions

In 2005, the U.S. Department of Energy (DOE) established the Next Generation Nuclear Plant (NGNP) project at Idaho National Laboratory (INL) to support near-term commercial deployment of a HTGR technology demonstration plant. A key part of the project was the development of a regulatory framework supportive of commercial HTGR deployment. These activities were closely coordinated with NRC staff and focused on adapting existing nuclear power plant regulatory requirements to the needs of NGNP licensing. DOE and NRC jointly formulated the approach for this licensing structure and communicated this approach to Congress in 2008.

Under the NGNP project, HTGR licensing precedents and NRC regulations were examined systematically as they relate to the HTGR safety case and associated plant design goals. NRC staff coordinated the scope of this examination and reviewed the results. In 2009, this information was used to develop a strategic implementation plan [4] for establishing the regulatory basis necessary to complete and submit an HTGR license application to NRC. The plan focused on key elements of plant safety design and licensing and included:

- Developing the basis for establishing a mechanistic radiological source term based primarily on particle fuel design and available qualification testing results
- Preventing and mitigating the release of the radiological source terms to the environment, including methods for the structured and comprehensive identification of licensing basis event sequences along with establishing multiple radionuclide release barriers

The design and licensing strategy of the NGNP centered on radionuclide retention capabilities of TRISO particle fuel. It also relied less on other barriers for limiting offsite releases of radionuclides compared to historical light water reactor (LWR) technology.

In July 2014, the NRC issued a report summarizing the results of these regulatory framework interactions with the NGNP. Important outcomes identified in that NRC staff report [5] included:

- General agreement was expressed with the proposed HTGR performance standard concerning HTGR functional containment. The functional containment approach limits radionuclide releases to the environment by emphasizing retention of radionuclides at their source in the fuel rather than allowing significant fuel particle failures and relying upon other external barriers to provide compliance with identified top-level regulatory dose acceptance criteria.
- The INL AGR Fuel Development and Qualification Program was determined to be reasonably complete within a context of pre-prototype fuel testing. Early fuel test results showed promise in demonstrating much of the desired retention capabilities of the TRISO particle fuel.

## 2.2 Current NRC Regulatory Framework

The NRC conducts its reactor licensing activities through a combination of regulatory requirements and guidance. The applicable regulatory requirements are found in Chapter I of Title 10, "Energy," of the *Code of Federal Regulations*, Parts 1 through 199. Regulatory guidance provides additional detailed information on specific acceptable means to meet the requirements in regulation. Guidance exists in several forms, including: Regulatory Guides (RGs), interim staff guidance, standard review plans, publications prepared by the NRC staff (NUREGs), review standards, and Commission policy statements. Appendix A summarizes these regulatory and guidance documents related to TRISO fuel. These regulatory requirements and guidance represent the entirety of the regulatory framework an applicant should consider when preparing an application for review by the NRC.

Establishing principal design criteria (PDC) for a reactor is a key part of the NRC's regulatory framework. The general design criteria (GDC) contained in Appendix A to 10 CFR Part 50 [6] were developed specifically for LWRs and provide minimum requirements for PDC, which establish the necessary design, fabrication, construction, testing, and performance requirements for SSCs which are important to safety, that is, SSCs "that provide reasonable assurance that the nuclear power plant can be operated without undue risk to the health and safety of the public."

The GDC also provide guidance in establishing the PDC for non-light-water reactor (non-LWR). The PDC serve as the fundamental criteria for the NRC staff when reviewing the SSCs that make up a nuclear power plant design particularly when assessing the performance of their intended safety functions in design basis events postulated to occur during normal operations, anticipated operational occurrences (AOO), and postulated accidents. All production and utilization facilities licensed under 10 CFR Part 50, including both LWRs and non-LWRs, are required to describe PDC in their preliminary safety analysis report supporting a construction permit application as described in 10 CFR 50.34(a)(3). All applicants for a standard design certification are also required to describe PDC in their final safety analysis report as described in 10 CFR 52.47(a)(3).

In April 2018, the NRC issued RG 1.232 "Guidance for Developing Principal Design Criteria for Non-Light-Water Reactors," which provides guidance for how the GDC in Appendix A may be adapted to develop PDC for non-LWR designs [7]. In addition, RG 1.232 provides guidance for adapting the LWR GDC for modular HTGRs and sodium-cooled fast reactors (SFRs). RG 1.232 guidance may be used to develop all or part of a design's PDC and users may choose among the Advanced Reactor design criteria (ARDC), modular HTGR design criteria (MHTGR-DC), or SFR design criteria (SFR-DC) to develop their PDC after considering the underlying safety basis a given criterion and evaluating the RG's rationale for the adaptation.

The work to develop and issue this regulatory guidance provides key regulatory underpinning for the path forward on advanced reactors. Specifically, MHTGR-DC 10 and MHTGR-DC 16, provide a model for evaluation of TRISO fuel performance in combination with plant systems performance and functional containment performance to achieve the overall radiological dose criteria. This work on particle fuel design and performance testing supports development of the basis for establishing a mechanistic radiological source term.

MHTGR-DC 10, *Reactor Design*, provides guidance related to acceptable system radionuclide releases. Other ARDC that pertain to the reactor core (that is, MHTGR-DC 11, 12, 13, and 26) do not directly pertain to the performance of the TRISO-coated particle fuel. MHTGR-DC 10, states [7]:

The reactor system and associated heat removal, control, and protection systems shall be designed with appropriate margin to ensure that specified acceptable system radionuclide release design limits are not exceeded during any condition of normal operation, including the effects of anticipated operational occurrences.

RG 1.232 includes the following rationale for MHTGR-DC 10 documenting the basis for wording changes from the original LWR GDC:

- “the concept of specified acceptable fuel design limits, which prevent additional fuel failures during anticipated operational occurrences (AOOs), has been replaced with that of the specified acceptable system radionuclide release design limits (SARRDL), which limits the amount of radionuclide inventory that is released by the system under normal and AOO conditions.” Design features within the reactor system must ensure the SARRDLs are not exceeded during normal operations and AOOs.
- The TRISO fuel used in the MHTGR design is the primary fission product barrier and is expected to have a very low incremental fission product release during AOOs.
- The SARRDLs will be established so that the most limiting license-basis event does not exceed the siting regulatory dose limits criteria at the exclusion area boundary (EAB) and low-population zone (LPZ), and also ensure the 10 CFR 20.1301 annualized dose limits to the public are not exceeded at the EAB for normal operation and AOOs.
- The concept of the TRISO fuel being the primary fission product barrier is intertwined with the concept of a functional containment for MHTGR technologies. See the rationale for MHTGR-DC 16 for further information on the Commission’s current position.

MHTGR-DC 16, *Containment Design*, provides guidance for a functional containment design, which relies on the use of multiple barriers to control the release of radioactivity. MHTGR-DC 16 states [7]:

A reactor functional containment, consisting of multiple barriers internal and/or external to the reactor and its cooling system, shall be provided to control the release of radioactivity to the environment and to ensure that the functional containment design conditions important to safety are not exceeded for as long as postulated accident conditions require.

RG 1.232 includes the following rationale for MHTGR-DC 16 documenting the basis for wording changes from the original LWR GDC, which include [7]:

- The term ‘functional containment’ is applicable to advanced non-LWRs without a pressure retaining containment structure. A functional containment can be defined as “a barrier, or set of barriers taken together, that effectively limit the physical transport and release of radionuclides to the environment across a full range of normal operating conditions, AOOs, and accident conditions.”

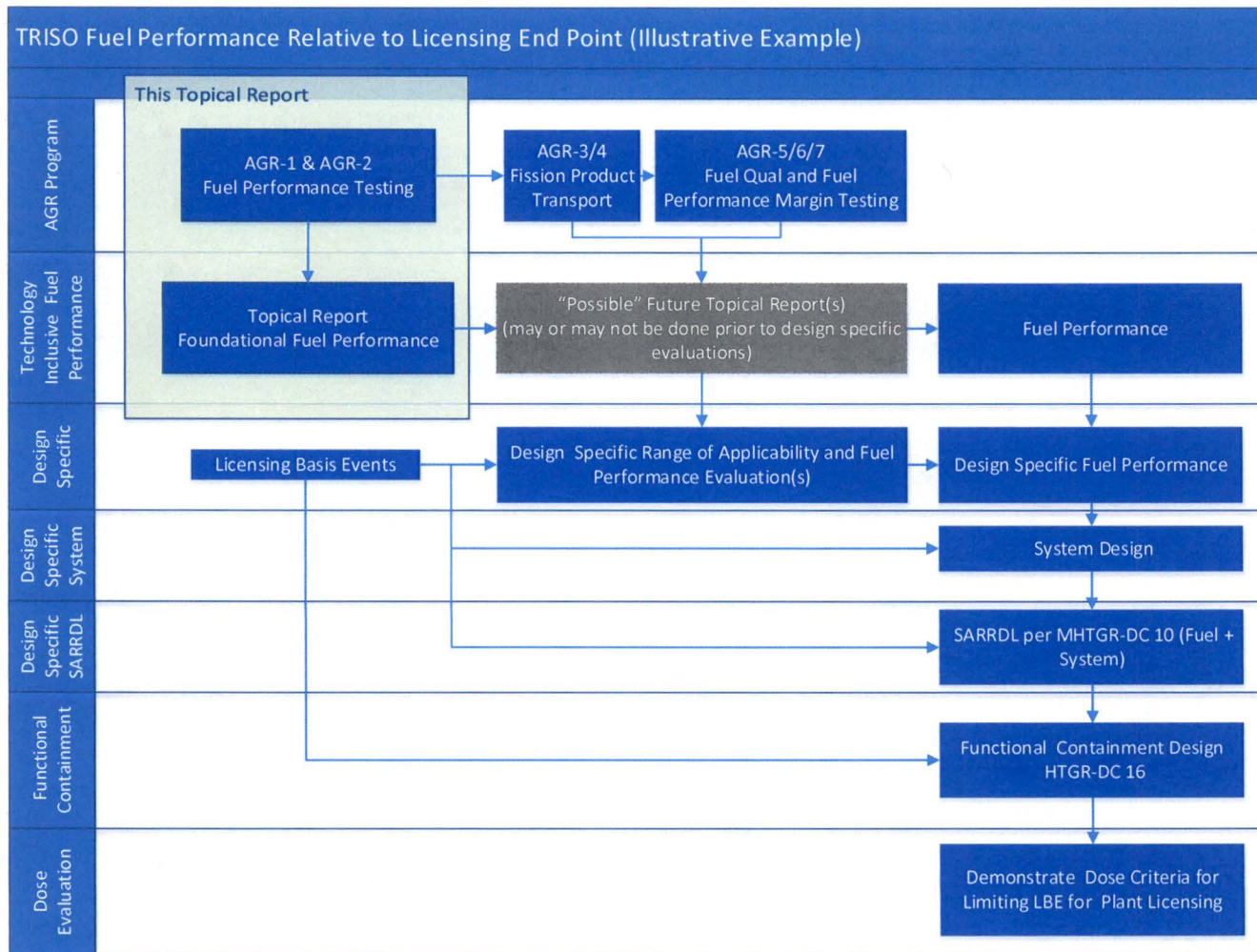
- “The NRC staff has brought the issue of functional containment to the Commission, and the Commission has found it generally acceptable.”
- “The NRC staff also provided feedback to the DOE on this issue as part of the NGNP project, (*see Appendix A to this document*). ... the area on functional containment and fuel development and qualification noted that “...approval of the proposed approach to functional containment for the MHTGR concept, with its emphasis on passive safety features and radionuclide retention within the fuel over a broad spectrum of off-normal conditions, would necessitate that the required fuel particle performance capabilities be demonstrated with a high degree of certainty.”

Figure 2-1 below illustrates how this topical report fits conceptually into the broader context of technology inclusive TRISO fuel performance, future AGR program data, manufacturing specifications and evaluation, design specific systems evaluation, functional containment evaluation, and finally, design specific demonstration of achieving acceptable dose criteria. This figure is intended to illustrate where and how this topical report provides valuable foundational information and finality to industry and the NRC. It is not intended to capture all of the steps in the future review process for the ultimate licensing of a plant.

As highlighted in the figure, this topical report addresses only the performance data obtained in the AGR-1 and AGR-2 tests. While limited in scope, these data are foundational to the design and licensing of reactors using TRISO fuel. This topical report, if endorsed, will provide TRISO fuel performance data from the AGR-1 and AGR-2 tests for use by future applicants during design of the plants and for use by NRC staff in accepting the design inputs and test data for fuel performance. The results presented here demonstrate the excellent performance of TRISO-coated fuel particles under normal and postulated accident conditions.

The completion of future AGR tests (discussed in Section 5 below) will provide additional information on statistical performance testing, fission product transport, and fuel performance margin tests. These data will also be important to future applicants and to NRC Staff for completion of safety evaluations. Applicants will utilize these data to formulate their fuel licensing case. The figure is intended to illustrate options that could include for example; an amendment to this report, a future stand-alone topical report, or use of test reports to support a future application and review.

The figure also indicates that future applicants will be required to develop LBE, demonstrate that the specific reactor design is within the range of applicability for the TRISO particle performance data, incorporate this information into the system design, establish SARRDLs, establish the functional containment design, and demonstrate that acceptable dose criteria are achieved for the plant.



**Figure 2-1**  
**TRISO fuel performance relative to licensing end point (illustrative example)**

# 3

## TRISO-COATED PARTICLE FUEL EXPERIENCE BASE

---

This section reviews the existing experience base supporting the development, qualification, and production of TRISO-coated particle fuel. A broad base of experience encompassing a range of coated particle designs and service conditions provides a general understanding of the important phenomena associated with particle fabrication and performance and has served to identify potential fuel failure mechanisms. This experience yields a common internationally recognized set of particle design features, which, in combination with restrictions on service conditions, mitigate or eliminate failure mechanisms.

The coated particles must be designed and fabricated to remain intact and retain radionuclides with a high level of effectiveness over the range of conditions that could be encountered in normal operation and under accident conditions. Historic modular gas reactor design concepts have been developed to limit the fuel service conditions (for example, burnup, fast fluence, temperature) to a range consistent with the performance capabilities of the fuel. The particles must be able to accommodate the following effects:

- Fission-induced changes in the kernel: production of a wide range of fission-product<sup>5</sup> isotopes, lattice dislocations by fission product recoil, kernel swelling due to solid and gaseous fission products, liberation of oxygen from fissioning of UO<sub>2</sub> molecules
- High-energy neutron-induced changes in material microstructure: anisotropic shrinkage and/or expansion in pyrocarbon layers, reductions in silicon carbide (SiC) layer strength
- Buildup of pressure within the particles: release of noble gas fission products from the kernel, production of CO and CO<sub>2</sub> from reaction of excess oxygen with buffer material, mainly in the case of UO<sub>2</sub> kernels
- Redistribution of fission products within the particle and chemical reactions with particle layers: chemical attack of the SiC layer and migration of the kernel within the particle

The last three effects are time and temperature dependent with a wide range of rate constants.

Particle physical characteristics established to meet anticipated performance requirements include dimensions (mean and variation), densities, pyrocarbon anisotropy, and defect levels. Rigorous statistically based procedures are used to characterize this fuel.

Experience with manufacturing coated-particle fuel has demonstrated the feasibility of producing large quantities of coated-particle fuel with low as-manufactured defect levels, approaching defect fractions of 10<sup>-5</sup>. This capability was first demonstrated in Germany with the production of reload fuel batches for the Arbeitsgemeinschaft Versuchsreaktor (AVR) and subsequently

---

<sup>5</sup> The term "fission product" here is used broadly to include isotopes that are produced as a result of fission processes (that is, direct fission products or isotopes that result from the radioactive decay of direct fission products) and isotopes resulting primarily from neutron activation of fission products (important examples include <sup>110m</sup>Ag and <sup>134</sup>Cs).

confirmed in fuel production campaigns in Japan for the High-Temperature Test Reactor (HTTR) first core and in China for the 10-MW High-Temperature Gas-Cooled Reactor (HTR-10) first core. Laboratory-scale production of high-quality fuel has also been demonstrated in Russia, South Africa, and the United States.

Appendix B summarizes the broad international experience with coated-particle fuel fabrication and performance covering a wide range of particle designs and material properties explored in the evolution toward the LEU TRISO particle under common development today. It also addresses the failure mechanisms that have been identified from this experience and the common particle design elements that have emerged.

The extensive international experience highlighted here and described in more detail in Appendix B includes particle designs exhibiting a wide variety of kernel properties. The kernel of the coated particle is substantially decoupled from the dense pyrocarbon and SiC layers by the low-density-carbon buffer layer. Thus, the experience generally applies to low-enriched uranium (LEU) UCO fuel from the standpoint of dense pyrocarbon and SiC-layer design and performance.

Section 4.2 describes the common elements of coated-particle designs that evolved from this broad experience and are under development. Section 4.3 addresses the potential particle failure mechanisms that were identified from the broad experience discussed in Section 3.1. These design elements, in combination with limitations established by the reactor designs on fuel-service conditions (for example, temperature, burnup, and fast fluence) under normal operation and accident conditions, effectively exclude most of the failure mechanisms and limit the remaining mechanisms to a very small fraction of the particles within a small fraction of the core.

### **3.1 Particle Development Experience**

#### ***3.1.1 General Experience and Coated Particle Evolution***

Coated particles start with a spherical kernel of fissile or fertile material surrounded by one or more refractory coatings. By the early 1960s, coated-particle fuel development for resinated graphite-moderated helium-cooled HTGRs was well under way in the United Kingdom in support of the DRAGON research reactor [8], in the U.S. in support of the Peach Bottom Unit 1 prototype power reactor [9] and in Germany in support of the AVR research and power reactor [10]. AVR fuel loadings evolved through many designs in the course of over two decades of plant operation, including the LEU TRISO design discussed in Section 4.2. As Figure 3-1 illustrates, coated particle designs for these early reactors varied considerably.



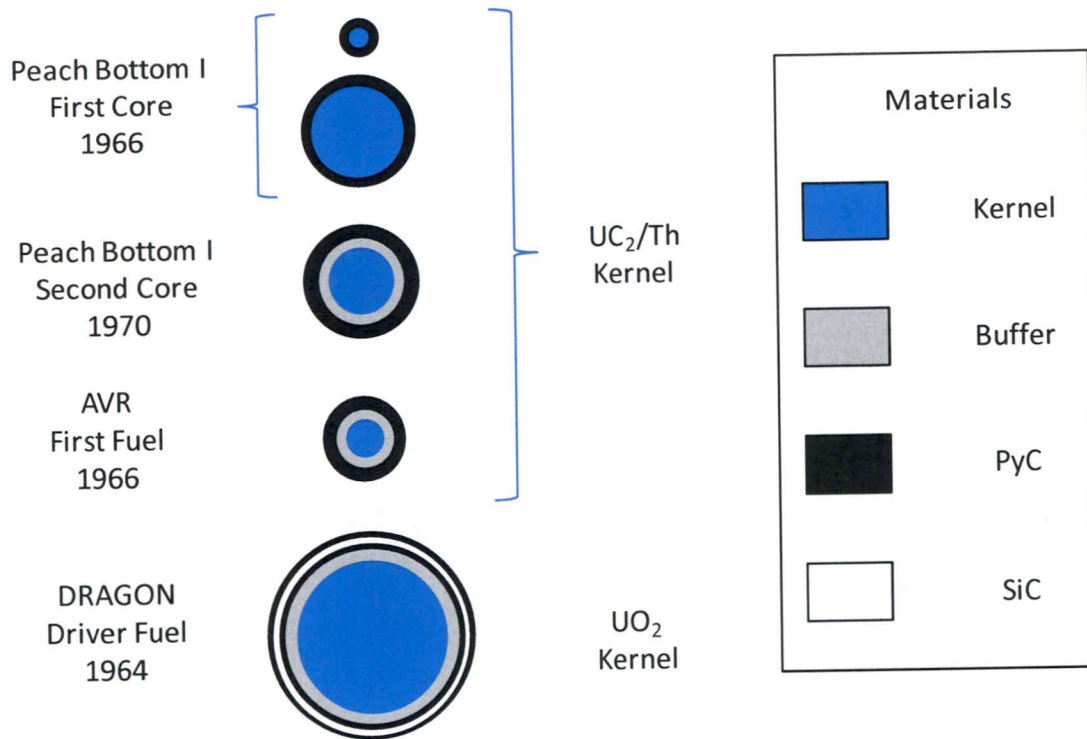


**Figure 3-1**  
**Early coated-particle designs**

*Courtesy of Idaho National Laboratory and used with permission of Battelle Energy Alliance, LLC*

As described in Appendix B, coated-particle fuel development programs have also been conducted in France, Russia, Japan, China, South Africa, and South Korea. The development of coated-particle fuel technology for both the pebble-bed and prismatic designs has drawn from an extensive international background of coated-particle fuel fabrication and testing experience spanning more than 50 years and covering a broad range of parameters:

- Kernel characteristics:
  - Diameter – 100 to 800  $\mu m$
  - Fissile/fertile materials – uranium, thorium, plutonium (mixed and unmixed)
  - Chemical forms – oxide, carbide, oxycarbide
  - Enrichment – ranging from natural to high-enriched uranium (HEU) and plutonium
- Coating characteristics:
  - Bistructural isotropic (BISO) – variations in buffer and pyrolytic carbon (PyC) coating thicknesses and properties
  - TRISO – variations in buffer, PyC and SiC (or zirconium carbide) thicknesses and properties

- Fuel forms:
  - Spheres – multiple geometries and fabrication methods
  - Compacts – cylindrical and annular shapes with variations in particle packing fractions and fabrication methods
- Irradiation facilities:
  - Material Test Reactors – High Flux Reactor (HFR, Netherlands), Forschungszentrum Jülich Research Reactor (FRJ 2 DIDO, Germany), IVV-2M (Russia), Siloe (France), R2 (Sweden), BR2 (Belgium), High-Flux Isotope Reactor (HFIR, United States) and Advanced Test Reactor (ATR, United States), with wide variations in neutron energy spectra and degree of irradiation acceleration
  - Research and Demonstration Reactors – DRAGON (United Kingdom), Peach Bottom I (United States), AVR (Germany), Fort St. Vrain (FSV, United States), Thorium High Temperature Reactor (THTR, Germany), HTTR (Japan), and HTR-10 (China)
- Irradiation and testing conditions:
  - Burnup – ranging from below 1% to above 70% fissions per initial metal atom (FIMA)
  - Fast fluence – ranging from below  $1 \times 10^{21}$  to above  $10 \times 10^{21}$  n/cm<sup>2</sup>
  - Irradiation temperature – ranging from 600 to 1950°C
  - Accident simulation temperature – ranging from 1400 to 2500°C

A detailed understanding of the parameters and phenomena of importance in the fabrication and performance of coated-particle fuel has emerged from this broad range of experience and data. Extensive bilateral and multilateral international information exchanges facilitated the incorporation of this broad experience base into German and other modern coated-particle fuels.

A detailed review of U.S. and German experience and the relationship to fuel performance and fuel performance modeling is documented in a 2004 EPRI report [11]. The evolution of the German fuel design, arriving at the LEU UO<sub>2</sub> TRISO pressed sphere selected as a basis for the pebble-bed reactor concept, is summarized in a historical review of AVR operation [10]. A broader range of international experience, focused mainly on LEU TRISO fuel, was addressed in an International Atomic Energy Agency (IAEA) coordinated research project conducted in the 1990s [12]. A more recent coordinated research project on TRISO-coated particle fuel was conducted in the early 2000s [13], which included two key elements: (1) an international quality control round robin test campaign for measuring important attributes of TRISO-coated particles; and (2) an international fuel performance benchmarking exercise to compare international codes that model TRISO-coated particle fuel under both normal operation and postulated accident conditions.

One important outcome of this international experience and data has been the convergence on common LEU TRISO particle designs, as discussed in Section 4.2, exhibiting similar coating thicknesses and properties with variations in kernel diameter, enrichment, and composition (UO<sub>2</sub> and UCO), depending on specific service conditions and requirements.

### **3.1.2 Experience Prior to U.S. AGR Program**

Experience prior to the AGR program with irradiation and safety testing of TRISO-coated UCO particles is discussed in this section.

#### **3.1.2.1 Fabrication**

In the 1960s and 1970s, a large-scale coated-particle fuel-fabrication facility was established at General Atomics (GA) in the United States to support the operation of the 115-MWth Peach Bottom Unit 1 (cylindrical annular fuel compacts containing BISO-coated (Th,U) $C_2$  fuel particles) and the 842-MWt FSV (prismatic fuel elements containing TRISO-coated (Th,U) $C_2$  fissile particles and TRISO-coated Th $C_2$  fertile particles) HTGRs [14]. Following the termination of FSV operations in 1989, the fuel fabrication facility was used for the fabrication of some fuel test articles and all the TRISO target test compacts for the NP-MHTGR. Following cancellation of the NP-MHTGR, the facility was decommissioned and dismantled—eliminating large-scale TRISO fuel fabrication capability in the United States.

High-density UCO kernels were irradiated in twelve irradiation test capsules in the United States and Germany. Three production lots of high-density UCO kernels supplied all U.S. irradiations. The first U.S. production lot of 350  $\mu$ m-diameter UCO was manufactured at GA. Compacts and loose particles from this batch were irradiated in capsules HRB-14, 15A, 15B, 16, 17, and 18, and R2-KI3. A second production run of 350- $\mu$ m-diameter UCO was made by this same process for capsule HRB-21. The fuel kernels for HRB-21 were coated with the TRISO-P coating (a particle design featuring a sacrificial overcoating of low-density PyC in a fluidized particle bed to increase crush strength and reduce coating failure during matrix injection). A third batch of high-density, 200- $\mu$ m-diameter UCO was made at Babcock and Wilcox (B&W) by the internal gelation process for use in the New Production Modular High-Temperature Gas-Cooled Reactor (NP-MHTGR) capsules. Subsequently, BWXT prepared UCO kernels for the AGR program starting in 2003 and developed coating for AGR-2 and later capsules in 2004 until recently. These coaters were pilot scale six-inch (152 mm) coaters. A more complete description of the fuel particles and the U.S. irradiation experiments is provided in a 2002 report by Petti et al. [15].

#### **3.1.2.2 Irradiation**

The U.S. irradiation program is described in a 2002 report [15]. Important results are presented here on irradiation of UCO fuel in both U.S. and German experiments prior to the AGR program.

Historical performance of UCO fuel in the early U.S. irradiation tests [15] does not meet the irradiation-performance requirements for current prismatic HTGR designs, but for reasons that appear unrelated to the performance of the UCO kernel. Instead, the performance issues appear to result from defective SiC coatings, which were created during coating and/or compacting processes. Examination of UCO particles during the PIE of these capsules did not reveal any evidence of failure that could readily be attributed to the UCO kernels. The irradiations confirmed the UCO kernels retained lanthanide fission products in the kernels and suppressed kernel migration and formation of CO in that no evidence of kernel migration or of attack on the SiC by CO or lanthanide fission products was observed. UO $_2$  particles mixed with UCO particles in the same compact exhibited significant kernel migration, while no kernel migration was observed in the UCO particles.

Capsule HRB-21 and the New Production Reactor (NPR) capsules all contained TRISO-P UCO particles. GA attributed the high-coating failure in these capsules to the poor design of the TRISO-P coating system, that is, rapid shrinkage of low-density outer pyrolytic carbon (OPyC) layer caused by introduction of a seal coat on the conventional OPyC layer, and the properties of the inner pyrolytic carbon (IPyC) layer (high anisotropy), and not to the UCO kernel itself [15,16,17]. HRB-21 LEU UCO was irradiated to 22% FIMA. The three NPR capsules containing 200- $\mu\text{m}$ -diameter HEU UCO fuel particles were irradiated up to approximately 78% FIMA.

By contrast, the German capsule FRJ2-P24 irradiation of UCO under representative prismatic HTGR temperatures and burnup (but very low fast fluence) showed excellent fuel performance with respect to fission-gas retention. TRISO-coated 300- $\mu\text{m}$ -diameter 20% enriched UCO particles formed into annular cylindrical fuel compacts were irradiated in this capsule. The UCO fuel achieved a burnup of up to 22% FIMA at a time-average temperature of about 1120°C with no in-service coating failures observed. No kernel migration or SiC corrosion because of fission product attack was reported by Borchardt et al. [18] and Bauer et al. [19].

In 1977, 5,354 fuel spheres (about 21% of the full AVR core) containing high-density TRISO-coated HEU UCO fuel kernels were inserted into the AVR. This was the first large-scale test of UCO in Germany. The fission-gas release in the AVR, as measured by the release-rate-to-birth-rate ratio ( $R/B^6$ ), remained at a level of  $2-3 \times 10^{-5} R/B^{85\text{mKr}}$  while the UCO fuel spheres were under irradiation (similar to levels prior to UCO insertion). This provided a gross indication there was not extensive UCO particle failure. Given these R/B levels and the presence of the other fuel types in the core, a quantitative determination of the fuel performance was not possible. HEU fuel development was discontinued in Germany due to non-proliferation considerations. In 1982, the German HTGR program selected  $\text{UO}_2$  for its reference fuel; consequently, no significant PIE or post-irradiation accident heating tests were performed on the HEU UCO fuel spheres irradiated in AVR.

Although the success of the German and Japanese fuel development programs (discussed in Appendix B) provides a high-level of confidence that TRISO fuel meeting prismatic HTR fuel performance requirements can be fabricated, this capability had not been demonstrated in the U.S. before DOE-sponsored commercial HTGR development ended in 1995. Consequently, DOE initiated the AGR program in 2002 to develop and qualify TRISO UCO fuel for HTRs to support future U.S. HTGR deployment.

---

<sup>6</sup> R/B is an indicator of initial fuel quality and fuel performance; it is defined as the ratio of the release rate (measured) over the birth rate (calculated) of short-lived fission gases that are released from exposed kernels (as a result of defective or failed coating layers) or dispersed uranium contamination outside of the coating layers. Fractional releases of short-lived fission gases can be expressed as R/B because the radioactive equilibrium is established relatively quickly in the fuel. Section 6.7 provides additional information on R/B ratios.

### 3.1.2.3 Safety Testing

While the German capsule FRJ2-P24 irradiation of UCO at representative prismatic HTGR temperatures and burnups showed excellent fuel performance with respect to retention of gaseous fission products, no post-irradiation simulated-accident heating tests were performed on the fuel from this capsule. In the U.S. program, fuel from irradiation tests HRB-15A and in HRB-15B was subjected to post-irradiation heating along with several other fuel types, including  $\text{UO}_2$  and  $\text{UC}_2$ .

In one test series, 186 initially intact LEU UCO fuel particles from HRB-15A and HRB-15B were heated in temperature ramp and isothermal accident-simulation tests [20]. Krypton-85 release from the fuel was used to indicate total TRISO coating failure. The temperature ramp tests covered the range from  $\sim 1100^\circ\text{C}$  to temperatures as high as approximately  $2700^\circ\text{C}$ , with heating rates in the range of  $\sim 19^\circ\text{C/h}$  to  $\sim 190^\circ\text{C/h}$ . The isothermal heating tests were conducted at  $2050^\circ\text{C}$ ,  $2200^\circ\text{C}$ , and  $2400^\circ\text{C}$ . These temperatures and heating rates were representative of those expected in the large HTGR (LHTGR) designs under consideration at that time and are much higher than anticipated in HTR designs under consideration today. The test series also involved heating of other TRISO fuel types:

- HEU, LEU, and depleted  $\text{UC}_2$
- $\text{ThO}_2$
- $(\text{Th,U})\text{O}_2$
- LEU  $\text{UO}_2$  and " $\text{UO}_2^*$ "<sup>7</sup>
- $\text{ThC}_2$  and  $(\text{Th,U})\text{C}_2$

Figure 3-2 (reproduced from reference 20) summarizes the results of thirty-hour ramp heating tests for the various LEU fuels and HEU  $\text{UC}_2$ . The primary mechanism for TRISO-coating failure and  $^{85\text{m}}\text{Kr}$  release under the simulated LHTGR accident conditions was found to be thermal decomposition of the SiC layer, followed by either diffusion of fission products through the PyC layers or breakage of the PyC. Within the temperature range tested, fuel-particle performance was found to depend on the inherent thermal stability of the SiC coating layer and not to be dependent upon variations in burnup, fast neutron fluence, or kernel composition.

---

<sup>7</sup>  $\text{UO}_2^*$  has a ZrC layer over the  $\text{UO}_2$  kernel.

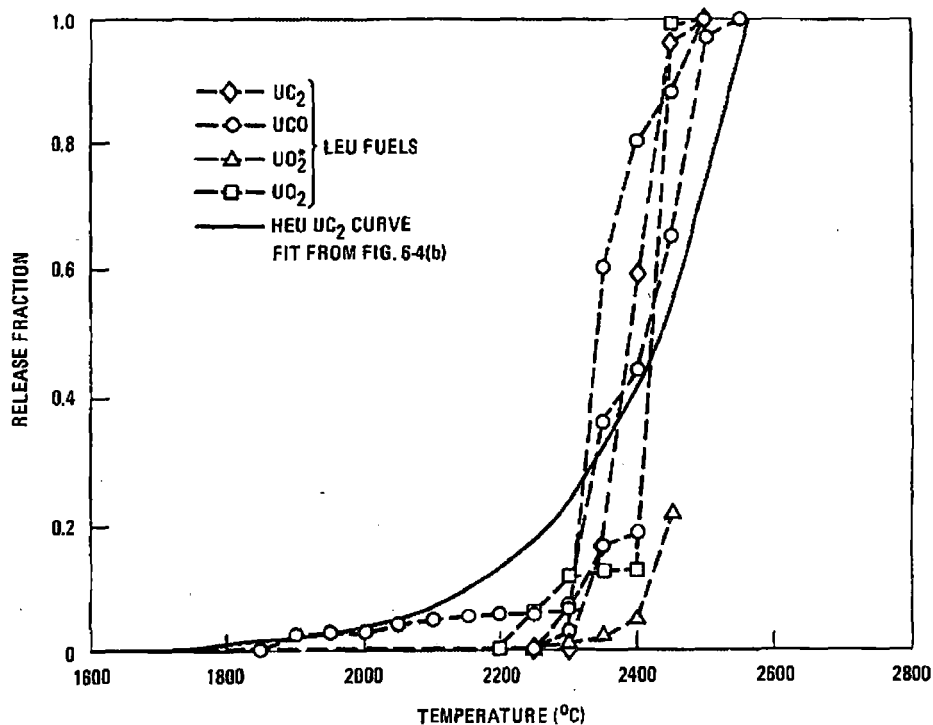


**Figure 3-2**

<sup>85m</sup>Kr release results for ramp heating tests of candidate HTGR fuel types [20].

*Courtesy of General Atomics; used with permission. All rights reserved.*

Given the different chemical compositions of the fuel types, the similarity of the release profiles in Figure 3-2 indicates that performance of the fuel particles for the LHTGR accident conditions simulated in this heating-test series is independent of kernel composition and depends only on the TRISO coating. It is worth noting the temperatures associated with the LHTGR accident conditions are much higher than the temperatures during loss-of-forced-cooling accidents in the HTR designs being considered today.

In another heating-test series, 30 initially intact LEU UCO fuel particles irradiated in HRB-15B were heated isothermally for 10,000 hours at temperatures of 1200, 1350, or 1500°C (10 particles at each temperature) [19]. LEU UO<sub>2</sub>, UC<sub>2</sub>, and two variations of UO<sub>2</sub>\*<sup>8</sup> were also tested under the same conditions. With respect to the relative heating test performance of the UCO and UO<sub>2</sub> particles, the following differences were observed:

- At 1500°C, <sup>154</sup>Eu release started much earlier in the UCO fuel particles than the UO<sub>2</sub> particles, and the total <sup>154</sup>Eu release from the UCO particles (~50%) was considerably higher than from the UO<sub>2</sub> particles (~15%). The UCO particles also released <sup>154</sup>Eu at both 1200°C and 1350°C, but the amount released decreased significantly with decreasing temperature.<sup>9</sup>

<sup>8</sup> One version of UO<sub>2</sub>\* had a ZrC-coated UO<sub>2</sub> kernel encapsulated by a standard TRISO coating. The ZrC coating layer on the kernel had a thickness of about 10 microns. The other version of UO<sub>2</sub>\* used standard TRISO-coated UO<sub>2</sub> particles, except that ZrC was distributed within the buffer coating layer.

<sup>9</sup> Eu is significantly retained by the graphite fuel blocks, so the increased release of Eu isotopes from UCO fuel particles relative to UO<sub>2</sub> fuel particles is not a significant issue for UCO fuel used in a prismatic HTGR.

The  $\text{UO}_2$  particles did not release  $^{154}\text{Eu}$  at  $1200^\circ\text{C}$  or  $1350^\circ\text{C}$ . (Similar results have been observed in AGR-1 and AGR-2 tests as discussed in Section 7.1.2.).

- At  $1500^\circ\text{C}$ ,  $^{110\text{m}}\text{Ag}$  release started much earlier in the  $\text{UO}_2$  particles than the UCO particles, and the total  $^{110\text{m}}\text{Ag}$  release from the  $\text{UO}_2$  particles (~90%) was considerably higher than from the UCO particles (<10%).
- $^{137}\text{Cs}$  was released only at  $1500^\circ\text{C}$  and only from three of the 150 particles tested. Two of these were  $\text{UO}_2$  particles. Diffusion through flawed, but intact, SiC layers was apparently responsible for the steadily increasing release from the two  $\text{UO}_2$  particles. None of the UCO particles released  $^{137}\text{Cs}$  at any temperature.

Although the above results indicate some differences in the accident-condition performance of UCO and  $\text{UO}_2$  fuel particles, it is important to note there were substantial differences in the SiC coatings on these two types of particles, which likely influenced fission product retention. The SiC layer on the UCO particles is characterized as having a laminar microstructure and a density of only  $3.16 \text{ Mg/m}^3$ ; the SiC layer on the  $\text{UO}_2$  particles is characterized as having a columnar microstructure and a density of  $3.21 \text{ Mg/m}^3$  [21].

In an additional heating test of U.S. UCO fuel, fuel-compact-containing carbonaceous matrix body sections from irradiation test R2-K13 were heated in Germany [22]. These samples were heated to  $2500^\circ\text{C}$ , resulting in total failure of the SiC.

# 4

## FISSION PRODUCT RETENTION, PARTICLE DESIGN, AND PERFORMANCE BASES

---

### 4.1 Fission Product Retention

High-temperature reactors possess design features that result in multiple barriers working together to attenuate the release of radionuclides. This concept is called “functional containment”<sup>10</sup> and encompasses a collection of design selections that, when taken together, ensure: (1) radionuclides are retained within multiple barriers arrayed in series, (with emphasis on retention at their source in the fuel); and (2) regulatory requirements and plant design goals for release of radionuclides are met (typically at the exclusion area boundary). The first three functional containment barriers consist of the fuel kernel, the fuel particle coatings, and the fuel matrix/material. For HTGRs, the fourth barrier is the helium pressure boundary. In the case of a fluoride salt-cooled high-temperature reactor (FHR), the salt coolant also acts as a barrier due to its ability to retain radionuclides. The reactor building serves as the final barrier.

Operational and design features of HTRs also play an important role in the functional containment concept of retaining radionuclides during normal and accident scenarios. The degree to which individual functional barriers are relied upon during a particular accident sequence is a design choice that considers tradeoffs between the required effectiveness of different barriers in a specific design approach [23]. Collectively these barriers operate to reduce fission product releases to very low levels during normal operations and under design basis events, including postulated accidents [24].

Successfully implementing a safety strategy based on functional containment will require:

- TRISO fuel that can be fabricated and characterized in a repeatable and consistent manner
- Fuel performance with very low in-service failures
- A mechanistic source term that can be calculated to the requisite level of accuracy for both normal and off-normal conditions

Historically, HTGR designers established fuel performance requirements that ensured offsite (plant boundary) dose limits would not be exceeded. Table 4-1 lists representative levels of allowable fuel defects and the allowable levels of in-service failures under normal operation and postulated core heatup accidents at 95% confidence. This information is based on the legacy MHTGR prismatic design and the 200 MWth High Temperature Gas-Cooled Reactor (HTR-MODUL) pebble-bed. These values are very similar despite differences in the design

---

<sup>10</sup> Functional containment, as defined by NRC Regulatory Guide 1.232: “a barrier, or set of barriers taken together, that effectively limit the physical transport and release of radionuclides to the environment across a full range of normal operating conditions, AOOs, and accident conditions” (see MHTGR-DC 16, *Containment Design*).



service conditions of the fuel (for example, burnup, fast fluence, temperature). While the actual values used in a particular HTGR or FHR design are at the discretion of the designer, the values presented here can be used as a metric when comparing the performance of UCO TRISO-coated particles against those fabricated and tested under the AGR program.

**Table 4-1**  
**Representative fuel defect levels and in-service failures for historic HTGR designs**

	Modular HTGR Prismatic	HTR-MODUL Pebble
<b>Manufacturing Defect Level</b>		
Heavy Metal Contamination	$2 \times 10^{-5}$	$6 \times 10^{-5}$
SiC Defects	$1 \times 10^{-4}$	
<b>In-Service Performance Requirements</b>		
Incremental Failures Normal Operation	$2 \times 10^{-4}$	$1.6 \times 10^{-4}$
Incremental Failures Core Heatup Accidents	$6 \times 10^{-4}$	$6.6 \times 10^{-4}$

## 4.2 Particle Design

The broad coated-particle fuel fabrication, irradiation, and testing experience discussed in Section 3.1 and Appendix B, combined with effective international information exchanges, has resulted in a consensus on basic coated-particle properties among ongoing fuel-development programs, as illustrated in Figure 4-1 and discussed below. The TRISO-coated particle is a spherical, layered composite. For the AGR program, it consists of a kernel of UCO surrounded by a porous carbon buffer layer that accommodates fission recoils preventing direct damage to the other coating layers and allows space for fission gases to accumulate. Surrounding the buffer layer is an IPyC layer, a SiC layer, and an OPyC layer. Historically, a broad range of TRISO particles have been fabricated and tested around the world, including: UO<sub>2</sub>, (U,Th)O<sub>2</sub>, UC<sub>2</sub>, (U,Th)C, PuO<sub>2</sub> and UCO (see Appendix B for more detail). Some of the designs also incorporated fertile particles, that is, ThO<sub>2</sub> or ThC<sub>2</sub> and natural or depleted UO<sub>2</sub>, as a part of a fissile-fertile fuel system.

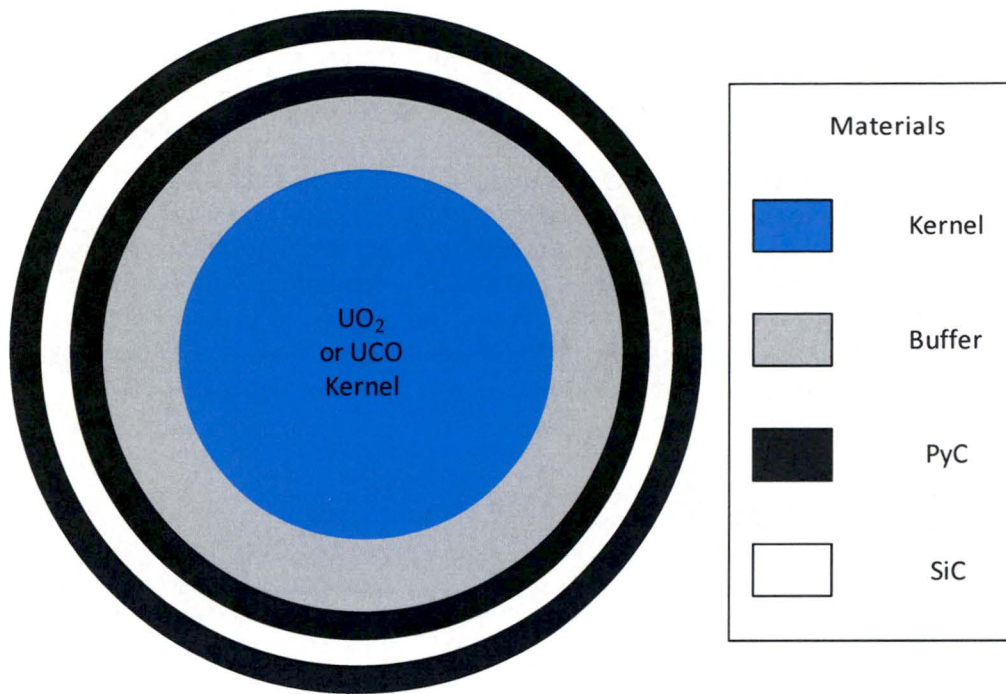


**Figure 4-1**  
**The international-consensus TRISO particle design**

*Courtesy of Idaho National Laboratory and used with permission of Battelle Energy Alliance, LLC*

The coating layers of the TRISO fuel particles work synergistically to inhibit the release and migration of fission products from the fuel particle. The TRISO particles are embedded inside a carbonaceous matrix that provides a rigid structure, improves heat transfer and temperature uniformity, and retards migration of fission products that are not retained within the TRISO particles. This coated-particle design mitigates or eliminates the failure mechanisms discussed in Section 4.3 and incorporates the elements listed below. The mean coating thicknesses are sufficient to perform the required functions with allowance for the particle-to-particle variation in thickness resulting from the coating process.

#### 4.2.1 Fuel Kernel

The spherical fuel kernel consists of high-assay, low-enriched (<20% <sup>235</sup>U) UO<sub>2</sub> or UCO. The kernel serves as an important barrier to radionuclide release by immobilizing many of the fission products and delaying the diffusive release of others, substantially reducing release from the particle by retention in the kernel and radioactive decay before release from the kernel.

UO<sub>2</sub> kernels perform effectively within the range of burnup and temperature gradients experienced in the German pebble-bed designs. Although some UO<sub>2</sub> kernels were fabricated as part of the AGR-2 campaign, the AGR program has focused efforts on characterizing and demonstrating the performance of UCO kernels. UCO kernels effectively limit the oxygen activity in the fuel, limiting the generation of CO and CO<sub>2</sub> and the associated kernel migration

and increased gas pressure in the particle. This allows higher burnup limits and thermal gradients associated with prismatic designs. The optimal kernel diameter is a function of enrichment and the related design burnup limits, with higher enrichment and burnup designs typically having smaller diameters.

The thermochemical basis for limited CO formation in UCO kernels is the oxidation of uranium carbide ( $UC_x$ ) phases in response to the increasing oxygen potential in the  $UO_{2+x}$  phase as irradiation proceeds [25,26]. Past experimental measurements of CO formation in  $UO_2 + UC_x$  kernels indicate a drastic reduction compared to  $UO_2$  [27]. In addition, both the historic UCO fuel irradiation testing database and the current AGR program results demonstrate the lower CO production based on the absence of any phenomena that are driven by CO pressure in the particles (for example, kernel migration or CO corrosion of the SiC layer).

#### **4.2.2 Buffer Layer**

The low-density (~50% of theoretical), porous PyC buffer coating layer protects the outer three layers by absorbing the kinetic energy of fission fragments ejected from the fuel kernel surface and providing space for the accumulation of gaseous fission products and carbon monoxide (in the case of  $UO_2$  kernels). As a compressible material, it serves to mechanically decouple the kernel from the inner pyrocarbon layer to accommodate kernel swelling, thereby reducing the buildup of stress in the outer coating layers during irradiation. The buffer layer shrinks under irradiation as the kernel swells. The buffer layer is not considered a retentive layer for fission products, but fission gases and carbon monoxide do collect within the buffer pores. The buffer thickness is typically 90 to 100  $\mu\text{m}$ .

#### **4.2.3 Inner Pyrolytic Carbon Layer**

The inner high-density (~85% of theoretical) isotropic layer of IPyC forms the second coating layer and the first load-bearing barrier against the pressure exerted by gaseous fission products and reaction products ( $CO$ ,  $CO_2$ ) within the fuel kernel and buffer layer. The IPyC layer also serves to protect the kernel from corrosive gases ( $HCl$ ,  $Cl_2$ ) liberated during the SiC coating process. Both the IPyC and OPyC layers retain gaseous fission products but become less effective in retaining metallic fission products at higher temperatures. The SiC occupies the surface-connected pores of the IPyC during deposition, thereby interlocking the two layers and providing extra mechanical support at the IPyC/SiC interface. The anisotropy of the IPyC layer is limited to control dimensional changes during irradiation where the IPyC and OPyC layers shrink at first, but may expand again if sufficiently high fast neutron dose levels are reached. Shrinkage of the IPyC layer during irradiation imparts a compressive load on the SiC layer. This reduces the maximum tensile hoop stress within the SiC, reducing the probability of in-pile particle failures. The IPyC thickness is typically 35 to 40  $\mu\text{m}$ .

#### **4.2.4 Silicon Carbide Layer**

The SiC layer functions as the structural “skeleton” of the TRISO particle and is the third and the most important coating layer for fission product retention. Since the pyrocarbon layers become less effective in retaining metallic fission products at higher temperatures, the SiC layer acts as the principal barrier to the release of these elements from the coated particle. A high-density SiC with a non-columnar grain structure is considered the most effective for fission product retention.

The SiC layer also has sufficient strength to withstand internal pressure produced during irradiation. The coated particle structure and dimensional stability of the SiC layer under irradiation, combined with the irradiation-induced shrinkage of the IPyC and OPyC, results in the SiC layer being kept under compression during irradiation. This provides a high level of assurance the SiC layer will remain intact. The SiC thickness is typically ~35  $\mu\text{m}$ .

#### 4.2.5 Outer Pyrolytic Carbon Layer

The OPyC coating layer is the final diffusion barrier for fission products and provides mechanical protection for the SiC layer during particle handling and during fuel form compaction operations. Irradiation-induced shrinkage of the OPyC leads to compression of the SiC layer because of its net shrinkage under fast-neutron irradiation during the fuel lifetime in the reactor core. This reduces the tensile stress in that layer. The OPyC serves as a redundant barrier to gaseous fission-product release. The anisotropy of the OPyC layer is limited to control dimensional changes during irradiation. The OPyC thickness is typically 35 to 40  $\mu\text{m}$ .

#### 4.2.6 Coated Particle

When the AGR program began, since a firm HTGR design had not yet been developed, the program decided to adopt the LEU fissile particle of the MHTGR and Gas Turbine Modular Helium Reactor (GT-MHR) designs as the reference fuel form for AGR-1: a 350- $\mu\text{m}$  19.7%-enriched UCO kernel. As design activities began under NGNP, evaluations were conducted to determine whether a single particle design instead of the fissile-fertile system could be used in the HTGR. While a complete assessment would have required significantly more design development, the initial study showed promise and thus a single particle was adopted for AGR-2: a 425- $\mu\text{m}$  14.0%-enriched UCO kernel.

In terms of fuel particle design, a relationship exists among the actual values of the kernel size, buffer volume, and the maximum burnup to achieve consistent fuel performance. The physical size of the particle components is up to the designer and the achievable burnup depends on the particle enrichment and core design. One such metric of fuel performance is the tensile stress in the SiC layer, which depends on the pressure of fission gas in the buffer. Assuming 100% fission gas release and the maximum burnup, the stress in the SiC layer is proportional to the following attributes:

$$\sigma \propto \frac{B \cdot V_k}{V_b} * \frac{r_{SiC}}{t_{SiC}} \quad \text{Equation 4-1}$$

where:

$\sigma$	=	Tensile stress
B	=	Maximum burnup
$V_k$	=	Volume of kernel
$V_b$	=	Volume of buffer
$r_{SiC}$	=	Radius of SiC layer
$t_{SiC}$	=	Thickness of SiC layer

Table 4-2 shows these physical attributes for a variety of particles that have been proposed or used in HTGRs. This includes previous U.S. LEU fissile/fertile dual particles designs, an HEU kernel for the DOE NPR project, the historical German TRISO particle, and the Japan Atomic Energy Research Institute (JAERI) TRISO particle used in their HTTR and the value proposed for their advanced commercial design. Normalizing all the tensile stress metrics to the historic German value shows the metrics are within 20% of the German value indicating the tensile stress component should be similar in all these particle designs. (This small deviation is because of rounding the physical size of the kernel and buffer for ease of fabrication.) It should be noted this analysis does not credit the very important role irradiation-induced PyC shrinkage plays in developing a strong compressive component to the stress in the SiC layer.

The values of thicknesses of the PyC and SiC layers are based on the successful German program and are used by the Chinese as well. The Japanese use slightly different dimensions. The AGR program adopted the German coating thicknesses for its fuel development.

**Table 4-2**  
**Particle design attributes contributing to tensile stress in SiC**

Parameter	German	JAERI HTTR	JAERI Advanced	U.S. LEU Fissile	U.S. Fertile	U.S. NPR	AGR
	<b>Particle Design Parameters</b>						
Kernel Composition	UO <sub>2</sub>	UO <sub>2</sub>	UO <sub>2</sub>	UCO	UCO	UCO	UCO
Kernel Diameter (μm)	500	600	550	350	500	200	425
Buffer Thickness (μm)	95	60	100	100	65	100	100
IPyC Thickness (μm)	40	30	35	35	40	50	40
SiC Thickness (μm)	35	30	35	35	35	35	35
OPyC Thickness (μm)	40	45	40	40	40	40	40
Enrichment (%)	10.6	6	10	19.9	0.7	93	14.0
Burnup (% FIMA)	10	3.6	10	26	6	80	17
	<b>Calculated Values</b>						
Particle Diameter (μm)	920	930	970	770	860	650	855
Kernel volume (mm <sup>3</sup> )	0.065	0.113	0.087	0.022	0.065	0.004	0.040
Buffer volume (mm <sup>3</sup> )	0.107	0.082	0.134	0.065	0.065	0.029	0.088
Simple tensile stress metric	0.676	0.643	0.763	0.799	0.608	0.816	0.785
Normalized to German value	1.00	0.95	1.13	1.18	0.90	1.21	1.16

To understand the behavior of the coating layers as a coating system requires more detailed modeling. The basic behavior of the three coating layers of the TRISO-coated particle is shown in Figure 4-2. Fission gas pressure builds up in the kernel and buffer regions, while the IPyC, SiC, and OPyC act to retain this pressure. The IPyC and OPyC layers both shrink and creep during irradiation of the particle while the SiC exhibits only elastic response. A portion of the gas pressure is transmitted through the IPyC layer to the SiC. This pressure increases as irradiation of the particle progresses, thereby contributing to a tensile hoop stress in the SiC layer. Countering the effect of the pressure load is the shrinkage of the IPyC and OPyC layers during irradiation, which causes them to push or pull inward on the SiC. Due to anisotropy in the PyC shrinkage behavior, the shrinkage histories differ in the radial and tangential directions. The shrinkage in the radial direction reverses to swelling at moderate fluence levels, whereas shrinkage in the tangential direction continues to high fluence levels.

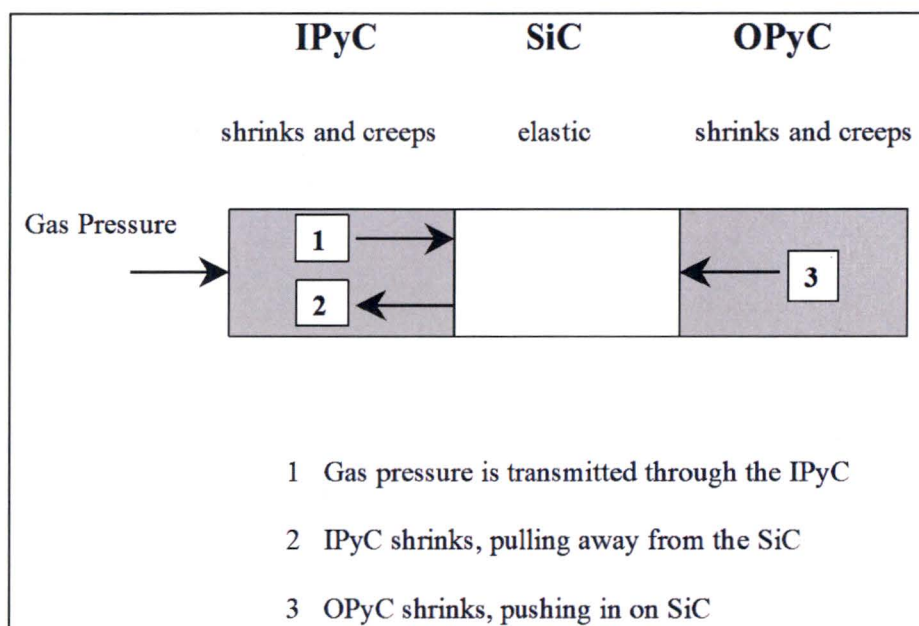


**Figure 4-2**  
**Behavior of coating layers in a fuel particle**

*Courtesy of Idaho National Laboratory and used with permission of Battelle Energy Alliance, LLC*

In the stress analyses of most models, an internal pressure is applied to the IPyC to simulate the fission gas build-up. The shrinkage strain rates and creep coefficients for the PyC and the elastic properties for the PyC and the SiC are based from data compiled in a report by GA in 1993 [28]. As such, the shrinkage strains are treated as functions of four variables: fluence level, pyrocarbon density, degree of anisotropy as measured by the Bacon Anisotropy Factor (BAF), and irradiation temperature. Irradiation-induced creep is treated as secondary creep, with a coefficient that is a function of PyC density and irradiation temperature. The creep coefficients used in the analyses described herein were set equal to twice the values recommended in the GA data. This is closer to what is used in older performance models [29-31] and has resulted

in predictions that are in better agreement with results from irradiation experiments of the NPR – MHTGR Program [32]. The elastic modulus for the PyC layers is applied as a function of four variables (the same variables as used for shrinkage), while the elastic modulus for the SiC is applied as a function of temperature only.

Figure 4-3 plots a time evolution for the tangential stress at the inner surface of the SiC layer for a normal spherical particle which is irradiated to a fluence level of  $3.0 \times 10^{25}$  n/m<sup>2</sup>. Early during irradiation, the shrinkage of the PyC layers induces an increasing compressive stress in the SiC. Eventually, creep in the PyC layers relieves stress in those layers, diminishing the beneficial effect of the shrinkage. Therefore, the tangential stress in the SiC reaches a minimum value, and then steadily increases through the remainder of irradiation. A pressure vessel failure is expected to occur if the tangential stress reaches a tensile value that exceeds the strength of the SiC for that particle.

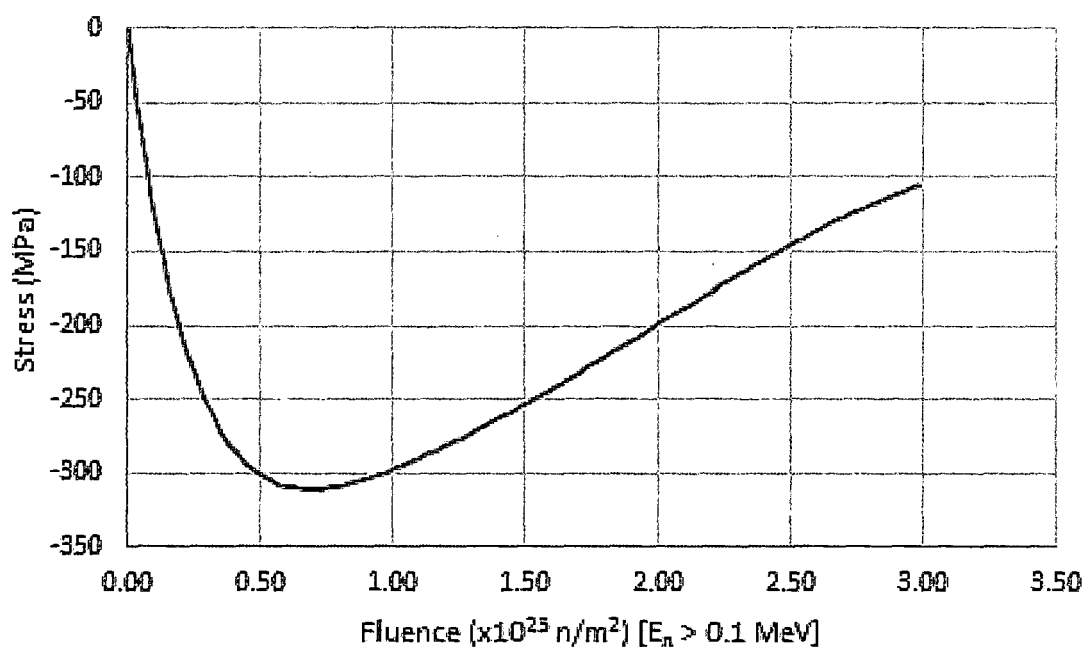


**Figure 4-3**  
**Tangential SiC stress history for a normal particle**

*Courtesy of Idaho National Laboratory and used with permission of Battelle Energy Alliance, LLC*

Sensitivity studies have been conducted using a thermomechanical fuel performance model to understand other potential failure modes of the particles (for example, cracking of the IPyC layer, excessive asphericity [33], thinning of the SiC layer [34]). In addition, the model has been used to study the impact of fuel particle attributes on the calculated stresses in the particles. Many of the coating properties measured during the AGR program evolved from those developed by GA based on their historical experience at FSV, modified as necessary to assure the high-level radionuclide release criteria could be met for their HTGR designs. During the

AGR program, more systematic calculations have been performed to determine which of the measured fuel attributes are the most critical from a fuel performance perspective and what are the appropriate critical limits for those attributes to be used in a specification. Results of the PARFUME analysis [35] indicate:

- Many of the fuel attributes have minimal impact on the thermomechanical performance of TRISO-coated UCO particles. The nominal thicknesses and densities of the German coatings are adequate for high-temperature reactor applications, and in many cases, there is performance margin. However, given the large experimental basis for these coatings, the models were not used to optimize/change layer thicknesses or densities from the German values.
- Minimal change was observed in the overall TRISO-coated particle failure probability as the PyC density (both IPyC and OPyC) and anisotropy were varied over the typical range of values. This is probably due to the uncertainties in the material properties, especially irradiation-induced creep.
- When varying the thickness of the SiC layer, the failure probability increased as the thickness decreased because there is less structural material to retain the fission gas pressure and subsequent increase in tangential stress in the layer. Thus, a critical limit<sup>11</sup> on the minimum thickness of SiC is warranted.
- Conversely, failure probability increased as the IPyC layer thickness increased because thicker PyC experience higher stress levels early in irradiation. This results in a higher IPyC cracking probability causing localized stress concentrations in the SiC layer. Thus, a critical limit on the maximum IPyC thickness is warranted.
- As the buffer thickness decreases, the volume available to store fission gas decreases resulting in a higher pressure and higher stress in the SiC layer. Thus, a critical limit on the minimum buffer thickness is warranted.
- For aspherical particles, as characterized by the aspect ratio (that is, largest diameter divided by smallest diameter on a particle), the model used in the analysis treats asphericity essentially as a flat plate on one side of the particle. Increasing the aspect ratio increases the surface area of the flat plate increasing the stress in the SiC layer due to pressure accumulation. Thus, a critical limit on aspect ratio is warranted.

These critical limits have been incorporated into the AGR fuel specification.

### **4.3 Failure Mechanisms**

The following failure mechanisms have been identified as capable of causing partial or total failure of the TRISO-coating system under irradiation and/or during postulated accidents:

- Pressure vessel failure of standard (“intact”) particles (particles without manufacturing defects)
- Pressure vessel failure of particles with defective or missing coatings
- Irradiation-induced failure of the OPyC coating

---

<sup>11</sup> A critical limit specifies that less than 1% of the population can have values above (upper critical limit) or below (lower critical limit) that limit at 95% confidence depending on the attribute in question.



- Irradiation-induced failure of the IPyC coating and potential SiC cracking
- Failure of the SiC coating caused by kernel migration in the presence of a temperature gradient
- Failure of the SiC coating caused by fission-product/SiC interactions
- Failure of the SiC coating caused by CO/SiC interactions
- Failure of the SiC coating resulting from thermal decomposition
- Failure of the SiC coating caused by heavy metal (HM) dispersion in the buffer and IPyC coating layers

These mechanisms are shown schematically in Figure 4-4. Phenomenological performance models, typically inspired by first principles and correlated with experimental data, have been developed to model each of these mechanisms [36,37].

As-manufactured HM contamination is not an in-service failure mechanism, but is very important with respect to fission product release. It is an extreme case of as-manufactured coating defects, whereby trace amounts of HM are not encapsulated by a single intact coating layer (analogous to “tramp uranium” in LWR fuel). Modern fuel product specifications allow only very small fractions of HM contamination ( $\sim 10^{-5}$  is typical). Nevertheless, when exposed kernel defects and in-service failure fractions are low, HM contamination can become a dominant source of fission product release.

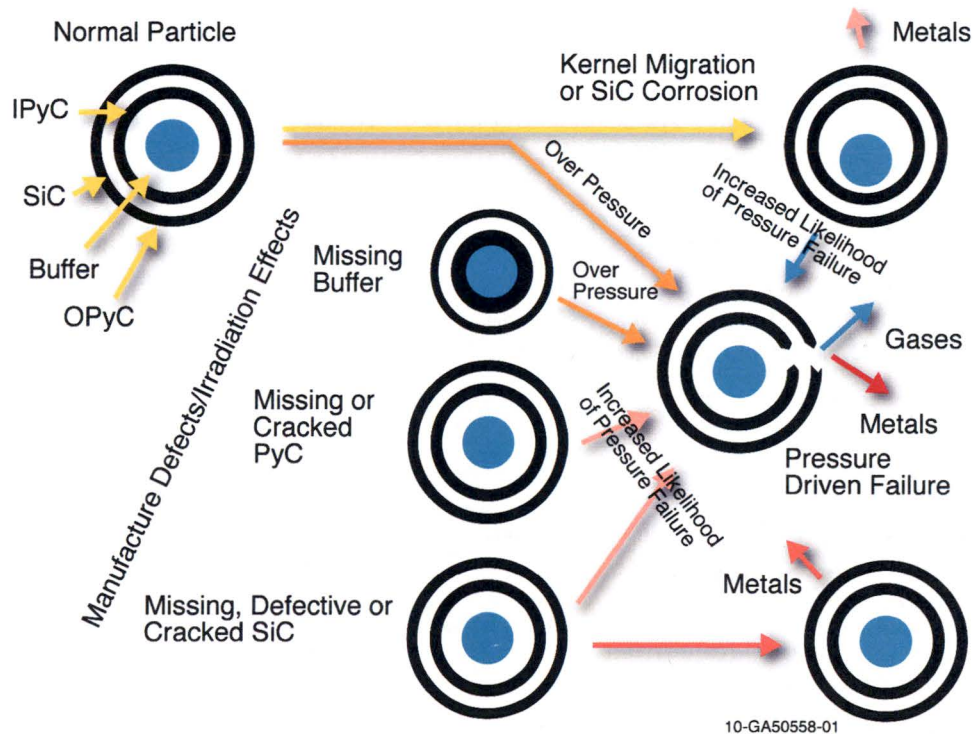


**Figure 4-4**  
**TRISO particle failure mechanisms**

*Courtesy of Idaho National Laboratory and used with permission of Battelle Energy Alliance, LLC*

The observed failure mechanisms for TRISO fuel can be categorized as structural/mechanical or thermochemical in nature. Failure mechanisms in both categories can be affected by the release of excess oxygen during fission and subsequent formation of carbon monoxide. The various failure mechanisms are discussed in greater detail in the following sections.

#### 4.3.1 Structural/Mechanical Mechanisms

During irradiation, long-lived and stable fission gases are released from the kernel into the buffer, which increases the internal gas pressure. For some particle designs (for example, UO<sub>2</sub> TRISO), carbon monoxide can also be generated during irradiation, which further increases the gas pressure. Because the SiC layer has a much higher elastic modulus than the PyC layers,<sup>12</sup> it would bear most of the internal pressure force, which produces a tensile stress if the irradiation-induced dimensional changes of the PyC and SiC were comparable. However, the PyC layers shrink during irradiation, subjecting the SiC layer to compression. Within the range of allowed fuel service conditions (for example, temperature and fast neutron fluence), the compressive forces from PyC shrinkage more than compensate for the tensile stresses from internal pressure, such that the SiC remains in compression provided at least one of the PyC layers remains intact. From a structural/mechanical perspective, the SiC layer will remain intact, provided it remains in compression or the tensile stress in the SiC layer does not exceed its strength.

##### 4.3.1.1 PyC Performance

As discussed above, shrinkage of the PyC layers during irradiation is a favorable attribute, as the resulting compressive forces acting upon the SiC layer counteract the tension arising from fission gas pressure. PyC shrinkage produces tensile stresses in the PyC layers themselves, which can lead to failure of these layers. The strains and stresses generated in the PyC layers are complex functions of fast neutron fluence, irradiation temperature, and coating-material properties.

A property to which PyC performance is quite sensitive is *anisotropy*, which can be quantified using x-ray or optical diffraction techniques. Anisotropy is usually expressed in terms of the BAF. For a perfectly isotropic material, BAF = 1, and for a perfectly oriented medium, BAF = ∞. Sufficiently isotropic PyC layers (BAF ≤ 1.035) are able to perform well out to high fast neutron fluences because the irradiation-induced strains and stresses are relaxed to some extent by irradiation-induced creep.

##### 4.3.1.2 Irradiation Induced Failure of IPyC Leading to SiC Cracking

PIE of fuel from the HRB-21 irradiation and the NP-MHTGR irradiations coupled with mechanical analyses showed fuel particle failures in these irradiation experiments were caused by irradiation-induced failure (cracking) of anisotropic IPyC. This leads to increased tension in the adjacent SiC layer to which it is bonded, increasing the probability of cracking the SiC layer [16,17]. These failure analyses led to changes in the coating conditions used in the fabrication of fuel particles in the AGR program [38] to ensure IPyC coatings with sufficient isotropy were produced.

<sup>12</sup> In other words, SiC is much stiffer than PyC. Because of this property, it is reasonable to assume the IPyC and OPyC are isolated from each other when evaluating performance of these layers and overall performance of the TRISO-coating system.

#### 4.3.1.3 Pressure Vessel Failure

In the absence of compressive forces from the PyC layers, the tensile stress,  $\sigma_{SiC}$ , in the SiC layer may be calculated with reasonable accuracy using the thin-shell approximation:

$$\sigma_{SiC} = \frac{Pr_{SiC}}{2t_{SiC}} \quad \text{Equation 4-2}$$

where

- P = Internal pressure inside the particle
- $r_{SiC}$  = Radius to the middle of the SiC layer
- $t_{SiC}$  = Thickness of the SiC layer

Pressure vessel failure occurs when the tensile stress in the SiC layer exceeds the strength of the SiC layer. The fraction of particles with a failed SiC coating,<sup>13</sup>  $f_{SiC}$ , is calculated using Weibull statistical strength theory, assuming volume flaws and a uniform stress distribution in the SiC layer, as:

$$f_{SiC} = 1 - \exp \left[ - \left( \frac{\sigma_{SiC}}{\sigma_o} \right)^m V_{SiC} \right] \quad \text{Equation 4-3}$$

Where:

- $\sigma_o$  = Weibull characteristic strength
- m = Weibull modulus
- $V_{SiC}$  = Volume of the SiC layer.

### 4.3.2 Thermochemical Mechanisms

Fuel failure caused by thermochemical mechanisms can be limited in large measure through the nuclear and thermal-hydraulic design of the reactor core. For the fuel to satisfy performance criteria, peak fuel temperatures must be kept sufficiently low, and the fraction of fuel that experiences relatively high temperatures for long periods of time must be kept sufficiently small. Thermochemical failure mechanisms that have been observed to occur in coated-particle fuel are described below.

#### 4.3.2.1 Kernel Migration

Local fuel temperatures and temperature gradients across the fuel can be relatively high when the reactor is producing power. Under these conditions, oxide and carbide fuel kernels can migrate up the thermal gradient. This phenomenon is often referred to as the "amoeba effect" and can lead to complete failure of the coating system. For oxide kernels, migration may be caused by carbon diffusion or gas-phase diffusion of CO or other gaseous carbon compounds [39]. Failure by this mechanism is correlated as a function of temperature, thermal gradient, and thicknesses of the buffer and IPyC layers. Failure is assumed to occur when the kernel material contacts the

---

<sup>13</sup> This fraction applies to the population of particles that have a failed IPyC layer and a failed OPyC layer.

SiC layer. The particle-to-particle variations in the buffer and IPyC thicknesses (expressed as normal distributions with measured variances) are accounted for when calculating the failure probability. In UCO kernels, this failure mechanism is not observed because CO or other gaseous carbon compounds are greatly reduced.

#### 4.3.2.2 Chemical Attack of SiC

Noble metals (for example, Ru, Rh, Pd, and Ag) are produced during fission of uranium, in some cases with relatively high yield. During irradiation, the thermochemical conditions are not conducive to the formation of stable oxides of these elements. They readily migrate out of the fuel kernel, regardless of its composition. Reactions of SiC with Pd have been observed during PIE of TRISO fuel [40]. Although the quantity of Pd is small compared with the mass of the SiC layer, the reaction is highly localized, and complete penetration of the SiC layer can occur if high temperatures are maintained for a sufficient period of time (see Figure 4-5). The reaction rate is highly dependent on temperature. The time required to penetrate the SiC layer decreases rapidly as the temperature increases above about 1300°C.

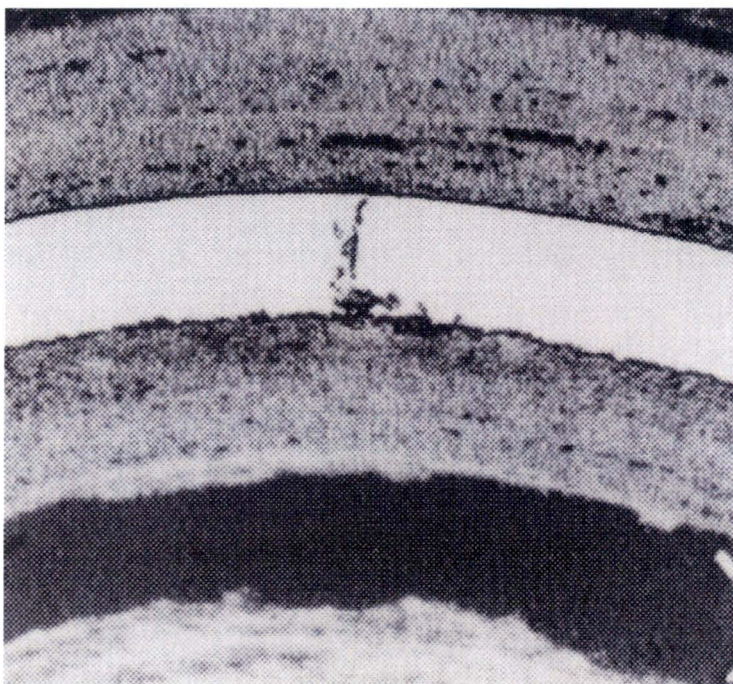


**Figure 4-5**  
**Localized fission-product attack of the SiC layer in an irradiated UCO particle from the HRB-16 experiment**  
*Courtesy of Idaho National Laboratory and used with permission of Battelle Energy Alliance, LLC*

Excess oxygen is produced in a  $\text{UO}_2$  kernel during irradiation because the oxygen liberated by fission is not completely consumed by reactions with fission products. At low burnup, some of the excess oxygen may remain trapped in the kernel. At high burnup the kernel becomes more porous, and it is likely nearly all of the oxygen will escape a  $\text{UO}_2$  kernel, after which it will quickly react with carbon in the buffer to predominately form CO. Excessive CO not only increases the pressure vessel and kernel migration failure probabilities, but can also corrode the SiC layer at accident-condition temperatures.

Chemical attack of the SiC layer by CO has been observed in  $\text{UO}_2$  particles irradiated at temperatures above approximately  $1400^\circ\text{C}$  [41]. Degradation occurred near locations where the IPyC layer was cracked. The kernels of particles with degraded SiC layers were examined with an electron microprobe, which showed the presence of silicon in the form of fission product silicides. Thermo-chemical calculations supported the hypothesis that silicon is transported to the kernel in the form of SiO gas produced by the reaction of CO with SiC. The SiO subsequently reacts with fission products.

#### 4.3.2.3 Thermal Decomposition of the SiC Layer

At very high temperatures, SiC will decompose into its constituent elements. The silicon vaporizes, leaving a porous carbon structure. Based on calculations performed for previous core designs, this failure mechanism is not an important contributor to fuel failure at normal operating or postulated accident conditions. However, thermal decomposition of SiC occurs rapidly at temperatures above  $2000^\circ\text{C}$ .

#### 4.3.2.4 Relationship between Fuel-Failure Mechanisms and Fuel-Particle Properties

The fuel service conditions and parameters that influence the fuel failure mechanisms are summarized in Table 4-3. The fuel particles must be designed and manufactured such that the properties defined in Section 5.3 are within limits that result in acceptable fuel performance (for example, fission product retention). The failure mechanisms are correlated with the reactor service conditions in models that are used to predict fuel performance. In addition, sensitivity studies have been conducted to assess the relative impact of various properties on calculated failure fractions, and results are summarized in Section 4.2.

### 4.4 Performance Bases

At the start of the AGR program, without a reactor design concept selected, the program decided to qualify fuel to an operating envelope that would bound potential options across a range of high-temperature reactor conceptual designs. Figure 4-6 is a radar plot of the five most important parameters for qualifying fuel performance. The parameters are listed below along with an explanation of their importance in influencing fuel performance:

- **Fuel temperature.** Many of the potential failure mechanisms and fission product transport mechanisms are dependent on both time at temperature during power operation and time at temperature under postulated accident condition.
- **Fuel burnup.** Determines the quantity of fission products in the kernel and thus the gas pressure and fission product concentration in the particles that can interact with the coating layers.

- **Fuel fast fluence.** Determines the level of radiation damage in the particles and the potential changes in properties and dimensions in the layers.
- **Power density.** Together with the thermal conductivity and the geometry of the fuel (for example, compact, pebble) determines the temperature gradient across the fuel specimen as some potential failure mechanisms depend on this temperature gradient. Note that the power density in Figure 4-6 is for the entire core volume not just the fuel specimen.
- **Particle packing fraction.** Packing fraction together with the global power density can be used to establish the power per particle, which establishes the temperature inside the particle.

Envelopes are shown in Figure 4-6 for the successful German and Japanese TRISO-coated particle fuel programs established in the 1980s and 1990s, respectively, along with bounds anticipated for the NGNP designs. The AGR program used the NGNP envelope to guide its irradiation testing.

**Table 4-3**  
**Relationship between mechanisms of fuel failure properties of fuel particles**

Failure Mechanism	Service Conditions	Parameters Influencing Failure Mechanism
Pressure vessel failure	Temperature, burnup, fast fluence	Strength of SiC Buffer density (void volume) Fission-gas release Kernel type (CO production) Layer thicknesses IPyC and OPyC performance
Irradiation-induced PyC failure leading to SiC cracking	Fast fluence, temperature	Dimensional change of PyC Irradiation-induced creep of PyC Anisotropy of PyC Strength of PyC PyC thickness PyC density Tensile stress in SiC at IPyC crack tip SiC strength
IPyC partial debonding	Temperature, fast fluence	Nature of IPyC-SiC interface Interfacial strength Dimensional change of IPyC Irradiation-induced creep of IPyC
Kernel migration	Temperature, burnup, temperature gradient	Kernel type (UO <sub>2</sub> , UCO, and so on) Buffer, and IPyC thickness
Diffusive release through intact layers	Temperature, burnup, temperature gradient, time at temperature	Chemical state/transport behavior of fission products Microstructure of SiC SiC thickness
Fission product attack of SiC	Temperature, burnup, temperature gradient, time at temperature	Chemical state/transport behavior of fission products Kernel type (UO <sub>2</sub> , UCO, and so on) Microstructure of IPyC and SiC
Corrosion of SiC by CO	Temperature, burnup, time at temperature	Kernel type (UO <sub>2</sub> , UCO, and so on) IPyC integrity
SiC thermal decomposition	Temperature, time at temperature	SiC thickness SiC microstructure
SiC permeability/SiC degradation	Burnup, temperature, fast fluence	Microstructure of SiC Thickness of SiC Permeability of SiC SiC layer impurities from fabrication process

This envelope resulted in the need for a fuel form that could survive at peak fuel temperatures of 1250°C on a time-average basis and high burnups in the range of 150 to 200 GWd/MTHM (metric tons of heavy metal) or 16.4 to 21.8% FIMA. The program selected UCO as the fissile kernel of choice because of its ability to limit CO production and kernel migration under irradiation phenomena that in 2003 were considered life limiting in the traditional UO<sub>2</sub> TRISO fuels if they were to operate at the upper temperature range (~1250°C) and high burnup anticipated in some of the designs.

For comparison, and as discussed in detail in Section 6, the UCO TRISO fuel compacts in the AGR-1 irradiation had a packing fraction of 37% and achieved burnups of between 11.3 and 19.6% FIMA and fast fluences between 2.2 and 4.3 × 10<sup>25</sup> n/m<sup>2</sup> (E > 0.18 MeV). Peak time-average temperatures ranged from 1069 to 1197°C and time-average volume-average (TAVA) temperatures ranged 955 to 1136°C. The UCO TRISO fuel compacts in the AGR-2 irradiation also had a packing fraction of 37% and achieved burnups between 7.3 and 13.2% FIMA and fast fluences between 1.9 and 3.5 × 10<sup>25</sup> n/m<sup>2</sup> (E > 0.18 MeV). Peak time-average temperatures ranged from 1080 to 1360°C and TAVA temperatures ranged from 987 to 1296°C. In both AGR-1 and AGR-2, capsule average power densities ranged from 4 to 14 W/cc and power per particle ranged between 20 and 160 mW/particle during the irradiations.

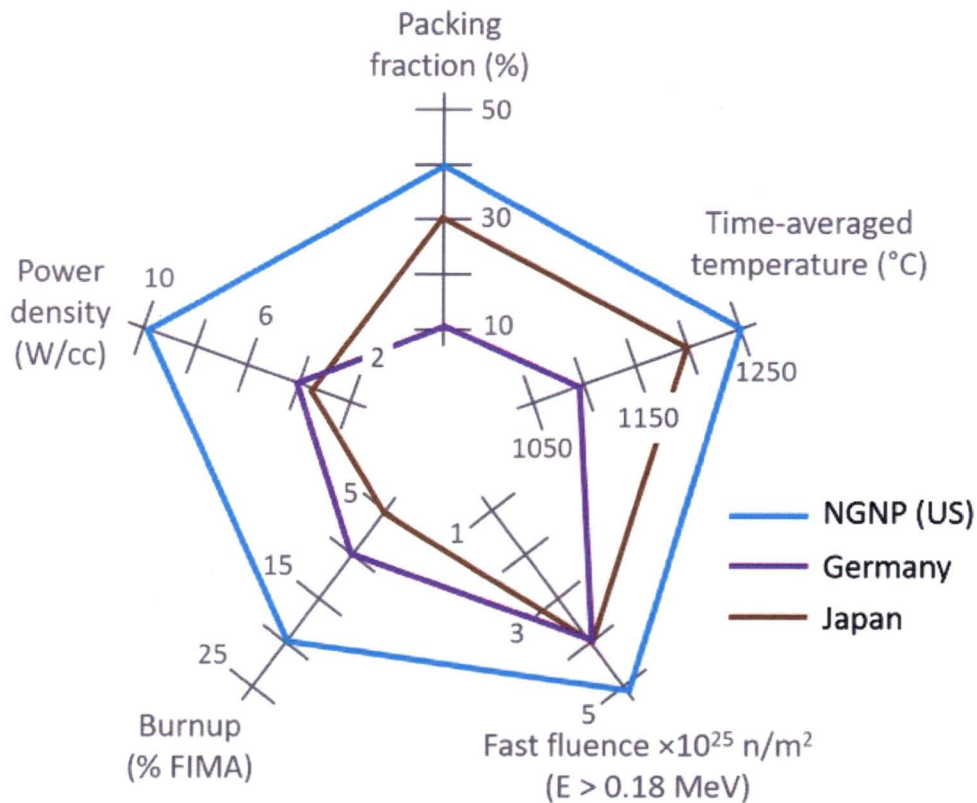


**Figure 4-6**  
**Radar plot of key parameters for TRISO-coated fuel performance. Germany and Japan plots represent historic values; NGNP indicates the performance envelope anticipated by the U.S. fuel development program.**

*Courtesy of Idaho National Laboratory and used with permission of Battelle Energy Alliance, LLC*



# 5

## ADVANCED GAS REACTOR FUEL DEVELOPMENT AND QUALIFICATION PROGRAM

---

### 5.1 Program Background and Objectives

In fiscal year 2002, the DOE Office of Nuclear Energy, Science, and Technology initiated development of the Advanced Gas Reactor Fuel Development and Qualification Program for coated-particle fuel. The resulting *Technical Program Plan for Advanced Gas Reactor Fuel Development and Qualification Program* [39] and subsequent revisions defined fuel development activities to support licensing and operating an HTGR in the U.S. under the umbrella of the NGNP project in accordance with the Energy Policy Act of 2005 when it was enacted. The AGR program is currently part of the DOE Advanced Reactor Technologies (ART) program and is pursuing irradiation and performance data for the qualification of TRISO particle fuel for use in high-temperature reactors [38].

TRISO particle fuel development and qualification activities support multiple HTR designs, including prismatic and pebble-bed HTGRs as well as FHRs. The AGR program to date has focused on manufacturing and testing the fuel design for HTR concepts using the most recent GT-MHR fuel product specification as a starting point [1]. Irradiation, safety testing, and PIE plans support fuel development and qualification in an integrated manner. Preliminary operating conditions and performance requirements for the fuel and preliminary fuel product specifications to guide the AGR program's fuel fabrication process development activities were based on previously completed HTGR design and technology development activities, operating conditions, and performance requirements.

A complete set of fuel design specifications for an HTGR has not been developed which could be used in the AGR program, but the maximum burnup envisioned in a prismatic HTGR is within the range of 150 to 200 GWd/MTHM or 16.4 to 21.8% FIMA. Maximum burnups for pebble-bed designs have historically been considerably less than this. Although Germany has demonstrated excellent performance of UO<sub>2</sub> TRISO particle fuel up to about 10% FIMA and 1150°C, UO<sub>2</sub> fuel is known to have limitations because of CO formation, including kernel migration at the higher burnups, power densities, temperatures, and temperature gradients that may be encountered in the prismatic HTGR design, and CO corrosion of the SiC layer. With UCO fuel, the kernel composition is engineered to minimize CO formation and kernel migration, which are key threats to fuel integrity at higher burnups, temperatures, and temperature gradients. The performance of German SiC-based, TRISO-coated-particle, UCO fuel up to 22% FIMA (as measured by the in-pile gas release in irradiation test FRJ2-P24 [18]) and the excellent performance of U.S.-made UCO TRISO fuel in AGR-1 and AGR-2 give added confidence that high-quality SiC-based, TRISO-coated-particle, UCO fuel can be made and its superior irradiation performance demonstrated statistically.

In addition to excellent fission product retention during normal operation at high burnups and high temperatures, HTGR fuel must exhibit satisfactory fission product retention under postulated accident conditions. Limited data on the accident performance of SiC-based TRISO-coated UO<sub>2</sub> fuel at high burnups indicate increased cesium releases at burnups  $\geq 14\%$  FIMA, so safety testing is an important element of any fuel qualification effort. The AGR program chose to develop coated-particle fuel using a low-enriched UCO kernel to qualify a fuel to meet fuel performance requirements under specified fuel service conditions. Thus, SiC-based TRISO-coated UCO was chosen as the baseline AGR fuel to be fabricated and tested. This fuel development path complemented particle fuel development with a UO<sub>2</sub> kernel that was being pursued by South Africa, China, and Europe. Safety testing of irradiated AGR-1 and AGR-2 UCO TRISO compacts has demonstrated the fuel's robust behavior for about 300 hours at 1600, 1700, and 1800°C, giving added confidence that SiC-based TRISO particle fuel can meet safety performance requirements (see Sections 6 and 7).

The TRISO-coated UCO fuel specification [42] utilizing SiC as the primary fission product retention layer was developed in response to extensive evaluations [16,17] of the fuel failures experienced in irradiations in the NPR and the MHTGR programs. This was the starting point for the fuel specification developed for the current program [43]. It was expected this fuel would exhibit acceptable fuel performance at higher burnups (16 to 22% FIMA) time-average fuel temperatures up to 1250°C for normal operation and 1600°C for potential accident conditions, and fast neutron fluences up to  $5 \times 10^{25}$  neutrons/m<sup>2</sup>.

The AGR program was established to achieve the following overall goals:

- Provide a fuel qualification data set in support of the licensing and operation of an HTGR. HTGR fuel performance demonstration and qualification comprise the longest duration research and development (R&D) tasks required for design and licensing. The fuel form is to be demonstrated and qualified for service conditions, which include normal operation and potential accident scenarios.
- Support deployment of HTGRs for hydrogen, process heat, and energy production in the U.S. by reducing market entry risks posed by technical uncertainties associated with fuel production and qualification.
- Extend the value of DOE Office of Nuclear Energy resources by using international collaboration mechanisms where practical.
- Establish a domestic TRISO particle fuel manufacturing capability for fabricating demonstration and qualification experiment fuel.
- Improve understanding of the fabrication process, its impact on as-fabricated fuel properties and attributes, and their impacts on in-reactor performance.

At the onset of the AGR program in 2002, facilities and personnel experienced in activities necessary to address the program goals existed in the U.S., primarily at INL and Oak Ridge National Laboratory (ORNL). INL and ORNL personnel with experience and knowledge of TRISO particle fuel, facility status, and capabilities were involved in developing the initial *Technical Program Plan for the Advanced Gas Reactor Fuel Development and Qualification Program* [44]. In addition, GA provided input regarding prismatic HTGR fuel performance requirements and perspectives from its experience in fuel development, fuel fabrication, and

fuel-related analytical capabilities needed to support licensing interactions. BWX Technologies Inc. (BWXT) provided input based on its experience and capabilities for fuel-kernel production and fuel-particle coating. Many of the individuals who helped develop this plan were directly involved in producing and testing previous U.S. fuel for the MHTGR and the NPR. They conducted extensive investigations and reviews in the early 1990s following the unexpectedly high fuel failure levels observed in those tests.

Following review by the NGNP project by the NEAC [45] DOE halted design-specific efforts on the NGNP project at the end of the conceptual design phase, in part because a viable public-private partnership for a demonstration reactor and follow-on commercialization was not established. To date no partnership has been formed, although recently several private companies have expressed interest in using UCO TRISO fuel based on the AGR program design in an advanced HTR design. Thus, the AGR program focus is to qualify a fuel form and establish a commercial fuel vendor in the U.S. The HTGR R&D will not perform verification or validation of any potential reactor vendor codes.

The AGR program involves the following five major program elements:

1. **Fuel Fabrication.** This program element—to fabricate TRISO particle fuel (that is, manufacturing fuel that meets the fuel quality and performance requirements for licensing an HTR)—requires development of a coating process that replicates, to the greatest extent practical, the HTGR particle design and properties of the coatings on German fuel particles that have previously exhibited superior irradiation and accident performance. Coating-process development has been accomplished in two phases: initially in a 2-in.-diameter, laboratory-scale coater (AGR-1) followed by scale-up to a 6-in., prototypic, engineering-scale coater (AGR-2). The Fuel Fabrication program element has included establishing the fuel fabrication infrastructure; developing the process for the low-enriched uranium oxycarbide kernels, TRISO particles, and compacts; developing coating process models; developing quality control methods; performing fuel process scale-up analyses; and developing process documentation for technology transfer to private industry. The fuel fabrication effort has produced TRISO particle fuel within cylindrical fuel compacts that met fuel product specifications and provided fuel and material samples for characterization, irradiation, safety testing, and PIE as necessary to meet the overall AGR program goals.
2. **Fuel and Material Irradiation.** This program element provides data on fuel performance during irradiation to support fuel process development, qualify a fuel design and fabrication process for normal operating conditions, and support development and validation of fuel performance and fission product transport models and codes. This program element also provides irradiated fuel and materials necessary for PIE and safety testing. Seven irradiation tests, designated as AGR-1 through AGR-7, have been defined to provide data and sample materials within the AGR program.
3. **Fuel PIE and Safety Testing.** This program element provides the facilities and processes to measure the performance of TRISO particle fuel under normal operating and potential accident conditions. Moisture and air ingress testing in quantities expected to exist within the typical helium and neon gas supplies used during irradiation (testing performed during AGR-3/4 irradiation) and safety testing (planned to be performed during AGR-5/6/7 PIE) will be performed to determine their effects on TRISO particle fuel. This work supports the fuel manufacturing effort by providing feedback on the performance of kernels, coatings, and

compacts during irradiation and under potential accident conditions. PIE and safety testing provide a broad range of data on fuel performance and fission product transport within TRISO-coated fuel particles, compacts, and carbonaceous matrix materials representative of fuel element blocks. These data, in combination with the in-reactor measurements (irradiation conditions and fission gas release-rate-to-birth-rate ratios), are necessary to demonstrate compliance with fuel performance requirements and support developing and validating computer codes.

4. **Fuel Performance Modeling.** This program element addresses the structural, thermal, and chemical processes that can lead to TRISO-coated particle failures. It considers the effects of fission product chemical interactions with the coatings, which can lead to degradation of the coated-particle properties. Fission product release from the fuel particles and transport in the fuel compact matrix and fuel element carbonaceous matrix during irradiation are also modeled. Computer codes and models will be further developed and refined as appropriate in response to irradiation, PIE, and safety testing data.
5. **Fission Product Transport and Source Term.** This program element addresses the transport within reactor core materials of fission products produced in the TRISO particle fuel and is intended to provide a technical basis for source terms for HTGRs under normal irradiation and potential accident conditions. Most of this work scope has not been performed because of funding shortfalls and higher priority work scope. Some initial fission product transport studies were performed on hydrogen and tritium permeation through high nickel superalloys with results that were included in published reports. An evaluation of data from irradiation and safety testing of "designed-to-fail" fuel particles will be performed as part of the AGR-3/4 PIE, see description below. The purpose of the evaluation is to characterize fission product release and transport from TRISO particle fuel into fuel compact matrix and fuel element carbonaceous matrix under normal and off-normal HTGR conditions.

## **5.2 Overview of AGR Program Irradiations**

The number and type of test trains to be irradiated were planned based on the needs of the fuel manufacturing, fuel performance modeling, and fission product transport activities. Seven experiments were identified based on discussions among the working groups during the course of developing the original program plan. Program budget constraints and further development of the test train designs have altered the type of test trains that were initially planned to be used for individual irradiations. In some cases, several originally planned individual experiments were combined into a single irradiation test train. This approach has taken advantage of the larger size of the ATR northeast flux trap (NEFT) irradiation position to accommodate a greater number of fuel specimens compared to the large B positions used for the AGR-1 and AGR-2 irradiations, allowing multiple experiment objectives to be accomplished in a single irradiation campaign. An eighth experiment, AGR-8, intended to provide radionuclide source term validation data was eliminated from the program plan in 2011 due to budget constraints and the absence of a reactor design effort going forward.

The four irradiation campaigns in the AGR program are outlined below.

### **5.2.1 Early Fuel Experiment (AGR-1)**

This multi-monitored capsule test train included six capsules, each containing 12 compacts made from TRISO particles produced in a small laboratory-scale (2-in.) coater in conjunction with fuel process development. This irradiation experiment provided experience with a multi-monitored test train design, fabrication, and operation, which facilitated the design, fabrication, and operation of subsequent irradiation experiments. The AGR-1 irradiation provided data on irradiated fuel performance for baseline and fuel variants that were selected based on data from fuel process development and existing irradiation experience. The early data on the performance of fuel variants supported the selection of a reference fuel for the AGR-2 irradiation experiment and development of an improved fundamental understanding of the relationship among the fuel fabrication process, as-fabricated fuel properties, normal operation, and potential accident condition performance.

### **5.2.2 Performance Test Fuel Experiment (AGR-2)**

This multi-monitored capsule test train included six independent capsules and had design very similar to AGR-1. Four of the capsules contained fuel manufactured in the U.S.: three capsules contained UCO fuel compacts and one capsule contained UO<sub>2</sub> fuel compacts. The U.S. UCO and UO<sub>2</sub> TRISO particles were fabricated in an engineering-scale 6-in. coater using process conditions derived from the production of AGR-1 Variant 3 (SiC layer produced using a mixture of hydrogen and argon diluent gases). Fuel compacts were fabricated using laboratory-scale processes and equipment at ORNL. The UCO compacts were subjected to a range of burnups and temperatures exceeding anticipated reactor service conditions in all three capsules. The two remaining capsules contained fuel manufactured by Westinghouse/Pebble-Bed Modular Reactor SOC Ltd., and Commissariat à l'Énergie Atomique et Aux Énergies Alternatives (the fabrication and performance of this fuel is not discussed in this report). This test train provided irradiated fuel performance data for coated particles fabricated at the engineering scale. It also provided fuel specimens for PIE and safety testing. The data obtained from the AGR-2 irradiation and subsequent PIE and safety testing further increase the fundamental understanding of the relationship among the fuel fabrication process, as-fabricated fuel properties, normal operation, and potential accident condition performance.

### **5.2.3 Fission Product Transport Experiments (AGR-3/4)**

This multi-monitored capsule test train was a combination of the AGR-3 and AGR-4 experiments originally planned as separate irradiations in large B positions but were combined and placed in the NEFT. This test train included compacts containing TRISO-coated "driver" fuel particles as well as 20 "designed-to-fail" (DTF) fuel particles, each within rings of carbonaceous material. DTF fuel particles for use in fission product transport testing consisted of reference kernels with only a ~20- $\mu$ m-thick pyrocarbon seal coating that was intended to fail during irradiation and provided known fission product source terms. The test train was designed to provide data on fission product diffusivities in fuel kernels and sorptivities and diffusivities in compact matrix and carbonaceous matrix materials for use in upgrading fission product transport models. The AGR-3/4 experiments also have provided irradiated fuel performance data on fission product gas release from failed particles and irradiated fuel samples for PIE. The in-pile

gas release and PIE data on fission gas and metal release from kernels will be used in developing improved fission product transport models to the extent possible from the experimental results. As this experiment was focused on fission product transport and not fuel performance, the results are not discussed in this report.

#### **5.2.4 Fuel Qualification and Fuel Performance Margin Testing Experiments (AGR-5/6/7)**

This multi-monitored capsule test train is a combination of the AGR-5, AGR-6, and AGR-7 experiments, which were planned originally for separate irradiations in large B positions, similar to AGR-1 and AGR-2, but were combined for irradiation in the NEFT. The test train includes a single fuel particle type, fabricated using process conditions and product parameters considered to provide the best prospects for successful performance based on process development results and available data<sup>14</sup> from AGR-1 and AGR-2 irradiations. This is the reference fuel design selected for qualification. Variations in capsule conditions (burnup, fast fluence, and temperature) were established in the irradiation test specifications.

The AGR-5/6 portion of this test train will provide irradiated fuel performance data and irradiated fuel samples for safety testing and PIE in a sufficient quantity to demonstrate compliance with statistical performance requirements under normal operating and potential accident conditions.

The AGR-7 portion of this test train includes the same fuel type as used in AGR-5/6 and occupies one of the five capsules. The irradiation will test fuel substantially beyond its operating temperature envelope, so some measurable level of fuel failure is expected to occur. This fuel performance margin test will provide irradiation data and irradiated fuel samples for PIE and post-irradiation heat-up testing in sufficient quantity to demonstrate the capability of the fuel to withstand conditions beyond AGR-5/6 normal operating conditions in support of plant design and licensing.

The experiment is notable for including a larger population of particles than previous irradiations (total particle count is approximately 570,000) and for extending the range of irradiation temperatures beyond the AGR-1 and AGR-2 experiments. The AGR-5/6 portion of the experiment is intended to contain particles with time-average irradiation temperatures ranging from 600 to 1400°C. The AGR-7 capsule contains a sub-population of approximately 54,000 particles and will have a time-average peak temperature of 1500 ± 50°C.

The AGR-5/6/7 irradiation experiment began in February 2018 and is expected to operate for approximately 3 years. The ongoing irradiation will not be discussed in this report.

---

<sup>14</sup> The decision to proceed with fabrication of qualification test fuel was made based on information available at the time, which included full irradiation of AGR-1 plus PIE, heat-up and fission product metal release data on AGR-1 fuel, as well as in-pile gas release data from AGR-2.

### 5.3 Summary of AGR-1 and AGR-2 Fuel Fabrication

Having decided on its fuel form, the AGR program began two fuel fabrication campaigns: (1) one focused on laboratory-scale coating at ORNL to support the AGR-1 testing program; and subsequently, (2) a second at engineering scale at BWXT to support the AGR-2 testing program. The decision was made to initiate activities at laboratory scale for two primary reasons: (1) the 15-year hiatus in producing TRISO fuel in the U.S. resulted in the need to re-establish the capabilities, procedures, and expertise; and (2) to address the historical failure in the U.S. to produce fuel that would meet HTGR performance requirements as evidenced by poor irradiation performance in the commercial MHTGR and NP-MHTGR programs in the early 1990s. Fuel fabrication development activities for the AGR program have spanned 15 years. Laboratory-scale equipment was used for process development to reduce the time and cost to complete the tests from feedstock consumables to waste generation. As the program progressed, aspects of fuel fabrication operations graduated from laboratory-scale to engineering-scale equipment.

This section describes the processes used to fabricate the AGR-1 and AGR-2 TRISO particles. *The fabrication techniques are provided for information only and are not intended to limit fabrication methods used to achieve the actual TRISO fuel specification provided in Table 5-5.*

As discussed in the following sections, the kernels and coatings of the UCO particles manufactured and tested in AGR-1 and AGR-2 exhibited some degree of property variation and were fabricated under different conditions and at different scales with remarkably similar excellent irradiation and accident safety performance. Thus, there is some allowance in terms of the actual values for key critical characteristics of the kernels and coatings necessary to impart satisfactory performance, as long as the TRISO particles meet the specification of Section 5.3.6.

#### 5.3.1 Kernel Production

Nuclear fuel kernels can be produced by either external or internal gelation where a uranium "broth" containing an acid-deficient uranyl nitrate (ADUN) solution reacts with high pH chemicals surrounding the droplet (external) or incorporated into the broth (internal) causing the ADUN to convert to a uranyl hydroxide gel. The AGR program focused its kernel fabrication efforts on internal gelation chemistry, using hexamethylenetetramine (HMTA) and urea as ammonium donors to affect the gelation when the broth droplets were warmed in an immiscible forming fluid. Carbon black was added to the broth, prior to gelation, as a carbon source to make uranium carbides. After forming, the gel spheres were aged in a collection pot to firm up the gels and then washed with ammonia water to ensure complete gelation and to remove residual reactants and soluble salts. The gel spheres were then air-dried and heat-treated at high temperature to form hard, dense ceramic UCO microspheres.

##### 5.3.1.1 AGR-1 Kernels

The AGR-1 UCO kernels were fabricated by BWXT in accordance with the AGR-1 Fuel Product Specification [46]. The fuel kernels had a nominal enrichment of 19.7% <sup>235</sup>U and a nominal diameter of 350 μm.

### 5.3.1.2 AGR-2 Kernels

For AGR-2, the U.S. kernels were fabricated by BWXT in accordance with the AGR-2 Fuel Product Specification [47]. The UCO kernels had a nominal enrichment of 14% and a nominal diameter of 425  $\mu\text{m}$ . Several changes were made to the fabrication processes to improve the chemistry, integrity, and density of the kernels relative to AGR-1. Differences in the fabrication are discussed in the following section.

The AGR-2  $\text{UO}_2$  kernels had a nominal enrichment of 9.6% and a nominal diameter of 500  $\mu\text{m}$  to be comparable with historic German fuel particles and to contrast the performance of domestic  $\text{UO}_2$  TRISO particles with that of UCO TRISO.

### 5.3.1.3 Diversity in Kernel Production

Target process parameters, given in Table 5-1, show the main changes made to the kernel fabrication processes. Although the same equipment was used for forming, washing, and drying the kernels, some additional changes were made that are not documented in the table. These include ancillary equipment enhancements, such as the broth mixer, which was replaced between AGR-1 and AGR-2 kernel fabrication campaigns along with the nozzle orifice sizes and pulsation parameters that were changed to produce the desired droplet sizes. The measured and calculated characteristics of the AGR-1 and AGR-2 kernels are given in Table 5-2. All quantified impurity levels in the kernels were less than the specified maxima and commonly below analytical detection limits; these data are not included in Table 5-2.

**Table 5-1**  
Differences in kernel production parameters for AGR-1 and AGR-2 [48-50]

Process Parameters	AGR-1 UCO	AGR-2 UCO	AGR-2 $\text{UO}_2$
HMTA : U mole ratio	1.3	1.55	1.55
Urea : U mole ratio	1.3	1.3	1.55
Carbon : uranium atom ratio (broth)	1.0	1.1	—
Carbon source	Powder	Aq. suspension	—
Carbon dispersion phase	ADUN solution	HMTA solution	—
Forming temperature	56°C	56°C	60°C
Broth droplet diameter (nominal)	1140 $\mu\text{m}$	1365 $\mu\text{m}$	1630 $\mu\text{m}$
Broth feed rate	27 cc/min	40 cc/min	30 cc/min
Calcination gas	100% $\text{H}_2$	8% $\text{H}_2$ : 92% Ar	13% $\text{H}_2$ : 87% Ar
Sintering gas	60% CO : 40% Ar	60% CO : 40% Ar	13% $\text{H}_2$ : 87% Ar
Sintering temperature	1890°C	1890°C	1500°C
Sintering hold time	4 hours	1 hour	2 hours



**Table 5-2**  
**AGR-1 and AGR-2 kernel properties [48-52]**

Kernel Properties	AGR-1 UCO	AGR-2 UCO	AGR-2 UO <sub>2</sub>
Diameter	349.7 $\mu\text{m}$	426.7 $\mu\text{m}$	507.7 $\mu\text{m}$
Density (g/cm <sup>3</sup> )	10.66	10.97	10.86
Fraction of theoretical density (%)	90.4	95.7	99.0
Aspect ratio ( $D_{\text{max}}/D_{\text{min}}$ )	1.015	1.012	1.009
C:U atom ratio	0.325	0.392	–
O:U atom ratio	1.361	1.428	2.003
[O+C]:U atom ratio	1.685	1.818	2.003
Calculated UO <sub>2</sub> : UC : UC <sub>1.86</sub> ( <sup>†</sup> )	68 : 31 : 01	71 : 16 : 12	100 : 00 : 00
Wt% U	90.06	89.46	87.97

<sup>†</sup>Assumes that only the listed compounds were present.

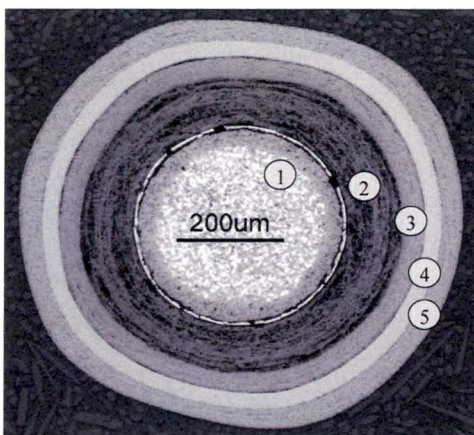


**Figure 5-1**  
**Sectioned TRISO fuel particle**

*Courtesy of Idaho National Laboratory and used with permission of Battelle Energy Alliance, LLC*

### 5.3.2 TRISO Fuel Particles

An example of a UCO TRISO fuel particle from the AGR program is presented in cross section in Figure 5-1, with labels for the: (1) fuel kernel; (2) buffer layer; (3) IPyC layer; (4) SiC layer; and (5) OPyC layer.

During SiC deposition and the heat treatment of the compacted fuel form, the uranium monocarbide phase converts to the dicarbide within the kernel and releases elemental uranium that subsequently reacts at the buffer/kernel interface to form a skin of UC<sub>1.86</sub>, evident as the thin, light ring between the kernel and the buffer layer in Figure 5-1.

### 5.3.2.1 TRISO Coating Deposition

The four coatings that comprise the TRISO fuel particle function the best in a reactor system if the coatings are sequentially deposited in the coater without an interruption that would necessitate keeping the bed fluidized for an extended time period or unloading the fuel. This is especially true for the IPyC and SiC layers, which provide the greatest fission product retention. Therefore, the coatings were sequentially applied without interruption. Uninterrupted coating is the baseline approach used by the successful German, Japanese, and Chinese programs and was adopted by the AGR program as well. The buffer is deposited by chemical vapor deposition from a mixture of acetylene and argon diluent. The inner and outer pyrolytic layers are deposited from a mixture of acetylene, propylene, and argon diluent. The SiC layer is deposited from methyltrichlorosilane (MTS) diluted with hydrogen and argon. Specifications are placed on the diameters, thicknesses, and densities of the kernel and coating layers; the sphericity of the kernel and coated particle; the stoichiometry of the kernel; the maximum anisotropy of the pyrocarbon layers; the microstructure of the SiC; and the acceptable defect levels for each layer. Statistical sampling techniques are used to demonstrate compliance with the specifications, usually at the 95% confidence level [53].

### 5.3.2.2 AGR-1 Particles

The AGR-1 UCO kernels were coated by ORNL, which also provided characterization data [54-57]. A baseline fuel and three variants were fabricated for AGR-1. These variants were purposely designed to explore a range of relevant process parameters to produce different physical values of key coating attributes, which had been the cause of the historical performance of U.S. TRISO fuel. Briefly, the baseline and variant fuels are described as:

- **Baseline.** Because of its excellent irradiation performance, coating process conditions used to fabricate historic German fuel were chosen as the starting point for the baseline fuel. Parametric studies refined these conditions for the specific coater used to coat AGR-1 fuel. This fuel was expected to perform successfully during irradiation.
- **Variant 1.** The IPyC coating temperature was increased relative to the baseline process for this variant. This change was expected to enhance the irradiation dimensional stability of the PyC, but with increased uranium dispersion. Also, the IPyC layer density was slightly lower than the baseline density.
- **Variant 2.** The IPyC coating gas fraction was increased relative to the baseline process for this variant. This change was also expected to enhance the irradiation dimensional stability of the PyC without significantly increasing uranium dispersion. Also, the IPyC layer density was slightly higher than the baseline density.
- **Variant 3.** The carrier gas composition for the SiC layer deposition was changed from hydrogen to an argon-hydrogen mixture, and deposition temperature was lowered. These changes were expected to change the microstructure of the SiC (including a finer grain size) and to reduce SiC defects.

The kernels were coated in a 2-in.-diameter retort tube. The 2-in.-diameter retort was selected, in part, because it facilitated fuel coating development studies without using a large amount of material resources or generating large quantities of waste.

### 5.3.2.3 AGR-2 Particles

The 425- $\mu\text{m}$  UCO and 500- $\mu\text{m}$   $\text{UO}_2$  kernels were coated and characterized by BWXT [49,50]. Based on the AGR-1 in-pile results available at the time, the AGR program decided the AGR-2 PyC coating would be applied using baseline conditions from AGR-1 and would use argon dilution during the SiC coating step, like AGR-1 Variant 3, for the best fluidization in the coater. The kernels were coated in a 6-in.-diameter retort increasing the coater capacity approximately 20-fold relative to AGR-1.

### 5.3.2.4 Diversity in TRISO Particle Properties

Properties of the resulting TRISO particles are given in Table 5-3.

**Table 5-3**  
**TRISO particle characterization data.**

Layer Properties	AGR-1 [49,54-59]				AGR-2 [48,50,51,52,58-61]	
	Baseline	Variant 1	Variant 2	Variant 3	UCO	UO <sub>2</sub>
<b>Buffer</b> Thickness (μm)	103.5	102.5	102.9	104.2	98.9	97.7
Density (g/cm <sup>3</sup> ) <sup>a</sup>	~1.10	~1.10	~1.10	~1.10	~1.04	0.99
<b>IPyC</b> Thickness(μm)	39.4	40.5	40.1	38.8	40.4	41.9
Density <sup>a</sup>	1.904	1.853	1.912	1.904	1.890	~1.89
BAF <sub>o</sub> (True) <sup>b</sup>	1.015	1.009	1.015	1.020	1.024	1.025
<b>SiC</b> Thickness (μm)	35.3	35.7	35.0	35.9	35.2	37.5
Density (g/cm <sup>3</sup> )	3.208	3.206	3.207	3.205	3.197	3.200
Aspect ratio <sup>c</sup>	–	–	–	–	1.037	1.034
Grain major axis (μm) <sup>d</sup>						
Twins	2.41	2.39	2.14	0.71	0.89	1.19
No Twins	5.82	5.10	5.29	1.29	1.67	2.37
<b>OPyC</b> Thickness (μm)	41.0	41.1	39.8	39.3	43.4	45.6
Density (g/cm <sup>3</sup> )	1.907	1.898	1.901	1.911	1.907	1.884
BAF <sub>o</sub> (True) <sup>b</sup>	1.013	1.009	1.012	1.014	1.018	1.015
Aspect ratio <sup>c</sup>	1.054	1.056	1.053	1.055	1.052	1.052
Missing OPyC	≤9.7×10 <sup>-5</sup>	≤9.7×10 <sup>-5</sup>	≤9.6×10 <sup>-5</sup>	≤9.7×10 <sup>-5</sup>	≤1.90×10 <sup>-4</sup>	≤5.8×10 <sup>-4</sup>

a. Layer density was not measured on batches with data preceded by a tilde (~). Values are inferred from similar runs.

b. The “true” Bacon anisotropy factor (BAF<sub>o</sub>) is calculated from diattenuation (N) as follows: BAF<sub>o</sub> = (1+N)/(1-N). Original AGR-1 BAF<sub>o</sub> anisotropies were calculated using a different conversion formula than later used for AGR-2. Data reported above use the same formula.

c. Aspect ratio is the ratio of major and minor radii. Measured only on the OPyC layer for AGR-1 fuel.

d. Grain major axis is reported only to indicate the impact on grain size of argon as a diluent gas combined with lower deposition temperatures. No correlation has yet been established between this property and SiC performance [58].

### 5.3.3 Sorting of Kernels and Particles

Various methods were employed to sort (separate by size and shape) the fuel kernels, TRISO-coated particles, and TRISO particles overcoated with resinated graphite powder. The methods described below have different sorting efficiencies and throughput rates. Table 5-4 is a summary of the methods employed to sort AGR-1 and AGR-2 materials at various stages of fuel fabrication.

**Table 5-4**  
**Sorting methods employed for AGR-1 and AGR-2 materials**

Material	Sieved	Tabled	Sorted by Roller Micrometer
AGR-1 kernels	X	X	–
AGR-2 kernels	X	X	–
AGR-1 TRISO	–	X	X
AGR-2 TRISO	X	X	X
AGR-1 overcoated TRISO	X	X	–
AGR-2 overcoated TRISO	X	X	–

#### 5.3.3.1 Sieving

Sieving is the most suitable method of sorting by size for full-scale production. Batch-wise sieving was employed for sorting of the AGR-1 and AGR-2 materials, but continuous methods could be employed for full-scale production. Sieving inherently sorts particles by the second largest dimension because the particle bed is in motion and particles can rotate to present different orientations to the apertures in the sieve, thus the longest axis is not always orthogonal to the plane of the sieve screen. The sieving rejected oversized and undersized kernels and particles and provided an opportunity to examine the reject fractions.

#### 5.3.3.2 Tabling

Tabling is an operation where kernels or particles are passed over an inclined, vibrating plane to sort the materials by shape. The more spherical materials readily traverse the plane and are collected in product bins opposite the feed port. Non-spherical materials do not roll well and move more orthogonally to the flow of spherical material and are collected in reject bins. Tabling is most efficient and has its greatest utility when the bulk of the materials are highly spherical. Faceted particles, such as TRISO particles, are more difficult to sort by shape due to increased comingling of the product and reject streams.

#### 5.3.3.3 Roller Micrometer Sorting

A roller micrometer consists of two cylindrical rods sloping away from the feed point and slightly diverging. The two rods rotate in opposite directions and away from the center line so as to roll the particles as they roll toward the widest and lowest end. Particles are sorted by their minimum dimension. Because particles are sorted in a single-file, this process is time-consuming and thus less well-suited for large-scale production.

### **5.3.4 Fuel Compact Fabrication**

Whether a cylindrical compact, a pebble, or another fuel form is to be pressed, a host matrix is needed to provide the structural integrity and thermal conductivity of the fuel form while benefiting the reactor physics. Graphite is a suitable medium, as it can provide exceptional high-temperature strength and good dimensional stability, and it moderates neutrons. A binder is needed to get graphite powders to remain in the compacted shape and to achieve the needed structural strength and integrity of the fuel form. Phenolic resins bind the graphite particles well, pyrolyze to an amorphous carbon phase, and are readily available in a highly pure form.

After coating, AGR-1 and AGR-2 particles were formed into right cylindrical compacts at ORNL. Prior to compacting, the AGR fuel particles were overcoated with resinated graphite powder. The resinated graphite powder becomes the compact matrix upon compaction and heat treatment. This overcoat also served to prevent particle-to-particle contact and to help achieve the desired volumetric packing fraction of fuel particles within the compacts. Resinated graphite powder was added to the die bodies before charging the overcoated TRISO particles and again afterward to form an unfueled end cap on the compacts as a precaution against damaging TRISO particles during compaction. The compacts were nominally 25 mm in length and 12.3 mm in diameter with fuel-free end caps of matrix material approximately 1.5 mm thick for AGR-1 and 0.5-mm thick for AGR-2. These end caps ensured smooth, protected surfaces that helped to prevent fuel particle damage during handling. The end cap thickness was reduced for AGR-2 and eliminated for subsequent AGR irradiation experiments. The AGR-1 compacts were pressed at room temperature using a single-acting die and a Carver press. The AGR-2 compacts were pressed at approximately 70°C using a Promess press, but utilized a die with a floating die body to function more like a double-acting press. The overcoated TRISO particles were pre-treated in a methanol atmosphere to soften the resin and make the overcoat more malleable.

### **5.3.5 Quality Controls and Statistical Methods for Characterizing Fuel**

Quality controls and statistical methods for characterizing unirradiated HTGR fuels from the fuel kernels to the final fuel form are outside of the scope of this report. Considerable information on analytical methods for characterizing fuel is available in *Characterization and Advanced Quality Control Techniques* in IAEA-TECDOC-1674, *Advances in High Temperature Gas Cooled Reactor Fuel Technology* [62].

Guidance on general statistical methods is available in report INL/EXT-05-00349, *Statistical Methods Handbook for Advanced Gas Reactor Fuel Materials* [63]. Experiment-specific guidance is found in the *Statistical Sampling Plan for AGR Fuel Materials* [53] and *Statistical Sampling Plan for AGR-2 Fuel Materials* [64].

### **5.3.6 Key Specifications and Property Ranges Observed in AGR-1 and AGR-2 TRISO Coated Particles**

Table 5-5 presents the ranges of means and dispersion critical limits for key TRISO fuel particle coating properties that impact fuel performance, compared to the applicable specifications. The data for all of the fuel types (that is, all four AGR-1 fuel types and the AGR-2 UCO) are combined into a single range and/or dispersion critical limits in cases where the specifications

for AGR-1 and AGR-2 were the same. In cases where the AGR-1 and AGR-2 specifications differed, separate values are given for AGR-1 and AGR-2. Note that when a specification exists for a mean value, this is provided as an acceptable minimum and/or maximum value(s) of the mean with 95% confidence.

In all cases, the dispersion critical limits are specified that no more than 1% of the particles may be above or below the indicated limits. The reported dispersion data indicate the calculated values above or below which 1% of the population statistically exists. From the range of measured mean and dispersion values for each parameter, the maxima and minima (as applicable) that define or bound the entire range for these five particle populations are highlighted in bold text. The only instance where a specification limit was exceeded is the upper range on the mean for AGR-2 OPyC thickness, which is highlighted in red.

Table 5-5, therefore, provides a summary of the ranges of key particle coating properties that were tested in the AGR-1 and AGR-2 irradiations. Note that selection of key particle properties for this list is influenced, in part, by extensive thermomechanical modeling of particle performance and sensitivity studies to determine which properties have the greatest impact on particle failure probability, as well as historic TRISO fuel experience.

As noted in Section 4.2, because the kernel is thermomechanically decoupled from the coating layers, there is not a *unique* set of kernel specifications that are critical to successful TRISO fuel as long as the scaling discussed in Section 4.2 is considered. Historically, a broad range of fissile and fertile kernels in a variety of chemical forms have been irradiated successfully around the world. In terms of UCO, work by Homan et al. [25] has shown that depending on the burnup desired a broad range of uranium carbide contents in the kernel (between ~10 and ~50%) can produce acceptable fuel performance that balances the reduction in CO that comes with the addition of uranium carbide to the kernel with the potential for increased mobility of lanthanide carbide fission products as more uranium carbide is added. More recent work by McMurray et al. [65] suggests even lower carbide contents (as low as 5%) could be acceptable based on a reassessment of the uranium oxycarbide system using the latest updates in thermodynamic databases. The AGR program chose to target about 30% uranium carbide in their kernel fabrication to meet a burnup of ~20% FIMA.

**Table 5-5**  
**Particle layer property 95% confidence values on means and dispersion limits**

Particle Property	Sample Population	Specified Range of Mean <sup>a</sup>	Measured Mean Confidence Extrema <sup>b</sup>	Maximum Allowable Fraction Beyond the Critical Limit(s) <sup>c</sup>	Measured Dispersion Extrema <sup>d</sup>
Buffer thickness (μm)	AGR-1	85 – 115	96.5 – 105.0	1% ≤ 55	1% ≤ 82.5
	AGR-2			1% ≤ 58	1% ≤ 74.9
IPyC thickness (μm)	AGR-1	36 – 44	38.6 – 41.1	1% ≤ 30 1% ≥ 56	1% ≤ 33.0 1% ≥ 47.2
	AGR-2			1% ≤ 30 1% ≥ 52	1% ≤ 33.3 1% ≥ 47.5
SiC thickness (μm)	AGR-1	32 – 38	34.4 – 36.1	1% ≤ 25	1% ≤ 32.0
	AGR-2			1% ≤ 23	1% ≤ 31.7
OPyC thickness (μm)	AGR-1, -2	36 – 44	39.1 – <b>44.3</b>	1% ≤ 20	1% ≤ 34.0
Buffer density (g/cm <sup>3</sup> )	AGR-1	0.88 – 1.18	1.08 – 1.12 <sup>e</sup>	Not specified	
	AGR-2	0.95 – 1.15	1.04 <sup>f</sup>		
IPyC density (g/cm <sup>3</sup> )	AGR-1, -2	1.85 – 1.95	1.851 – 1.914	1% ≤ 1.80 1% ≥ 2.00	1% ≤ 1.822 1% ≥ 1.951
SiC density (g/cm <sup>3</sup> )	AGR-1, -2	≥ 3.19	≥ 3.204	1% ≤ 3.17	1% ≤ 3.198
OPyC density (g/cm <sup>3</sup> )	AGR-1, -2	1.85 – 1.95	1.895 – 1.914	1% ≤ 1.80 1% ≥ 2.00	1% ≤ 1.881 1% ≥ 1.935
IPyC anisotropy (BAF <sub>True</sub> ) <sup>g</sup>	AGR-1	≤ 1.035	≤ 1.023	1% ≥ 1.06	1% ≥ 1.044
	AGR-2	≤ 1.045	≤ 1.026		
OPyC anisotropy (BAF <sub>True</sub> ) <sup>g</sup>	AGR-1, -2	≤ 1.035	≤ 1.020	1% ≥ 1.06	1% ≥ 1.038
Aspect Ratio <sup>h</sup>	AGR-1, -2	Not specified		1% ≥ 1.14	1% ≥ 1.098

- a. Conformance of the measured mean to the specified range is with a single-sided, 95% confidence tests.
- b. Reported for the 95% single-sided confidence limit for each extreme. Values beyond specified limits are given in red.
- c. No more than 1% of the particle population may reside beyond the specified critical limit(s) with 95% confidence.
- d. 95% confidence test that no more than 1% of the population lies beyond the reported value. Calculated population fractions beyond the specified critical limits for each property within all particle batches/lots are no more than 1.5E-5.
- e. Data are from interrupted coating runs and not the irradiated particle batch/lot.
- f. Single datum for the mean. No confidence range is available.
- g. Data converted from ellipsometer diattenuation (N) to Bacon Anisotropy Factor using: BAF True = (1+N)/(1-N).
- h. Ratio of the major and minor axes. Measured on OPyC layer for AGR-1 and SiC layer for AGR-2.



# 6

## AGR-1 AND AGR-2 IRRADIATIONS

---

The irradiation performance of the TRISO fuel produced in the 1990s compared to the successful German program led to a broad review of all aspects of fabrication and testing of TRISO fuel, providing lessons learned for future TRISO fuel work in the United States [66]. The review suggested changes in the fabrication process to improve coating performance, recommended a reduction in the level of acceleration in fuel irradiations, and urged an expansion of PIE to fully characterize the fuel following irradiation and/or accident safety testing. With this historical backdrop, the following objectives and goals were defined for AGR-1 and AGR-2.

- **AGR-1.** The goal was to fabricate different types of UCO TRISO fuel particles using a 2-in. laboratory-scale coater at ORNL under a set of systematic, well-characterized coating conditions. As discussed in Section 5.3.2.2, a baseline fuel particle composite and three variant fuel particle composites were fabricated. The variants included two particle composites coated using different IPyC coating conditions and one particle composite coated using different SiC coating conditions. In the area of irradiation, a key objective was to gain experience with multi-capsule test train design, fabrication, and operation to reduce chances of operational problems in subsequent test trains. Such types of capsules had been used successfully in Europe to support German TRISO fuel qualification. Another goal was to obtain early data on irradiated fuel performance and support development of a fundamental understanding of the relationship between the fuel fabrication process, fuel product properties and irradiation performance. If the fuel performance under irradiation was acceptable, there would be ample irradiated UCO fuel for accident simulation testing (that is, heating tests) and other PIE activities. In terms of accident testing, two separate furnaces were established at INL and ORNL to conduct long-term high-temperature heating tests to simulate accident performance similar to the German program. In addition, significant infrastructure and capabilities were established at hot cells at both laboratories to: (1) characterize particles after irradiation and accident heating; (2) establish fission product mass balances; and (3) search for and recover any failed or degraded particles to understand the causes for such behavior.
- **AGR-2.** The objective was to demonstrate the performance of TRISO-coated UCO particles fabricated in a 6-in. engineering-scale coater. The irradiation capsule design for AGR-2 was essentially the same as demonstrated in AGR-1; it had six independently monitored and controlled capsules in a test train. Three capsules contained UCO fuel. Two of these were irradiated under normal conditions, while one UCO capsule was operated with a maximum time-average temperature of about 1360°C as a performance margin test of the fuel. The remaining three capsules tested UO<sub>2</sub> TRISO fuel (one containing U.S.-manufactured UO<sub>2</sub> particles, while the other two contain particles from France and South Africa). Although the focus of this report is on the performance of TRISO-coated UCO particles, the results on the UO<sub>2</sub> performance in AGR-2 are also provided as a benchmark given it is the historic fuel form used around the world (that is, Germany, China, and Japan).

## 6.1 Capsule Design and Operation

AGR-1 and AGR-2 were irradiated in the 38.1 mm (1.5 in.) diameter east and west large B positions (B-10 and B-12), respectively, at the INL ATR [59,61]. A cross-sectional view of the ATR core indicating the location of the east large B position is displayed in Figure 6-1. *A priori* physics calculations [67] showed anticipated very high-temperature reactor end-of-irradiation conditions (that is, burnup to about 20% FIMA and maximum fast neutron fluence of  $5 \times 10^{25}$  n/m<sup>2</sup>, E > 0.18 MeV) were best matched by the conditions obtained from irradiation in these large B positions after about 550 to 600 days of irradiation.

Conducting irradiations in these locations results in a slight acceleration in the accumulation of burnup and fast fluence compared to that expected in historic HTRs. Target burnups can be reached in about 550 to 600 effective full power days in the ATR compared with 1000 days in historic HTRs. The actual acceleration factors observed in AGR-1 and AGR-2 are less than 2, consistent with the bulk of the historic German irradiation experience and much slower than the bulk of the historic U.S. irradiations that were highly accelerated (x5-10) [66]. The effect of accelerated irradiation has been examined based on the current understanding of TRISO fuel performance. Accelerated irradiations can lead to higher peak temperatures in the fissile kernels of coated particles and for very high acceleration factors, the temperatures can be 100 to 500°C higher depending on the design of the coated particle [68]. However, the more modest accelerations of the AGR irradiation and the historical German testing show little to no effect on fuel performance. Furthermore, as discussed later in this report, the PIE of AGR-1 and AGR-2 TRISO fuel show no indication of any potential incipient failure that could have occurred had the time at temperature been longer as would be the case in a real time irradiation.

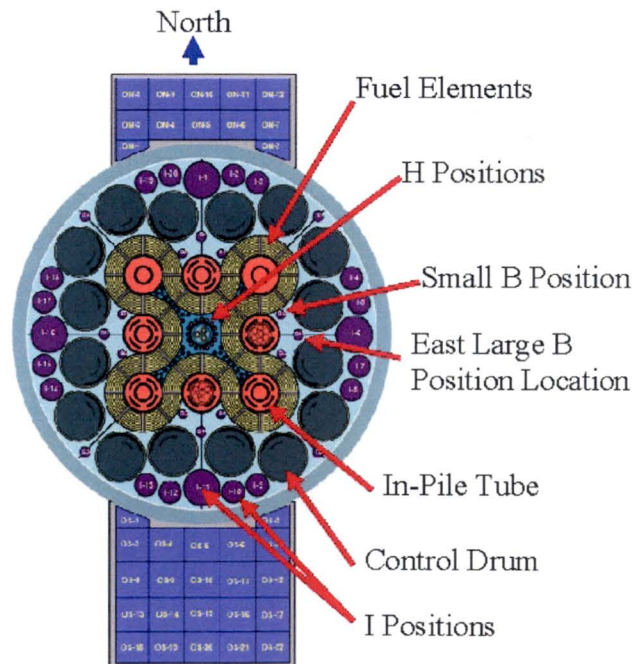


**Figure 6-1**  
**ATR core cross section**

*Courtesy of Idaho National Laboratory and used with permission of Battelle Energy Alliance, LLC*

The AGR-1 and AGR-2 test trains were multi-capsule, instrumented lead experiments with very similar design. Each test train contained six capsules, each independently controlled for temperature and independently monitored for fission product gas release. An axial view of the test train is illustrated in Figure 6-2. Each capsule was 152.4 mm (6 in.) long and contained 12 fuel compacts arranged in three vertical stacks, with each stack containing four compacts. Figure 6-3 shows a cutaway view of an AGR-1 capsule illustrating the arrangement of the three compact stacks and showing the hafnium shroud used to suppress flux on the west side of the capsule.

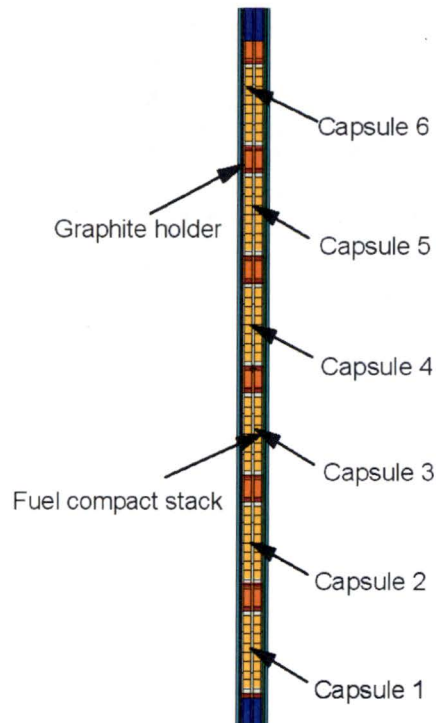


**Figure 6-2**  
**Axial schematic of the AGR-1 capsules**

*Courtesy of Idaho National Laboratory and used with permission of Battelle Energy Alliance, LLC*

Independent gas lines routed a mixture of helium and neon gases through each of the six capsules to provide temperature control and to sweep released fission product gases to the fission product monitoring system (FPMS). Temperature control was based upon temperature feedback from the thermocouples (TCs) in each capsule and was performed by varying the sweep gas composition (between 100% helium for high conductivity and 100% neon for low conductivity). This blending of sweep gases before the gas enters the test train could be accomplished either automatically (by a computerized mass flow controller) or manually. The arrangement of the gas lines can be seen in the three dimensional (3-D) rendering of a test capsule shown in Figure 6-3.

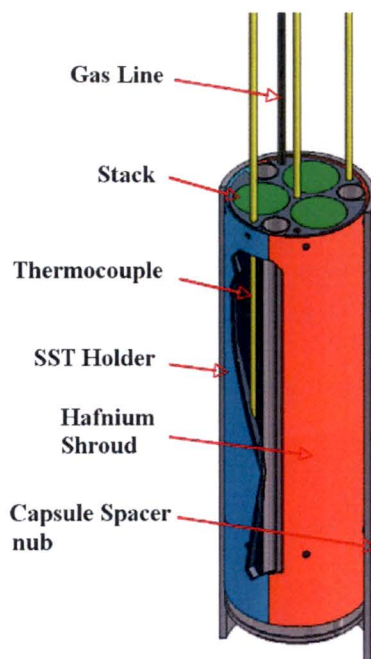


**Figure 6-3**  
**Three-dimensional cutaway rendering of single AGR-1 capsule**

*Courtesy of Idaho National Laboratory and used with permission of Battelle Energy Alliance, LLC*

A horizontal capsule cross section at the top of the AGR-1 test train is shown in Figure 6-4. AGR-2 was similar in design but was a mirror image of AGR-1 since it was irradiated in an identical position on the other side of the ATR core in the west large B position.<sup>15</sup> In both experiments, the compacts were placed inside a boronated graphite sleeve. The boron allowed a reduction in heat generation early in the experiment to provide more uniform heating (compared to the exponential drop in heating expected in the case of no boron as the fuel was completely depleted of <sup>235</sup>U) and better thermal control of the experiment.

Each capsule contained only one fuel type or variant. In AGR-1, baseline fuel was irradiated in Capsules 6 and 3, Variant 1 in Capsule 5, Variant 2 in Capsule 2, and Variant 3 in Capsules 1 and 4. In AGR-2, U.S. UCO fuel was irradiated in Capsules 2, 5, and 6; U.S. UO<sub>2</sub> fuel in Capsule 3; French UO<sub>2</sub> fuel in Capsule 1; and South African UO<sub>2</sub> fuel in Capsule 4. The capsules are numbered consecutively from the bottom (Capsule 1) to the top (Capsule 6). Fuel compacts are identified by their location in the test train using a three-digit (X-Y-Z) nomenclature, where X refers to the capsule number, Y refers to the axial level within the capsule (Level 4 is at the top of the capsule and Level 1 is at the bottom), and Z refers to the stack number.

<sup>15</sup> Note that the AGR-2 test train was removed from the core several times to avoid higher-power cycles, and was irradiated for one cycle in the I-24 position. Details can be found in Reference 60.

The FPMS continuously measured the sweep gas from each capsule to provide an indicator of fuel irradiation performance [69]. Spectrometer detector systems measured the concentrations of various krypton and xenon isotopes in the sweep gas from each capsule. Eight-hour counting intervals were used to measure the concentrations of  $^{85m}\text{Kr}$ ,  $^{87}\text{Kr}$ ,  $^{88}\text{Kr}$ ,  $^{89}\text{Kr}$ ,  $^{90}\text{Kr}$ ,  $^{131m}\text{Xe}$ ,  $^{133}\text{Xe}$ ,  $^{135}\text{Xe}$ ,  $^{135m}\text{Xe}$ ,  $^{137}\text{Xe}$ ,  $^{138}\text{Xe}$ , and  $^{139}\text{Xe}$ .

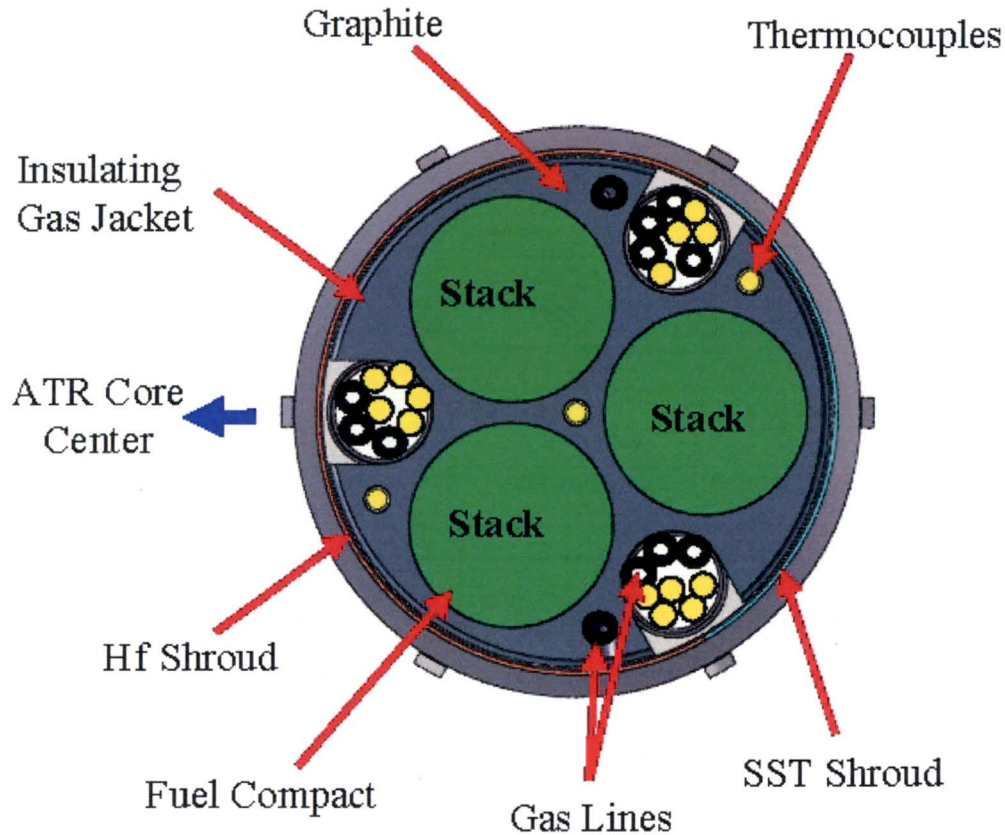


**Figure 6-4**  
**Horizontal cross section of an AGR-1 experiment capsule**

*Courtesy of Idaho National Laboratory and used with permission of Battelle Energy Alliance, LLC*

The FPMS incorporated seven individual monitoring systems: one for each of the individual capsule effluent lines, and one that could monitor any individual effluent line or any combination of the six lines. This seventh monitor was primarily provided as a backup unit capable of providing effluent line monitoring should any of the primary monitoring systems fail. Each monitor consisted of a high purity germanium (HPGe) detector-based, gamma-ray spectrometer, and a thallium-activated, sodium iodide (NaI (Tl)) scintillation detector-based total radiation detector (often termed the “gross” radiation detector). The gross detectors were able to detect the failure of individual TRISO particles, while the gamma-ray spectroscopy was used for isotopic quantification of the noble gas release. These detector units are located in the ATR-2C secondary cubicle. Figure 6-5 illustrates the flow path used for both the AGR-1 and AGR-2 irradiations.

The sweep gas from each test capsule was routed via sampling lines to the monitoring station associated with that capsule. The sample lines, valves, and filters are predominately contained in the 2C primary cubicle. The sample lines have only two short, shielded segments in the 2C secondary cubicle. These short segments run through the gross detector monitoring station and into the HPGe spectrometer shield.

Each gross detector monitoring station (seven stations implemented) incorporates a  $\text{O}25 \times 25 \text{ mm}$  NaI (TI) scintillation detector viewing a 25-mm-long segment of the capsule effluent line just before its entry into the HPGe spectrometer shield. The scintillation detector counting rate is monitored using a computer-controlled multi-channel scaler.

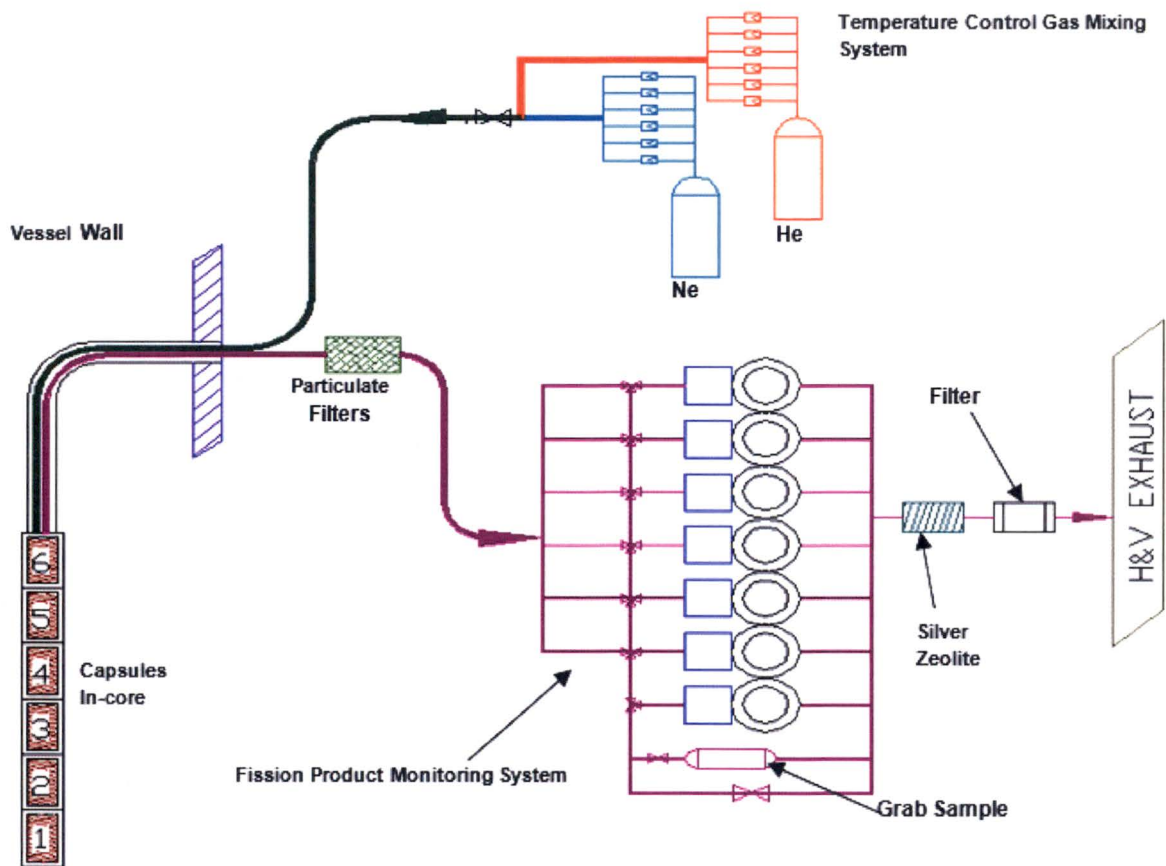


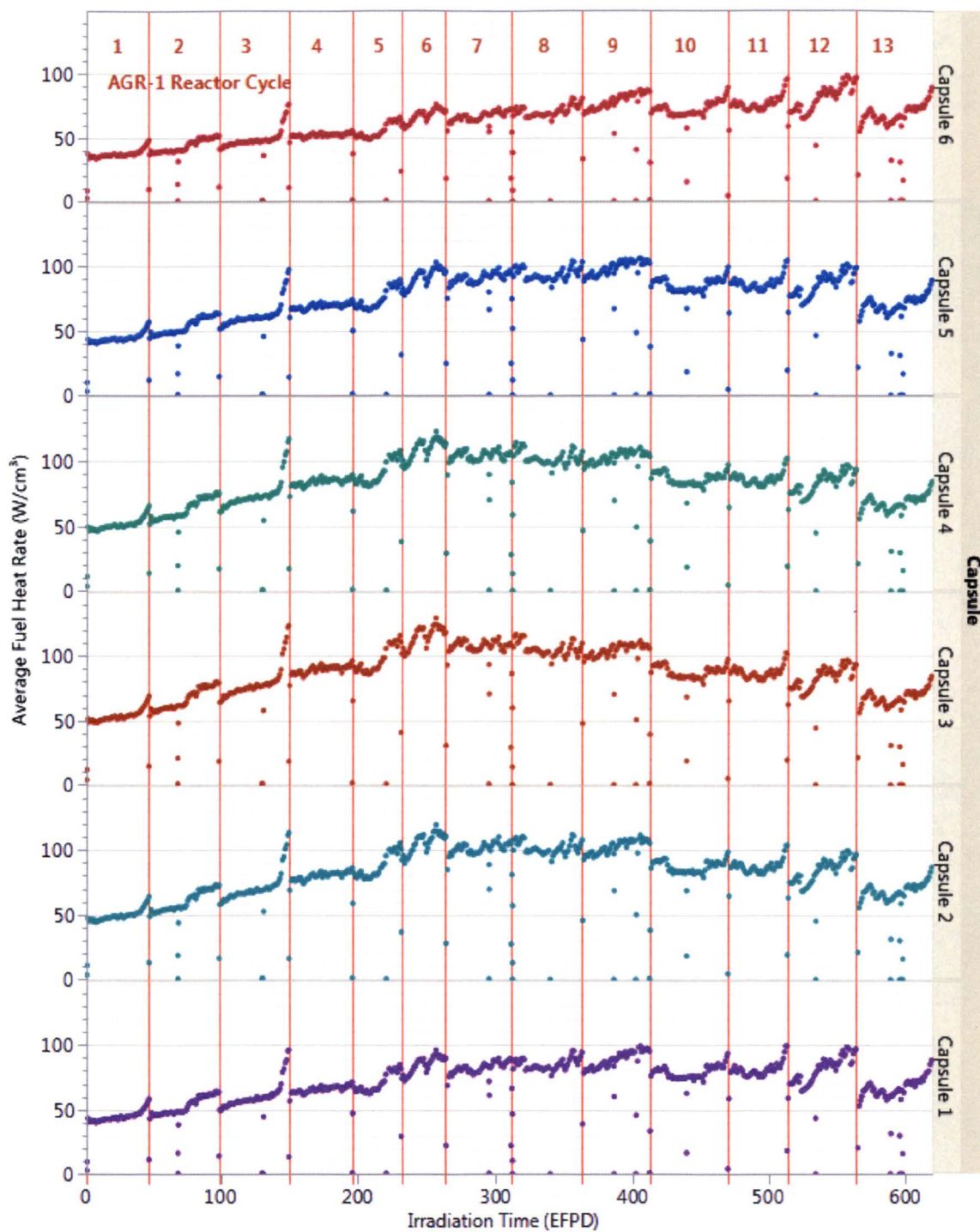
**Figure 6-5**  
**AGR-1 and AGR-2 experiment gas flow path**

*Courtesy of Idaho National Laboratory and used with permission of Battelle Energy Alliance, LLC*

## **6.2 Fission Rate, Burnup, and Fast Fluence**

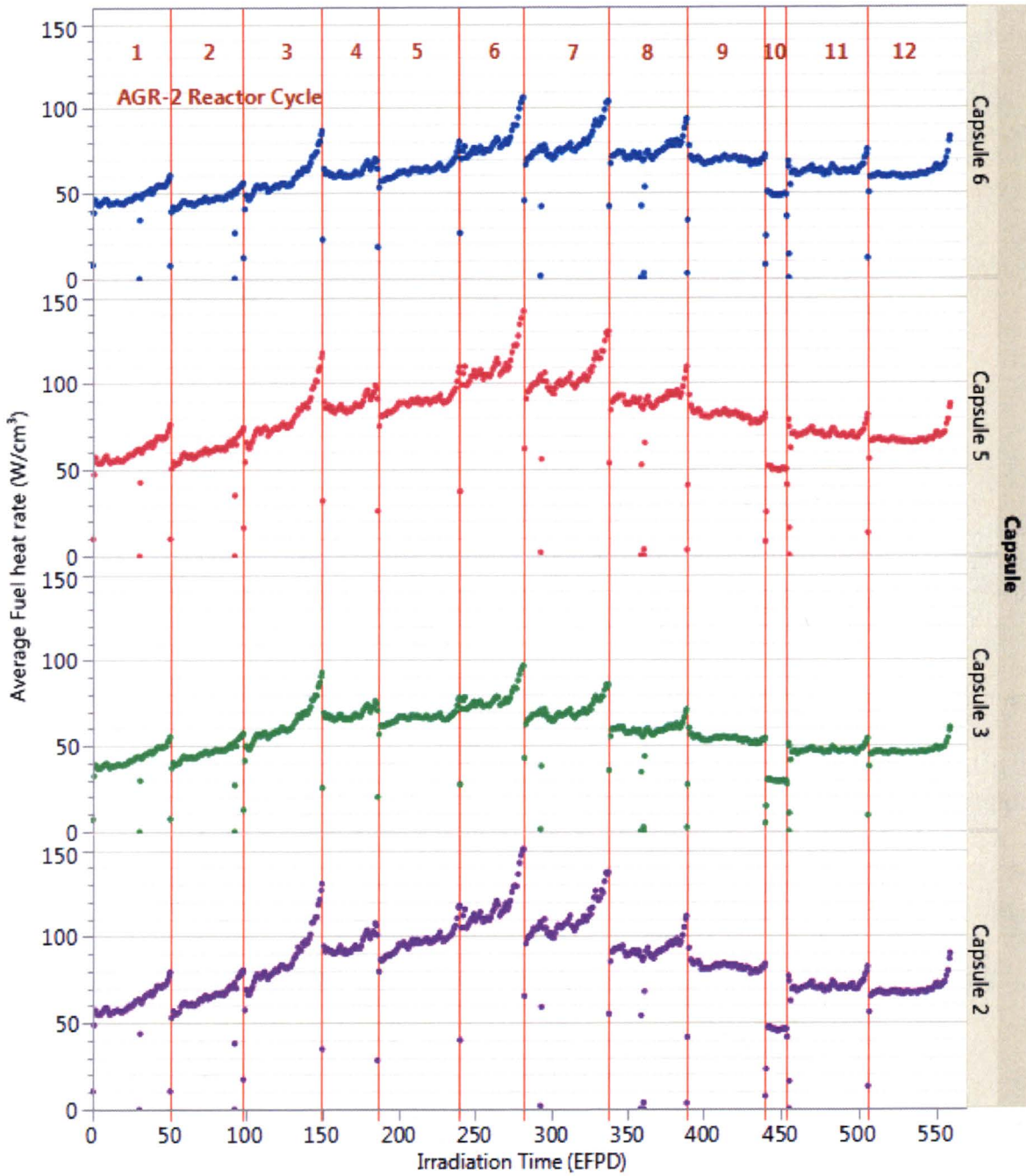
Neutronics analysis of the experiments was performed using JMOCUP, a depletion calculation code developed at INL combining the continuous energy Monte Carlo N-Particle (MCNP) transport code [70] and the depletion code ORIGEN 2.2 [71]. The JMOCUP depletion methodology was used to model and deplete the AGR-1 and AGR-2 TRISO fuel compacts.

Figure 6-6 and Figure 6-7 show the calculated capsule-average heat generation rate in the AGR-1 and AGR-2 compacts versus time in effective full power days (EFPDs). The compact fission power densities varied between ~50 and 150 W/cc for both irradiations, but in rare cases exceeded 150 W/cc at the end of some of the irradiation cycles. The general trend shared by each capsule is an increase over the first several cycles as the boron in the graphite was depleted, followed by a leveling-off over the remaining cycles.



**Figure 6-6**  
**AGR-1 capsule average power density versus irradiation time in EFPDs**  
 Courtesy of Idaho National Laboratory and used with permission of Battelle Energy Alliance, LLC





**Figure 6-7**  
**AGR-2 capsule average power density versus irradiation time in EFPDs**  
*Courtesy of Idaho National Laboratory and used with permission of Battelle Energy Alliance, LLC*

In many of the individual irradiation cycles, an increase in power density can be observed towards the end. This is because late in the cycle, outer shim cylinders (also called control drums), as shown in Figure 6-1, were often rotated such that the hafnium absorbers are oriented further away from the core to compensate for driver fuel burnup over the cycle. This operation also tends to increase the thermal flux substantially in the region of the B-10 and B-12 positions. This increase at the end of the cycle was not observed during Cycle 153B (the tenth AGR-2 power cycle) because the test train was located in the I-24 position of the ATR where the effect of the rotation of the outer shims is opposite.

These power densities are converted to maximum, minimum, and average power per particle in Figure 6-8. The power per particle ranged from 20 to 110 mW/particle in the AGR-1 irradiation. For AGR-2, which had UCO fuel particles with larger fissile kernels compared to AGR-1, the power per particle was somewhat higher and ranged from 20 to 160 mW/particle. The power per particle was even higher in the AGR-2 UO<sub>2</sub> capsule although the fissile inventory was less in the compact (the flux is higher in this axial position in the core relative to the U.S. AGR-2 UCO capsules so the power was greater).

Calculated burnups of the AGR-1 fuel compacts (in %FIMA) as a function of EFPDs are shown in the left pane of Figure 6-9, with vertical lines delineating the irradiation cycles. Capsule average burnup is shown for each capsule, along with the values for the peak and minimum compact in each capsule. The capsules at the top and bottom of the reactor (that is, Capsules 6 and 1, respectively) have the lowest burnup, with higher values found in the center capsules.

Capsule-average burnups ranged from 13.4% FIMA in Capsule 6 to 18.6% FIMA in Capsule 3. The right pane of Figure 6-9 shows fast neutron fluence ( $E > 0.18$  MeV) versus time in EFPDs, with vertical lines delineating the irradiation cycles. As would be expected, the trends of fast fluence follow quite closely those of burnup. The capsule with the lowest average fluence at the end of the irradiation was Capsule 6 with a value of  $2.65 \times 10^{25}$  n/m<sup>2</sup> ( $E > 0.18$  MeV), and the capsule with the highest was Capsule 3 at  $4.07 \times 10^{25}$  n/m<sup>2</sup> ( $E > 0.18$  MeV).

For AGR-2, the left pane of Figure 6-10 shows capsule-average burnups ranged from 9.3% FIMA in Capsule 6 to 12.2% FIMA in Capsule 2 for UCO. The fast neutron fluence ( $E > 0.18$  MeV) versus time in EFPDs, shown in the right pane, indicates the trends of fast fluence closely follow those of burnup.

The AGR-2 UCO capsule with the lowest average fluence at the end of the irradiation was Capsule 6 with a value of  $2.39 \times 10^{25}$  n/m<sup>2</sup>, and the UCO capsule with the highest was Capsule 2 at  $3.25 \times 10^{25}$  n/m<sup>2</sup>. The lower burnup of AGR-2 UCO compacts compared to AGR-1 compacts is associated with the different enrichments of the fuel particles in the two experiments (19.7% versus 14.0%). Given their low enrichment, the AGR-2 UO<sub>2</sub> compacts received lower peak burnup (10.7% FIMA) compared to the AGR-2 UCO fuel (13.2% FIMA).

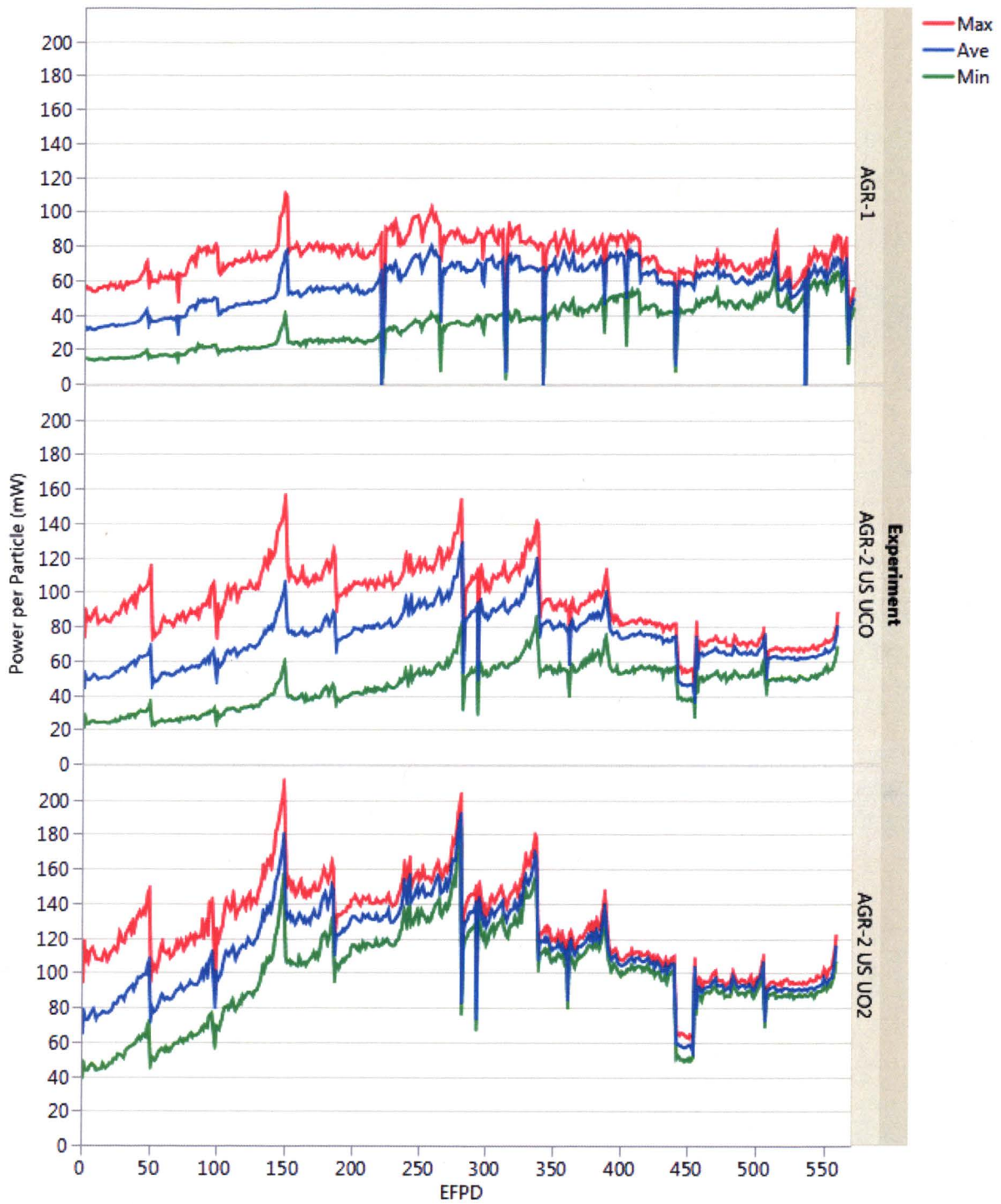


**Figure 6-8**  
**Power per particle for AGR-1 and AGR-2 irradiations**  
*Courtesy of Idaho National Laboratory and used with permission of Battelle Energy Alliance, LLC*

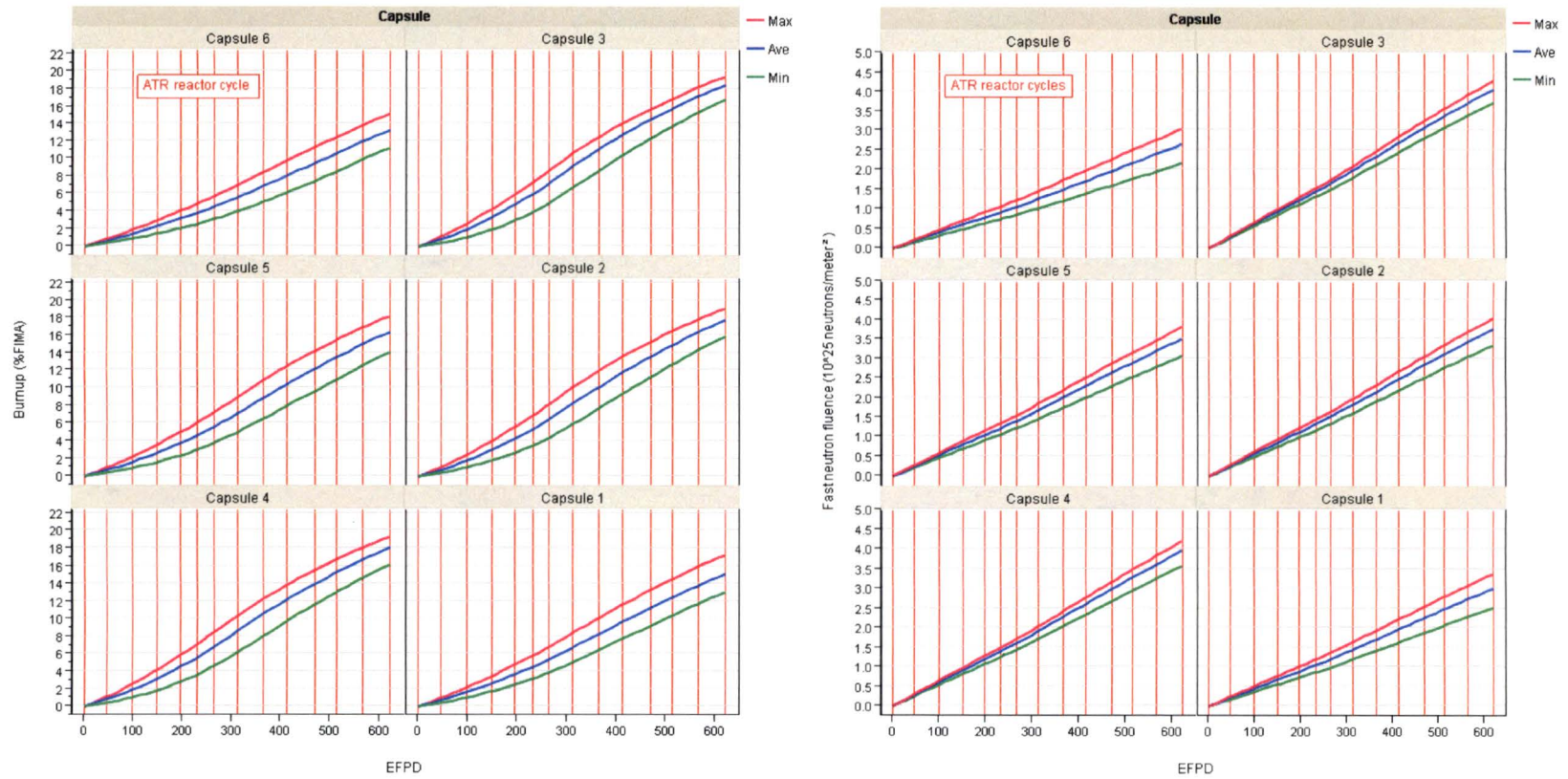


**Figure 6-9**  
**AGR-1 burnup (%FIMA) and fast neutron fluence ( $E > 0.18$  MeV) versus EFPD by capsule**  
*Courtesy of Idaho National Laboratory and used with permission of Battelle Energy Alliance, LLC*

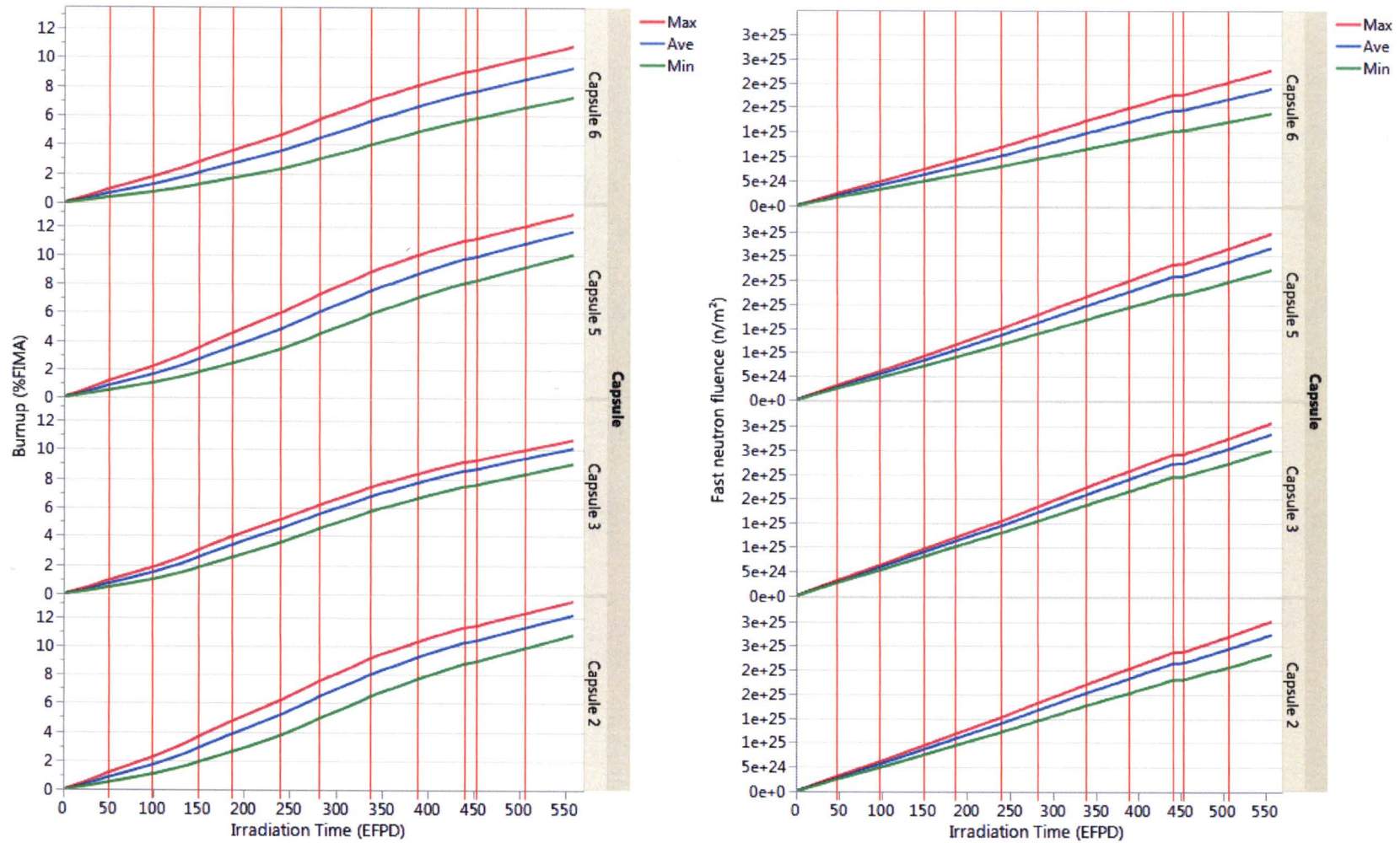


**Figure 6-10**  
**AGR-2 burnup (FIMA) and fast neutron fluence (E > 0.18 MeV) versus EFPD by capsule**  
 Courtesy of Idaho National Laboratory and used with permission of Battelle Energy Alliance, LLC

Figure 6-11 shows the correlation between burnup and fast fluence for the 72 AGR-1 compacts and the 48 AGR-2 compacts. The minimum, average, and maximum burnups of the AGR-1 and AGR-2 compacts by capsule are tabulated in Table 6-1. Collectively, the AGR-1 and AGR-2 irradiations provided compacts with a broad range of irradiation conditions with which to elucidate the performance of TRISO-coated UCO particles.

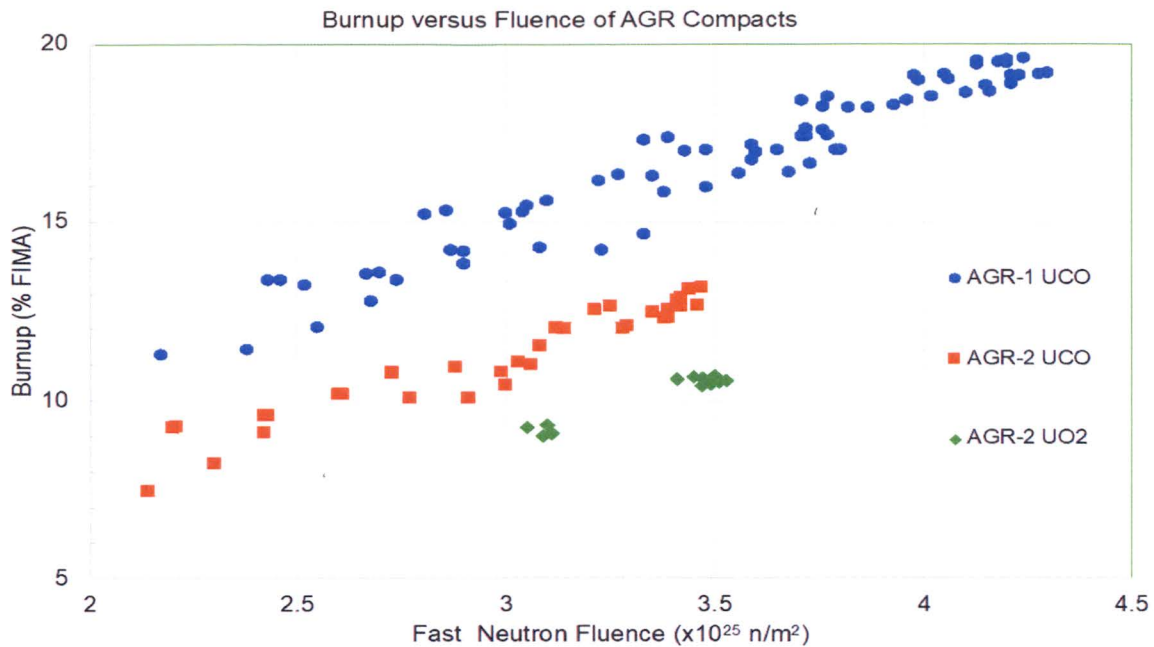


**Figure 6-11**  
**Fast neutron fluence ( $E > 0.18$  MeV) vs. burnup (%FIMA) for AGR-1 and AGR-2 compacts**  
 Courtesy of Idaho National Laboratory and used with permission of Battelle Energy Alliance, LLC

Both the AGR-1 and AGR-2 experiments contained fluence wires embedded in the graphite sample holders in each capsule. Analysis of the fluence wires yielded the thermal and fast fluence that accumulated during the irradiation. The wires were gamma counted to determine the inventory of the relevant activation products. Following gamma counting, the packages containing the niobium wires were opened, and the wires were removed and dissolved in acid. Aliquots of the solution were placed on filter paper for x-ray counting using low-energy photon spectrometers. The inventory of five different isotopes were ultimately determined for the wires (that is, <sup>54</sup>Mn, <sup>59</sup>Fe, <sup>60</sup>Co, <sup>93m</sup>Nb, <sup>94</sup>Nb), and these were used to calculate neutron fluences in the capsules in the thermal, epithermal, and fast energy ranges.

**Table 6-1**  
**AGR-1 and AGR-2 minimum, average, and peak compact burnup and fast fluence at the end of irradiation**

Capsule	Compact Burnup (% FIMA)			Compact Fast Neutron Fluence ( $10^{25}$ n/m <sup>2</sup> E >0.18 MeV)		
	Minimum Compact	Capsule Average	Peak Compact	Minimum Compact	Capsule Average	Peak Compact
<b>AGR-1 UCO</b>						
1	13.2	15.3	17.4	2.52	3.02	3.39
2	16.0	17.8	19.1	3.35	3.77	4.05
3	17.0	18.6	19.6	3.72	4.07	4.30
4	16.4	18.2	19.4	3.59	3.98	4.21
5	14.2	16.5	18.2	3.08	3.52	3.82
6	11.3	13.4	15.3	2.17	2.65	3.04
<b>AGR-2 UCO</b>						
2	10.8	12.2	13.2	2.88	3.25	3.47
5	10.1	11.7	12.9	2.77	3.18	3.42
6	7.3	9.3	10.8	1.94	2.39	2.73
<b>AGR-2 UO<sub>2</sub></b>						
3	9.0	10.1	10.7	3.05	3.35	3.53

For the AGR-1 experiment, the results for fast neutron fluence (E >0.18 MeV) based on fluence wire measurements have been compared with the predicted values from the as-run AGR-1 physics calculations for each capsule (with the exception of Capsule 1, for which no fluence wires were recovered). The comparison is shown in Table 6-2. The results demonstrated excellent agreement, as the difference between values from the two methods was within <7% for all five capsules compared.

**Table 6-2**  
**Comparison of AGR-1 capsule fast neutron fluence ( $E > 0.18$  MeV) determined from measurement of fluence wires and from physics calculations [72]**

Capsule	Fast fluence ( $10^{25}$ n m <sup>-2</sup> )		Difference
	Measured	Calculated	
6	2.33 ± 7%	2.42	+3.7%
5	3.06 ± 7%	3.05	-0.3%
4	3.25 ± 7%	3.43	+5.2%
3	3.33 ± 7%	3.39	+1.8%
2	3.19 ± 7%	2.99	-6.7%
1	–	2.29	–

Burnup of compacts from both experiments was determined experimentally using nondestructive gamma spectrometry and agreement with calculated values across all compacts in the experiments is good [73,74]. Burnup was also determined in selected fuel compacts from the AGR-1 experiment through dissolution of fuel kernels and mass spectrometry measurements. Similar measurements on AGR-2 fuel are in progress. Table 6-3 shows the comparison between measured and calculated burnup values for four AGR-1 compacts [72,75]. Note that two different approaches were used to derive burnup values using gamma spectrometry data [75].

**Table 6-3**  
**Comparison of measured and calculated burnup values for AGR-1 fuel compacts**

Compact	Mass Spectrometry	Gamma Spectrometry Direct	Gamma Spectrometry Ratio	Calculated
6-3-2	10.7 (±0.5) %	10.7 (±0.5) %	11.0 (±0.3) %	11.31%
3-2-1	19.3 (±1.0) %	18.2 (±0.9) %	18.6 (±0.6) %	18.98%
5-3-1	16.3 (±0.8) %	16.9 (±0.8) %	15.9 (±0.5) %	16.88%
1-3-1	16.3 (±0.8) %	16.0 (±0.8) %	15.6 (±0.5) %	15.98%

### 6.3 Thermal Analysis

The temperature at which the fuel compacts were irradiated is an essential component of assessing the performance of the fuel. 3-D finite element thermal calculations were performed on a daily basis using Abaqus FEA [76,77]. These calculations were performed using compact heat generation rates provided by the as-run neutronics analysis described earlier and with additional operational input for sweep gas composition versus time. Figure 6-12 shows a cross section of the AGR-2 finite element mesh formed from eight-node hexahedral bricks. The model contains approximately 350,000 nodes per capsule for both AGR-1 and AGR-2.



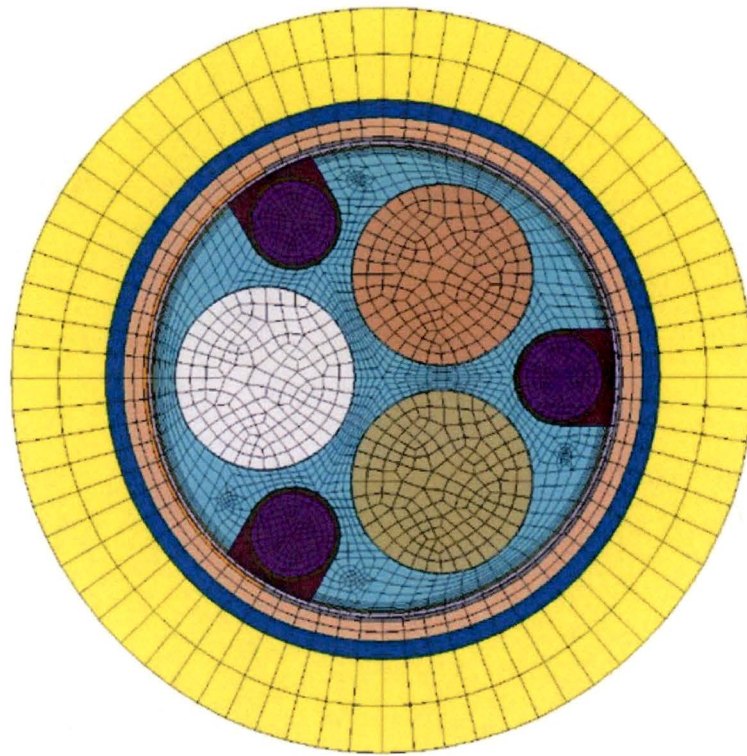


**Figure 6-12**

**Two-dimensional cross-section of Abaqus FEA model for AGR-2 irradiation**

*Courtesy of Idaho National Laboratory and used with permission of Battelle Energy Alliance, LLC*

Figure 6-13 shows a sample temperature profile calculated by Abaqus FEA after ~250 EFPDs in AGR-1 Capsule 4 (top) and after 290 EFPDs in AGR-2 Capsule 3 (bottom). Higher temperatures were in the center of the fuel stacks, with lower temperatures on the edges that were closer to the periphery of the capsule. The lowest temperatures were found on the compacts in Stack 2 on the left in the top pane of Figure 6-13 (AGR-1) since it was the compact furthest away from the ATR core. Because AGR-2 was a mirror image of AGR-1, the compacts in Stack 3 had the lowest temperatures as this stack was facing away from the core.

Figures 6-14 and 6-15 show the daily calculated fuel temperatures (capsule volume average, capsule maximum, and capsule minimum) for each of the six AGR-1 capsules versus time in EFPDs, Figures 6-16 and 6-17 show the time-average values of these temperatures plotted as a function of time for the six AGR-1 capsules. Similar plots are shown in Figures 6-18 and 6-19 for the U.S. AGR-2 capsules.

The end-of-irradiation time-average temperatures are summarized for each capsule in Table 6-4. In this table, the values listed are the lowest of the time-average minimum temperatures for the 12 compacts, the highest of the time-average maximum temperatures, and the average of the time-average, volume-average temperatures for the compacts. Thus, the table indicates, for example, the highest compact time-average maximum temperature in AGR-2 Capsule 2 was 1360°C and the lowest compact time-average minimum temperature was 1034°C.

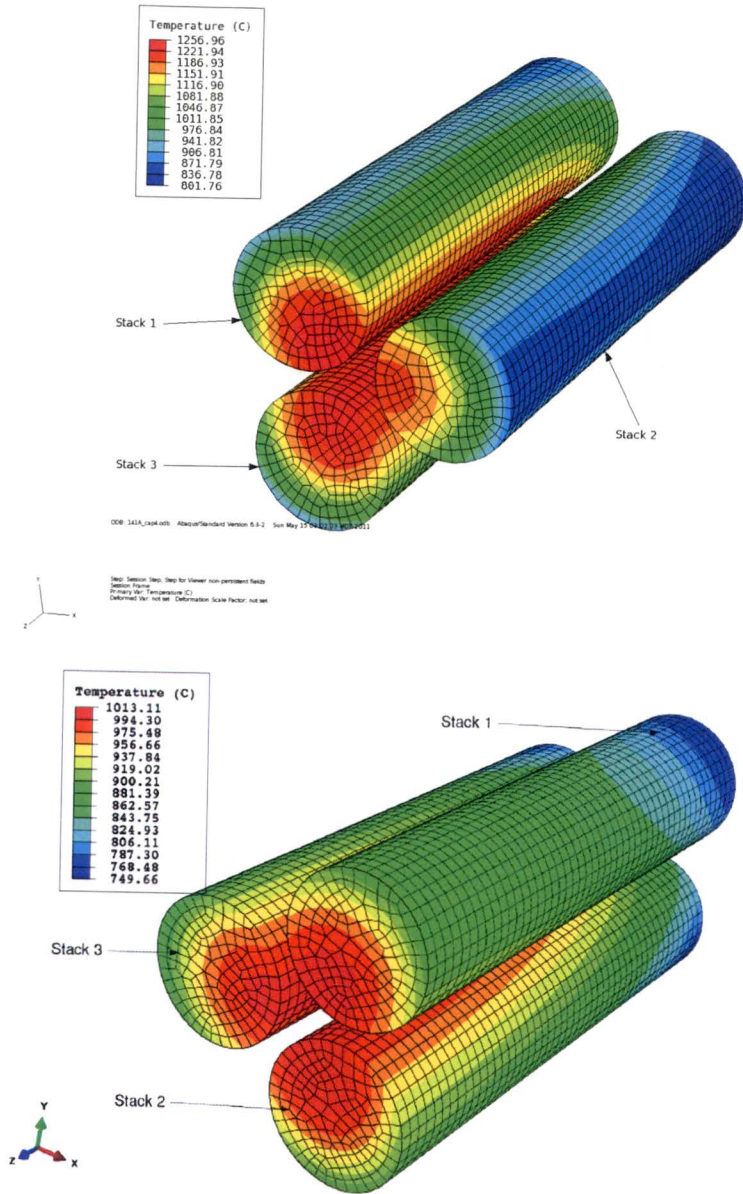


**Figure 6-13**  
**Sample temperature profile in AGR-1 Capsule 4 after ~250 EFPDs (top) and AGR-2 Capsule 3 after 290 EFPDs (bottom)**  
 Courtesy of Idaho National Laboratory and used with permission of Battelle Energy Alliance, LLC

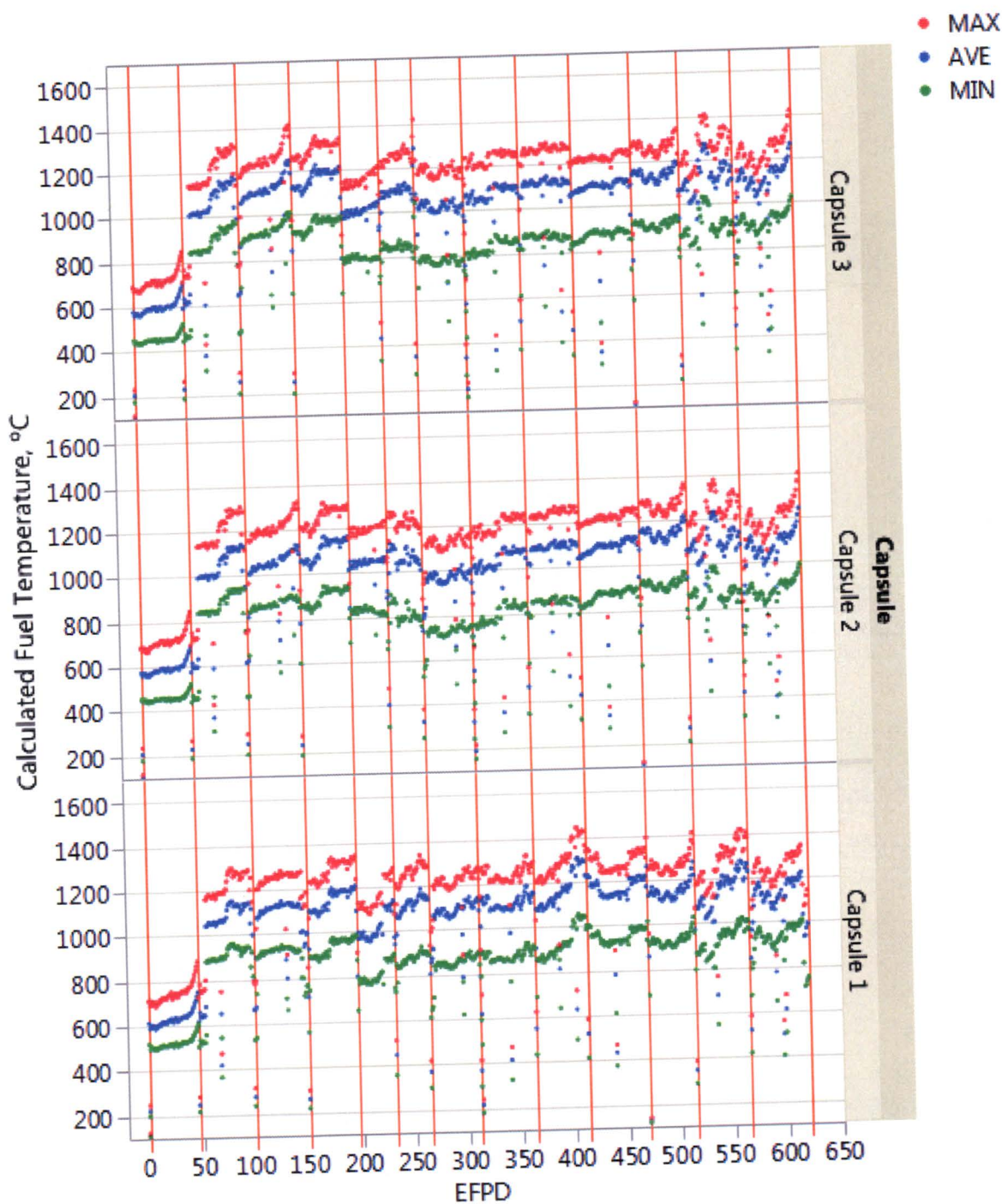


**Figure 6-14**  
 AGR-1 calculated daily minimum, maximum and volume average temperatures for capsules 1-3  
 Courtesy of Idaho National Laboratory and used with permission of Battelle Energy Alliance, LLC

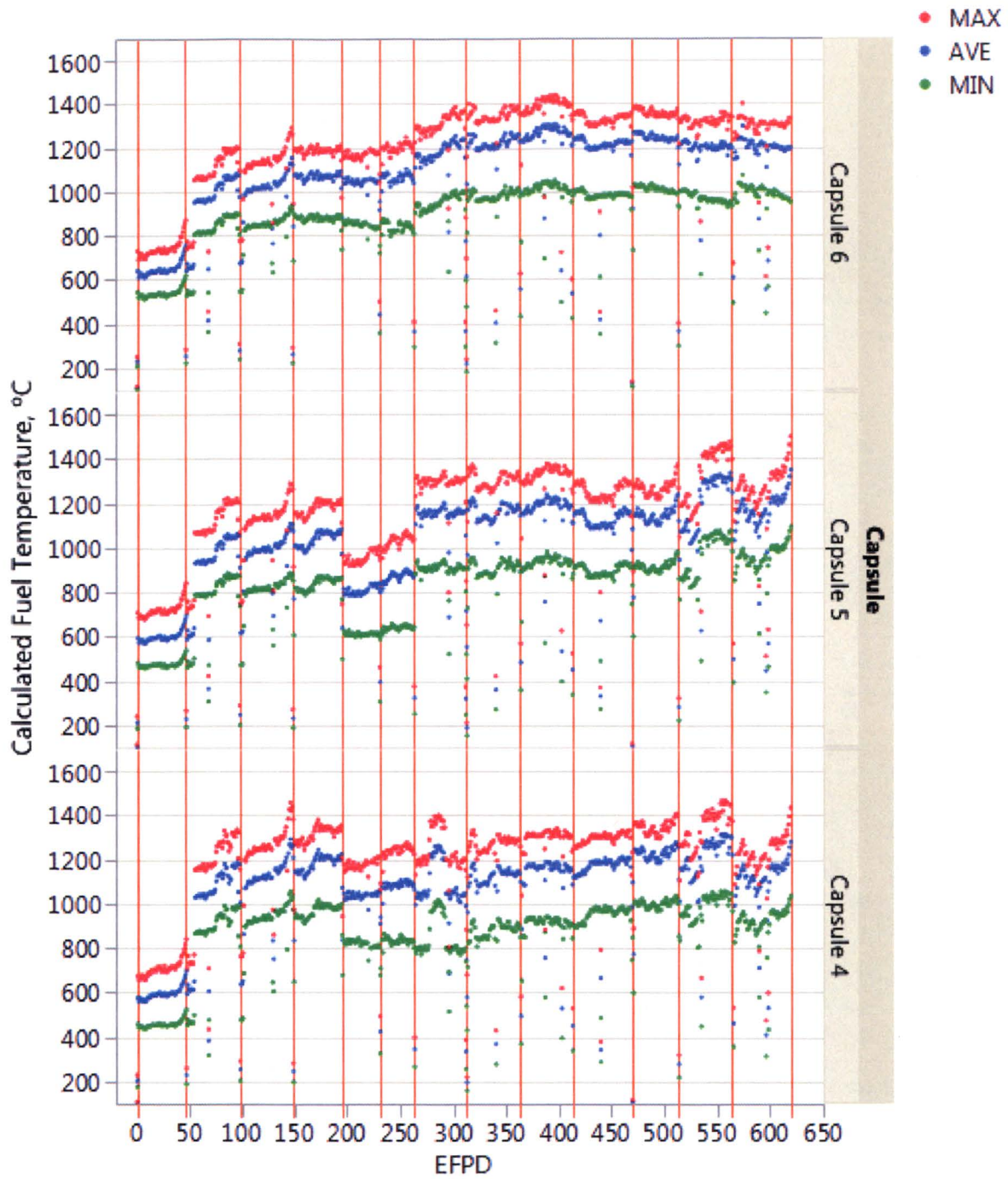


**Figure 6-15**  
AGR-1 calculated daily minimum, maximum, and volume average temperatures for capsules 4-6  
*Courtesy of Idaho National Laboratory and used with permission of Battelle Energy Alliance, LLC*

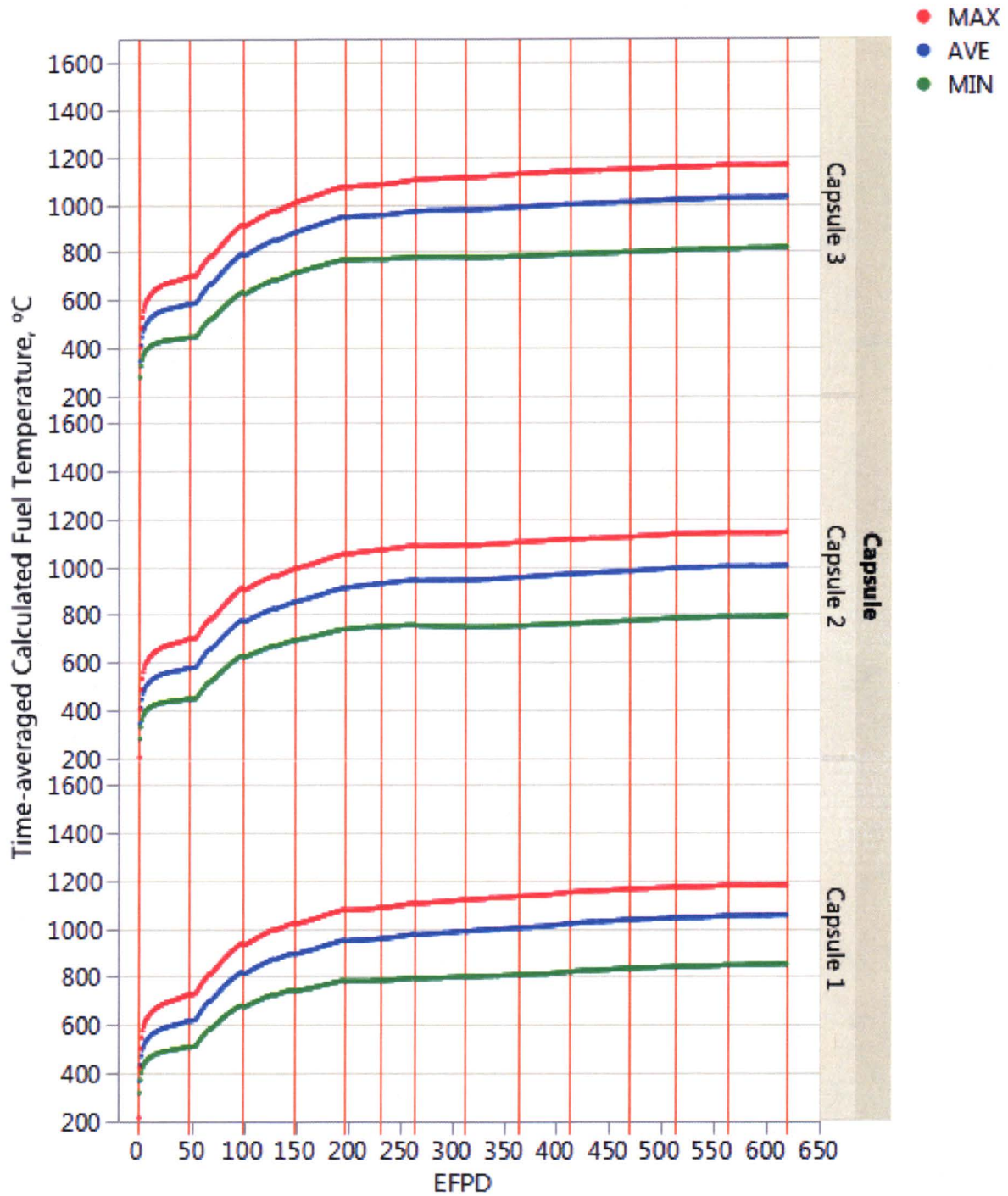


**Figure 6-16**  
 AGR-1 calculated time-average minimum, time-average maximum and time-average volume-average temperatures for capsules 1-3  
 Courtesy of Idaho National Laboratory and used with permission of Battelle Energy Alliance, LLC

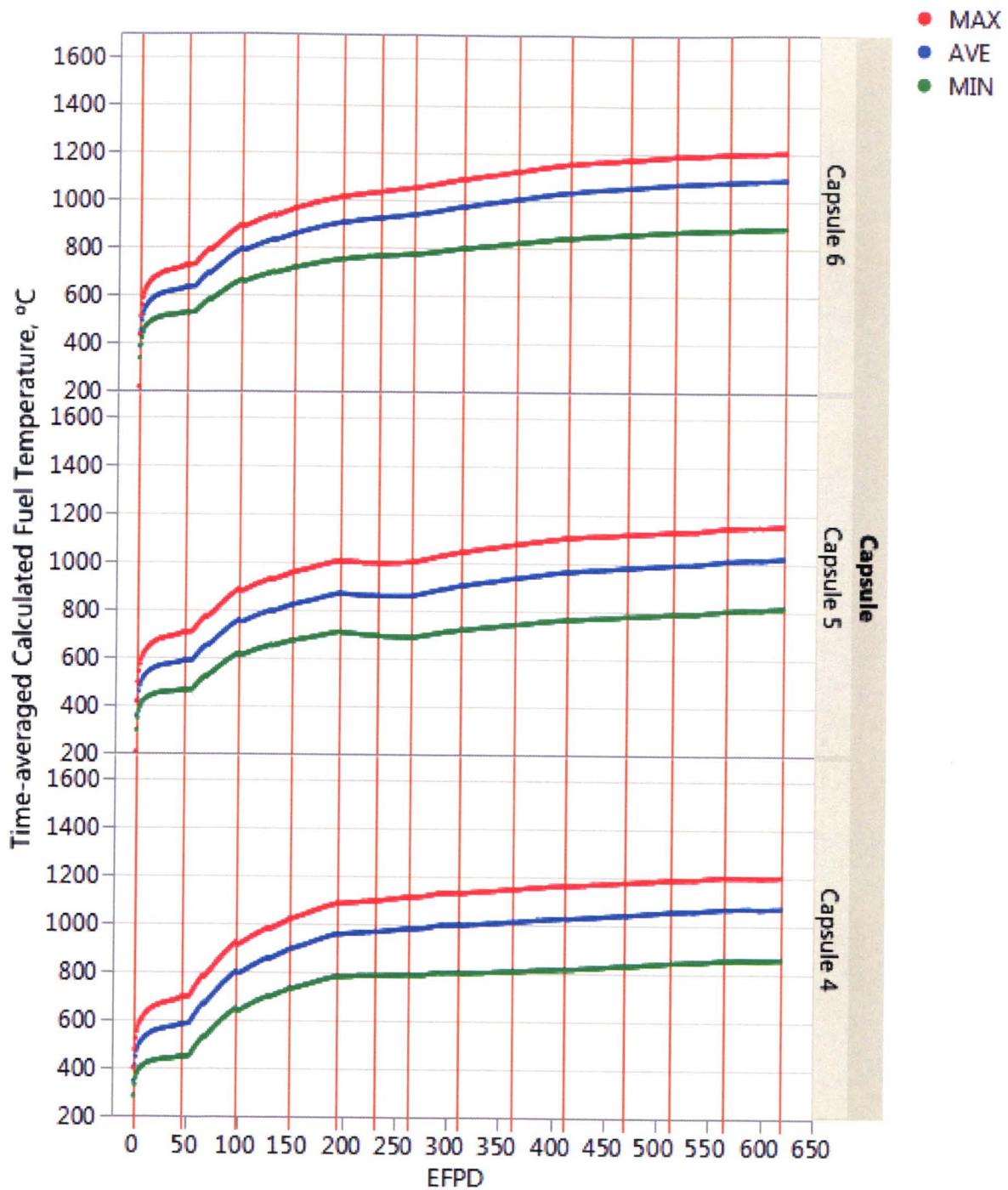


**Figure 6-17**  
**AGR-1 calculated time-average minimum, time-average maximum and time-average volume-average temperatures for capsules 4-6**  
 Courtesy of Idaho National Laboratory and used with permission of Battelle Energy Alliance, LLC

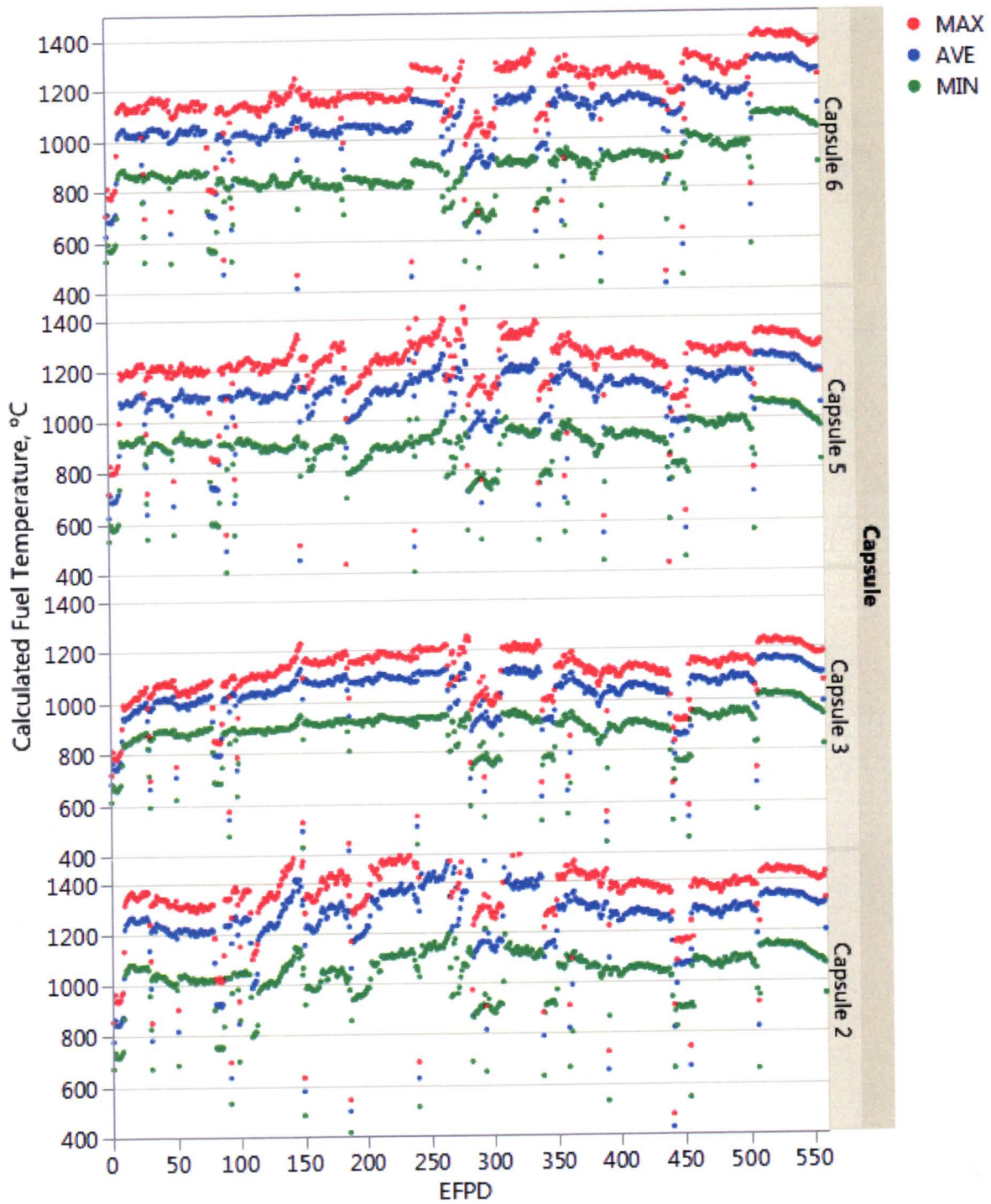


**Figure 6-18**  
AGR-2 calculated daily minimum, maximum, and volume average temperatures  
Courtesy of Idaho National Laboratory and used with permission of Battelle Energy Alliance, LLC

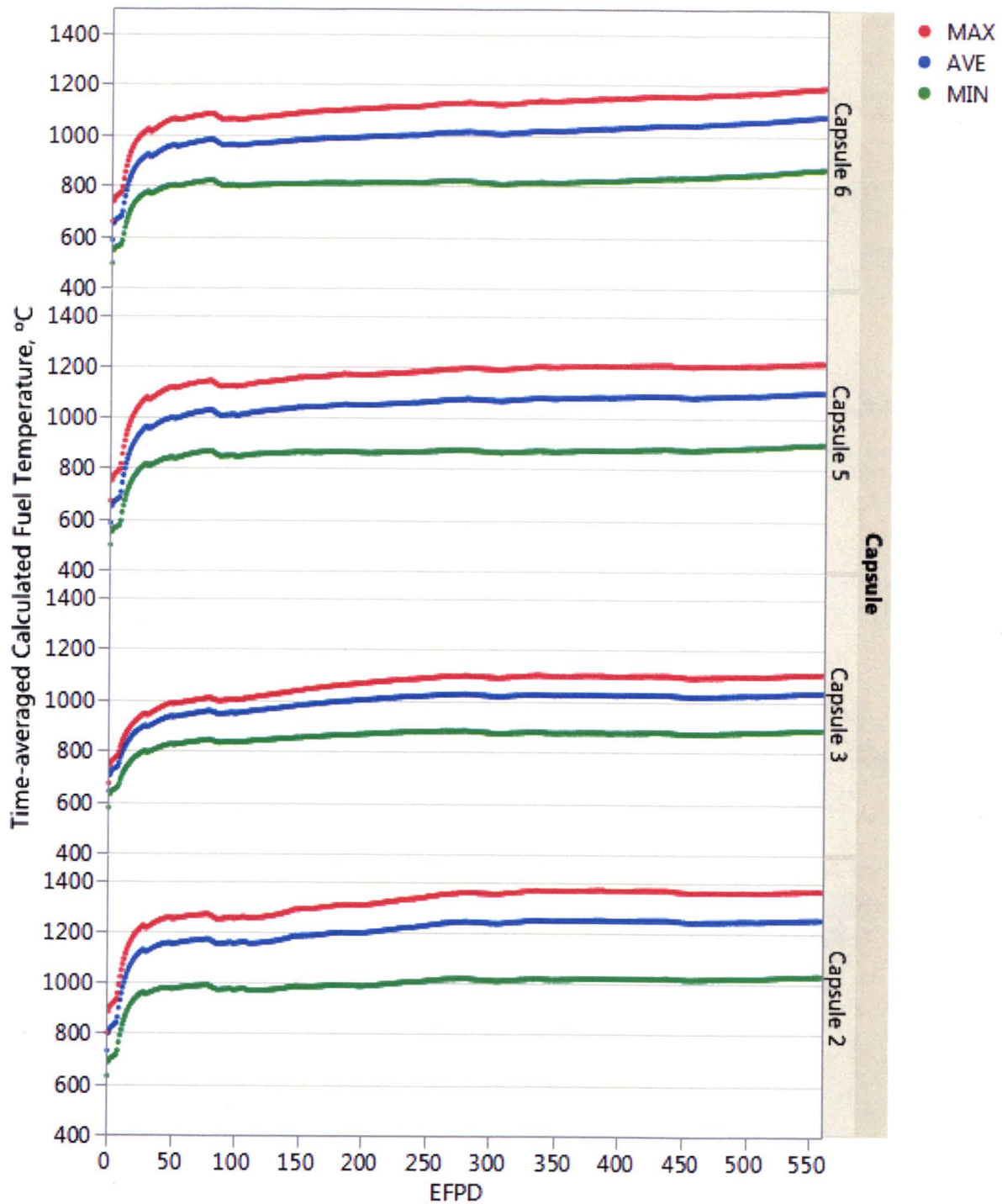


**Figure 6-19**  
**AGR-2 calculated time-average minimum, time-average maximum, and time-average volume-average temperatures**  
 Courtesy of Idaho National Laboratory and used with permission of Battelle Energy Alliance, LLC



**Table 6-4**  
**End-of-irradiation time-average temperatures for AGR-1 and AGR-2 capsules**

Capsule Number	Time-Average Minimum Temperature (°C)	Time-Averaged Volume-Average Temperature (°C)	Time-Average Maximum Temperature (°C)
<b>AGR-1 UCO</b>			
1	854	1054	1167
2	800	1002	1124
3	828	1028	1147
4	866	1070	1187
5	818	1023	1144
6	885	1087	1197
<b>AGR-2 UCO</b>			
2	1034	1252	1360
5	923	1101	1210
6	868	1074	1183
<b>AGR-2 UO<sub>2</sub></b>			
3	889	1032	1105

#### 6.4 Thermocouple Measurement and Performance

Temperature measurements for both AGR-1 and AGR-2 were performed by TCs terminating within the graphite sample holders of each capsule. These measurements supported temperature control of the experiment where designated control TCs provided feedback to the automated sweep gas control system that adjusted gas blends to maintain reference temperatures. TC measurements are also used to support thermal analyses of the test train, which are used to calculate fuel temperatures. When a control TC failed during the irradiation, a previously selected back-up TC within the same capsule was used as the control TC and the reference control temperature reset based on thermal analysis calculations. When all TCs failed within a capsule, results from physics and thermal analyses, and operating history of adjacent capsules were used to manually set the gas blends of the affected capsule.

The AGR-1 test train was designed with 19 TCs; three TCs failed during fabrication and seven more failed during operation. The two failure mechanisms for the TCs were the formation of virtual junctions and open circuit failures where the signal ceases altogether. Virtual junctions are detected by perturbing the temperature in a single capsule using gas flow, then observing the TC readings from capsules below this one to see if they respond. If a capsule TC responds to temperature changes in a capsule above it, it is likely a virtual junction has formed, and the TC can be considered failed. TC-2 in Capsule 5 was damaged during fabrication of the test train and was never operational. By the end of irradiation, all TCs in Capsules 1, 2, and 3, plus TC-3 in Capsule 4, had been declared failed.

The AGR-2 TCs did not perform as well as in AGR-1. Fewer TCs were used in AGR-2 than in AGR-1, but their diameters were larger to accommodate larger thermo-elements, which were expected to provide better survivability. The sheath material was changed from the Inconel 600 used in AGR-1 to niobium. It is hypothesized the sheaths became brittle during irradiation and started fracturing in the later stages of irradiation due to both thermal expansion and contraction upon heat-up and cool-down, as well as from handling of the test train when it was moved for high-power cycles in ATR, causing the TCs to fail. Of the 11 TCs in Capsules 2, 3, 5, and 6, one failed during fabrication and the other 10 TCs failed during operation between the second and final AGR-2 irradiation cycles. All TC failures were attributed to open circuit failure, which is typically caused by breakage of a thermo-element wire or the junction itself. However, temperature control of all capsules was maintained using thermal analysis calculations that were benchmarked against the TC measurements before the TCs failed.

TC drift was assessed by analysis, which used as-run sweep gas mixes and heat generation rates from physics analyses, where thermal model results for the specific TC location were compared to TC readings. Figure 6-20 shows the differences between the measured and calculated TC temperatures in the AGR-1 irradiation while the TCs were considered operational. Data are not shown for TCs after they were declared failed. A downward drift of measured TC temperatures relative to calculated TC temperatures over irradiation time can be observed in TC-2 (red dots in Figure 6-20) in Capsules 2, 3, and 4. Readings from other TCs are consistent with their simulation results. The differences between what was measured and what was calculated was generally within  $\pm 100^{\circ}\text{C}$ , although this threshold was exceeded in some instances, particularly in the second half of the irradiation.

Similar results are shown in Figure 6-21 for AGR-2. TC-3 in Capsule 6, and to a lesser extent TC-2 and TC-5 in Capsule 6, show evidence of drift. Except for TC-3 in Capsule 6, the agreement between the measured and calculated TC temperatures for the UCO capsules were within  $\pm 100^{\circ}\text{C}$ . For Capsule 3 ( $\text{UO}_2$  fuel) the agreement is much better, within  $\pm 20\text{-}50^{\circ}\text{C}$ .

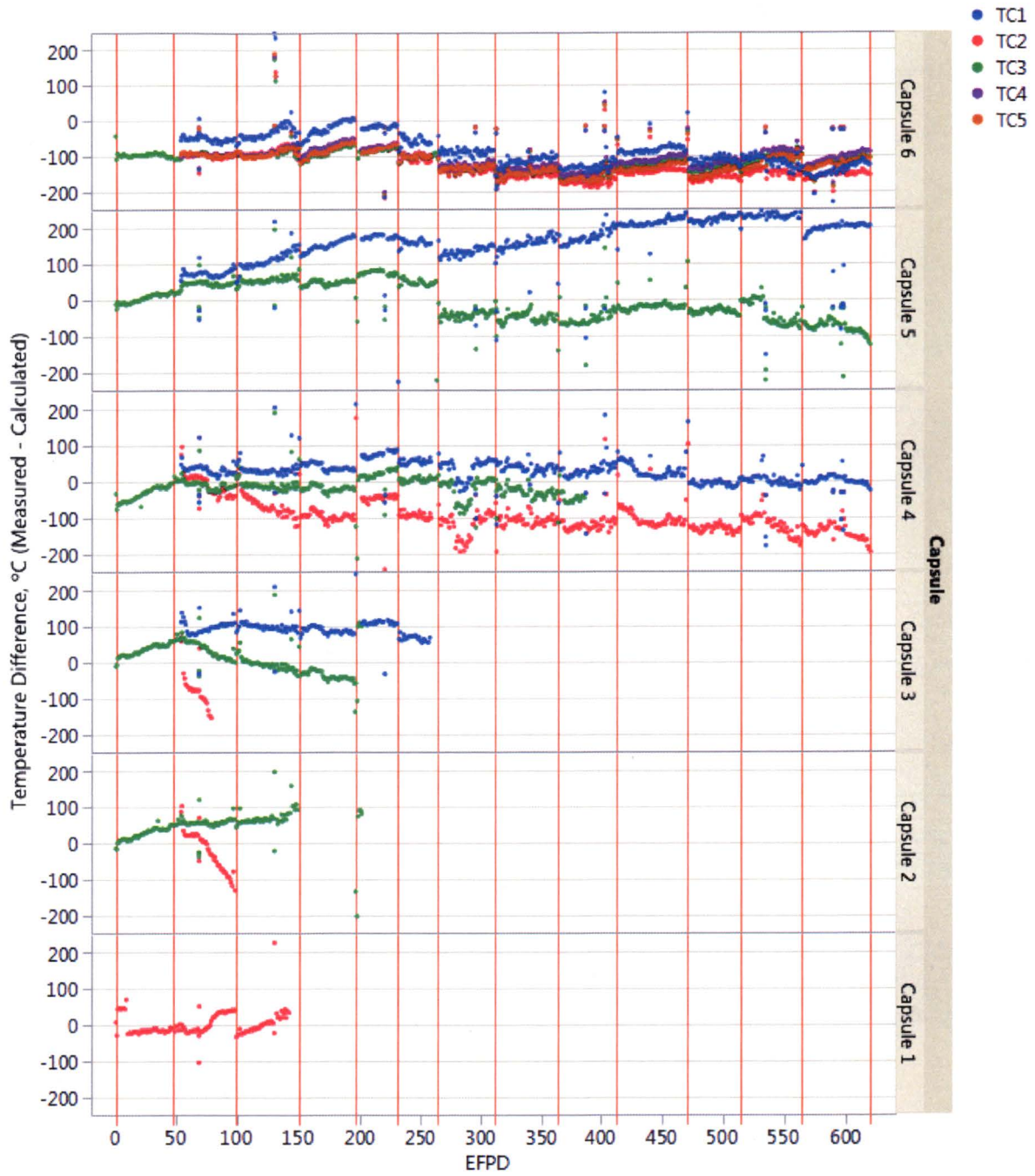


**Figure 6-20**  
**Difference between measured and calculated TC temperatures for AGR-1 versus EFPDs**  
*Courtesy of Idaho National Laboratory and used with permission of Battelle Energy Alliance, LLC*

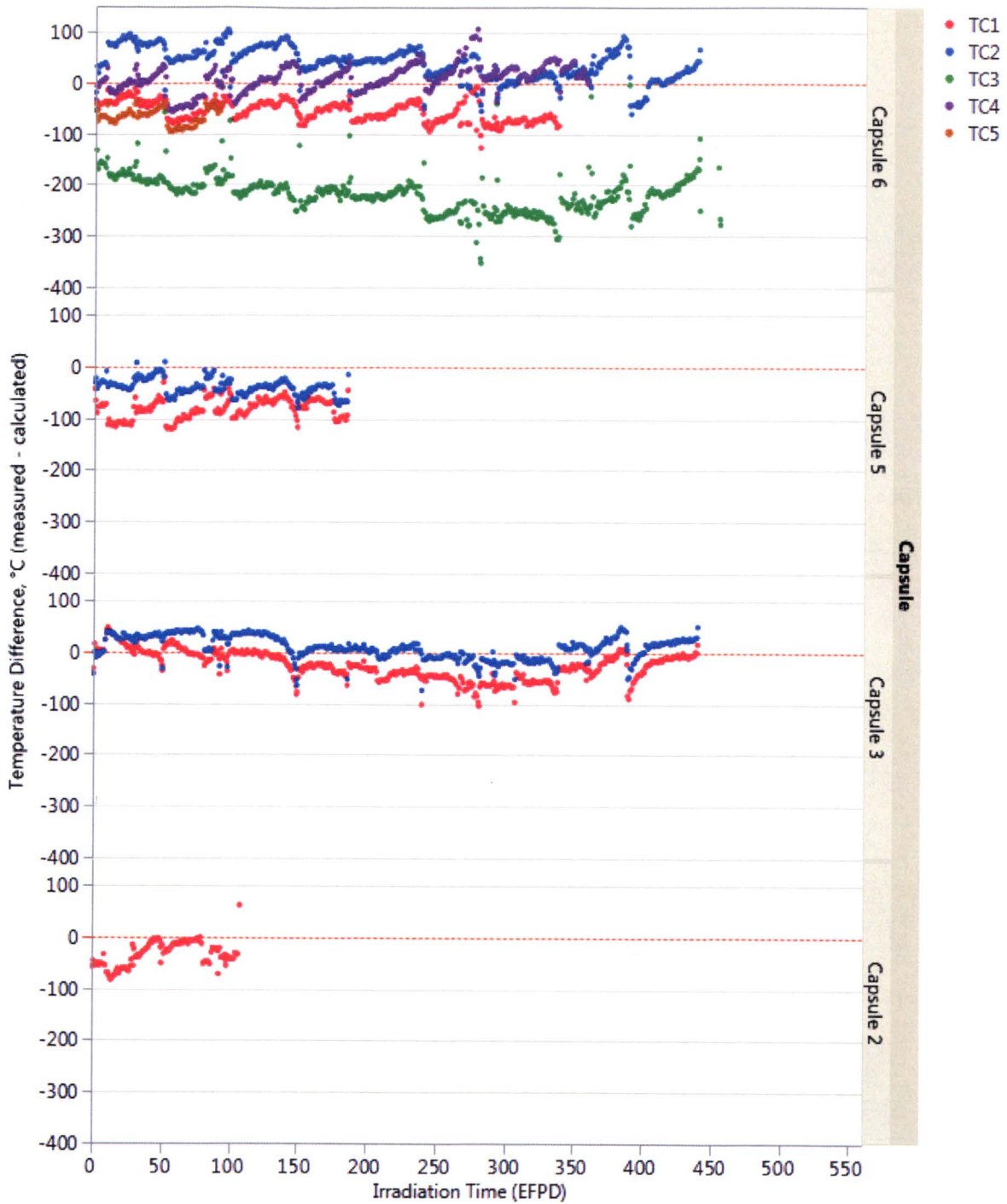


**Figure 6-21**  
**Difference between measured and calculated TC temperatures for AGR-2 versus EFPDs**  
*Courtesy of Idaho National Laboratory and used with permission of Battelle Energy Alliance, LLC*

## 6.5 Uncertainty Quantification of Calculated Temperatures

An uncertainty analysis has been performed for the temperature estimates in AGR-1 using a formal uncertainty propagation protocol that considers both the traditional uncertainties of each key variable used in the calculation, but also includes the first order cross-correlation effects of the key variables in the uncertainty estimates [78]. The uncertainties in predicted temperatures using this approach change over the course of the irradiation since uncertainties in key inputs like gas gap size increased with time due to carbonaceous matrix shrinkage (primarily an effect of accumulated fast fluence) and fuel heat rate changes due to fissile burnup and changes in ATR operation. The uncertainties also vary by capsule and experiment given the different gas gap sizes used in each capsule. The results identify those input parameters having the greatest impact on the overall uncertainty, which has been helpful in designing the follow-on capsules.

To quantify the uncertainty of AGR-1 calculated temperatures, the uncertainty assessment identified and analyzed Abaqus FEA model parameters of potential importance to the AGR-1 predicted fuel temperatures. Specifically, the key variables include: (1) the width of the control gas gap; (2) the neon gas fraction; (3) the fuel heat rate; (4) the graphite holder thermal conductivity; and (5) the fuel compact thermal conductivity. Expert judgments were used as a basis to specify the uncertainty range for a set of select parameters, including those with high sensitivity and those with large uncertainty. The overall effect of a parameter uncertainty on the model prediction variation is a product of input uncertainty and its sensitivity coefficient. Propagation of model parameter uncertainty was then used to quantify the overall uncertainty of AGR-1 calculated temperatures.

The overall uncertainty in the calculated temperatures for AGR-1 ranged from 2.0 to 6.5% (~40 to 60°C at  $1\sigma$  and 100 to 120°C at  $2\sigma$ ), depending on irradiation time (thermal conditions), capsule, and the temperature parameter being predicted (for example, peak fuel temperature, volume-average fuel temperature, or TC temperature). Table 6-5 presents temperatures and their relative and absolute standard deviations for TAVA and time-average maximum fuel temperatures at the end of AGR-1 for six capsules.

**Table 6-5**  
**Temperatures (T) and uncertainty ( $\sigma_T$ ) for time-average fuel temperatures at the end of AGR-1**

Capsule	Time-Average Volume-Average Fuel			Time-Average Maximum Fuel		
	T, °C	$\sigma_T$ , %	$\sigma_T$ , °C	T, °C	$\sigma_T$ , %	$\sigma_T$ , °C
Capsule 6	1088	5.014	55	1204	5.012	60
Capsule 5	1023	3.700	38	1157	4.301	50
Capsule 4	1070	3.743	40	1202	4.327	52
Capsule 3	1029	3.777	39	1162	4.330	50
Capsule 2	1003	3.830	38	1141	4.379	50
Capsule 1	1055	3.165	33	1178	3.776	45

Temperatures differ from those reported in Table 6-2 and in the AGR-1 Irradiation Test Final As-Run Report [59] due to the method used to convert daily temperature data to capsule-average and capsule-maximum values [79].

In some cases, the uncertainty is dominated by uncertainty in fuel heat rate (for example, Capsule 6). For peripheral TCs, the uncertainty is driven by the increasing uncertainty of the control gas gap distance, especially for the middle capsules at the end of irradiation. The increase of gap uncertainty has more effect on the temperature uncertainty of peripheral TCs than on the uncertainty of the center TC. The fuel temperature uncertainty is dominated by uncertainties in fuel and graphite thermal conductivity. The center TC uncertainty is dominated by uncertainties in graphite thermal conductivity.

The daily capsule volume-average and capsule peak temperatures, along with one standard deviation (indicated by the shaded regions) in AGR-1 Capsule 4 are presented in Figure 6-22 (instantaneous) and Figure 6-23 (time-average) as illustrations.

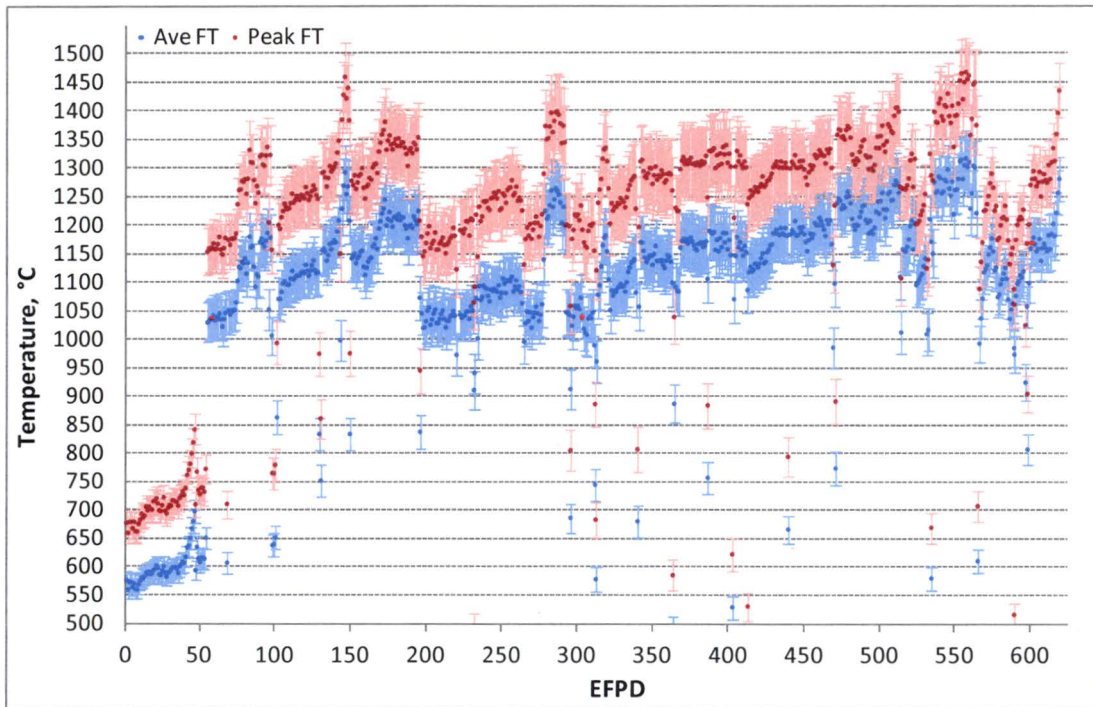


**Figure 6-22**  
**Instantaneous peak and average fuel temperature (FT) and associated uncertainty for AGR-1 Capsule 4**

*Courtesy of Idaho National Laboratory and used with permission of Battelle Energy Alliance, LLC*

A similar analysis was performed for the AGR-2 capsules [80]. Uncertainties in the fuel heat rate and gas gap dominate the uncertainties in the time-average volume-average temperatures and in TC temperatures. The fuel and graphite thermal conductivities have minor impacts on the TC uncertainty. Uncertainties at one sigma range from 30°C to 40°C for the TAVA temperatures and 35°C to 45°C for the time-average maximum temperatures, similar to AGR-1.

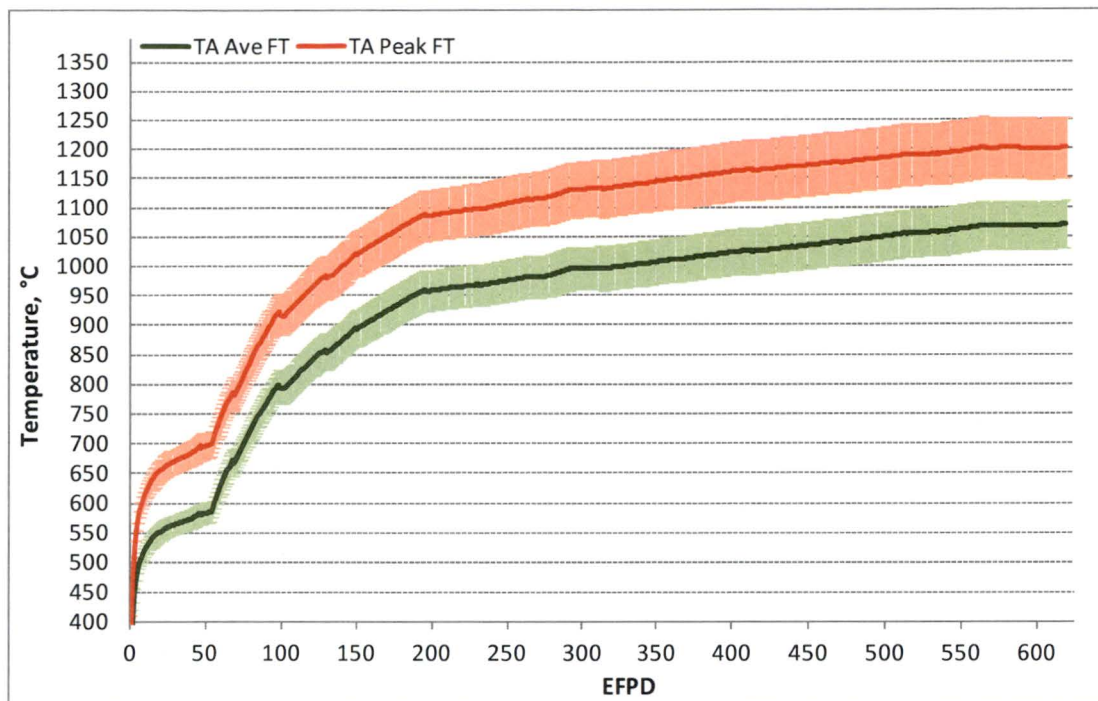


**Figure 6-23**

**Time-average (TA) peak and time-average volume-average fuel temperatures (FT) for AGR-1 Capsule 4**

*Courtesy of Idaho National Laboratory and used with permission of Battelle Energy Alliance, LLC*

## 6.6 Broader Comparisons of Key Service Conditions

The fuel particles in both AGR-1 and AGR-2 experienced a range of burnups, TAVA temperatures, and fluences during their exposure in ATR. Each particle experienced a unique “trajectory” to its final service conditions in the experiment. Figure 6-24 presents 3-D scatter plots of burnup, fluence, and TAVA temperatures for the 72 compacts in AGR-1 (left pane) and the 36 UCO compacts in AGR-2 (right pane). Also shown on each two-dimensional projection are the burnup-temperature, fluence-temperature, and burnup-fluence combinations experienced by each compact. The particles in AGR-1 and AGR-2 experienced a broad range of temperature-burnup-fluence trajectories under irradiation, which serve as a solid foundation to demonstrate the performance of UCO TRISO-coated particles for use in HTRs. The distribution of individual fuel compact TAVA temperatures and burnup is further highlighted in Figure 6-25. The data demonstrate the approximately 200°C distribution in temperatures for all of the fuel with the exception of AGR-2 Capsule 2, which had appreciably higher temperatures.

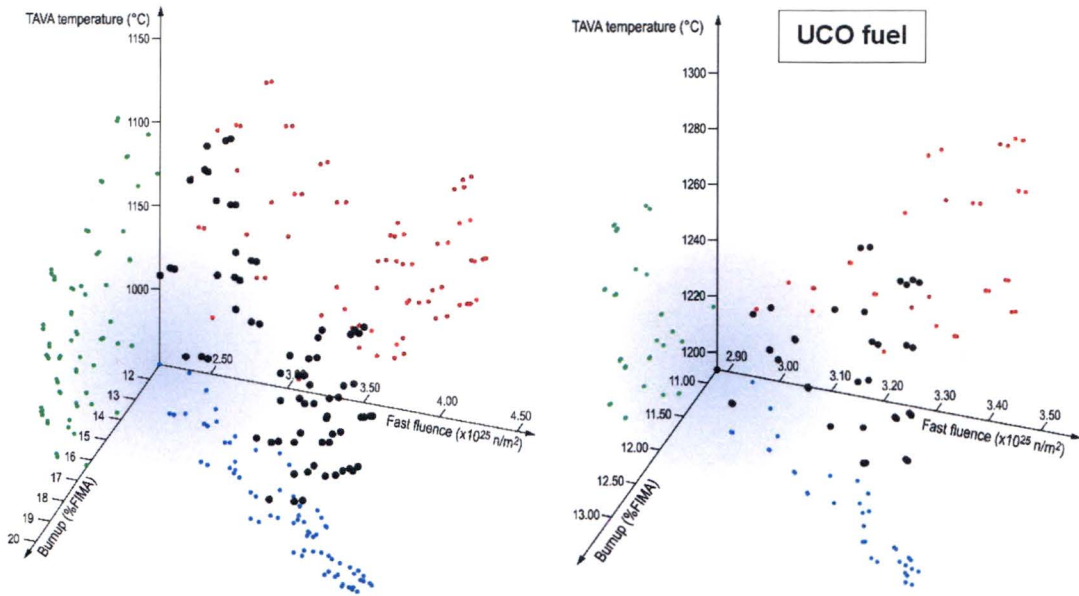


**Figure 6-24**  
**3-D scatter plot of the irradiation characteristics of the 72 AGR-1 (left pane) and 36 AGR-2 (right pane) UCO compacts**  
 Courtesy of Idaho National Laboratory and used with permission of Battelle Energy Alliance, LLC

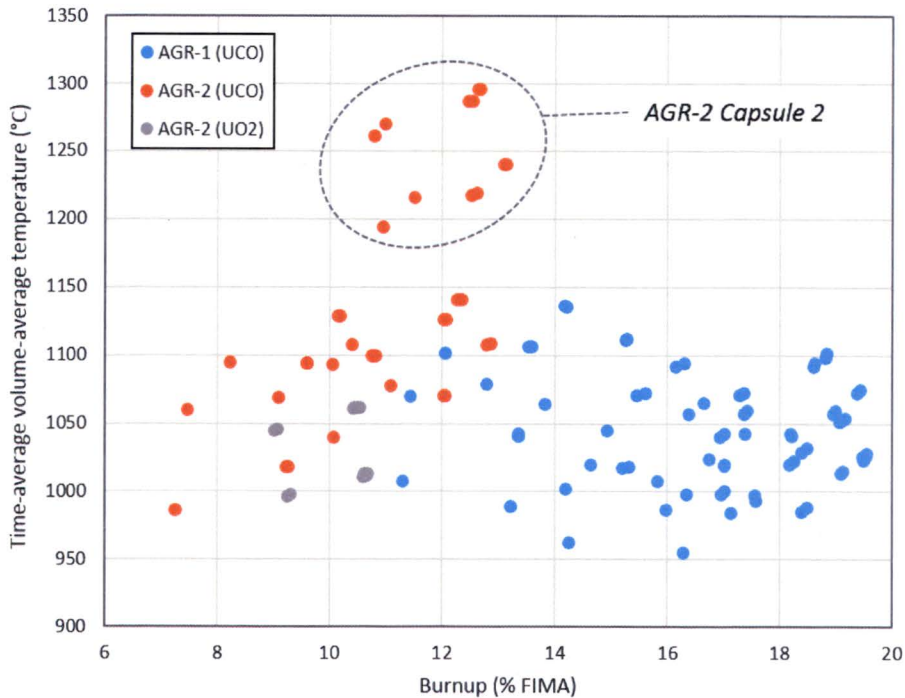


**Figure 6-25**  
**AGR-1 and AGR-2 fuel compact TAVA temperatures as a function of burnup**  
 Courtesy of Idaho National Laboratory and used with permission of Battelle Energy Alliance, LLC



Further detail on the fuel temperature distributions is provided in Figure 6-26, which presents a cumulative distribution of the duration that fractions of the particle population spent in specific temperature ranges in the AGR-1 irradiation. The data indicate the UCO TRISO fuel was exposed to very high temperatures for long durations, well in excess of those expected in an actual HTGR. Peak time-average temperatures in prismatic HTGRs are usually less than 1250°C. Based on the figure, about 15% of the particle population experienced temperatures in excess of 1250°C for 200 days, 10% of particle population experienced temperatures in excess of 1300°C for 100 days, 5% of particle population experienced temperatures in excess of 1350°C for 50 days, and 2% of particle population experienced temperature in excess of 1400°C for 25 days.

The more severe AGR-1 irradiation conditions compared to the vast majority of historic HTGR designs, demonstrate substantial fuel performance margin. Similar plots are provided in Figure 6-27 and Figure 6-28 for AGR-2 where the results from Capsule 2 are separated from Capsules 5 and 6 because it was designed to operate at a time-averaged peak temperature of 1400°C (an early margin test), whereas the other two capsules were designed to be operated at a time-average peak temperature of  $\leq 1250^\circ\text{C}$ .

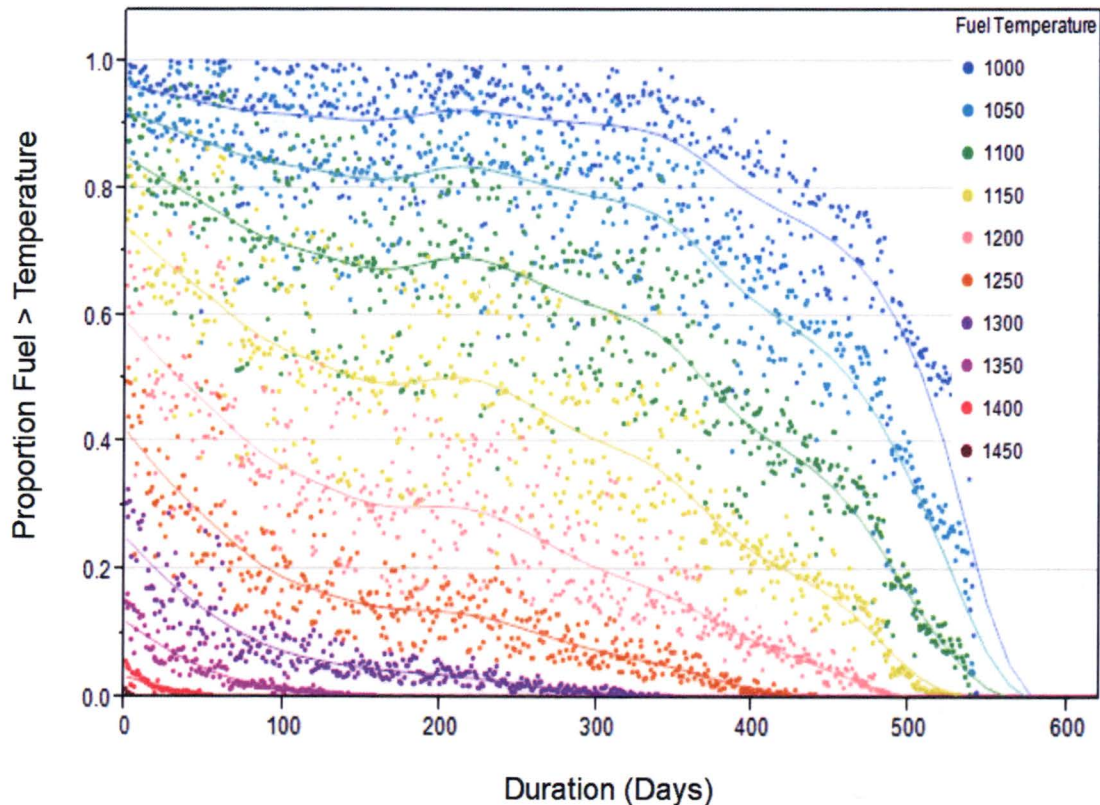


**Figure 6-26**

**Distribution of time at temperature experienced by TRISO fuel particles in AGR-1**

*Courtesy of Idaho National Laboratory and used with permission of Battelle Energy Alliance, LLC*

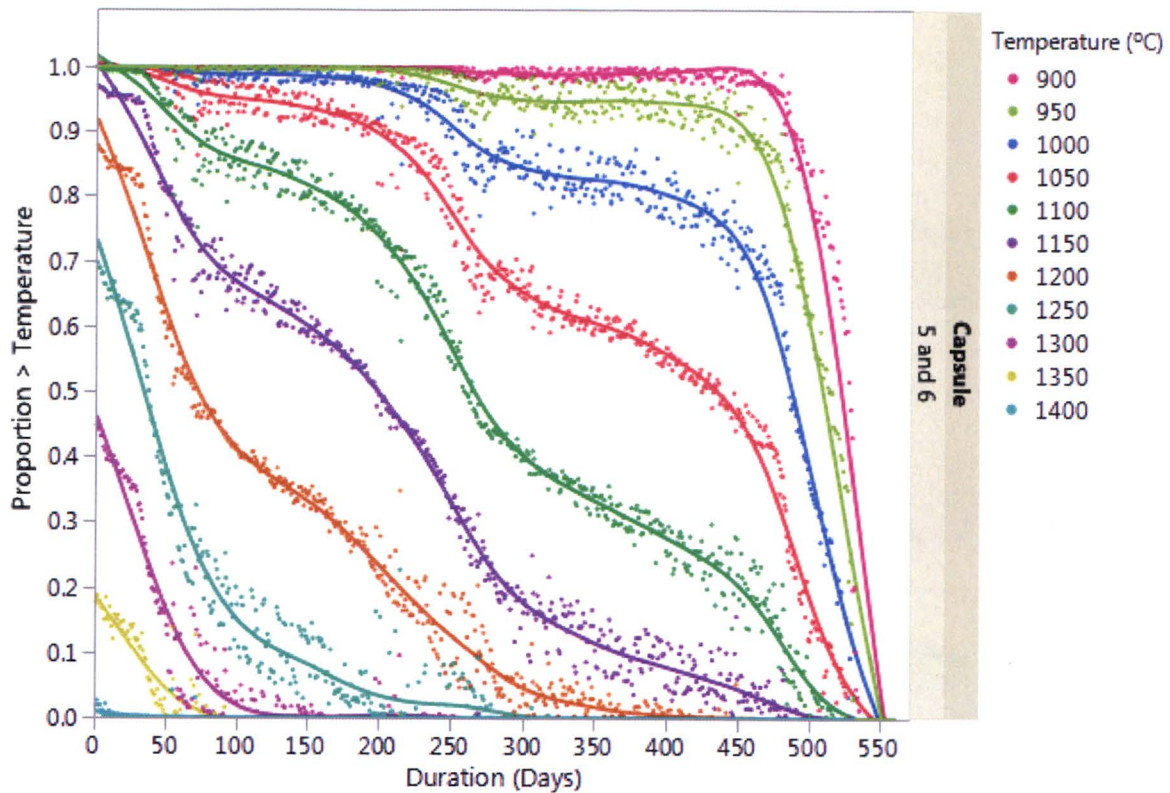


**Figure 6-27**  
**Distribution of AGR-2 time at temperature for Capsules 5 and 6 UCO fuel (designed to operate at a time-average temperature of 1250°C)**  
 Courtesy of Idaho National Laboratory and used with permission of Battelle Energy Alliance, LLC

The calculated temperatures in AGR-2 are similar to those in AGR-1 in that much of the fuel operated at high-temperature for significant amounts of time. A key facet of the AGR-2 experiment is the performance results of the UCO in Capsule 2, in which large fractions of the fuel operated at very high temperature (for example, approximately 25% of the particles experienced temperatures in excess of 1400°C for more than 100 days and approximately 10% of the fuel experienced temperatures in excess 1500°C for 30 days).

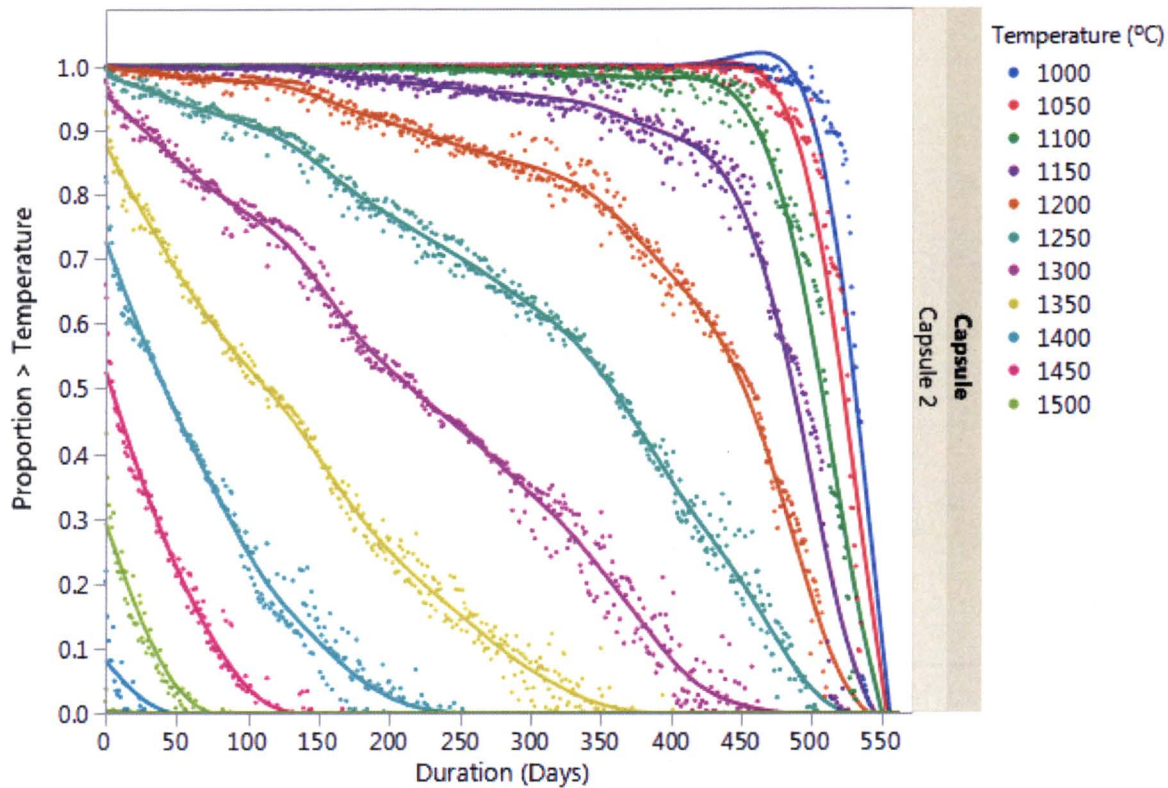


**Figure 6-28**  
**Distribution of AGR-2 time at temperature for Capsule 2 UCO fuel (designed to operate at a time-average peak temperature of 1400°C)**  
*Courtesy of Idaho National Laboratory and used with permission of Battelle Energy Alliance, LLC*

To provide another perspective of the severity of the AGR irradiations, the temperature distributions from the six capsules in AGR-1 and in Capsules 2, 5, and 6 of AGR-2 (comprising all U.S. UCO fuel) are compared to the distribution calculated for the SC-MHR reactor, a GA MHTGR design with an outlet temperature of 750°C. As can be seen in Figure 6-29, the irradiations are very bounding in terms of temperature relative to that expected in the GA design. The effect would be even more exacerbated in a pebble-bed since the fuel in pebble-bed reactors tends to run cooler than prismatic reactors at the same outlet temperature. These fuel temperatures are significantly higher than expected in FHR designs.

The AGR program recognizes the temperatures in the AGR-1 and AGR-2 irradiations are overly conservative relative to that expected in an operating reactor, but the temperatures were appropriate given the objectives of each experiment: (1) AGR-1 was a proof-of-concept experiment to determine the performance of UCO TRISO-coated particle fuel at the aggressive high-burnup high-temperature conditions proposed for some HTGR designs; and (2) AGR-2 had as its goal to demonstrate the performance of UCO TRISO-coated particle fuel produced in an engineering-scale coater and to perform an early high-temperature margin test.

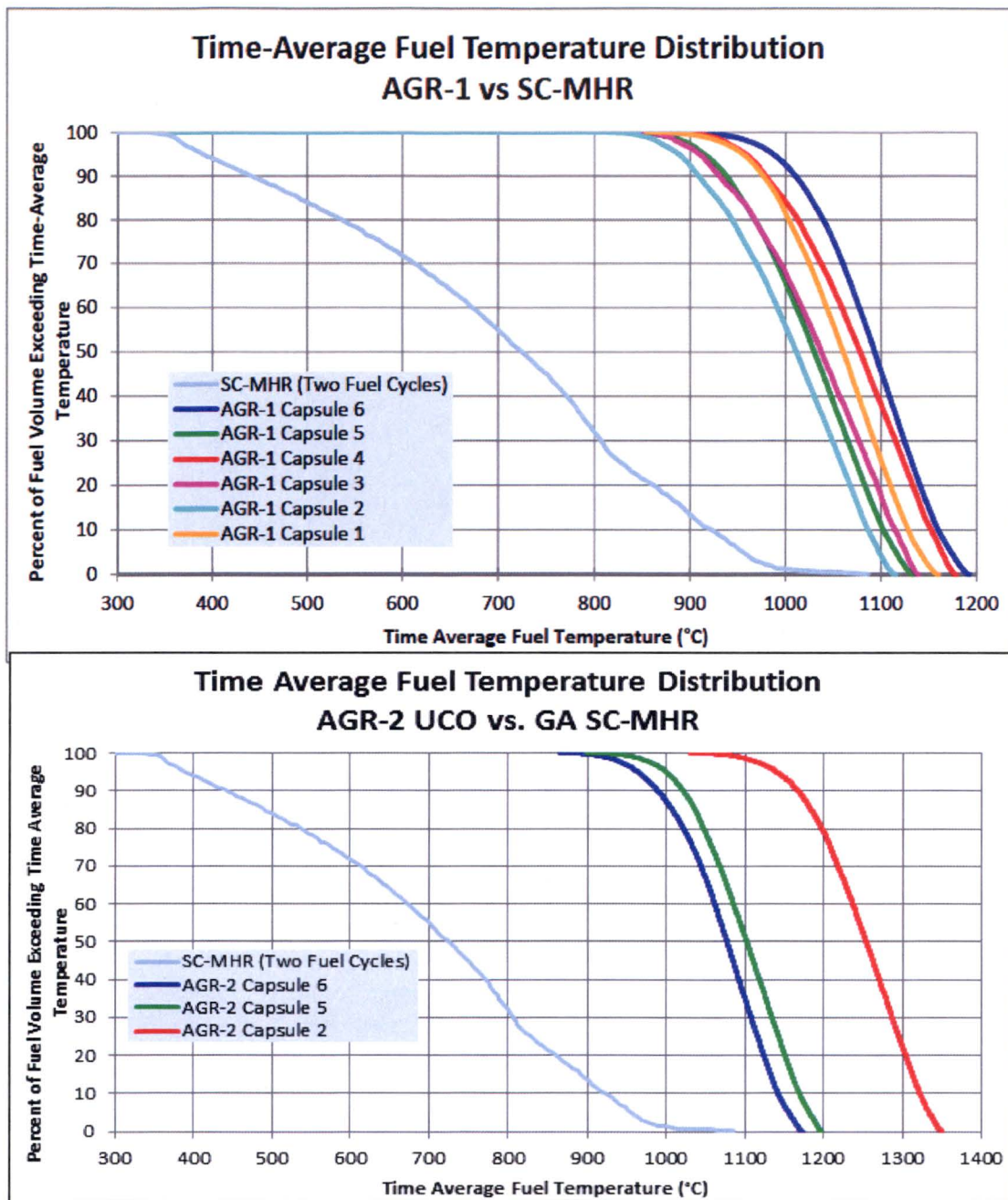


**Figure 6-29**  
 Comparison of fuel temperature distribution in AGR-1 and AGR-2 capsules with that expected from a 750°C outlet temperature HTGR (the GA SC-MHR)  
 Courtesy of Idaho National Laboratory and used with permission of Battelle Energy Alliance, LLC

## 6.7 Fission Gas Release

The release rate of fission product gases from TRISO fuel particles is a direct method of assessing fuel performance. Fission product R/B ratio values provide indicators of initial fuel quality (that is, level of contamination and as-manufactured exposed fuel kernels) and fuel performance (subsequent TRISO failures) during irradiation. The fission gas isotopes measured by the FPMS during AGR-1 and AGR-2 include  $^{85m}\text{Kr}$ ,  $^{87}\text{Kr}$ ,  $^{88}\text{Kr}$ ,  $^{89}\text{Kr}$ ,  $^{90}\text{Kr}$ ,  $^{131m}\text{Xe}$ ,  $^{133}\text{Xe}$ ,  $^{135}\text{Xe}$ ,  $^{135m}\text{Xe}$ ,  $^{137}\text{Xe}$ ,  $^{138}\text{Xe}$ , and  $^{139}\text{Xe}$ . These nuclides were selected for the R/B evaluations because they have relatively short half-lives, allowing each isotope to reach equilibrium concentration in the fuel during each ATR irradiation cycle. The FPMS system described earlier was used to quantify release rates during irradiation giving the R/B ratios for the radionuclides of interest.

The spectrometer detector systems measure the concentrations of various krypton and xenon isotopes in the sweep gas from each capsule. Eight-hour counting intervals are used to measure the isotope concentrations in the sweep gas. The radionuclides of interest decay in transit from the capsule to the counters. Given a certain measured activity,  $A$  ( $\mu\text{Ci}$ ), the radionuclide release rate,  $R$  (atoms/s), of a particular nuclide can be calculated as:

$$R = 3.7 \times 10^4 \frac{Ae^{\lambda V_T/f}}{(1 - e^{-\lambda V_S/f})}$$

Equation 6-1

Where:

$V_S$  is the sample volume (mL)

$\lambda$  is the nuclide decay constant ( $\text{s}^{-1}$ )

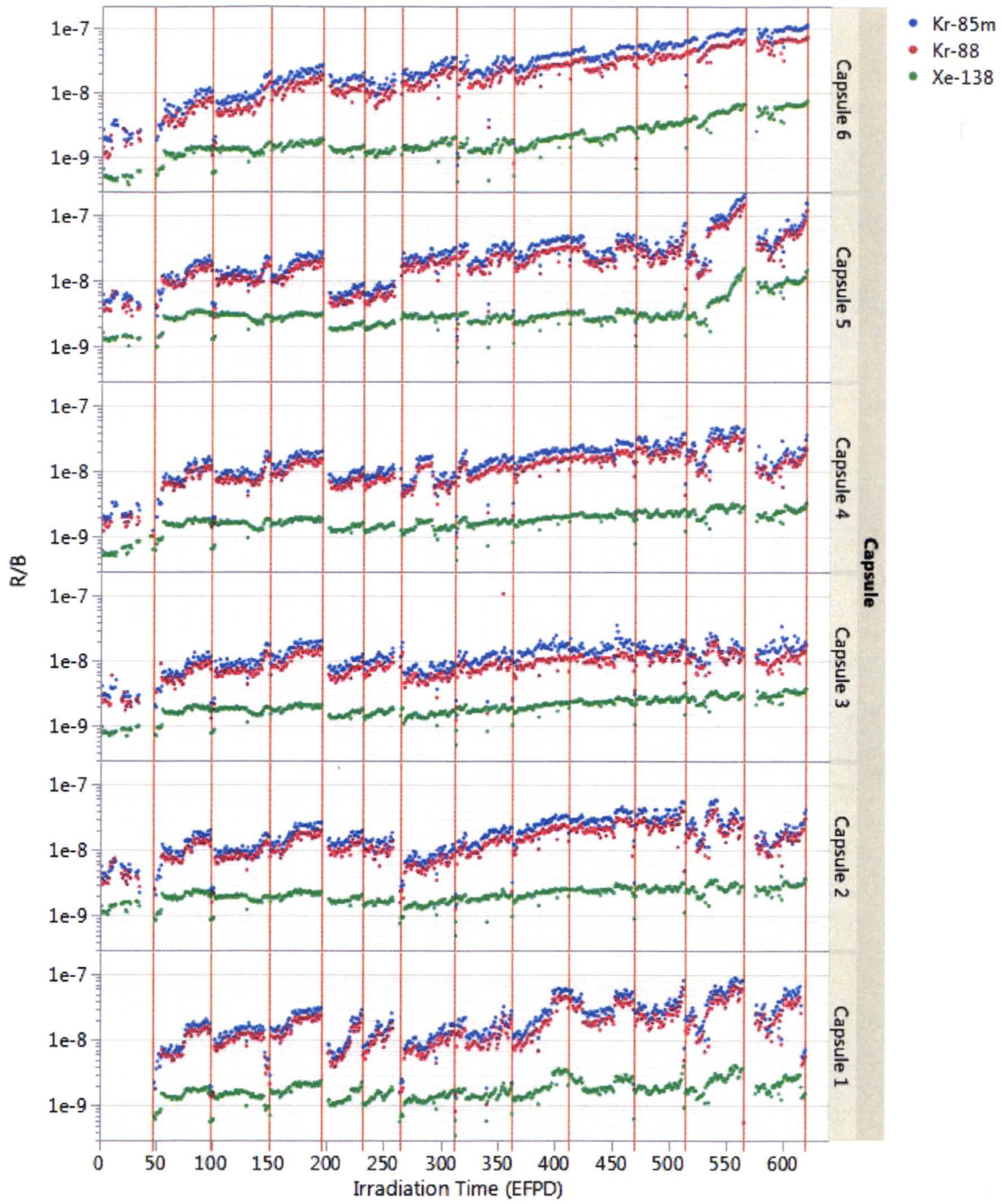
$f$  is the capsule volumetric flow rate (mL/s)

$V_T$  is the transport volume from the capsule to the sample volume (mL).

The transport volumes were determined during a lead-out flow experiment performed at the beginning of each irradiation.

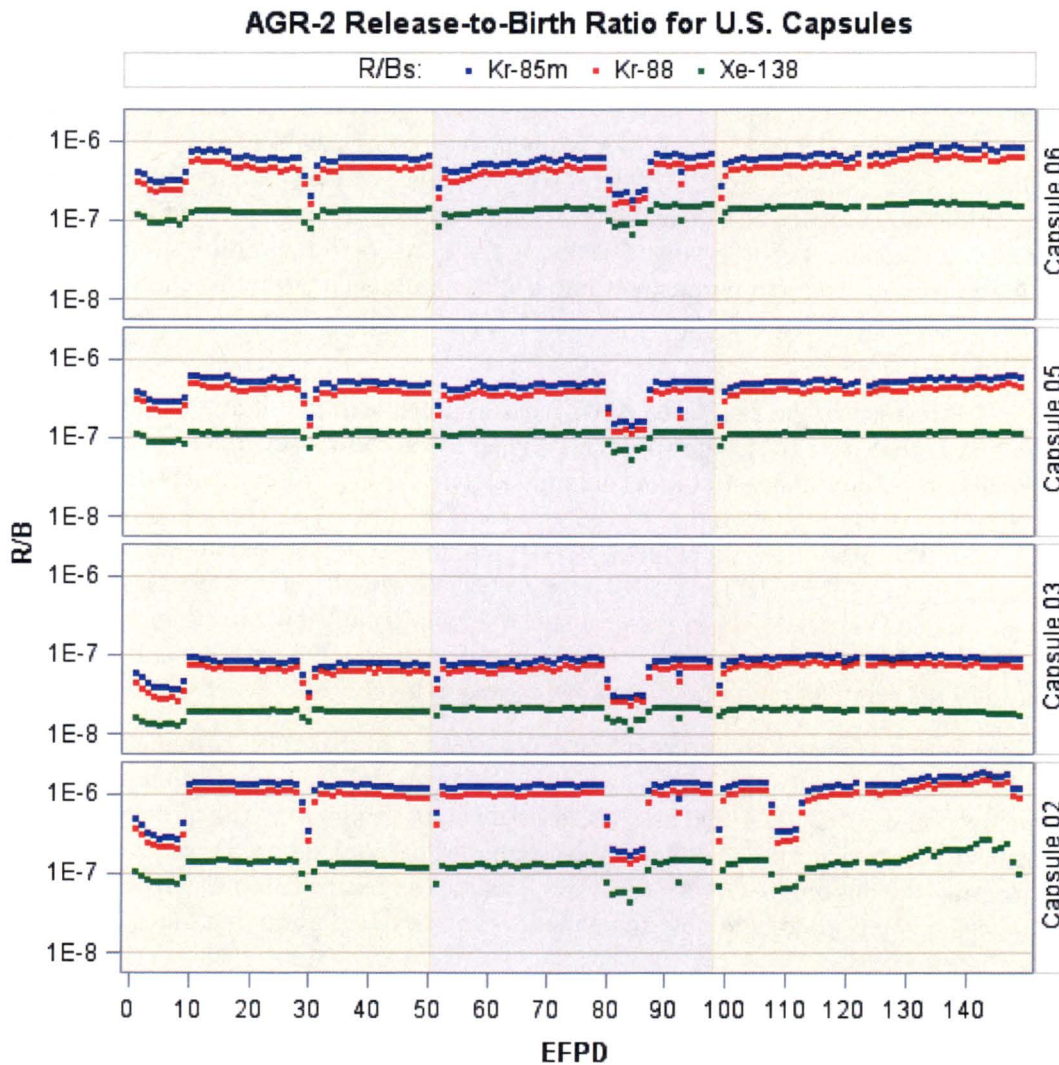
The birth rates of noble gas fission products of interest were calculated using ORIGEN2, Version 2.2. These calculations used compact flux and reaction rates from MCNP. The ORIGEN2 libraries used in the calculation were modified to remove the isotope depletion methods (transmutation and decay) for the isotopes of interest for birthrates. The increase in the concentration of the isotope during the irradiation time interval divided by the irradiation time interval was determined to be the birthrate of the isotope during the time interval. The ratio of the experimentally determined release rates to the calculated birth rates was then computed.

Figure 6-30 shows R/B versus time for  $^{85m}\text{Kr}$ ,  $^{88}\text{Kr}$ , and  $^{135}\text{Xe}$  for the AGR-1 irradiation. AGR-1 irradiation cycle numbers are shown across the top of the figure. These are daily average values filtered such that data coinciding with low reactor power or large helium flow rates are removed. The R/B ratios for these nuclides are below approximately  $10^{-7}$  for the duration of the test with the exception of Capsule 5, which reaches higher temperatures during the last two cycles than other capsules and ends the irradiation with an R/B of approximately  $2 \times 10^{-7}$ . (Note: An R/B of  $10^{-7}$  indicates for every 10 million fission gas atoms generated in fission only one is released.)



**Figure 6-30**  
**AGR-1 R/B ratios for  $^{85m}\text{Kr}$ ,  $^{88}\text{Kr}$ , and  $^{135}\text{Xe}$  versus time in EFPDs**  
*Courtesy of Idaho National Laboratory and used with permission of Battelle Energy Alliance, LLC*

Figure 6-31 shows R/B versus time for  $^{85m}\text{Kr}$ ,  $^{88}\text{Kr}$ , and  $^{138}\text{Xe}$  plotted for AGR-2 for the first three irradiation cycles. Gas flow problems were encountered following test removal from and re-insertion after 150 EFPDs to avoid irradiation during a high-power cycle in ATR. The physical handling of the capsule damaged the refractory gas lines and caused unintentional intermixing of the gas flows between the capsules. As a result, the fission gas data beyond 150 EFPDs (the third irradiation cycle) could not be qualified, and no conclusions about fuel performance beyond Cycle 3 can be drawn based on the R/B data. Accordingly, these data are not shown in Figure 6-31. The capsule gas flows were set to a uniform gas mixture in all capsules until the end of the irradiation so thermal analyses could be performed with a known gas mixture from that point on.



**Figure 6-31**  
**AGR-2 R/B ratios for  $^{85m}\text{Kr}$ ,  $^{88}\text{Kr}$ , and  $^{138}\text{Xe}$  versus time in EFPDs**  
 Courtesy of Idaho National Laboratory and used with permission of Battelle Energy Alliance, LLC

## 6.8 Implications on Fuel Performance

AGR-1 end-of-life  $^{85\text{m}}\text{Kr}$  fission gas release and AGR-2  $^{85\text{m}}\text{Kr}$  release through the first three irradiation cycles are compared to historic German and U.S. irradiations in Figure 6-32. The historic data in this figure are taken from the compilation by Petti et al. [66]<sup>16</sup>. Mean values for each subset of data are given by the hashmarks and indicate that on average, the R/B results for historic U.S. irradiations were approximately three orders of magnitude higher than the German tests.

The gas release for AGR-1 was extremely low. The UCO fuel in AGR-1 was irradiated to a peak compact-average burnup of 19.6% FIMA, a peak fast neutron fluence of about  $4.3 \times 10^{25}$  n/m<sup>2</sup>, and a maximum time-average fuel temperature of approximately 1200°C. About 300,000 TRISO fuel particles were irradiated without a single particle failure, as indicated by the fission-gas measurements on the purge gas from each of the capsules [81]. Thus, AGR-1 is the best irradiation performance of a large quantity of TRISO fuel achieved in the U.S., and the experiments exceeded the German levels of burnup (the reported peak burnup of the German irradiations ranged from 6.9 to 15.6% FIMA, with an average of 10.5% FIMA). These results have confirmed the expected superior irradiation performance of UCO at high burnup in that no kernel migration, no evidence of CO attack of SiC, and no indication of severe SiC attack by noble metal or lanthanide fission products has been observed. Zero fuel failures out of 300,000 particles in the AGR-1 irradiation translates into a 95% confidence failure fraction of  $<1.1 \times 10^{-5}$ , a factor of 18 better than the prismatic reactor design in-service failure fraction requirement of  $2 \times 10^{-4}$ .

The in-pile R/B results for the first three AGR-2 cycles are shown in Figure 6-31 and summarized in Figure 6-32 [61]. The values are higher than the first several cycles of the AGR-1 irradiation, due in part to higher uranium contamination in the AGR-2 compacts compared to AGR-1 (uranium contamination in the AGR-2 compacts was  $\sim 4 \times 10^{-6}$  compared to an average value of  $3 \times 10^{-7}$  for the AGR-1 fuel types). In addition, the mean exposed kernel defect fraction for the AGR-2 fuel was  $9.5 \times 10^{-6}$  ( $\leq 2.5 \times 10^{-5}$  at 95% confidence). At this level it is possible to have had an exposed kernel defect in each capsule that would contribute to fission gas release, although the presence of such a defect particle cannot be confirmed based on the R/B data, in part because of the relatively high uranium contamination levels.

No particle failure was observed during the first three cycles of the AGR-2 irradiation. However, because of the cross-talk between capsules due to damage in the gas lines, fission gas release measurements could not be qualified after the third cycle of irradiation. Thus, the possibility of a small number of failures during the later cycles cannot be precluded based on the irradiation data. As a result, the ongoing AGR-2 PIE, which includes an examination of particle failures in the capsules, is being used to help determine the level of particle failure that may have occurred during irradiation.

---

<sup>16</sup> Reference 66 includes  $^{85\text{m}}\text{Kr}$  R/B results from eight additional spheres taken from the HFR-K5 and HFR-K6 irradiations. These results are not included in Figure 42, as the end-of-life values are given only as  $<3 \times 10^{-7}$ .



The preliminary PIE data currently available indicates at most four particles that experienced TRISO failure in the three UCO capsules using a somewhat conservative approach in identifying particles with failures (discussed in further detail in Section 7.5). Four failures out of 114,000 UCO particles in the experiment corresponds to an actual failure fraction  $\leq 8.1 \times 10^{-5}$  at 95% confidence, which is approximately a factor of 2.5 below historic reactor design specification of  $2 \times 10^{-4}$ . In addition, the high-temperature UCO capsule in AGR-2 showed excellent behavior under irradiation, at time-average peak temperature of  $\leq 1360^\circ\text{C}$ , and 25% of the particles in that capsule saw temperatures in excess of  $1400^\circ\text{C}$  for over a hundred days. The PIE completed to date has indicated no significant difference in coating failure rates between Capsule 2 and the other two, lower-temperature capsules. This early margin test demonstrated the high-temperature capability of these fuel particles.

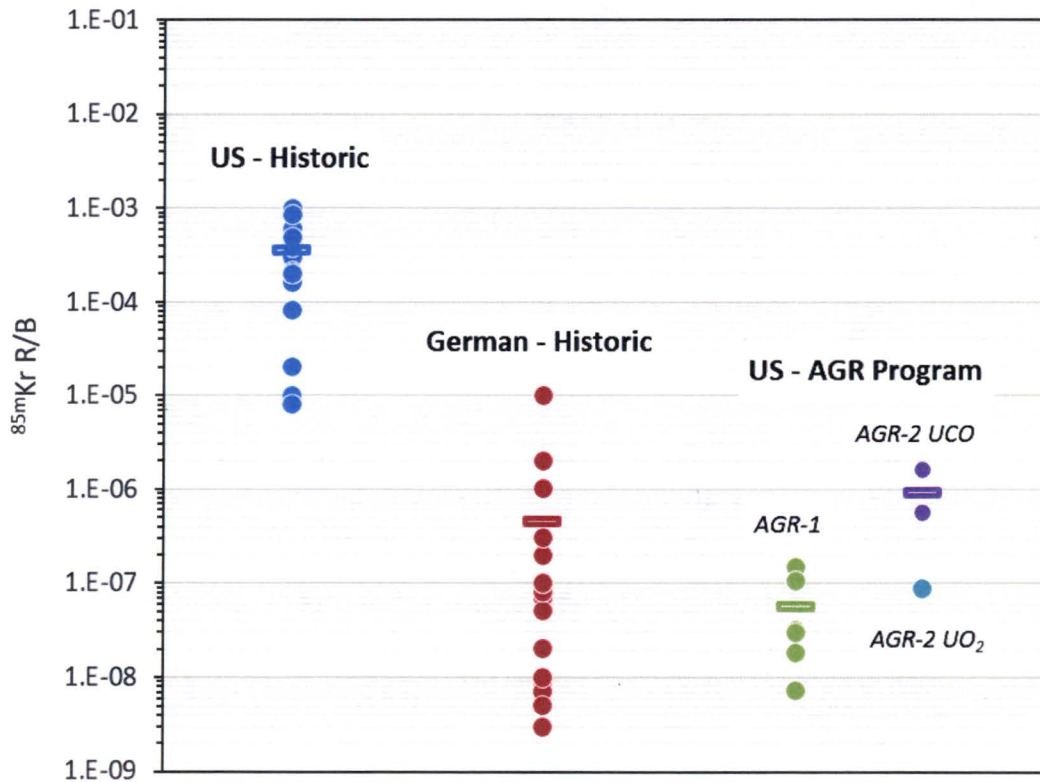


**Figure 6-32**  
 $^{85\text{m}}\text{Kr}$  fission gas release for AGR-1 (end of life) and AGR-2 (after the first three irradiation cycles) compared to historic performance in U.S. and German TRISO fuel irradiations  
 Courtesy of Idaho National Laboratory and used with permission of Battelle Energy Alliance, LLC

**The results from the AGR-1 and AGR-2 irradiations demonstrate excellent performance of UCO TRISO-coated particles that meet historic designer specifications with significant margin.** The data confirm the use of the AGR-2 particle as a reference for future high-temperature reactor designs. Beyond the actual performance, it is important to note the fissile kernels of the particles in AGR-1 and AGR-2 were of different size and enrichment, the coatings were applied in coaters of two different sizes (that is, a 2-in. laboratory-scale coater and a 6-in. engineering-scale coater), and further the coating conditions were varied so different microstructures and properties of the coatings were produced.

The excellent behavior with two different UCO kernels confirms the performance of the coatings is the primary factor in achieving good fuel performance and the kernel is of secondary importance. In terms of coating characteristics, AGR-1 particles were fabricated using a range of coating conditions that produced: (1) different combinations of PyC anisotropy and density, which in some cases were intentionally at the edge of the historic specification range; and (2) different microstructures of the SiC—a larger grain, made with traditional hydrogen and MTS coating gases, and a finer grain, by introducing argon gas as a diluent to improve fluidization during SiC deposition.

Based on the in-pile results available at the time, the AGR program decided the AGR-2 PyC coating would be applied using baseline conditions from AGR-1 and would use argon dilution during the SiC coating step, like Variant 3 in AGR-1 for the best fluidization in the coater. Despite these variations in coating conditions, the performance of intact TRISO particles was similar, albeit with slightly higher fission gas release in AGR-2 due to slightly higher uranium contamination of the particle batch in the larger engineering-scale coater and a higher as-fabricated exposed kernel fraction.

**The kernels and coatings of the UCO TRISO-coated fuel particles tested in AGR-1 and AGR-2 exhibited property variations and were fabricated under different conditions and at different scales, with remarkably similar excellent irradiation and accident safety performance results. The ranges of those variations in key characteristics of the kernels and coatings are reflected in measured particle layer properties provided in Table 5-5 from AGR-1 and AGR-2. UCO TRISO-coated fuel particles that satisfy the parameter envelope defined by these measured particle layer properties in Table 5-5 can be relied on to provide satisfactory performance.**

# 7

## ASSESSMENT OF FUEL PERFORMANCE FROM POST-IRRADIATION EXAMINATION AND SAFETY TESTING

---

The objective of the PIE and safety testing is to characterize and measure the performance of TRISO fuel after irradiation and during postulated accident conditions. These activities also support the fuel development effort by providing feedback on the performance of kernels, coatings, and compacts. Data from PIE and safety testing in combination with the in-reactor measurements will provide the data necessary to demonstrate compliance with fuel performance requirements and to support the development and validation of computer codes. PIE of UCO TRISO fuel irradiated in AGR-1 is complete, while similar work for AGR-2 is nearing completion.

Key aspects of fuel performance that were investigated were fission product release from particles and compacts, radiation-induced changes in kernel and coating microstructures, and coating failure.<sup>17</sup> Safety tests were performed by heating the fuel compacts in helium at temperatures of 1600, 1700, or 1800°C, with nominal hold times of 300 hours. An additional AGR-1 test was performed involving three compacts heated using a temperature profile resembling the peak temperature trajectory during an HTGR depressurized loss of forced cooling accident. These results are discussed in the following sections.

### 7.1 Fission Product Release During Irradiation

#### 7.1.1 Methods

Several different experimental measurements are used to assess the extent of fission product release from the fuel particles and compacts. These involve quantifying either the fission product inventory remaining in the fuel specimen, or the inventory that has been released from the specimen. When compared with the predicted inventory generated during irradiation (based on physics calculations), the numbers can indicate a fraction of total inventory retained or released.

---

<sup>17</sup> In Section 7, coating failures are commonly categorized as either *SiC failure* or *TRISO failure* to differentiate between the two. *SiC failure* is defined as loss of integrity of the SiC layer with at least one pyrocarbon layer remaining intact, such that fission gases will be retained but fission products such as cesium may be released in significant quantities. *TRISO failure* is defined as loss of integrity of all three dense coating layers, such that fission gases will be released from the particle. This is also often referred to as an exposed kernel.

The basic measurements that were part of the AGR-1 and AGR-2 PIE are listed below. The methods have been summarized in the *AGR-1 Post Irradiation Examination Final Report* [82], with numerous specific references provided containing additional details on methods and results. Similar methods are being used for the AGR-2 PIE:

- **Fission product inventory on the capsule components outside of the fuel compacts.** This is obtained by gamma counting of certain components, burn-leach of carbonaceous matrix components, and acid leaching of metallic components. The results provide the capsule-average fractional release from the fuel compacts. AGR-1 and AGR-2 results are provided in dedicated reports [83,84].
- **Fission product inventory in the compacts outside of intact SiC.** This includes any inventory residing in the OPyC layer and the compact matrix and is determined by deconsolidation-leach-burn-leach (DLBL) analysis of selected compacts. This inventory represents fission products that were released from the fuel particles but not released from the compact.
- **Gamma counting of individual particles.** This provides the total gamma-emitting fission product inventory in each particle. In most cases, the fractional release of fission products from an individual particle is sufficiently small (for example, <1%) and the uncertainty on the inventory sufficiently large (minimum uncertainty typically in the range of 5%) that no conclusions can be drawn regarding the extent of fission product release using these data. Two notable exceptions include (1) assessing silver release from intact particles and (2) assessing cesium release from particles with failed coatings. In these cases, the release from a particle can be sufficiently large that the approximate fractional release can be estimated by examining the remaining inventory.
- **Gamma counting of individual compacts.** This provides the total gamma-emitting fission product inventory in each compact. This is primarily of use for assessing silver release from a compact, which can be very significant (that is, tens of percent).

All of the release fractions expressed in this report are based on calculated inventories determined from neutronics simulations of the irradiation experiments. Some measurements of whole compact and individual particle inventories have been performed and compared to the calculated values to assess the accuracy of the calculations. This includes gamma spectrometry measurements of total fuel compact inventories for gamma-emitting fission products and gamma counting of individual particles from numerous compacts.

The data for AGR-1 compacts indicate that the measured inventories for certain fission products (including  $^{134}\text{Cs}$ ,  $^{137}\text{Cs}$ ,  $^{144}\text{Ce}$ , and  $^{106}\text{Ru}$ ) are in good agreement with the calculated inventories: the measured-to-calculated (M/C) inventory ratios (averaged for all AGR-1 compacts) are between 0.96 and 1.0 for these isotopes. For other isotopes there is evidence of a bias in the calculation as the measured inventories are somewhat less than the calculated inventories; the average M/C ratio is 0.83 for  $^{154}\text{Eu}$  and 0.70 for  $^{125}\text{Sb}$  for AGR-1 fuel compacts. Similar analysis is being performed on the AGR-2 fuel, including an analysis of  $^{90}\text{Sr}$  inventories to compare with the calculated values ( $^{90}\text{Sr}$  is not detected by gamma spectrometry as it decays with no gamma

ray emission). Nonetheless, calculated values are used exclusively in the results presented here for consistency. For certain isotopes, reliable M/C values may not be available for all specimens analyzed, and the variation in M/C ratio for individual specimens means that no single correction can be applied to account for these differences.

### 7.1.2 Results

Several aspects of fission product behavior in the AGR-1 fuel are graphically highlighted in Figure 7-1. Two sets of data are presented: red columns represent the range of fission product inventories measured in selected compacts outside of intact SiC [82], expressed as a fraction of the total compact inventory, and blue columns represent the range of fission product inventories measured outside of the fuel compacts in the six capsules [83], expressed as a fraction of the total capsule inventory.

Preliminary data for the AGR-2 UCO fuel compacts [85] and capsules [84] are presented in Figure 7-2. Note that for  $^{154}\text{Eu}$  and  $^{90}\text{Sr}$ , the data ranges for Capsule 2 are plotted separately because they fall significantly outside the range of values for Capsules 5 and 6, a result of the higher fuel temperature in Capsule 2. For the remaining isotopes, all data are plotted together since the ranges of values overlap.

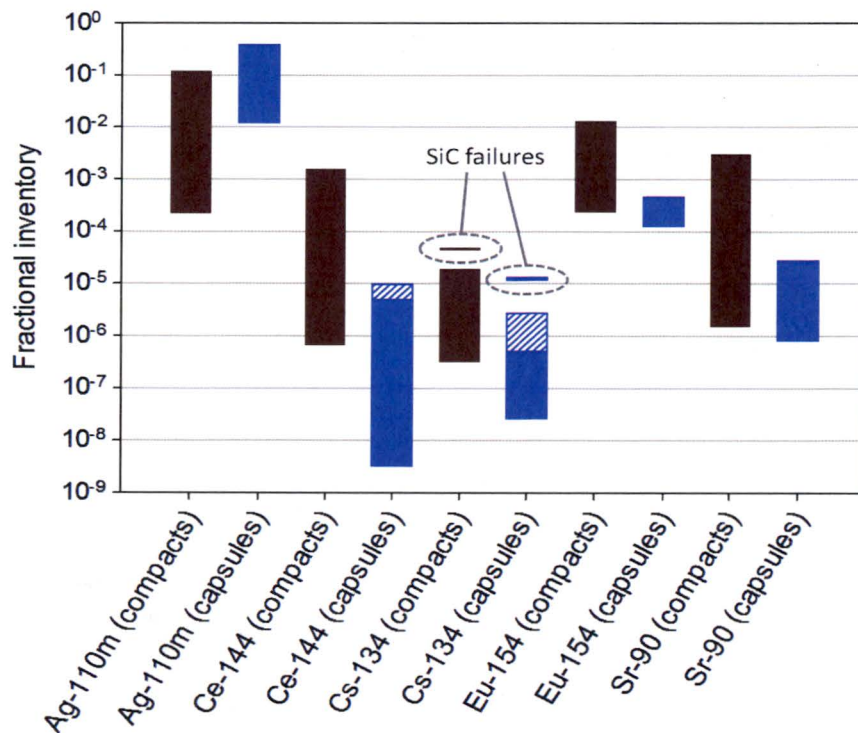


**Figure 7-1**  
 Range of AGR-1 fractional fission product inventories found in the matrix of examined compacts (red columns) and on the irradiation capsule components (blue columns). Instances where compacts and capsules contained SiC failures are indicated separately on the plot. Hatched areas indicate that the inventory on some capsule components was below the detection limit of the techniques. Therefore, the sum of contributions from all components represents a conservative upper bound for the total inventory in several of the capsules.  
 Courtesy of Idaho National Laboratory and used with permission of Battelle Energy Alliance, LLC

Interpretation of the AGR-2  $^{154}\text{Eu}$  data is complicated because almost all components from Capsules 5 and 6 contained no measurable inventory and the techniques used in some cases resulted in relatively high minimum detectable activities. Therefore, the range denoted by the hatched regions were established based on these minimum detectable activities. However, given the similarities in temperature between AGR-1 capsules and AGR-2 Capsules 5 and 6, as well as the generally similar trends in Eu and Sr behavior in the two experiments, it is likely that the actual  $^{154}\text{Eu}$  fractional releases from the fuel compacts are in the  $\sim 10^{-4}$  range. The behavior of specific elements presented in Figures 7-1 and 7-2 is discussed further below.

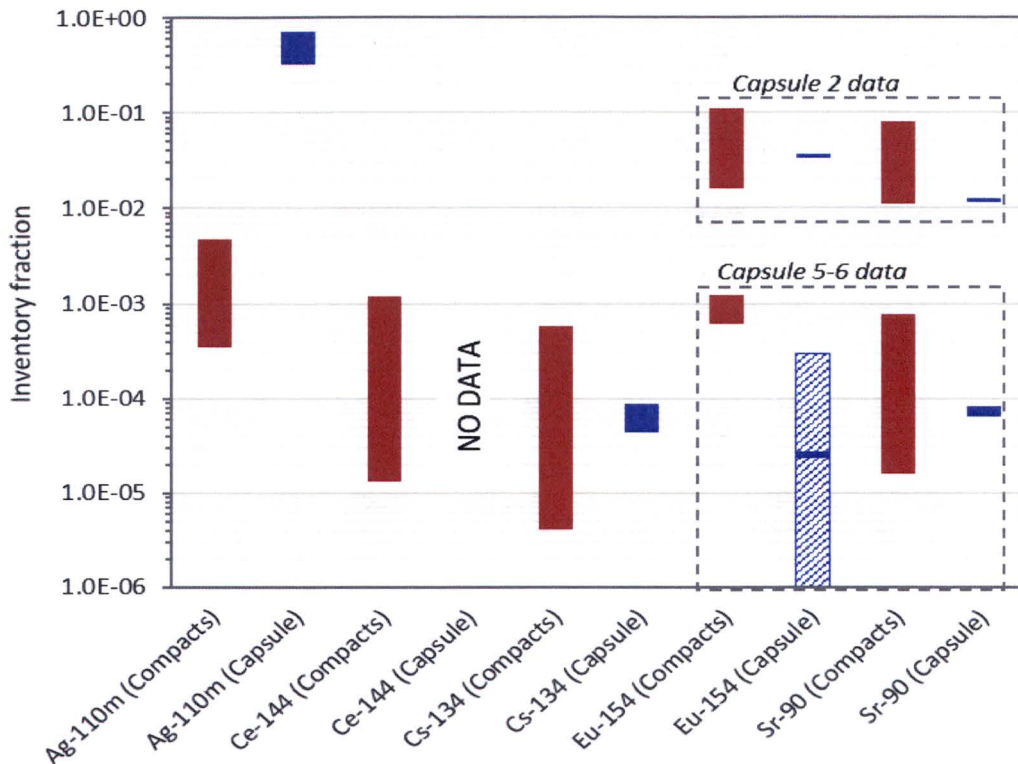


**Figure 7-2**  
**Range of AGR-2 fractional fission product inventories found in the matrix of examined compacts (red columns) and on the irradiation capsule components (blue columns). See text for explanation of the multiple data sets for  $^{154}\text{Eu}$  and  $^{90}\text{Sr}$ .**

*Courtesy of Idaho National Laboratory and used with permission of Battelle Energy Alliance, LLC*

**Cesium.** As indicated in Figure 7-1, the Cs release from the AGR-1 fuel compacts was very low based on the inventory measured on the capsule components. The PIE of the capsule components and fuel compacts indicated two capsules (Capsules 5 and 6) contained a small number of particles with SiC layer failure (see Section 7.4 for further discussion), and these particles released higher levels of cesium relative to intact particles. As a result, the inventory of cesium in the compact matrix was found to be higher in compacts containing particles with SiC failures. Similarly, cesium release from fuel compacts was higher in capsules where SiC layer failures occurred. This distinction is indicated in Figure 7-1 by the separate data sets labeled “SiC failures.”

In compacts containing SiC failures, the  $^{134}\text{Cs}$  fractional inventory was approximately  $5 \times 10^{-5}$ , while in compacts containing only intact particles the fractional inventory was  $<2 \times 10^{-5}$ . In capsules containing SiC failures, the fractional release was approximately  $1 \times 10^{-5}$ , while in capsules with only intact particles the fractional release was  $<3 \times 10^{-6}$  (with the highest measured inventory outside of compacts amounting to approximately  $5 \times 10^{-7}$ ). At these low levels, the contribution of cesium from the dispersed uranium contamination in the matrix could be a significant portion of the total release from the compacts. These data therefore demonstrate that release from intact particles is extremely small. In addition, the higher peak compact matrix inventory relative to the inventory released from the compacts indicates a significant amount of retention of cesium in the matrix during irradiation.

The cesium inventories for AGR-2 shown in Figure 7-2—both the inventory in the matrix of analyzed compacts and the inventory released from the compacts to the capsule components—are notably higher compared to AGR-1. This is due in part to the higher overall temperatures in AGR-2 and the presence of exposed kernels and/or particles with failed SiC in all three capsules, and exacerbated by elevated incidence of SiC failure driven by proximity to test train components and not related to fuel performance (discussed further in Section 7.4). For this experiment, cesium fractional inventory in the matrix of compacts was found to peak at approximately  $6 \times 10^{-4}$ . Total fractional release of cesium from the compacts in UCO Capsules 5 and 6 (similar temperature to AGR-1 fuel) was  $4.4 \times 10^{-5}$ , while fractional release in Capsule 2 was  $\sim 9 \times 10^{-5}$ .

**Europium and strontium.** Both the  $^{154}\text{Eu}$  and  $^{90}\text{Sr}$  data for AGR-1 in Figure 7-1 exhibit a trend of higher fractional inventory in the matrix of compacts compared to the inventory released from compacts, indicating significant retention in the matrix during irradiation. This trend is evident for AGR-2 as well (Figure 7-2), with the range of values for Capsules 5 and 6 significantly overlapping those from AGR-1. Both experiments exhibit a similar trend in slightly lower Sr release relative to Eu. The AGR-2 Capsule 2 data demonstrate the notably higher inventory of Eu and Sr in the matrix of compacts at the higher irradiation temperature, peaking at around  $10^{-1}$  and  $8 \times 10^{-2}$ , respectively.

**Silver.** Ag behavior is unique among the elements presented in Figure 7-1 and Figure 7-2 in that the release from the compacts to the capsule components generally exceeded the inventory retained in the matrix. AGR-2 matrix fractional inventory values overlap the range for AGR-1 but exhibit a maximum ( $5 \times 10^{-3}$ ) which is significantly less than the AGR-1 maximum ( $1.1 \times 10^{-1}$ ). The fractional release from compacts for the two experiments ranges from  $10^{-2}$  to  $7 \times 10^{-1}$ . The temperature dependence of the Ag release from compacts is demonstrated in Figure 7-3, which presents the total  $^{110\text{m}}\text{Ag}$  inventory measured outside of fuel compacts in all AGR-1 and AGR-2 capsules as a function of capsule time-average maximum temperature.

At the individual compact level, total Ag release varied considerably, from essentially complete retention to complete release. Figure 7-4 shows the measured  $^{110\text{m}}\text{Ag}$  inventory in AGR-1 and AGR-2 compacts [73,74] divided by the calculated inventory from physics simulations (defined as the M/C ratio) as a function of time-average maximum compact temperature. Note values in excess of 1.0 result from more  $^{110\text{m}}\text{Ag}$  measured in the compact than was predicted, which could be due to uncertainty on the measured inventory as well as a low bias on the predicted inventory. Similarly, at the individual particle level, Ag release could range from complete retention to complete release, as demonstrated from particle gamma counting data [82].

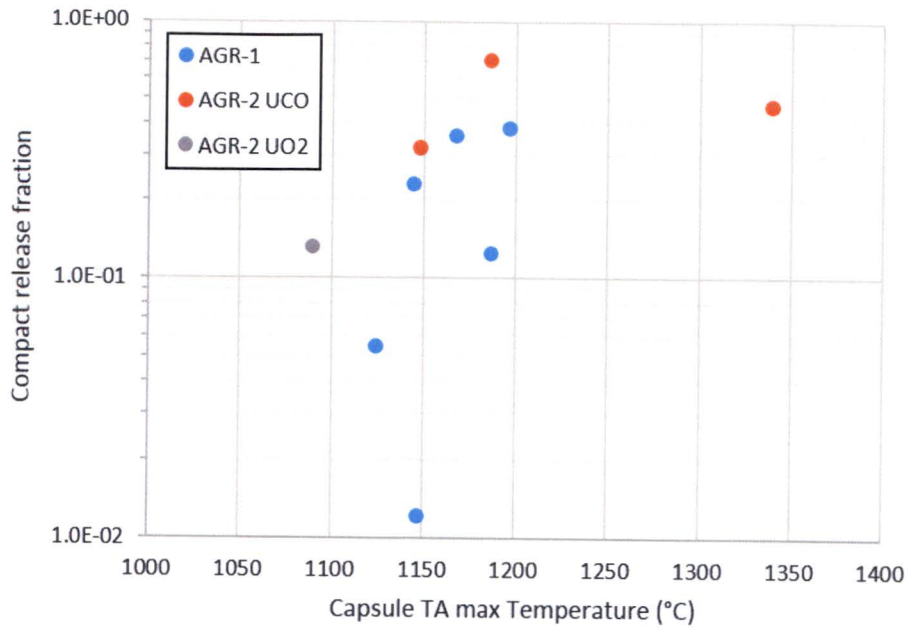


**Figure 7-3**  
**AGR-1 and AGR-2 capsule-average compact  $^{110m}\text{Ag}$  release based on total inventory measured on capsule components as a function of the capsule time-average maximum temperature**  
*Courtesy of Idaho National Laboratory and used with permission of Battelle Energy Alliance, LLC*

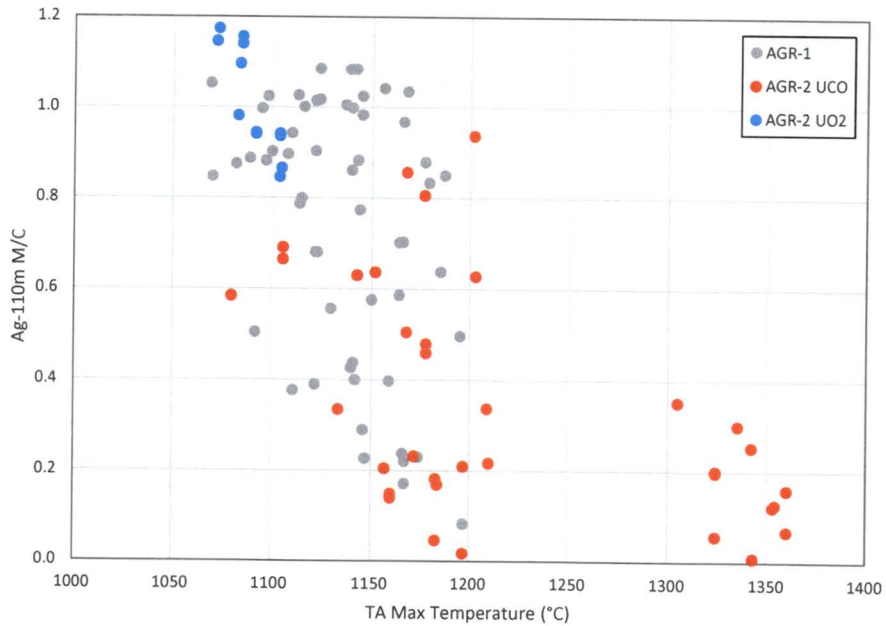


**Figure 7-4**  
**Ratio of measured  $^{110m}\text{Ag}$  inventory to calculated inventory in AGR-1 and AGR-2 fuel compacts plotted vs. time-average maximum temperature**  
*Courtesy of Idaho National Laboratory and used with permission of Battelle Energy Alliance, LLC*



**Palladium.** The level of Pd found in the compacts outside the SiC was approximately 1% in five AGR-1 compacts for which this element was analyzed in the DLBL solutions. Despite this large amount of Pd in the fuel matrix, no widespread Pd corrosion or attack of SiC has been observed during metallographic examination of the as-irradiated TRISO particles. This was unexpected since Pd attack of SiC at high burnup in TRISO fuel has been postulated as a potential failure mode [68]. As will be described further below, Pd attack appears only to be a cause of SiC layer failure when IPyC layer failure allows localized Pd concentration at the inside of the SiC layer.

## **7.2 Irradiated Fuel Particle Microstructural Evolution**

Extensive microscopic examination of particle cross sections has been performed to understand kernel and coating layer morphology evolution during irradiation. This included cross sections of select as-irradiated AGR-1 and AGR-2 compacts [86,87], as well as loose particles deconsolidated from numerous as-irradiated or safety-tested compacts [82,85]. In addition, a select number of particles were analyzed using x-radiography with 3-D tomographic reconstruction, which has enabled nondestructive examination of the kernel periphery and the coating layers. Common features observed in the irradiated particles include densification of the buffer layer and swelling of the kernel with related formation of gas-filled bubbles, as shown in Figure 7-5. High-burnup kernel migration (the so-called “amoeba effect”) has not been observed in any particles, indicating the efficacy of the UCO fuel in limiting the oxygen partial pressure in the fuel and the formation of carbon monoxide.

In the majority of particles, the buffer layer debonded from the IPyC layer, driven by buffer densification and volume shrinkage, and leaving a void between the buffer and IPyC layer. This was observed as either complete (see Figure 7-5a) or partial (see Figure 7-5b) debonding in the polished plane analyzed. Much less common were particles in which the buffer and IPyC layers remained completely bonded in the plane observed (see Figure 7-5c), where the buffer densification resulted in the inner diameter increasing while the kernel swelled to fill the increasing volume. Such particles constituted 4% of approximately 1,000 particles observed in a study of AGR-1 compact cross sections [86], and no such particles were observed in a study of over 500 AGR-2 UCO particles in compact cross sections [87].

While all of the coating layers appeared intact for most particles in the plane examined, fracture of the buffer layer was not uncommon in the AGR-1 and AGR-2 particles. Buffer fracture was often accompanied by expansion of the kernel into the gap formed at the point of fracture (see Figure 7-5d). The percentage of particles with observable buffer fracture was relatively consistent among six AGR-1 compacts examined in cross section, varying 13 to 35% with an average of 23% [86]. The extent of buffer fracture exhibited much greater variation in AGR-2 UCO compacts (compact-average values from 0 to 86% based on examination of particles from seven UCO compacts), and this appeared to be influenced to some degree by irradiation temperature.

Comparing compacts irradiated to a calculated fast fluence of  $3 \times 10^{25} \text{ n/m}^2 \pm 0.12 \times 10^{25}$ , those irradiated at TAVA temperatures of approximately 1100°C exhibited an observed buffer failure fraction of 86%, while those irradiated at TAVA temperatures >1200°C exhibited buffer failure fractions of 1–2%. This is believed to be due to greater magnitude of thermal creep occurring at

the higher temperatures, which relaxes stresses developed due to buffer densification and shrinkage. Given the relatively high rates of buffer fracture observed in many of the UCO compacts along with the very low SiC and TRISO coating failure fractions, it is clear that buffer fracture does not represent a significant threat to particle integrity.

While particles with buffer and IPyC layer separation and the representative buffer fracture shown in Figure 7-5d were fairly common, there appeared to be no obvious detrimental effects on the outer, dense coating layers that resulted in layer failure, even in cases where the kernel was in direct contact with the IPyC layer. However, if the buffer-IPyC interface remained intact as in Figure 7-5c, fracture of the buffer layer was always accompanied by fracture of the IPyC layer, and often included debonding of the IPyC from the SiC layer (see Figure 7-5e).

Fracture of the buffer layer was not necessary for IPyC fracture to occur. In some particles, partial debonding of the buffer-IPyC layer apparently led to development of sufficient stress in the IPyC layer to cause fracture (see Figure 7-5f), often with resultant debonding between the IPyC and SiC layers and in rare cases, partial fracture of the SiC at the IPyC-SiC interface (as shown in Figure 7-5f) that did not lead directly to SiC failure.

Because partial buffer-IPyC debonding (see Figure 7-5b) was much more common than no debonding (see Figure 7-5c), this type of IPyC fracture was more common than the type shown in Figure 7-5e. IPyC fracture and IPyC-SiC debonding of this nature was found to be an important contributor to SiC layer failure, as discussed in detail in Section 7.4.

A notable difference between the AGR-1 and AGR-2 irradiated particles is the absence of through-layer IPyC fractures observed in random AGR-2 particles examined in compact cross sections [87]. It is postulated this may be due to a less adherent buffer-IPyC interface strength (potentially a result of the longer fluidization time between buffer layer and IPyC layer deposition, which may result in fewer sites on the buffer surface for integration of the IPyC layer), such that the layers more easily detach during irradiation in the AGR-2 fuel. This would also tend to provide less opportunity for SiC layer failure from IPyC-SiC delamination.

## **7.3 Safety Testing**

### **7.3.1 Isothermal Safety Tests in Dry Helium**

Post-irradiation accident simulation heat-up testing (“safety testing”) in dry helium has been performed on the AGR-1 and AGR-2 fuel compacts. The majority of these tests have been isothermal tests at a temperature of 1600, 1700, or 1800°C for a nominal duration of 300 hours. Tests have been performed using the Fuel Accident Condition Simulator (FACS) furnace at INL and the Core Conduction Cooldown Test Facility (CCCTF) at ORNL. Fifteen such tests were performed on AGR-1 fuel compacts. AGR-2 safety testing is still in progress, with seven AGR-2 UCO fuel compacts and three AGR-2 UO<sub>2</sub> fuel compacts tested to date.

Safety testing has demonstrated excellent robustness of the AGR UCO TRISO fuel. Figure 7-6 presents 1600°C test results from an AGR-2 UCO compact (AGR-2 5-2-2) that are typical of a significant number of the UCO safety tests [88]. In particular, the compact exhibited very low fractional release of Cs isotopes for the duration of the test, modest release of Eu and Sr isotopes (with the overall release behavior of these two isotopes being relatively similar), and fairly high release of <sup>110m</sup>Ag.

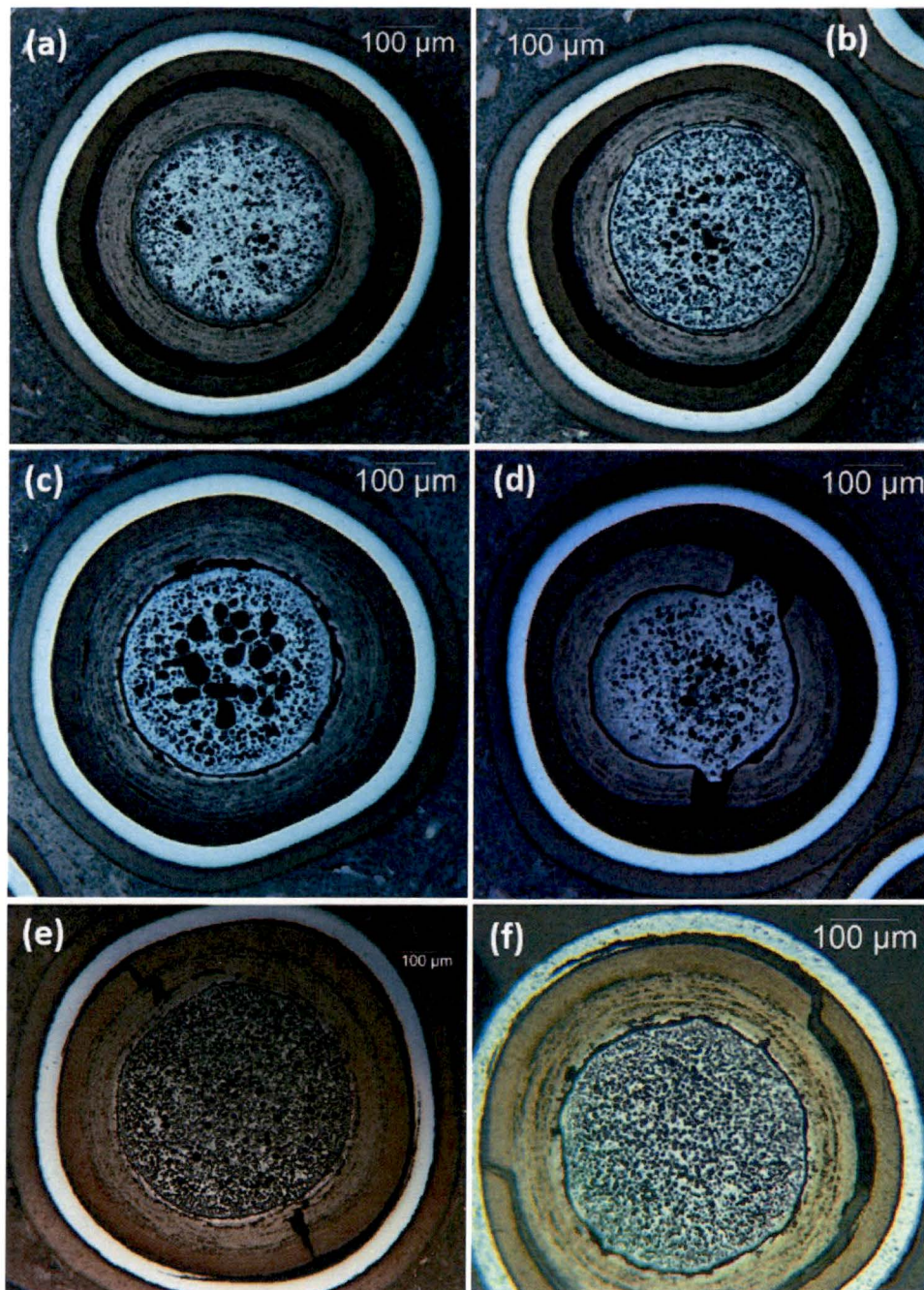


**Figure 7-5**  
**Examples of various AGR-1 irradiated particle microstructures**  
*Courtesy of Idaho National Laboratory and used with permission of Battelle Energy Alliance, LLC*

Typical of a number of the AGR safety tests to date, no  $^{85}\text{Kr}$  was detected in the gas effluent during this test, with the total estimated detection limit corresponding to fractional release in the range of  $1 \times 10^{-6}$  to  $5 \times 10^{-6}$ . Note in most tests, the fractional release of several other isotopes was also quantified, including  $^{137}\text{Cs}$  and  $^{155}\text{Eu}$ . The discussion below omits these, as the behavior of these elements is better characterized using the isotopes  $^{134}\text{Cs}$  and  $^{154}\text{Eu}$ . For Cs, the isotope  $^{137}\text{Cs}$  tends to be influenced to a greater degree by contamination in shielded hot cells because of its long half life ( $t_{1/2} = 30$  years), with for Eu, the isotope  $^{154}\text{Eu}$  has gamma emissions that make detection more favorable than for  $^{155}\text{Eu}$ .

Summary plots of  $^{134}\text{Cs}$ ,  $^{110\text{m}}\text{Ag}$ ,  $^{154}\text{Eu}$ , and  $^{90}\text{Sr}$  fractional release from all AGR-1 and AGR-2 isothermal safety tests completed to date are shown in Figure 7-7 and Figure 7-8. The x-axis represents elapsed time after reaching the target hold temperature. Releases are expressed as a fraction of the total calculated inventory generated in the compact during irradiation. Test temperature is indicated by the plot colors: 1600°C (blue), 1700°C (green), or 1800°C (red). The inventory fraction corresponding to a single particle is indicated by the dashed horizontal lines on the plots (as labeled on the  $^{110\text{m}}\text{Ag}$  plots in each figure).

The total number of particles per compact was approximately 4100 for AGR-1, 3180 for AGR-2 UCO, and 1540 for AGR-2  $\text{UO}_2$ . The AGR-2  $\text{UO}_2$  test data are represented by dotted lines and gray-filled symbols in Figure 7-8. The key trends in fractional release behavior based on these data are summarized for specific elements in the discussion below. Krypton fractional release data are not provided in Figure 7-7 and Figure 7-8, as the level of  $^{85}\text{Kr}$  released during many of the tests was below detection limits.  $^{85}\text{Kr}$  release observations are included in the discussion below.

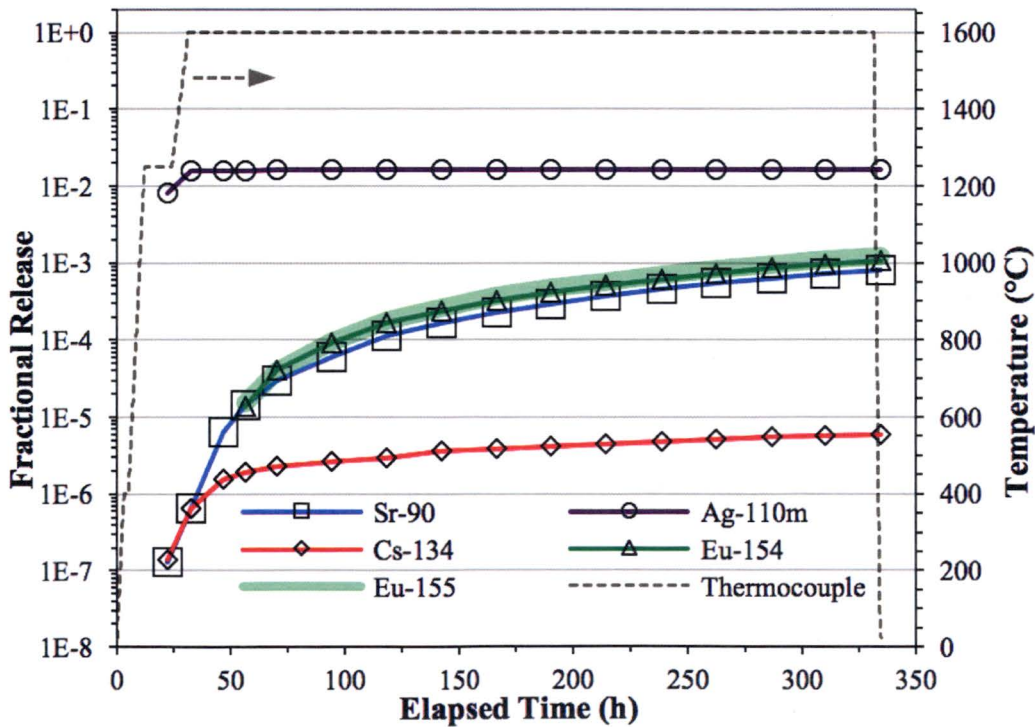


**Figure 7-6**  
**Fission product release from heating of AGR-2 compact 5-2-2 at 1600°C**  
 Courtesy of Idaho National Laboratory and used with permission of Battelle Energy Alliance, LLC

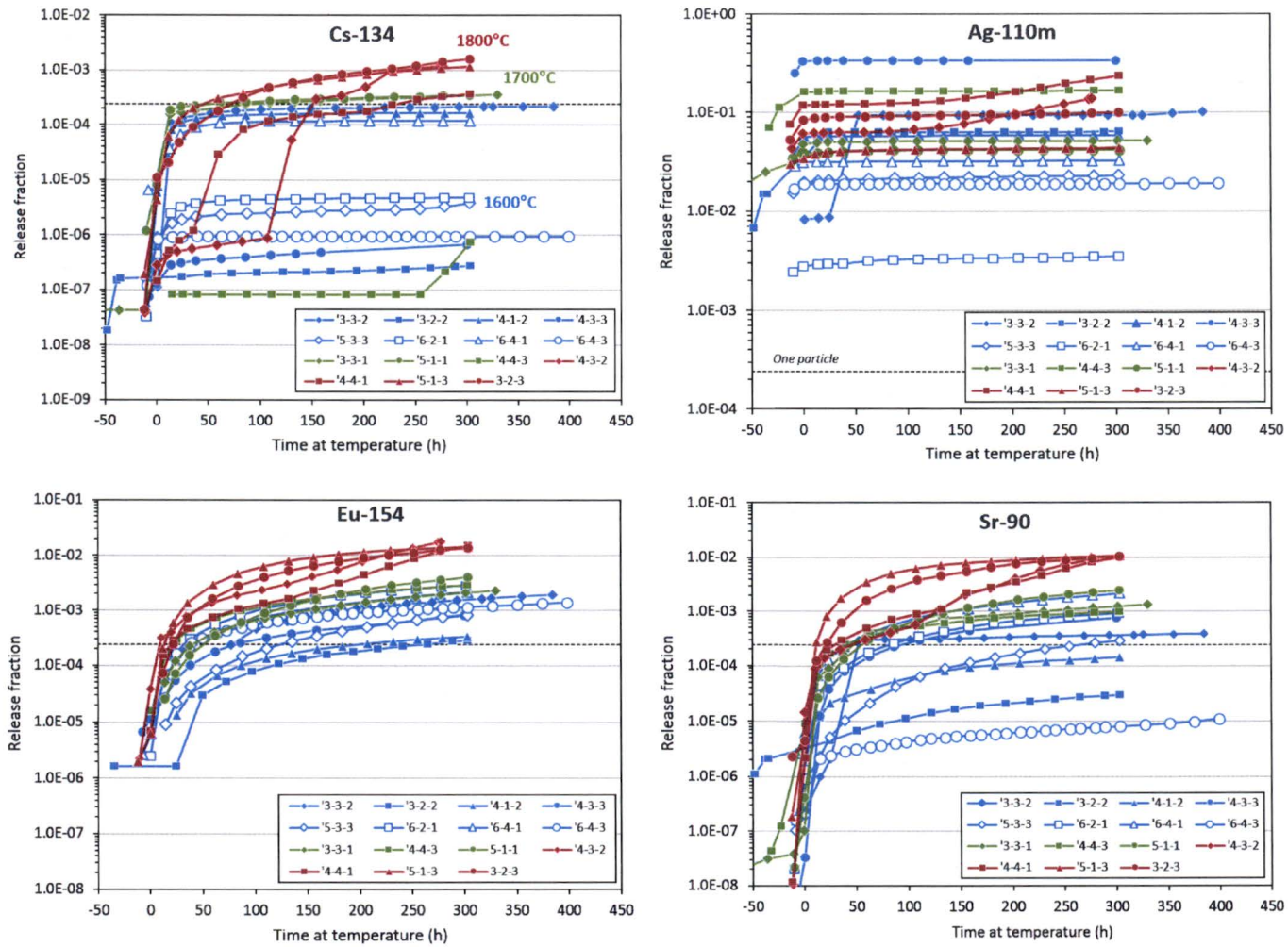


**Figure 7-7**  
**Fission product releases from AGR-1 compacts during isothermal safety tests. Plot color indicates test temperature: 1600°C (blue), 1700°C (green), or 1800°C (red)**

*Courtesy of Idaho National Laboratory and used with permission of Battelle Energy Alliance, LLC*

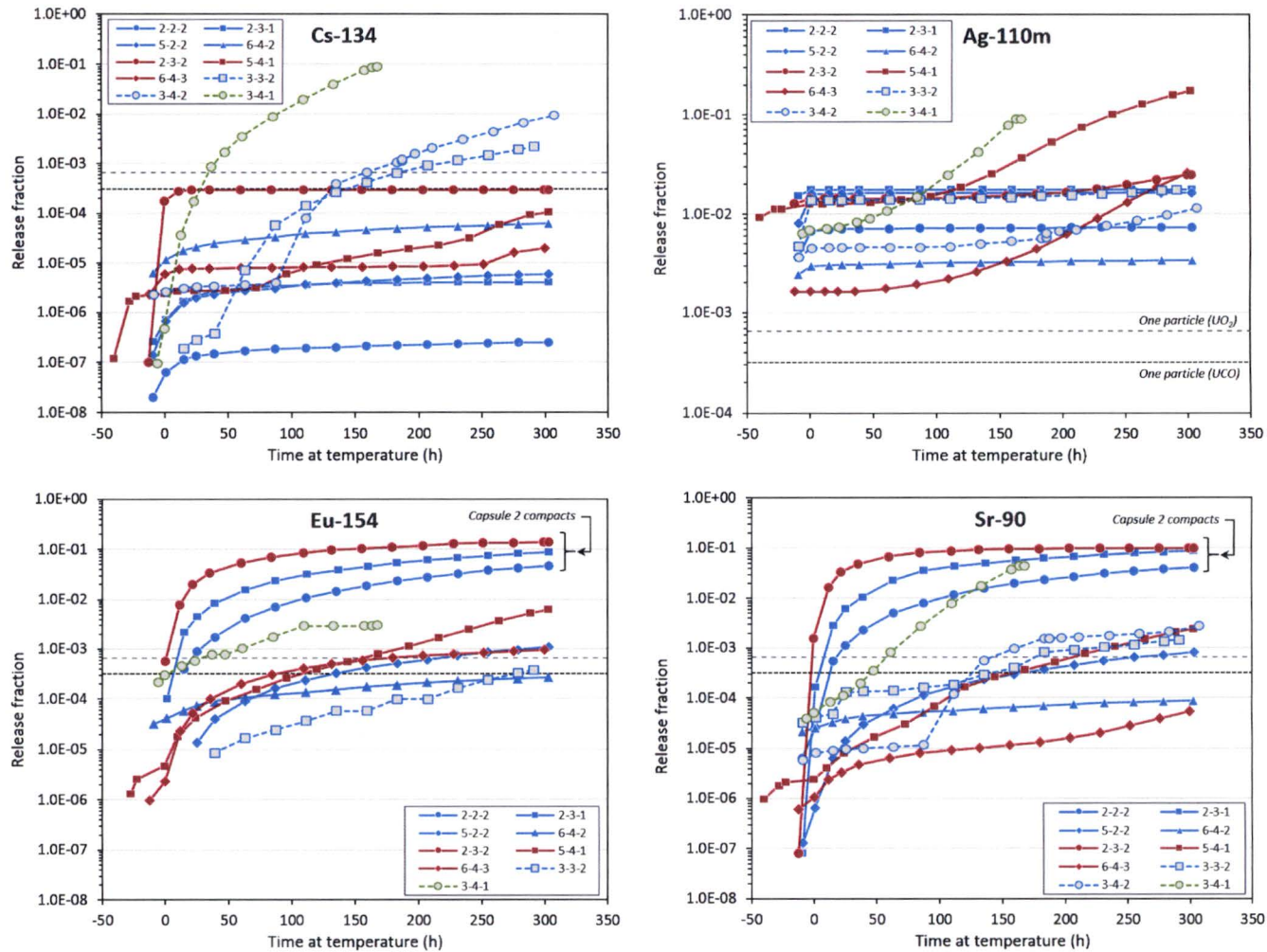


**Figure 7-8**  
 Fission product releases from AGR-2 compacts during isothermal safety tests. Plot color indicates test temperature: 1600°C (blue), 1700°C (green), or 1800°C (red). UO<sub>2</sub> tests are indicated by dotted lines with gray-filled symbols  
 Courtesy of Idaho National Laboratory and used with permission of Battelle Energy Alliance, LLC

### 7.3.2 Cesium

The AGR-1  $^{134}\text{Cs}$  release data indicate two distinct sets of release curves, exhibiting end-of-test release  $>10^{-4}$  or  $<5 \times 10^{-6}$ . Extensive PIE following the safety tests has demonstrated all compacts with releases  $>1 \times 10^{-4}$  contained one or more particles with a SiC layer that had failed (in some cases these were found to be particles with as-fabricated defective layers) [82,85]. These particles typically retained an intact pyrocarbon layer, such that  $^{85}\text{Kr}$  release remained low (the exception was Compact 4-3-2, which experienced two TRISO failures). Recovery and inspection of the particles with SiC failures has helped to understand the failure mechanism, as discussed further in Section 7.4. In the remaining compacts with release  $<5 \times 10^{-6}$ , no evidence of any coating failures was found.

The results demonstrate cesium release through intact SiC is extremely low; therefore, cesium release from the fuel is dictated largely by the number of particles experiencing SiC layer failure. Peak  $^{134}\text{Cs}$  release was approximately  $2 \times 10^{-4}$  after 300 hours at  $1600^\circ\text{C}$  and approximately an order of magnitude higher at  $1800^\circ\text{C}$ . Note during the safety test of Compact 4-3-2, the  $^{134}\text{Cs}$  release remained below  $1 \times 10^{-6}$  for approximately 100 hours before a suspected SiC failure resulted in a significant increase, demonstrating excellent retention by intact SiC even at  $1800^\circ\text{C}$ .

Cesium release during the AGR-1 UCO tests (Figure 7-7) was lower compared to AGR-2 (Figure 7-8), primarily reflecting a lower incidence of SiC failure. The highest release at  $1600^\circ\text{C}$  was approximately  $6 \times 10^{-5}$  (Compact 6-4-2). While this is roughly an order of magnitude higher than releases from AGR-1 compacts containing only intact particles, it is still  $\sim 5\times$  lower than the level of one particle. This observation, along with a lack of evidence of failed particles during post-test destructive examination of the compact, suggest no particles suffered SiC failure.

One of the compacts tested at  $1800^\circ\text{C}$  experienced an early TRISO failure (Compact 2-3-2), with  $^{134}\text{Cs}$  release reaching  $3 \times 10^{-4}$  by the end of the test (equivalent to a single particle inventory, and the highest  $^{134}\text{Cs}$  release observed from all AGR-2 UCO compacts), and a second compact (Compact 5-4-1) experienced a SiC layer failure with  $^{134}\text{Cs}$  release reaching  $1 \times 10^{-4}$  at the end of the test. The third compact tested at  $1800^\circ\text{C}$  (Compact 6-4-3) experienced no SiC layer failure during the test and  $^{134}\text{Cs}$  release was  $2 \times 10^{-5}$  at the end of the test, the lowest for any  $1800^\circ\text{C}$  UCO fuel tested to date. Notably, the AGR-2 data do not exhibit the same bifurcated  $^{134}\text{Cs}$  release behavior as observed for AGR-1. This is largely a consequence of the lower number of SiC failures (and zero failures at  $1600^\circ\text{C}$ ), which limited the number of tests with  $^{134}\text{Cs} > 10^{-4}$  to only Compact 2-3-2 ( $1800^\circ\text{C}$ ).

Recovered AGR-1 and AGR-2 particles that experienced SiC layer failure during safety tests were found to have widely varying levels of Cs retention. Values ranged from extremely low (less than 10%) to relatively high (values as high as approximately 80% were measured). Higher levels of retention are possible, but particles with such high retention would be indistinguishable from particles with intact SiC and could not be isolated during PIE.

A key observation with regard to AGR-2  $\text{UO}_2$   $^{134}\text{Cs}$  release during the tests is the obviously higher values compared to UCO. Total release at  $1600^\circ\text{C}$  was  $2 \times 10^{-3}$  to  $10^{-2}$ , and nearly  $10^{-1}$  at  $1700^\circ\text{C}$  (note the  $1700^\circ\text{C}$  test was terminated prior to the originally planned 300-hour duration due to the rapidly increasing release of fission products). Post-test analysis of the compacts revealed a significant number of particles that experienced measureable cesium release.

Analysis of these particles revealed the cause to be reaction of CO(g) with the SiC layer and concomitant degradation of the layer, such that cesium retention was impacted while fission gas remained largely retained in the particles due to an intact OPyC layer. An example is shown in Figure 7-9. The observed corrosion of the SiC layer is similar to that observed in previous tests with UO<sub>2</sub> TRISO particles [89]. It is estimated approximately 400–800 particles in AGR-2 Compact 3-4-1 (1700°C) had a SiC layer with degraded Cs retention [85]. The significantly increased level of SiC failure and Cs release in the UO<sub>2</sub> fuel highlights one of the key advantages of UCO fuel, which results in far less production of CO(g) within the particle. With an average end-of-test release of  $5.7 \times 10^{-3}$  at 1600°C, the UO<sub>2</sub> fuel exhibited over 300x higher <sup>134</sup>Cs release compared to the average release from UCO tested under the same conditions ( $1.8 \times 10^{-5}$ ).

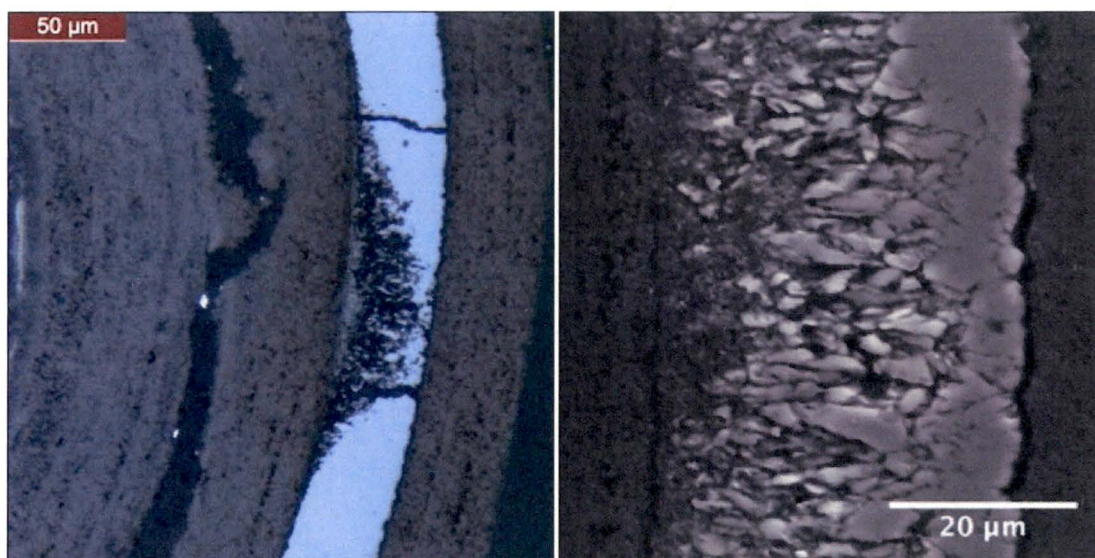


**Figure 7-9**  
Optical (left) and electron (right) micrographs of a region of the SiC layer corroded by CO in an irradiated UO<sub>2</sub> particle heated to 1600°C  
Courtesy of Idaho National Laboratory and used with permission of Battelle Energy Alliance, LLC.

### 7.3.3 Silver

The most common Ag release behavior for UCO at 1600 and 1700°C was rapid early release of a fraction between  $3 \times 10^{-3}$  and  $3 \times 10^{-1}$  followed by little measurable additional release for the remaining duration of the test. This released inventory is roughly comparable to the range of inventories found in the matrix of as-irradiated compacts (Figure 7-1 and Figure 7-2) and is believed to be due to depletion of silver in the compact matrix at the end of irradiation.

A notable behavior during 1800°C safety tests of AGR-1 compacts was an increase in <sup>110m</sup>Ag release after approximately 100 hours for Variant 3 (that is, Capsule 4) compacts (see the <sup>110m</sup>Ag data for Compacts 4-3-2 and 4-4-1 in Figure 7-7). The Variant 3 fuel was fabricated with a variation in the SiC coating process that resulted in a finer-grain microstructure relative to the Baseline fuel (Sections 5.3.2.2 and 5.3.2.4). A similar increase in <sup>110m</sup>Ag release was not observed for the other two compacts heated at 1800°C. These two compacts both had SiC with the larger-grained, Baseline microstructure. All three of the AGR-2 UCO compacts heated at 1800°C exhibited increasing <sup>110m</sup>Ag release similar to the similar AGR-1 Variant 3 compacts



(see red data plots in Figure 7-8). The AGR-2 fuel particles were fabricated with SiC layer deposition conditions based on the AGR-1 Variant 3 process, and a similar fine-grained microstructure (Sections 5.3.2.3 and 5.3.2.4). The conclusion is the finer-grain SiC allows Ag diffusion to a greater extent than the larger-grain AGR-1 Baseline microstructure, but the effect is only detectable after ~100 hours at 1800°C.

The AGR-2 UO<sub>2</sub> tests at both 1600°C and 1700°C exhibited an increase in <sup>110m</sup>Ag release rate after the initial release observed at the start of the test. The onset of this release occurred earlier in the 1700°C test compared to the 1600°C tests. It is likely this increase is related to the significant number of particles experiencing failure of the SiC layer rather than diffusion through intact SiC, which was fabricated using a similar process as the AGR-2 UCO fuel.

### 7.3.4 Europium and Strontium

The release behavior for Eu and Sr was typically very similar during the AGR UCO safety tests. AGR-1 data exhibit similar release curves for the two elements and a similar range of total release values at each temperature (with the exception of a greater spread in 1600°C <sup>90</sup>Sr data toward lower values, as shown in Figure 7-7). For both elements, the data demonstrate a clear trend of increasing release with increasing temperature. In the 1600 and 1700°C tests, the data exhibit relatively constant release rate throughout the tests, and the final release is within the range of values quantified in the matrix of as-irradiated AGR-1 compacts (Figure 7-1). This suggests the release during these tests was primarily from inventory present in the compact matrix at the end of irradiation that was slowly released at elevated temperature.

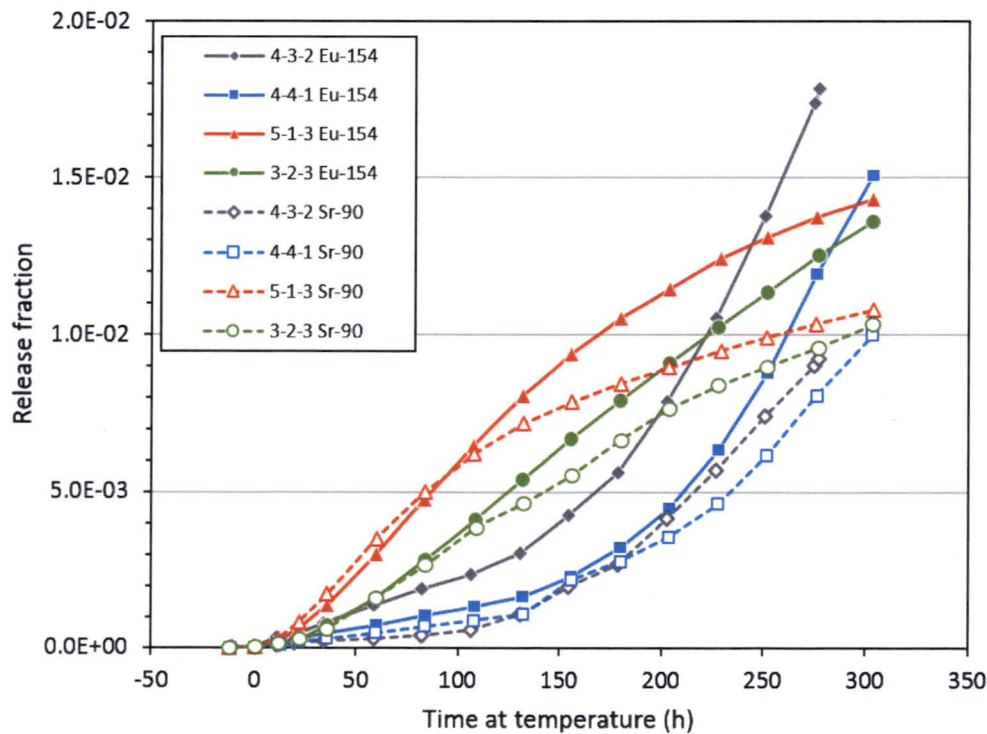


**Figure 7-10**  
<sup>154</sup>Eu and <sup>90</sup>Sr release from AGR-1 compacts heated to 1800°C  
 Courtesy of Idaho National Laboratory and used with permission of Battelle Energy Alliance, LLC

The 1800°C tests displayed differing behavior depending on the fuel type. Release from the two AGR-1 Variant 3 compacts (4-3-2 and 4-4-1) exhibited an increase in rate at around 100 hours, similar to that observed for  $^{110\text{m}}\text{Ag}$ . This suggests the onset of additional release through intact particle coatings. By contrast, the Baseline (3-2-3) and Variant 1 (5-1-3) compacts exhibited a slightly decreasing rate over the same time period. These trends are highlighted in Figure 7-10. The decrease in release rate for the Baseline and Variant 1 compacts may be due to the total  $^{154}\text{Eu}$  and  $^{90}\text{Sr}$  source in the matrix of these compacts becoming depleted toward the end of the test. Note the final  $^{154}\text{Eu}$  and  $^{90}\text{Sr}$  release in the 1800°C tests was very near or slightly exceeding the range of values quantified in the matrix of as-irradiated compacts (Figure 7-1).

The AGR-2 Eu and Sr release data in Figure 7-8 are more complex due to (1) the Capsule 2 compacts that were irradiated at significantly higher temperatures compared to other AGR UCO fuel and (2) the  $\text{UO}_2$  compacts from Capsule 3. The 1600°C  $^{154}\text{Eu}$  and  $^{90}\text{Sr}$  releases from Capsule 5 and 6 UCO compacts (5-2-2 and 6-4-2)—which had irradiation conditions more closely comparable to AGR-1—were in the same range as the AGR-1 values. However, the 1800°C releases from Capsule 5 and 6 compacts (5-4-1 and 6-4-3) were somewhat lower than the AGR-1 values, particularly in the case of  $^{90}\text{Sr}$ ; the  $5.4 \times 10^{-5}$   $^{90}\text{Sr}$  fractional release from

Compact 6-4-3 is the lowest value observed at 1800°C in the AGR program to date. Furthermore, only Compact 5-4-1 exhibited the characteristic increase in  $^{154}\text{Eu}$  and  $^{90}\text{Sr}$  release rate after ~50–100 hours. Compact 6-4-3 exhibited a minor increase in  $^{90}\text{Sr}$  release rate near 150–200 hours, and a gradual decrease in  $^{154}\text{Eu}$  release rate. Figure 7-11 highlights the 1800°C  $^{154}\text{Eu}$  and  $^{90}\text{Sr}$  behavior of these two compacts.

The data from AGR-2 Capsule 2 compacts are labeled on the  $^{154}\text{Eu}$  and  $^{90}\text{Sr}$  plots in Figure 7-8. The end-of-test releases were notably higher compared to other AGR UCO fuel compacts, reaching approximately  $10^{-1}$  at 1800°C, and  $4 \times 10^{-2}$  to  $10^{-1}$  at 1600°C. These high release values during the safety tests are related to the much higher inventory in the matrix of the Capsule 2 compacts, a result of significant diffusion through intact coatings at the relatively high irradiation temperatures. Note these release fractions are near the upper end of the range of values quantified in the matrix of as-irradiated AGR-2 compacts (Figure 7-2).

The AGR-2  $\text{UO}_2$   $^{154}\text{Eu}$  and  $^{90}\text{Sr}$  releases differed from the UCO behavior. While the final  $^{154}\text{Eu}$  fractional release at 1600°C was of a similar magnitude as the UCO values, the  $^{90}\text{Sr}$  values were slightly higher and in one instance (Compact 3-4-2) the release experienced noticeable increase at approximately 100 hours, which corresponds to the increase in  $^{134}\text{Cs}$  release. The 1700°C  $^{154}\text{Eu}$  fractional release from Compact 3-4-1 was approximately  $3 \times 10^{-3}$  at the end of the test, while the  $^{90}\text{Sr}$  was over an order of magnitude higher ( $4.5 \times 10^{-2}$ ). It can be concluded the relatively high number of particles with SiC failure contributed significantly to the Eu and Sr release in the  $\text{UO}_2$  compacts.

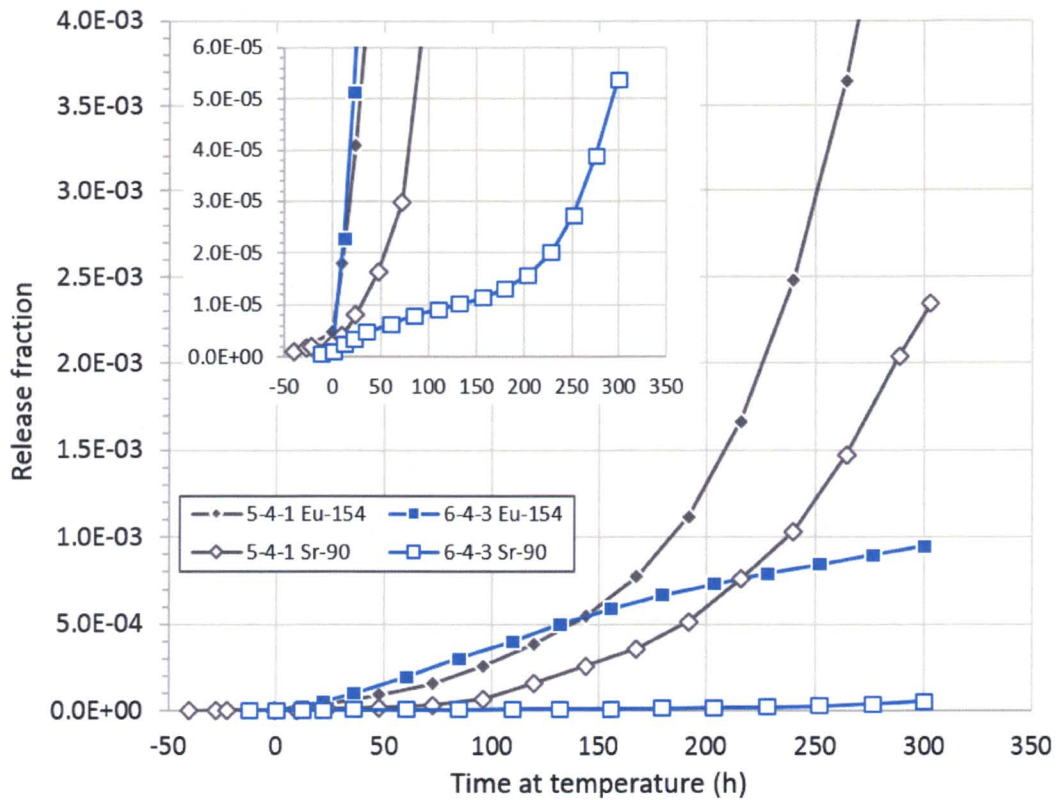


**Figure 7-11**  
 $^{154}\text{Eu}$  and  $^{90}\text{Sr}$  release from AGR-2 Capsule 5 and 6 compacts heated to 1800°C  
 Courtesy of Idaho National Laboratory and used with permission of Battelle Energy Alliance, LLC

### 7.3.5 Krypton

Krypton release curves are not presented here, as there was no  $^{85}\text{Kr}$  detected in the gas effluent in a significant number of the safety tests. Table 7-1 summarizes the Kr release observations from all AGR-1 safety tests and AGR-2 safety tests completed to date for a nominal heating duration of 300 hours. No TRISO failures have been observed in any 1600 or 1700°C tests for both UCO and  $\text{UO}_2$  fuel, and two 1800°C tests exhibited one (AGR-2 Compact 2-3-2) or two (AGR-1 Compact 4-3-2) TRISO failures.

### 7.3.6 Transient Temperature Accident Simulation Tests in Dry Helium

The nominal 300 hours hold at the peak temperature used in the isothermal tests described in the previous section greatly exceeds the duration that fuel will experience peak temperature in a reactor accident. The German  $\text{UO}_2$  TRISO development program in the 1980s performed several accident tests that involved heating the compacts in dry helium using a time-temperature profile that closely simulated the expected peak fuel temperature trajectory in the reactor core during a depressurized loss of forced cooling accident, based on the HTR-MODUL reactor design [90,91]. Several tests were performed in which the peak temperature reached approximately 1620°C. In two of these tests using spherical fuel elements with burnup of 9-10% FIMA,  $^{85}\text{Kr}$

releases exceeded the level of a single particle, indicating one or more particles experiencing TRISO failure. A separate test using an element with burnup of 9% FIMA (element AVR-91/31) was performed with the temperature curve shifted upwards to obtain a maximum of 1700°C. During this test, <sup>85</sup>Kr levels reached approximately 10<sup>-3</sup>, also indicating several TRISO failures.

**Table 7-1**  
**Maximum <sup>85</sup>Kr release fractions for AGR UCO and UO<sub>2</sub> fuel after ~300 hours at 1600, 1700, and 1800°C**

Fuel Type	Temperature	Remarks
UCO	1600°C	<5 × 10 <sup>-6</sup> ; undetectable in majority of tests
	1700°C	<10 <sup>-5</sup>
	1800°C	<6 × 10 <sup>-5</sup> in 5 tests with no TRISO failures ~4 × 10 <sup>-4</sup> in 2 tests where either 1 or 2 TRISO failed
UO <sub>2</sub>	1600°C	<2.5 × 10 <sup>-6</sup> (estimated detection level as no <sup>85</sup> Kr was measured)
	1700°C	4 × 10 <sup>-5</sup> after 174 h; increase probably due to diffusion through OPyC in particles with failed SiC layer

The spheres that experienced failures during the tests were at the upper end of normal burnup for UO<sub>2</sub> TRISO fuel and the uncertainty in the actual irradiation temperature for fuel spheres in AVR was large (with the possibility irradiation temperatures could significantly exceed the reported values). These factors may have contributed to the elevated particle failure fractions observed. Nonetheless, the results of these tests have raised concerns that variable temperature tests with relatively rapid rise to temperature at the start of the accident phase could result in more particle damage than seen in isothermal tests. To address this concern, the AGR program has repeated the more extreme 1700°C test of fuel element AVR-91/31 using three AGR-1 compacts from Capsule 1 (approximately 12,300 particles) [92].

The average burnup of the compacts was 15% FIMA, the average compact TAVA temperature was 1027°C, and the average compact time-average peak temperature was 1123°C. Results of the heating tests are shown in Figure 7-12. The test involved an isothermal hold at a temperature of 857°C for approximately 70 hours before executing a rapid rise to the peak temperature of 1700°C, followed by a relatively gradual temperature decrease to ~1200°C over the next 270 hours (the temperature profile was based on the previous German test of AVR-91/31).

The results are consistent with the isothermal AGR-1 and AGR-2 UCO tests. <sup>110m</sup>Ag fractional release rapidly reached a relatively high level (7 × 10<sup>-2</sup>) and did not change appreciably for the remainder of the test. <sup>134</sup>Cs, <sup>154</sup>Eu, and <sup>90</sup>Sr release all increased initially during the rapid temperature rise but little additional release was observed after a total elapsed time of approximately 215 hours (corresponding to a test temperature of ~1500°C).

The final release of these isotopes was lower than observed for the AGR-1 or AGR-2 1600°C isothermal tests, which would be expected based on the shorter duration at high temperatures (total duration at temperatures >1600°C was approximately 70 hours). <sup>85</sup>Kr fractional release was low throughout the test, with a final value of 3 × 10<sup>-6</sup>. The <sup>134</sup>Cs and <sup>85</sup>Kr data indicate zero particles with SiC layer failure or complete TRISO layer failure during the test.

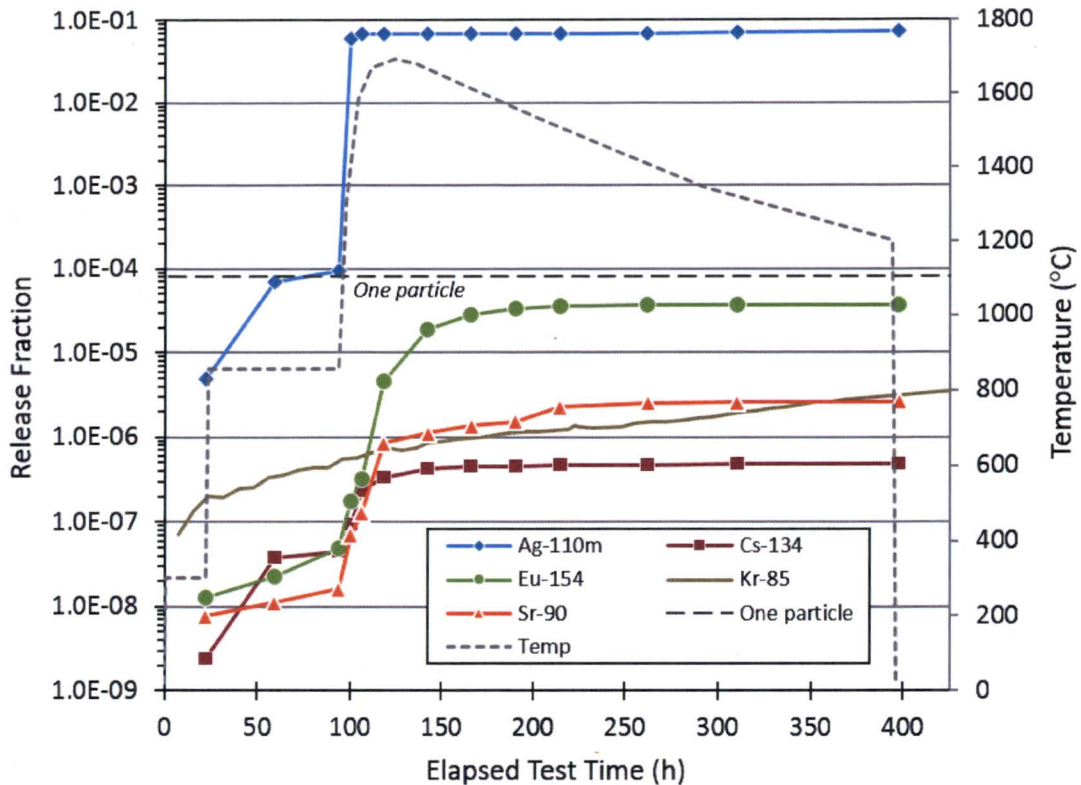


**Figure 7-12**  
**Fission product release during an accident simulation test in dry helium using three AGR-1 compacts**  
*Courtesy of Idaho National Laboratory and used with permission of Battelle Energy Alliance, LLC*

A similar test is planned using three AGR-2 compacts from Capsule 5 (average burnup of 12.7% FIMA, average compact time-average maximum temperature of 1200°C) to compile additional data and confirm the results from the AGR-1 test.

#### 7.4 SiC Failure Mechanisms

Coating layer failure was relatively rare in the AGR UCO fuel particles, both during irradiation and during safety tests. For the AGR-1 and AGR-2 irradiations combined, TRISO failure occurred in approximately 1 out of every 103,000 particles (with none observed in the AGR-1 irradiation), and no TRISO failures occurred in any of the 1600°C or 1700°C safety tests. Instances of SiC layer failure occurred with higher frequency, but were still relatively rare: approximately one in every 52,000 particles during irradiation and one in every 15,000 particles during 1600°C safety tests (detailed failure statistics are compiled and discussed in Section 7.5). Furthermore, the actual degradation and failure of a SiC layer has been found to occur in a localized region within the particle.

A consequence of the low failure fractions and localized corrosion is that the likelihood of observing the layer failure by random examination of particle cross sections (the method commonly employed during historical PIE of particle fuel) is extremely small. In previous TRISO fuel development and testing efforts, particle failure mechanisms were only observed and understood when the rate was sufficiently high that random observation was likely, often at the percent level or higher. Prior to initiating the AGR-1 PIE, methods were developed to locate particles with failures for further study.

Particles that experienced SiC layer failure during irradiation or during safety tests were identified based on elevated cesium release, and many of these were analyzed in detail both nondestructively, using x-ray imaging with tomographic reconstruction, and by cross-sectioning and microanalysis using a number of analytical characterization methods. The basic approach used for the AGR-1 fuel has been described previously [82] and is being repeated for the AGR-2 fuel [85,93].

For SiC failures during irradiation, the examination process started with gamma-scanning the empty graphite holders to locate regions with elevated cesium activity. The compacts that were adjacent to these regions during irradiation were identified as likely to contain one or more particles that experienced SiC failure in-pile. These as-irradiated compacts, as well as compacts that exhibited Cs release indicative of SiC failure during safety testing, were then deconsolidated to liberate the particles, which were individually gamma counted to quantify the inventory of  $^{137}\text{Cs}$ ,  $^{134}\text{Cs}$ , and  $^{144}\text{Ce}$ . Particles that exhibited abnormally low cesium inventory were then collected, and x-ray imaging was used to nondestructively observe the interior particle morphology.

In total, three particles with high cesium release during the AGR-1 irradiation were found in two compacts and examined. (A fourth particle was detected during deconsolidation-leach-burn-leach analysis of another compact but was destroyed in the process; therefore, the particle was not subjected to detailed microstructural analysis). In all of these particles, a similar failure mechanism was implicated. Buffer shrinkage contributed to IPyC fracture due to incomplete debonding at the buffer-IPyC interface.

In one case, arrowhead-like fracture occurred (similar to that shown in Figure 7-5e), while in the other two particles, IPyC fracture was related to stress from the buffer pulling away from the IPyC (similar to Figure 7-5f). The IPyC fracture then exposed the SiC layer to concentrated chemical attack of fission products (notably Pd), which caused degradation through the entire layer (see Figure 7-13).

It is noteworthy significant attack of the SiC layer was never observed in particles without this sort of IPyC fracture, nor in these three particles in areas away from the IPyC fracture. So, while these failures were ultimately caused by Pd attack on SiC, prior fracture of the IPyC layer appears to be a prerequisite for the attack to occur.

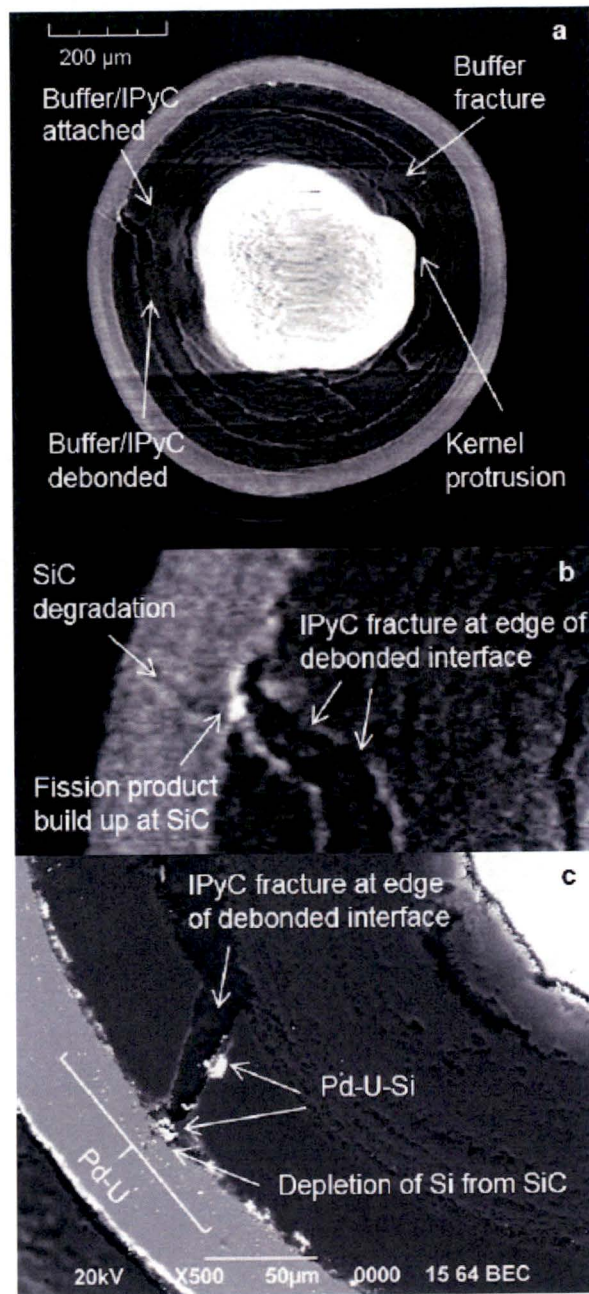
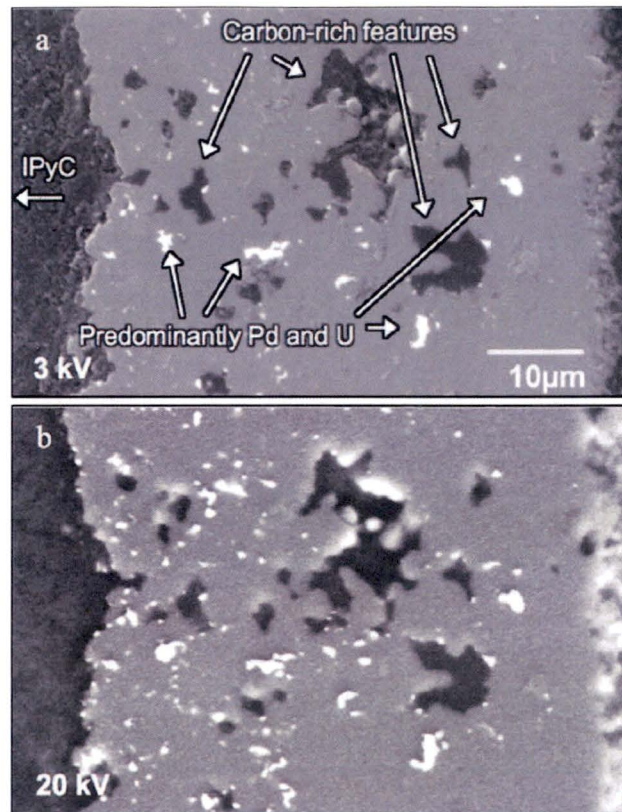


Figure 7-13

(a) X-ray tomogram showing microstructure in as-irradiated AGR-1 Compact 5-2-3 particle that led to SiC failure and cesium release; (b) x-ray close-up of degraded pathway through SiC; and (c) SEM micrograph of degraded region with EDS identification of Pd and U in the SiC and Si outside the SiC

*Courtesy of Idaho National Laboratory and used with permission of Battelle Energy Alliance, LLC*

AGR-1 safety testing produced SiC failures in fractions higher than during irradiation, with the failure fractions increasing with test temperature. At 1600°C, two of the three AGR-1 particles with SiC failures that were identified were examined in detail, and the cause of the SiC failure was determined to be an as-fabricated defect in the SiC layer (the third particle was not recovered for analysis). At 1700 and 1800°C, nearly all of the particles recovered exhibited a similar SiC failure mechanism to the one identified for the as-irradiated particles. However, the elevated temperature increased the severity of the SiC degradation due to enhanced reaction with fission products. Figure 7-14 shows the local corrosion of the SiC layer in an AGR-1 particle from a 1700°C safety test.



**Figure 7-14**

**Corroded region of the SiC layer of an AGR-1 particle safety tested at 1700°C**

*Courtesy of Idaho National Laboratory and used with permission of Battelle Energy Alliance, LLC*

Examination of SiC failures in AGR-2 particles has been less conclusive, as it appears some particles experiencing SiC failure (both during irradiation and during safety testing) may have been destroyed during the DLBL process, eliminating the opportunity to perform detailed examination. In addition, several particles from AGR-2 Capsule 2 that experienced failed SiC were recovered and examined in detail. Evidence was present of significant degradation of the SiC layer from nickel [93]. The evidence suggests that these particles failed due to interaction



with Ni contamination, likely originating from a failed thermocouple in the graphite holder located very close to these compacts during the irradiation as the TCs contain Ni in their thermoelements. However, some of the AGR-2 particles that have been observed with SiC failure indicate a similar mechanism as described above for the AGR-1 particles.<sup>18</sup>

The dominant SiC failure mechanism described here is significantly different from those currently embedded in fuel performance models.<sup>19</sup> Incorporation of this failure mode into the models is likely to be challenging due to its complex nature (essentially a two-part mechanism, involving thermomechanical behavior of the buffer and IPyC under irradiation, followed by focused chemical attack of the SiC layer) and a lack of some key data (including buffer strength, buffer-IPyC bond strength, fission product partitioning coefficients at the site of the IPyC fracture, and reaction kinetics for the chemical degradation). It is also unclear whether this type of SiC layer failure acts as a precursor to complete TRISO failure (that is, whether eventual failure of the OPyC layer in these particles and related release of fission gas is a likely scenario). While this seems plausible, particles with TRISO failure are sufficiently rare and are not usually recovered intact for further study, such that their specific cause in the AGR UCO particles is not known with certainty in most instances.

## **7.5 Particle Failure Statistics**

The statistics for both SiC layer failure and full TRISO failure for AGR-1 and AGR-2 UCO fuel—both during irradiation and during safety tests—are compiled in Table 7-2. The table lists the total number of compacts and particles for each test condition, the number of observed failures of each type based on current best estimate values from irradiation and PIE data, the actual failure fraction (number of failures divided by number of particles tested), and the upper 95% confidence limit on the failure fraction calculated using binomial statistics. Explanation of the AGR-1 data has been provided by Demkowicz et al. [82].

The AGR-2 data are preliminary and are based on PIE and safety testing completed to date. As mentioned in Sections 6.7 and 6.8, exact numbers of particles that experienced failed TRISO during the irradiation could not be reliably determined based on R/B ratios. A conservative approach was taken in assessing available AGR-2 PIE data in this regard, and is described briefly here.

Particles with exposed kernels in AGR-2 compacts were assessed based on a combination of capsule fission product inventory data (data on fission product—primarily Cs—release from compacts during irradiation), DLBL results (for example, the presence of uranium from dissolved kernels in the pre-burn leach solutions), particle gamma counting and subsequent x-ray analysis of selected particles, and safety testing data (which could indicate exposed kernels in a compact if fission gas release is elevated from the start of the test). This analysis is significantly

---

<sup>18</sup> This excludes the particles in AGR-2 Compact 2-2-3 that exhibited obvious evidence of external nickel attack on the SiC layer, which is believed to be due to the combination of a very close proximity to a failed thermocouple in the graphite holder and the relatively high irradiation temperature. See discussion by Hunn et al. for details (Reference 100). These particles are not included in the calculated AGR-2 failure statistics. However, they did contribute to overall Cs release from the fuel compacts in Capsule 2, artificially elevating the reported values.

<sup>19</sup> Note that the PARFUME code does not consider the possibility of SiC failure with the OPyC remaining intact, as failure of SiC layer automatically results in OPyC failure in the model. Nonetheless, this mode of SiC layer failure (that is, localized Pd attack resulting from IPyC failure and IPyC-SiC debonding) is not considered in the model.

complicated by several issues, including: (a) particles with failed SiC, but intact OPyC, will release Cs during irradiation along with exposed kernels and therefore the two cannot be distinguished based on Cs release alone; (b) the results of leaching to assess exposed kernels (that is, the uranium content in the leaching solutions) is not always definitive with regard to quantifying the number of kernels leached; (c) kernels that are leached in pre-burn leach solutions could be from particles that had exposed kernels in-pile or to particles that experienced SiC failure in-pile but subsequently experienced OPyC failure during the deconsolidation process; and (d) there is usually no effective means during post-irradiation analysis to distinguish an exposed kernel defect from a particle that experienced TRISO failure in-pile.

In cases where the source of the exposed kernel could not be definitively determined (for example, as-fabricated exposed kernel, in-pile TRISO failure, or TRISO failure during destructive PIE analysis), all suspected exposed kernels were conservatively assessed as in-pile TRISO failure. The result is an estimate of  $\leq 4$  in-pile AGR-2 TRISO failures (Table 7-2). Given the measured exposed kernel defect fractions for the AGR-2 compacts discussed in Section 6.8, it is possible that one or more of these particles was in fact an as-fabricated defect.

Data for AGR-1 and AGR-2 are listed separately in Table 7-2, and the data are combined for both experiments at the bottom of the table. AGR-2 values may change slightly upon completion of PIE and safety testing. The results of the AGR-1 transient temperature test have not been included in the totals.

The TRISO failure fraction during AGR-1 irradiation for was  $\leq 1.1 \times 10^{-5}$  at 95% confidence. The conservative approach for assigning TRISO failure to the AGR-2 capsules during irradiation results in a failure fraction  $\leq 8.1 \times 10^{-5}$ . Combining the data from both experiments gives a value of  $\leq 2.3 \times 10^{-5}$ . This is approximately a factor of 9 lower than typical reactor design specifications for allowable in-service TRISO failures under normal operating conditions ( $2 \times 10^{-4}$ ).

No TRISO failures were observed in any of the 1600°C safety tests. Combining the results gives a total TRISO failure fraction of  $\leq 6.6 \times 10^{-5}$  at 95% confidence. This is a factor of 9 lower than typical reactor design specifications for allowable failures during 1600°C accidents ( $6 \times 10^{-4}$ ). It is also important to note a relatively small percentage of the fuel in the reactor core experiences the peak temperature of 1600°C during an accident, whereas in the AGR safety tests 100% of the particles experienced the target test temperature. In addition, the dwell time of the fuel at peak temperature during an accident is relatively short (for example, the fuel compacts in the AGR-1 transient test shown in Figure 7-12 were within 100°C of peak temperature for 70 h), while the AGR isothermal safety tests have a nominal duration of 300 hours.

The combined AGR-1 and AGR-2 TRISO failure fraction at 1800°C is  $\leq 3.0 \times 10^{-4}$  at 95% confidence. While reactor design specifications do not extend to this temperature, given it is significantly beyond peak core temperatures expected during an accident, it is noteworthy this value is still a factor of 2 below the specification for allowable failures at 1600°C mentioned above.

The combined (AGR-1 + AGR-2) SiC failure fractions are  $\leq 3.6 \times 10^{-5}$  during irradiation and  $\leq 1.7 \times 10^{-4}$  and  $\leq 1.3 \times 10^{-3}$  during safety testing at 1600°C and 1800°C, respectively (all values are the upper limit at 95% confidence). While there are currently no reactor design specifications for SiC layer failure, it is noteworthy the irradiation and 1600°C values are lower than the allowable TRISO failures under these conditions. Another important observation from the safety testing data in this regard is the appreciably lower incidence of SiC layer failure in the AGR-2

fuel; particularly at 1800°C (roughly half the number of particles were tested, but only 13% of the number of AGR-1 SiC failures were observed). It is not known for certain if this may be related to the lower incidence of IPyC failure observed in random particle samples (see discussion in Section 7.2).

Figure 7-15 shows a plot of the total combined (AGR-1 + AGR-2) SiC layer and full TRISO failure fractions for irradiation and for each of the safety test temperatures (note that no combined 1700°C test data are provided, as no 1700°C tests were performed on AGR-2 UCO compacts).

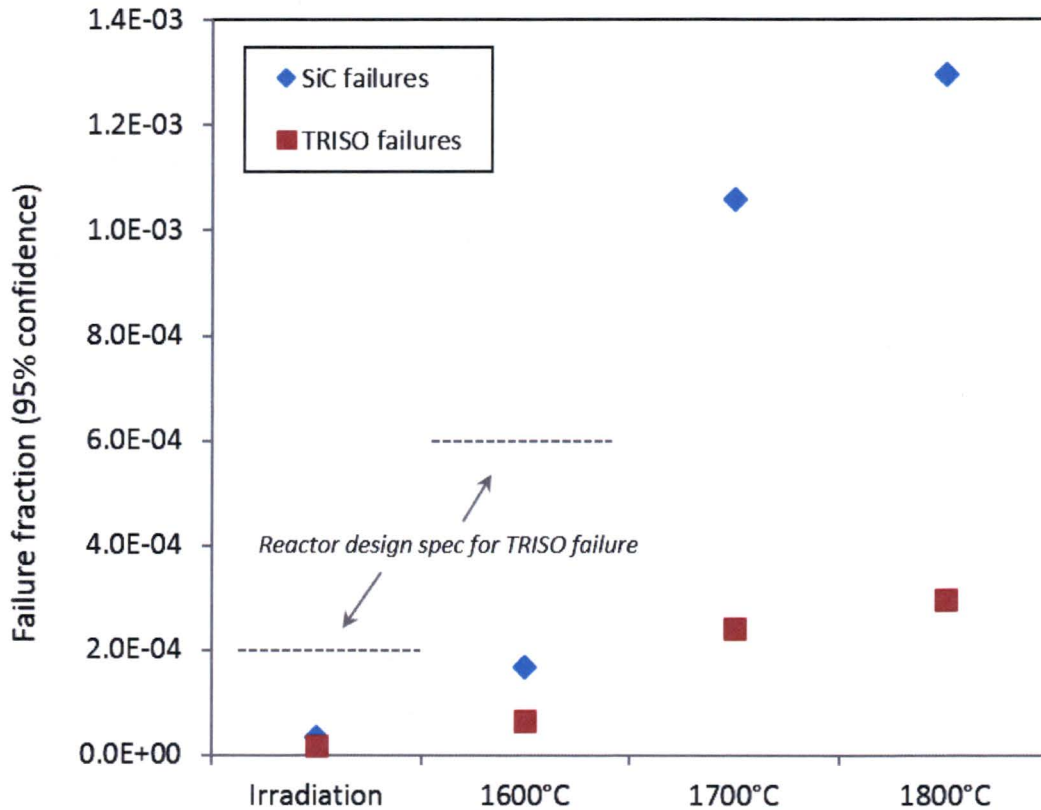


**Figure 7-15**  
**SiC layer and full TRISO failure fractions (upper limit at 95% confidence) for combined AGR-1 and AGR-2 UCO results during irradiation and during safety tests**  
 Courtesy of Idaho National Laboratory and used with permission of Battelle Energy Alliance, LLC

No TRISO failures were observed in the AGR-2 UO<sub>2</sub> (Capsule 3) fuel compacts. In spite of the much higher frequency of SiC failure during safety tests relative to UCO, no TRISO failures were observed in the three safety tests completed to date. However, the much smaller number of particles involved in these tests prevents determination of statistically significant failure fractions. Zero observed TRISO failures out of 18,480 particles in the irradiation results in a failure fraction of  $\leq 1.7 \times 10^{-4}$  at 95% confidence. The true failure fraction for this population is likely much lower than this, but a significantly greater number of particles need to be tested to confirm this. Zero observed TRISO failures in the 4,630 particles in safety tests results in a failure fraction of  $\leq 6.5 \times 10^{-4}$  at 95% confidence.

Calculation of SiC failure fraction during irradiation suffers from the same statistical penalty of low particle numbers, and the value is the same as the TRISO failure fraction since zero failures were observed. During safety testing, there were significantly more SiC failures compared to UCO fuel (as discussed in Section 7.3.1), and quantification of the exact number of particles has not been possible.

**Testing of UCO TRISO-coated fuel particles in AGR-1 and AGR-2 constitutes a performance demonstration of these particle designs over a range of normal operating and off-normal accident conditions. Therefore, the testing provides a foundational basis for use of these particle designs in the fuel elements of TRISO-fueled HTR designs (that is, designs with pebble or prismatic fuel and helium or salt coolant).**

**Aggregate AGR-1 and AGR-2 fission product release data and fuel failure fractions, as summarized in this report, can be used for licensing of reactors employing UCO TRISO-coated fuel particles that satisfy the parameter envelope defined by measured particle layer properties in Table 5-5 from AGR-1 and AGR-2.**

Table 7-2

SiC layer and full TRISO failure statistics for AGR-1 and AGR-2 UCO fuel during irradiation and during safety tests. AGR-2 data are preliminary, pending completion of PIE and safety testing.

Test Conditions	Number of Compacts	Number of Particles	SiC Failures			TRISO Failures		
			Number of Failures	Failure Fraction	95% Conf	Number of Failures	Failure Fraction	95% Conf
<b>AGR-1</b>								
Irradiation	72	298,000	4	$1.3 \times 10^{-5}$	$\leq 3.1 \times 10^{-5}$	0	0	$\leq 1.1 \times 10^{-5}$
1600°C	8	33,100	3	$9.1 \times 10^{-5}$	$\leq 2.4 \times 10^{-4}$	0	0	$\leq 9.1 \times 10^{-5}$
1700°C	3	12,400	7	$5.6 \times 10^{-4}$	$\leq 1.1 \times 10^{-3}$	0	0	$\leq 2.5 \times 10^{-4}$
1800°C	4	16,500	23	$1.4 \times 10^{-3}$	$\leq 2.0 \times 10^{-3}$	2	$1.2 \times 10^{-4}$	$\leq 3.9 \times 10^{-4}$
<b>AGR-2</b>								
Irradiation	36	114,336	4	$3.5 \times 10^{-5}$	$\leq 8.1 \times 10^{-5}$	$\leq 4^a$	$\leq 3.5 \times 10^{-5}$	$\leq 8.1 \times 10^{-5}$
1600°C	4	12,704	0	0	$\leq 2.4 \times 10^{-4}$	0	0	$\leq 2.4 \times 10^{-4}$
1800°C	3	9,528	1	$1.0 \times 10^{-4}$	$\leq 5.0 \times 10^{-4}$	1	$1.0 \times 10^{-4}$	$\leq 5.0 \times 10^{-4}$
<b>AGR-1 + AGR-2</b>								
Irradiation	108	412,336	8	$1.9 \times 10^{-5}$	$\leq 3.6 \times 10^{-5}$	$\leq 4^a$	$\leq 9.7 \times 10^{-6}$	$\leq 2.3 \times 10^{-5}$
1600°C	12	45,804	3	$6.5 \times 10^{-5}$	$\leq 1.7 \times 10^{-4}$	0	0	$\leq 6.6 \times 10^{-5}$
1800°C	7	26,028	24	$9.2 \times 10^{-4}$	$\leq 1.3 \times 10^{-3}$	3	$1.2 \times 10^{-4}$	$\leq 3.0 \times 10^{-4}$

<sup>a</sup>This value is the upper bound on the estimated number of in-pile failures. The precise value is not known but is estimated to be between 0 and 4.

# 8

## SUMMARY/CONCLUSIONS

---

The AGR-1 and AGR-2 data and analyses on UCO TRISO-coated particle fuel performance presented in Sections 5 – 7 of this topical report supports the following conclusions for NRC approval:

### Conclusion 1:

*Testing of UCO TRISO-coated fuel particles in AGR-1 and AGR-2 constitutes a performance demonstration of these particle designs over a range of normal operating and off-normal accident conditions. Therefore, the testing provides a foundational basis for use of these particle designs in the fuel elements of TRISO-fueled HTR designs (that is, designs with pebble or prismatic fuel and helium or salt coolant).*

The AGR program has demonstrated excellent irradiation performance of a statistically large population of UCO TRISO fuel particles under conditions of high burnup and high temperature. Compact-average burnup ranged from 7.3 to 19.6% FIMA and fuel compact time-average maximum temperatures ranged from 1069 to 1360°C. Results for irradiation, PIE, and safety testing from two experiments (AGR-1 and AGR-2), with fuel fabricated using a range of process parameters, show consistently robust performance.

### Conclusion 2:

*The kernels and coatings of the UCO TRISO-coated fuel particles tested in AGR-1 and AGR-2 exhibited property variations and were fabricated under different conditions and at different scales, with remarkably similar excellent irradiation and accident safety performance results. The ranges of those variations in key characteristics of the kernels and coatings are reflected in measured particle layer properties provided in Table 5-5 from AGR-1 and AGR-2. UCO TRISO-coated fuel particles that satisfy the parameter envelope defined by these measured particle layer properties in Table 5-5 can be relied on to provide satisfactory performance.*

Beyond the empirical performance data, it is important to note the fissile kernels of the particles in AGR-1 and AGR-2 were of different size and enrichment and the coatings were applied in an uninterrupted manner in coatiers of two different sizes (that is, a 2-in. laboratory-scale coater and a 6-in. engineering-scale coater). Further, the coating conditions were varied so different microstructures and properties of the coatings were produced. The behavior with two different UCO kernels confirms the performance of the coatings is the primary factor for achieving good fuel performance such that the kernel is of secondary importance.

In terms of coating characteristics, AGR-1 coated particles were fabricated using a range of coating conditions that produced: (1) different combinations of PyC anisotropy and density, which in some cases were intentionally at the edge of the historic specification range; and (2) different microstructures of the SiC—a larger grain, made with traditional hydrogen and MTS coating gases, and a finer grain, by introducing argon gas as a diluent to improve fluidization

during SiC deposition. Based on the in-pile results available at the time, the AGR program decided the AGR-2 PyC coating would be applied using baseline conditions using in AGR-1 and would use argon dilution during the SiC coating step (similar to Variant 3 in the AGR-1 fuel) for the best fluidization in the 6-in. coater. Despite these variations in coating conditions, the performance of intact TRISO particles was nominally the same, albeit with slightly higher fission gas release in AGR-2 due to slightly higher uranium contamination of the particle batch in the larger engineering-scale coater.

These results demonstrate TRISO-coated particles can be made in a variety of coaters under a range of process conditions with some flexibility in coating parameter space in terms of acceptable values of density and anisotropy of the PyC and the microstructure of the SiC to achieve satisfactory irradiation performance.

### Conclusion 3:

*Aggregate AGR-1 and AGR-2 fission product release data and fuel failure fractions, as summarized in this report, can be used for licensing of reactors employing UCO TRISO-coated fuel particles that satisfy the parameter envelope defined by measured particle layer properties in Table 5-5 from AGR-1 and AGR-2.*

The fission gas release measured during AGR-1 was extremely low. About 300,000 TRISO fuel particles were irradiated without a single particle failure, making it the best irradiation performance of a large quantity of TRISO fuel ever achieved in the U.S., and substantially exceeding the German levels of burnup. These results have confirmed the expected superior irradiation performance of UCO at high burnup in that no kernel migration, no evidence of CO attack of SiC, and no indication of severe SiC attack by noble metal or lanthanide fission products has been observed. Zero fuel failures out of 300,000 particles in the AGR-1 irradiation translates into a 95% confidence failure fraction of  $<1.1 \times 10^{-5}$ , a factor of 18 better than the prismatic reactor design in-service failure fraction requirement of  $2 \times 10^{-4}$ .

The in-pile fission gas release for AGR-2 was higher than AGR-1, partly due to a higher level of HM contamination measured on the fabricated fuel. No particle failures were conclusively identified during irradiation based on fission gas release; however, because of the experimental anomalies associated with the AGR-2 irradiation capsule, the possibility of a small number of failures cannot be precluded.

The preliminary PIE data available indicates that  $\leq 4$  particles experienced TRISO failure in the three UCO capsules. Four failures out of a total of 114,000 UCO particles in the experiment corresponds to an actual failure fraction  $\leq 8.1 \times 10^{-5}$  at 95% confidence, which is approximately a factor of 2.5 below the historic MHTGR design specification of  $2 \times 10^{-4}$ . Additionally, the high-temperature UCO capsule in AGR-2 showed excellent behavior under irradiation, at a time-average peak temperature of 1360°C, and 10 to 20% of the particles in that capsule were exposed to temperatures in excess of 1400°C for hundreds of days. This early margin test demonstrated the high-temperature capability of these fuel particles.

Aggregate AGR-1 and AGR-2 data yield a TRISO particle failure fraction of  $\leq 2.3 \times 10^{-5}$  at 95% confidence, approximately a factor of 9 below historic MHTGR design specifications.

Cesium fractional release from compacts containing only particles with intact SiC was very low ( $<3 \times 10^{-6}$  for  $^{134}\text{Cs}$ ), and as a result, the total Cs release from the fuel compacts is primarily dependent on the extent of SiC layer failure. Total  $^{134}\text{Cs}$  fractional release from compacts under normal operating temperatures in both experiments (including all AGR-1 capsules and AGR-2 Capsules 5 and 6) was  $\leq 4.4 \times 10^{-5}$ . Eu and Sr exhibited modest release through intact coatings, although significant retention was observed in the fuel matrix. Inventory in the compact matrix could be as high as  $\sim 10^{-2}$  ( $^{154}\text{Eu}$ ) and  $3 \times 10^{-3}$  ( $^{90}\text{Sr}$ ) for fuel irradiated at normal operating temperatures, but fractional release from fuel compacts was  $\leq 4.6 \times 10^{-4}$  ( $^{154}\text{Eu}$ ) and  $\leq 8.2 \times 10^{-5}$  ( $^{90}\text{Sr}$ ).

At higher irradiation temperatures (up to a time-average maximum of  $1360^\circ\text{C}$ ), Eu and Sr release from compacts is notably higher (approximately  $4 \times 10^{-3}$  for  $^{154}\text{Eu}$  and  $10^{-3}$  for  $^{90}\text{Sr}$ ). Silver release was high, consistent with historical observations. No widespread Pd attack or corrosion of SiC was observed despite finding large amounts of Pd outside of the SiC layer.

Safety testing in the  $1600 - 1800^\circ\text{C}$  range has demonstrated the robustness of UCO TRISO under depressurized conduction cooldown conditions. No full TRISO particle failures have been observed at  $1600$  or  $1700^\circ\text{C}$ . Fractional release of  $^{134}\text{Cs}$  from compacts containing only intact particles at  $1600^\circ\text{C}$  was  $<6 \times 10^{-5}$ . When a SiC layer in a particle failed, some of the Cs from that particle was released.

Releases of Ag, Sr, and Eu at  $1600$  and  $1700^\circ\text{C}$  are attributed to diffusion of these fission products into the fuel matrix during irradiation and subsequent release from the matrix upon high-temperature heating. Overall, the results indicate low incremental release of safety-relevant fission products under accident conditions. These results obtained to date from AGR-2 UCO fuel produced at engineering scale are similar to those from AGR-1 laboratory-scale fuel.

These results demonstrate the UCO TRISO-coated particles that underwent irradiation and subsequent high-temperature heating as part of the AGR-1 and AGR-2 experiments exhibited excellent performance and meet historic design specifications for allowable particle failures with significant margin. The data support the use of LEU UCO TRISO fuel for future high-temperature reactor designs, with specific kernel geometry and enrichment dependent on reactor design and burnup goals, provided overall particle design remains similar to those demonstrated by the AGR program.



# 9

## REFERENCES

---

1. W. Scheffel and J. Saurwein. *Preliminary Fuel Product Specifications for the Baseline Advanced Gas Reactor Fuel Design*. General Atomics, San Diego, CA: September 2003. 911034, Rev. 0.
2. U.S. Nuclear Regulatory Commission, Office of Nuclear Reactor Regulation. *Office Instruction: Topical Report Process*. LIC-500, Rev. 6. Washington, D.C.: March 2018.
3. P.A. Demkowicz, D.A. Petti, D.W. Marshall, M.R. Holbrook, and W.L. Moe, *Technical Bases for the Performance Demonstration of TRISO-coated UCO Fuel Particles*. Idaho National Laboratory: September 2018. INL/LTD-18-46060, Rev. 0.
4. *NGNP Licensing Plan*. Idaho National Laboratory, Idaho Falls, ID: June 26, 2009. PLN-3202.
5. G.M. Tracy, Director, U.S. Nuclear Regulatory Commission, Office of New Reactors, Letter to Dr. J. Kelly, DOE Deputy Assistant Secretary for Nuclear Technologies, “NGNP – Assessment of Key Licensing Issues,” ML14174A734, with Enclosure 1 (“Summary Feedback on Four Key Licensing Issues,” ML14174A774) and Enclosure 2 (“Assessment of White Paper Submittals on Fuel Qualification and Mechanistic Source Terms,” Rev.1, ML14174A845).
6. U.S. Code of Federal Regulations. *Domestic Licensing of Production and Utilization Facilities*. 10 CFR Part 50. [http://ecfr.gpoaccess.gov/cgi/t/text/text-idx?c=ecfr&tpl=/ecfrbrowse/Title10/10cfr50\\_main\\_02.tpl](http://ecfr.gpoaccess.gov/cgi/t/text/text-idx?c=ecfr&tpl=/ecfrbrowse/Title10/10cfr50_main_02.tpl)
7. U.S. Nuclear Regulatory Commission. *Guidance for Developing Principal Design Criteria for Non-Light-Water Reactors*. RG 1.232. Washington, D.C.: April 2018.
8. R.A. Simon and P.D. Capp, 2002, “Operating experience with the Dragon High Temperature Reactor Experiment”, *Proceedings of the Conference on High Temperature Reactors (HTR-2002)*, Petten, the Netherlands, April 22-24, 2002. International Atomic Energy Agency, Vienna: 2002.
9. K.I. Kingrey. *Fuel Summary for Peach Bottom Unit 1 High-Temperature Gas-Cooled Reactor Cores 1 and 2*, Idaho National Laboratory, Idaho Falls, ID: April 2003. INEEL/EXT-03-00103.
10. *AVR – Experimental High-Temperature Reactor, 21 Years of Successful Operation for a Future Energy Technology*. VDI-Verlag GmbH, Düsseldorf: June 1990.

---

References

11. *A Review of Radionuclide Release from HTGR Cores During Normal Operation*. Electric Power Research Institute, Palo Alto, CA: February 2004. 1009382.
12. *Fuel Performance and Fission Product Behaviour in Gas Cooled Reactors*. International Atomic Energy Agency, Vienna: November 1997. IAEA-TECDOC-978.
13. *Advances in High Temperature Gas Cooled Reactor Fuel Technology*. International Atomic Energy Agency, Vienna: June 2012. IAEA-TECDOC-1674.
14. D. McEachern, R. Noren, and D. Hanson, "Manufacture and irradiation of Fort St. Vrain fuel," *International HTR Fuel Seminar*, Brussels, Belgium, February 2001.
15. D.A. Petti, J.T. Maki, J. Buongiorno, R.R. Hobbins, and G.K. Miller. *Key Differences in the Fabrication, Irradiation and Safety Testing of U.S. and German TRISO-coated Particle Fuel and Their Implications on Fuel Performance*. Idaho National Laboratory, Idaho Falls, ID: April 2002. INEEL/EXT-02-00300.
16. R.R. Hobbins and R.K. McCardell. *Summary of NP-MHTGR Fuel Failure Evaluation*. September 1993. EGG-NPR-10967.
17. *MHTGR TRISO-P Fuel Failure Evaluation Report*. General Atomics, San Diego, CA: October 1993. DOE-HTGR-90390, Rev. 0.
18. G. Bourcharadt, B. Hürttlen, and G Pott. *Experiment FRJ2-P24 Bestrahlungsbericht*. Kernforschungsanlage Jülich, Jülich, Germany: August 1982. Interner Bericht KFA-ZBB-1B-19/82.
19. C. Bauer and H. Klöcker. *Elektrolytische Desintegration an 3 Compacts aus dem Experiment FRJ2-P24*. Kernforschungsanlage Jülich, Jülich, Germany: March 17, 1983. Interne Notiz IRW-IN – 8/83.
20. D.T. Goodin. *Accident Condition Performance of High-Temperature Gas-Cooled Reactor Fuels*, GA Technologies, Inc., San Diego, CA: October 1983. GA-A16508.
21. R.E. Bullock, "Fission-product release during postirradiation annealing of several types of coated fuel particles," *Journal of Nuclear Materials*, Vol. 125, pp. 304–319 (1984).
22. B. Myers et al. *Capsule R2-K13: Final Report on Cells 2 and 3*. GA Technologies, Inc., San Diego, CA: September 1985. HTGR-85-08668.
23. *Mechanistic Source Terms White Paper*. Idaho National Laboratory, Idaho Falls, ID: July 2010. INL/EXT-10-17997.
24. D.A. Petti, R.R. Hobbins, P. Lowry and H. Gougar, "Representative source terms and the influence of reactor attributes on functional containment in modular high temperature gas-cooled reactors," *Nuclear Technology*, Vol. 184, pp. 181–197 (2013).

25. F.J. Homan, T.B. Lindemer, E.L. Long, Jr., T.N. Tiegs, and R.L. Beatty, "Stoichiometric effects on performance of high-temperature gas-cooled reactor fuels from the U-C-O system," *Nuclear Technology*, Vol. 35, pp. 428-441 (1977).
26. D. Olander, "Nuclear fuels – Present and future," *Journal of Nuclear Materials*, Vol. 389, pp. 1-22. (2009).
27. E. Proksch, A. Strigl, and H. Nabielek, "Carbon monoxide formation in UO<sub>2</sub> kernalled HTR fuel particles containing oxygen getters," *Journal of Nuclear Materials*. Vol. 139, pp. 83-90 (1986).
28. *NP-MHTGR Material Models of Pyrocarbon and Pyrolytic Silicon Carbide*. Combustion Engineering General Atomics Corporation, San Diego, CA: July 1993. CEGA-002820, Rev. 1.
29. J. Kaae, D. Stevens, and C. Luby, "Prediction of the irradiation performance of coated particle fuels by means of stress-analysis models," *Nuclear Technology*, Vol. 10, p. 44 (1971).
30. H. Walther, "On mathematical models for calculating the mechanical behaviour of coated fuel particles," *Nuclear Engineering and Design*, Vol. 18, No. 1, pp. 11–39 (1972).
31. D.G. Martin, "An analytical method of calculating, to a reasonable accuracy, stresses in the coatings of HTR fuel particles," *Journal of Nuclear Materials*. Vol. 48, No. 1, pp. 35–46 (1973).
32. G.K. Miller, D. A. Petti, D. J. Varacalle, and J. T. Maki, "Statistical approach and benchmarking for modeling of multi-dimensional behavior in TRISO-coated fuel particles," *Journal of Nuclear Materials*, Vol. 317, pp. 69–82 (2003).
33. G.K. Miller, G. K., D. A. Petti, and J. T. Maki, "Consideration of the effects of partial debonding of the IPyC and particle asphericity on TRISO-coated fuel behavior," *Journal of Nuclear Materials*, Vol. 334, p. 79 (2004).
34. G.K. Miller, G. K., D. A. Petti, J. T. Maki, and D. L. Knudson, "An evaluation of the effects of SiC layer thinning on failure of TRISO-coated fuel particles," *Journal of Nuclear Materials*, Vol. 355, pp. 150–162 (2006).
35. W.F. Skerjanc, J. T. Maki, B. P. Collin, and D. A. Petti, "Evaluation of design parameters for TRISO-coated fuel particles to establish manufacturing critical limits using PARFUME," *Journal of Nuclear Materials*, Vol., 469, pp. 99–104 (2016).
36. J.J. Powers and B.D. Wirth, "A review of TRISO fuel performance models," *Journal of Nuclear Materials*, Vol. 405, pp. 74–82 (2010).
37. W.F. Skerjanc and P.A. Demkowicz. *PARFUME Theory and Model Basis Report*. Idaho National Laboratory, Idaho Falls, ID: September 2018. INL/ EXT-08-14497, Rev. 1.

---

References

38. *Technical Program Plan for INL Advanced Reactor Technologies Advanced Gas Reactor Fuel Development and Qualification Program*. Idaho National Laboratory, Idaho Falls, ID: June 2018. PLN-3636, Rev. 7.
39. M. Wagner-Löffler, "Amoeba behavior of UO<sub>2</sub> coated particle fuel," *Nuclear Technology*, Vol. 35, p. 392 (1977).
40. J.W. Ketterer and B. F. Myers. *Capsule HRB-16 Postirradiation Examination Report*. General Atomics, San Diego, CA: September 1985. HTGR-85-053.
41. K. Minato, T. Ogawa, S. Kashimura, K. Fukuda, I. Takahashi, M. Shimizu, and Y. Tayama, "Carbon monoxide - silicon carbide interaction in HTGR fuel particles," *Journal of Materials Science*, Vol. 26, p. 2379 (1991).
42. S. Muñoz. *Fuel Product Specification*. General Atomics, San Diego, CA: May 1994. DOE-HTGR-100209. Rev. 0.
43. *Preliminary AGR Fuel Specification*. Idaho National Laboratory, Idaho Falls, ID: April 2004. EDF-4198, Rev. 1.
44. *Technical Program Plan for the Advanced Gas Reactor Fuel Development and Qualification Program*. Oak Ridge National Laboratory, Oak Ridge, TN: April 2003. ORNL/TM-2002/262.
45. William F. Martin, Chairman, and John Ahearne, Vice Chairman, Nuclear Energy Advisory Committee, Letter to Dr. Steven Chu, Secretary of Energy, Washington, D.C. June 30, 2011.
46. C.M. Barnes. *AGR-1 Fuel Product Specification and Characterization Guidance*. Idaho National Laboratory, Idaho Falls, ID: April 25, 2006. EDF-4380, Rev. 8.
47. C.M. Barnes. *AGR-2 Fuel Specification*. Idaho National Laboratory, Idaho Falls, ID: January 9, 2009. SPC-923, Rev. 3.
48. B&W Nuclear Operations Group, G73AA, "Industrial Fuel Fabrication and Development," Lot G73AA-10-69308, December 2008.
49. BWXT Nuclear Products Division, G73, Industrial Fuel Fabrication and Development, Lot G73D-20-69302, March 2005.
50. BWXT Nuclear Products Division, G73I, Industrial Fuel Fabrication and Development, Lot G73I-14-69307, July 2008.
51. B&W Nuclear Operations Group, G73H, Industrial Fuel Fabrication and Development, Lots: G73H-10-93085B, March 2009.
52. B&W Nuclear Operations Group, G73J, Industrial Fuel Fabrication and Development, Lots: G73J 14-93071A, G73J 14-93073A, G73J 14-93074A, September 2008.

53. J. Einerson. *Statistical Sampling Plan for AGR Fuel Materials*. Idaho National Laboratory, Idaho Falls, ID: February 2006. EDF-4542, Rev. 7.
54. J.D. Hunn and R.A. Lowden. *Data Compilation for AGR-1 Baseline Coated Particle Composite LEU01-46T*. Oak Ridge National Laboratory, Oak Ridge, TN: April 2006. ORNL/TM-2006/019.
55. J.D. Hunn and R.A. Lowden. *Data Compilation for AGR-1 Variant 1 Coated Particle Composite LEU01-47T*. Oak Ridge National Laboratory, Oak Ridge, TN: April 2006. ORNL/TM-2006/020.
56. J.D. Hunn and R.A. Lowden. *Data Compilation for AGR-1 Variant 2 Coated Particle Composite LEU01-48T*. Oak Ridge National Laboratory, Oak Ridge, TN: May 2006. ORNL/TM-2006/021.
57. J.D. Hunn and R.A. Lowden. *Data Compilation for AGR-1 Variant 3 Coated Particle Composite LEU01-49T*. Oak Ridge National Laboratory, Oak Ridge, TN: May 2006. ORNL/TM-2006/022.
58. T.J. Gerczak, J.D. Hunn, R.A. Lowden, and T.R. Allen, "SiC layer microstructure in AGR-1 and AGR-2 TRISO fuel particles and the influence of its variation on the effective diffusion of key fission products," *Journal of Nuclear Materials*, Vol. 480, pp. 257–270 (2016).
59. B. Collin. *AGR-1 Irradiation Test Final As-Run Report*. Idaho National Laboratory, Idaho Falls, ID: January 2015. INL/EXT-10-18097, Rev. 3.
60. *AGR-2 Fuel Compact Pre-Irradiation Characterization Summary Report*. Oak Ridge National Laboratory, Oak Ridge, TN: November 2010. ORNL/TM-2010/226, Rev. 0.
61. B. Collin. *AGR-2 Irradiation Test Final As-Run Report*. Idaho National Laboratory, Idaho Falls, ID: February 2018. INL/EXT-14-32277, Rev. 4,
62. *Advances in High Temperature Gas Cooled Reactor Fuel Technology*. International Atomic Energy Agency, Vienna: December 2012. IAEA-TECDOC-1674.
63. *Statistical Methods Handbook for Advanced Gas Reactor Fuel Materials*. Idaho National Laboratory, Idaho Falls, ID: May 2005. INL/EXT-05-00349, Rev. 0.
64. *Statistical Sampling Plan for AGR-2 Fuel Materials*. Idaho National Laboratory, Idaho Falls, ID: January 2009. PLN-2691, Rev. 4.
65. J.W. McMurray, T.B. Lindemer, N.R. Brown, T.J. Reif, R.N. Morris, and J.D. Hunn, "Determining the minimum required uranium carbide content for HTGR UCO fuel kernels," *Annals of Nuclear Energy*, Vol. 104, pp. 237-242 (2017).

---

References

66. D.A. Petti, J. Buongiorno, J.T. Maki, R.R. Hobbins, and G.K. Miller, "Key differences in the fabrication, irradiation and high temperature accident testing of U.S. and German TRISO-coated particle fuel and their implications on fuel performance," *Nuclear Engineering and Design*, Vol. 222, pp. 281–297 (2003).
67. G.S. Chang and M.A. Lillo, *Confirmatory Neutronics Analysis of the AGR-1 Experiment Irradiated in ATR B-10 Position*. Idaho National Laboratory, Idaho Falls, ID: February 13, 2007. EDF-7120, Rev. 1.
68. J.T. Maki, D.A. Petti, D.L. Knudson, and G.K. Miller, "The challenges associated high burnup, high temperature, and accelerated irradiation for TRISO-coated particle fuel," *Journal of Nuclear Materials*, Vol. 371, pp. 270–280 (2007).
69. J.K. Hartwell, D.M. Scates, and M.W. Drigert. *Design and Expected Performance of the AGR-1 Fission Product Monitoring System*. Idaho National Laboratory, Idaho Falls, ID: September 2005. INL/EXT-05-00073.
70. *MCNP—A General Monte Carlo N-Particle Transport Code, Version 5—Volumes I and II*. Los Alamos National Laboratory, Los Alamos, NM: April 24, 2003 (Revised 6/30/2004). LA-UR-03-1987 and LA-CP-0245.
71. A.G. Croff, "ORIGEN2: A Versatile Computer Code for Calculating the Nuclide Compositions and Characteristics of Nuclear Materials," *Nuclear Technology*, Vol. 62, pp. 335–352 (1983).
72. J. Sterbentz, J.M. Harp, P.A. Demkowicz, G.L. Hawkes, and G.S. Chang, "Validation of the physics analysis used to characterize the AGR-1 TRISO fuel irradiation test," Paper 15497, *Proceedings of the 2015 International Congress on Advances in Nuclear Power Plants (ICAPP 2015)*, Nice, France, May 3-6, 2015.
73. J.M. Harp. *Analysis of Individual Compact fission Product Inventory and Burnup for the AGR-1 TRISO Experiment Using Gamma Spectrometry*. Idaho National Laboratory, Idaho Falls, ID: May 21, 2014. ECAR 1682, Rev. 3.
74. J.M. Harp, P.A. Demkowicz, and J.D. Stempien. *Fission Product Inventory and Burnup Evaluation for Gamma Spectrometry of the AGR-2 Irradiation*. Idaho National Laboratory, Idaho Falls, ID: September 2016. INL/EXT-16-39777.
75. Harp, J. M., P. A. Demkowicz, P. L. Winston, and J. W. Sterbentz, "An analysis of nuclear fuel burnup in the AGR-1 TRISO fuel experiment using gamma spectrometry, mass spectrometry, and computational simulation techniques," *Nuclear Engineering and Design*, Vol. 278, pp. 395–405 (2014).
76. G.L. Hawkes. *AGR-1 Daily As-Run Thermal Analyses*. Idaho National Laboratory, Idaho Falls, ID: 2014. ECAR-968, Rev. 4.
77. G.L. Hawkes. *AGR-2 As-Run Daily Thermal Analyses*. Idaho National Laboratory, Idaho Falls, ID: 2014. ECAR-2476, Rev. 1.

78. B.T. Pham, J.J. Einerson, G.L. Hawkes, N.J. Lybeck, and D.A. Petti, "Impact of gap size uncertainty on calculated temperature uncertainty for the advanced gas reactor experiments," *Proceedings of the 8th International Topical Meeting on High Temperature Reactor Technology (HTR-2016)*, Las Vegas, Nevada, November 6-10, 2016.
79. B.T. Pham, J.J. Einerson, and G.L. Hawkes. *Uncertainty Quantification of Calculated Temperatures for the AGR-1 Experiment*. Idaho National Laboratory, Idaho Falls, ID: 2013. INL/EXT-12-25169, Rev. 1.
80. B.T. Pham, J.J. Einerson, and G.L. Hawkes. *Uncertainty Quantification of Calculated Temperatures for the U.S. Capsules in the AGR-2 Experiment*. Idaho National Laboratory, Idaho Falls, ID: March 2015. INL/EXT-15-34587.
81. S.B. Grover, D.A. Petti, and J.T. Maki, "Completion of the First NGNP Advanced Gas Reactor Fuel Irradiation Experiment, AGR-1, in the Advanced Test Reactor," *Proceedings of the 5th International Topical Meeting on High Temperature Reactor Technology (HTR 2010)*, Prague, Czech Republic, October 18–20, 2010.
82. P.A. Demkowicz, J.D. Hunn, R.N. Morris, I. van Rooyen, T. Gerczak, J.M. Harp, and S.A. Ploger. *AGR-1 Post Irradiation Examination Final Report*. Idaho National Laboratory, Idaho Falls, ID: 2015. INL/EXT-15-36407.
83. P.A. Demkowicz, J.M. Harp, P.L. Winston, and S.A. Ploger. *Analysis of Fission Products on the AGR-1 Capsule Components*. Idaho National Laboratory, Idaho Falls, ID: 2013. INL/EXT-13-28483.
84. J.D. Stempien and P.A. Demkowicz. *AGR-2 Irradiation Experiment Fission Product Mass Balance*. Idaho National Laboratory, Idaho Falls, ID: May 2019. INL/EXT-19-53559.
85. J.D. Hunn, R.N. Morris, F.C. Montgomery, T.J. Gerczak, D.J. Skitt, C.A. Baldwin, J.A. Dyer, G.W. Helmreich, B.D. Eckhart, Z.M. Burns, P.A. Demkowicz, and J.D. Stempien, "Post-irradiation examination and safety testing of US AGR-2 irradiation test compacts," *Proceedings of the 9th International Topical Meeting on High Temperature Reactor Technology (HTR-2018)*, Warsaw, Poland, October 8-10, 2018.
86. S. Ploger, P. Demkowicz, J. Hunn, and J.S. Kehn, "Microscopic analysis of irradiated AGR-1 coated particle fuel compacts," *Nuclear Engineering and Design*, Vol. 271, pp. 221–230 (2014).
87. F.J. Rice, J.D. Stempien, and P.A. Demkowicz, "Ceramography of irradiated TRISO fuel from the AGR-2 experiment," *Nuclear Engineering and Design*, Vol. 329, pp. 73–81 (2018).
88. R.N. Morris, J.D. Hunn, C.A. Baldwin, F.C. Montgomery, T. Gerczak, and P.A. Demkowicz, "Initial results from safety testing of US AGR-2 irradiation test fuel," *Nuclear Engineering and Design*, Vol. 329, pp. 124–133 (2018).

---

References

89. K. Minato, T. Ogawa, S. Kashimura, K. Fukuda, I. Takahashi, M. Shimizu, and Y. Tayama, "Carbon monoxide-silicon carbide interaction in HTGR fuel particles," *Journal of Materials Science*, Vol. 26, pp. 2379–2388 (1991).
90. H. Hantke. *Performance of High Quality HTR LEU Fuel Elements with TRISO Coated Particles*. Forschungszentrum Jülich, Jülich, Germany: 1992. Internal Report HTA-IB-7/92.
91. W. Schenk, D. Pitzer, and H. Knauf. *Simulation der Maximalen MODUL-Störfallaufheizkurve (AVR-GLE 3, 90/20) und deren Extrapolation auf 1700 °C (AVR-GLE 3, 91/31)*. Forschungszentrum Jülich, Jülich, Germany: 1993. Technical Note FZJ-IWE-TN-17/93.
92. J.D. Stempien, P.A. Demkowicz, E.L. Reber, and C.L. Christensen. "High-temperature safety testing of irradiated AGR-1 TRISO fuel," *Proceedings of the 9th International Topical Meeting on High Temperature Reactor Technology (HTR-2018)*, Warsaw, Poland, October 8-10, 2018.
93. J.D. Hunn, C.A. Baldwin, F.C. Montgomery, T.J. Gerczak, R.N. Morris, G.W. Helmreich, P.A. Demkowicz, J.M. Harp, and J.D. Stempien, "Initial examination of fuel compacts and TRISO particles from the US AGR-2 irradiation test," *Nuclear Engineering and Design*, Vol. 329, pp. 89–101 (2018).



# A

## U.S. REGULATORY BASES

---

### A.1 NRC Regulations

Regulations related to light water reactor (LWR) design are codified primarily in the General Design Criteria (GDC) contained in Appendix A of 10 CFR Part 50 [1]. The U.S. Nuclear Regulatory Commission's (NRC) Regulatory Guide (RG) 1.232 [2] provides guidance for how the GDC in Appendix A may be adapted for non-light-water reactor (non-LWR) designs.

RG 1.232 provides Advanced Reactor Design Criteria (ARDC), which may be used by non-LWR designers and future applicants to develop principal design criteria (PDC) for any non-LWR designs. In addition, RG 1.232 provides guidance for adapting the LWR GDC for modular HTGRs and sodium-cooled fast reactors (SFRs). The design criteria serve as the fundamental criteria for the structures, systems, and components (SSC) that make up a nuclear power plant design, particularly when assessing the performance of their intended safety functions during applicable licensing basis events. RG 1.232 guidance may be used to develop all or part of a design's PDC and users are free to choose among the ARDC, modular HTGR design criteria (MHTGR-DC), or SFR design criteria (SFR-DC) to develop their PDC after considering the underlying safety basis for the criterion and evaluating the RG's rationale for the adaptation.

MHTGR-DC 10, *Reactor Design*, provides guidance related to acceptable system radionuclide releases. Other ARDC that pertain to the reactor core (that is, MHTGR-DC 11, 12, 13, and 27), do not directly pertain to the performance of the tristructural isotropic (TRISO)-coated particle fuel. MHTGR-DC 10, states [2]:

- “The reactor system and associated heat removal, control, and protection systems shall be designed with appropriate margin to ensure that specified acceptable system radionuclide release design limits are not exceeded during any condition of normal operation, including the effects of anticipated operational occurrences.”

RG 1.232 includes the following rationale for MHTGR-DC 10 documenting the basis for wording changes from the original LWR GDC [2]:

- “the concept of specified acceptable fuel design limits, which prevent additional fuel failures during anticipated operational occurrences (AOOs), has been replaced with that of the specified acceptable system radionuclide release design limits (SARRDL), which limits the amount of radionuclide inventory that is released by the system under normal and AOO conditions.” Design features within the reactor system must ensure the SARRDLs are not exceeded during normal operations and AOOs.
- The TRISO fuel used in the MHTGR design is the primary fission product barrier and is expected to have a very low incremental fission product release during AOOs.

- The SARRDLs will be established so that the most limiting license-basis event does not exceed the siting regulatory dose limits criteria at the exclusion area boundary (EAB) and low-population zone (LPZ), and also so that the 10 CFR 20.1301 annualized dose limits to the public are not exceeded at the EAB for normal operation and AOOs.
- The NRC has not approved the concept of replacing specified acceptable fuel design limits with SARRDLs. The concept of the TRISO fuel being the primary fission product barrier is intertwined with the concept of a functional containment for MHTGR technologies. See the rationale for MHTGR-DC 16 for further information on the Commission's current position.

MHTGR-DC 16, *Containment Design*, provides guidance for a functional containment design, which relies on the use on multiple barriers to control the release or radioactivity. MHTGR-DC 16 states [2]:

- "A reactor functional containment, consisting of multiple barriers internal and/or external to the reactor and its cooling system, shall be provided to control the release of radioactivity to the environment and to ensure that the functional containment design conditions important to safety are not exceeded for as long as postulated accident conditions require."

RG 1.232 includes the following rationale for MHTGR-DC 16 documenting the basis for wording changes from the original LWR GDC, which include [2]:

- "The term "functional containment" is applicable to advanced non-LWRs without a pressure retaining containment structure. A functional containment can be defined as "a barrier, or set of barriers taken together, that effectively limit the physical transport and release of radionuclides to the environment across a full range of normal operating conditions, AOOs, and accident conditions."
- "The NRC staff has brought the issue of functional containment to the Commission, and the Commission has found it generally acceptable"
- "The NRC staff also provided feedback to the DOE on this issue as part of the NGNP project, (*see Appendix to this document*). ... the area on functional containment and fuel development and qualification noted that "...approval of the proposed approach to functional containment for the MHTGR concept, with its emphasis on passive safety features and radionuclide retention within the fuel over a broad spectrum of off-normal conditions, would necessitate that the required fuel particle performance capabilities be demonstrated with a high degree of certainty."

10 CFR Part 52.79 (a)(24) provides guidance on the content for Combined License Applications regarding designs that differ significantly from LWR designs licensed before 1997, or utilize simplified, inherent, passive, or other innovative means to accomplish their safety functions. It references 10 CFR Part 50.43(e) which, in summary, requires a combination of analyses and test programs to demonstrate the performance of safety features and ensure sufficient data exist to assess the analytical tools used for safety analyses.

## **A.2 NRC Policy Statements**

No U.S. Nuclear Regulatory Commission policy statements directly apply to TRISO-coated particle fuel or address testing or monitoring of the fuel, nor does the NRC policy statement on the regulation of advanced nuclear power plants explicitly address nuclear fuel. However, NRC policy issues specific to the MHTGR concept are identified in NRC Commission paper (SECY)-93-092 [3] and in Section 5 of NUREG-1338 [4]. Of the ten issues identified in SECY-93-092, both “Containment Performance” and “Source Term” policy issues are related to TRISO fuel. Their use of a multi-barrier containment configuration and associated mechanistic source terms for accident analyses are based on the performance of the TRISO fuel being both excellent and predictable.

### **A.2.1 Functional Containment Performance**

The current LWR containment leakage requirements are outlined in GDC 16 and Appendix J of 10 CFR Part 50. The containment performance issue involves whether an advanced reactor design should be allowed to employ alternative approaches to the traditional “essentially leak-tight” containment structures used in LWRs to provide for the control of fission-product releases to the environment.

Fundamental to the HTGR and FHR concepts is their emphasis on release prevention by utilizing high-integrity fuel particles, rather than a leak-tight containment barrier to minimize radionuclide releases to the environment. In SECY-03-0047 [5], SECY-04-0103 [6], and SECY-05-006 [7], the NRC approved the use of a standard based on functional containment performance to evaluate the acceptability of the proposed designs, rather than relying on prescriptive containment design criteria. As part of the containment evaluation, the NRC instructed the staff to address the failure of the fuel particles, among other issues.

There is a strong linkage between TRISO particle behavior, functional containment performance, and licensing. Recognizing the importance of this relationship, NRC staff released a draft SECY paper seeking NRC approval of a recommendation that adopts a technology-inclusive, risk-informed, performance-based approach when establishing performance criteria for structures, systems, and components and corresponding programs that limit the release of radioactive materials from non-LWR designs [8]. The staff determined formal Commission direction on functional containment would be beneficial to support development and deployment of advanced reactor technologies seeking to utilize this approach to safety.

The draft SECY was submitted to the Advisory Committee on Reactor Safeguards (ACRS) in early 2018 for review. On May 10, 2018, the ACRS communicated its findings to the Commission and noted the proposed SECY set forth a rational basis for developing functional containment performance criteria. The letter recommended the methodology be further developed for licensing use [9].

On June 27, 2018, the staff indicated its intention to finalize the draft SECY paper and then send it to the Commission for formal approval [10]. SECY-18-0096 entitled, “Functional Containment Performance Criteria for Non-Light Water Reactor Designs,” [11] was approved by the Commission on December 4, 2018.

## **A.2.2 Source Term**

The source term for the MHTGR or FHR technology is defined as the set of quantities of radionuclides released from a reactor building to the environment. This definition is judged appropriate for greater emphasis on fuel retention of radionuclides for events rather than reactor building retention following an event.

In its Staff Requirements Memorandum for SECY-93-092, the Commission approved the staff's recommendation the source terms for non-LWRs be based on a mechanistic analysis, relying on the staff's assurance three conditions are met [3]. One of the conditions was "the performance of the reactor and fuel under normal and off-normal conditions is sufficiently well understood to permit a mechanistic analysis. Sufficient data should exist on the reactor and fuel performance through research, development, and testing programs to provide adequate confidence in the mechanistic approach."

The purpose of this report is to provide the NRC with data on fuel performance through research, development, and testing programs to provide a functional basis for this adequate confidence necessary to support the mechanistic analysis source term approach.

## **A.3 NRC Guidance/References**

### **A.3.1 NUREG-1338, "Pre-application Safety Evaluation Report for the MHTGR"**

In 1989, a draft of a pre-application safety evaluation report (PSER) [12] documented the NRC staff's pre-application review of the MHTGR design and its conclusions. Following DOE submission of additional information for the fuel design in 1991 and 1992 and meetings with the NRC on fuel design and fission-product transport in 1991, a draft of the final PSER was completed in December 1995 [13] and was based upon the draft PSER issued in 1989 and upon a number of reports completed after the draft PSER was issued.

The final PSER draft confirmed the following overall conclusions of the earlier draft with respect to the fuel design, specifically [13]:

- The NRC staff believes that fuel design and quality can be developed to meet the performance objectives proposed by DOE and required by the safety analyses, but notes this conclusion is dependent on the successful outcome of the research program
- The NRC staff notes actual fuel performance in Federal Republic of Germany reactors, together with reported laboratory and in-pile tests, gives promise fuel performance objectives can eventually be demonstrated.

However, NUREG-1338 also states the information provided for the MHTGR up to that time had not demonstrated the necessary design and quality of fuel to meet these performance objectives. It identifies the following information that the NRC needs to reach a determination on the fuel [13]:

- Design thicknesses of fuel particle coatings and the bases for these thicknesses given the proposed fuel failures from manufacturing, normal operation (neutron fluence), and accidents (temperature)

- Quality control of the manufacturing process for the fuel and resulting tolerances on the coatings
- Fuel performance of specific coated particles and coating tolerances demonstrated from irradiation and safety tests
- Expected fuel temperatures throughout the core during accidents and the resulting volume-averaged failed fuel fraction
- Potential dose consequences shown to be within acceptable limits for the predicted volume-averaged failed fuel fraction

NUREG-1338 also includes the following conclusions to be considered in qualifying TRISO-coated particle fuel [13]:

- The statistical question of how many fuel particles are needed in irradiation and safety tests to justify the proposed low failed-fuel fraction within 95% certainty
- The fuel design and containment proposed for the MHTGR, which the NRC staff considers a licensability issue for the MHTGR (licensability issues occur when the design departs significantly from what the NRC has accepted in the past or when changes in the design to resolve a staff concern could fundamentally alter the proposed design.)
- The credible mechanisms for “weak fuel” (fuel that performs acceptably during normal reactor operation, but is subject to failure under more stringent conditions during accidents) to ensure that all mechanisms for fuel failure are recognized and quantitatively accounted for in fuel performance models

The NRC guidance provided in NUREG-1338 indicates successful completion of the Fuel Research and Development (R&D) program must provide a statistically significant demonstration [13]:

- The reference fuel manufacturing processes and quality-control methods ensure the production of fuel meeting specification requirements
- The fuel fabricated using the reference fuel manufacturing processes meets the fuel performance requirements under normal operation and all credible accident conditions
- Validated methods are available to accurately predict fuel performance and fission-product transport.

### **A.3.2 NUREG-0111, “Evaluation of High Temperature Gas-Cooled Reactor Particle Coating Failure Models and Data”**

NUREG-0111[14] addresses highly enriched uranium (HEU) UC<sub>2</sub> TRISO fissile particles with a 200- $\mu$ m kernel and ThO<sub>2</sub> bistructural isotropic (BISO) fertile particles with a 500- $\mu$ m kernel for service in a large prismatic HTGR. Major differences in particle design, fabrication specifications, and service conditions relative to the fuel for MHTGRs or FHRs limit the applicability of this report to the current low-enriched uranium (LEU) fuel. Experience with this and other diverse fuel types over the course of TRISO-coated particle fuel development has provided valuable insights into the development and understanding of the LEU UCO TRISO fuel.

### **A.3.3 NUREG-0800, Standard Review Plan, Section 4.2, "Fuel System Design"**

The existing NUREG-0800 Standard Review Plan [15] Section 4.3 for LWRs is technology-specific and deals with fuel performance phenomena that do not apply to HTGR fuel performance. The HTGR design criteria for fuel design limits must be appropriately adapted to reflect the underlying intent in preserving TRISO particle fuel performance and integrity.

Any review of TRISO particle fuel must consider statistically significant measurements that reliably indicate overall fuel system performance. Billions of TRISO fuel particles (each independently functioning as a separate radionuclide containment vessel) are in a HTGR core. These coated fuel particles are embedded in a solid carbonaceous matrix nominally shaped as either a spherical pebble or a compact cylinder. This type of fuel design makes it infeasible for direct damage assessment of individual coated particles after manufacture while loaded in the core. Therefore, a HTGR fuel system design review must encompass the coated particle fuel manufacturing process and rely on appropriate indirect methods of measurement (such as SARRDL) that communicate coated particle fuel failure rates and enable predictions of overall radionuclide barrier performance. Review requirements should focus on:

- Evaluating the quality of TRISO particle fuel during manufacture
- Understanding fuel system performance impacts as a result of normal operation and AOOs
- Characterizing fuel system performance as it relates to reactivity control
- Establishing in-service performance requirements and fission product release requirements for postulated accidents
- Enabling fuel performance and fission product release prediction/modeling under normal operating and postulated accidents with desired statistical certainty

### **A.3.4 TRISO-Coated Particle Fuel Phenomenon Identification and Ranking Tables**

In anticipation of future licensing applications for HTGRs, the NRC commissioned a panel to identify and rank the phenomena associated with TRISO-coated-particle fuel to obtain a better understanding of the significant features of TRISO-coated-particle fuel design, manufacture, and behavior during both normal reactor operation and accidents [16]. Six Phenomena Identification and Ranking Tables (PIRTs) were developed by the panel, including PIRTs on:

- Manufacturing
- Operations
- Depressurized heat-up accident
- Reactivity accident
- Depressurized accident with water ingress
- Depressurization accident with air ingress

In preparing the PIRTs, the panel assumed the plant to be a pebble-bed reactor with UO<sub>2</sub> fuel, except for the reactivity accident PIRT, in which a prismatic reactor was considered instead. The panel also identified and evaluated the importance and knowledge rankings that would be different for prismatic reactor UCO fuel. The PIRTs are documented in NUREG/CR-6844, Vol. 1 [16].

According to NUREG/CR-6844, the NRC will use the PIRT results to:

- Identify key attributes of gas-cooled reactor fuel manufacture that may require regulatory oversight.
- Provide a valuable reference for the review of vendor HTGR fuel qualification plans.
- Provide insights for developing plans for fuel safety margin testing.
- Assist in defining test data needs for the development of fuel performance and fission product transport models.
- Inform decisions regarding the development of the NRC's independent HTGR fuel performance code and fission product transport models.
- Support the development of the NRC's independent models for source term calculations.
- Provide insights for the review of vendor HTGR fuel safety analyses.

### **A.3.5 Next Generation Nuclear Plant**

In 2005, DOE established the Next Generation Nuclear Plant (NGNP) Project at Idaho National Laboratory (INL) to support near-term commercial deployment of a HTGR technology demonstration plant. A key part of the project was the development of a regulatory framework supportive of commercial HTGR deployment. Framework activities were closely coordinated with NRC staff and focused on adapting existing nuclear power plant regulatory requirements to the needs of NGNP licensing. DOE and NRC jointly formulated the approach for this licensing structure and communicated this approach to Congress in 2008.

Under the NGNP project, HTGR licensing precedents and NRC regulations were examined systematically as they relate to the NGNP safety case and associated plant design goals. NRC staff coordinated the scope of this examination and reviewed the results. In 2009, this information was used to develop a strategic implementation plan [17] for establishing the regulatory basis necessary to complete and submit an HTGR license application to NRC. The plan focused on key elements of plant safety design and licensing, and included:

- Developing the basis for establishing a mechanistic radiological source term (based primarily on particle fuel design and available qualification testing results).
- Preventing/mitigating the release of the radiological source terms to the environment, including methods for the structured and comprehensive identification of licensing basis event sequences, along with establishing multiple radionuclide release barriers.
- Developing an updated emergency planning structure that considers collocated industry energy end-users to assure protection of public health and safety in the unlikely event of a radiological release.

- The design and licensing strategy of NGNP centered on radionuclide retention capabilities of TRISO particle fuel. It also relied less on other barriers for limiting offsite releases of radionuclides compared to historical LWR technology. This approach in conjunction with the related HTGR design goals aligns with the NRC's Advanced Reactor Policy Statement [18] regarding pursuit of less complex reactor designs with longer response time constants, passive reactor shutdown, and passive heat removal with limited reliance on operator actions, minimization of severe accident potential, and providing multiple barriers to potential radionuclide releases.

The NGNP project yielded a series of complementary pre-licensing "white papers" that were submitted to NRC staff for formal review and feedback. The review and feedback process included extensive public meeting interactions, conference calls, and written correspondence focused on requests for additional information. Responses were provided to all NRC requests for additional information regarding the Fuel Qualification White Paper.

In early 2012, four licensing framework topics were identified as key focus areas because they represented areas of significant and longstanding regulatory uncertainty for the entire HTGR industry. The four key topical areas targeted for joint examination were:

- HTGR functional containment performance
- Licensing basis event selection
- Source terms
- Emergency planning

Ensuing interactions resulted in NRC staff drafting initial regulatory positions on the four framework topics and submitting them to the NRC's Advisory Committee on Reactor Safeguards (ACRS) for review in early 2013. Staff findings were then updated and released again in July 2014. Major items addressed in the NRC staff position report [19] included:

- The DOE INL AGR program was determined to be reasonably complete within a context of pre-prototype fuel testing. Early fuel test results showed promise in demonstrating much of the desired retention capabilities of the TRISO particle fuel. Outcomes of the regulatory interactions related to the NGNP Fuel Qualification White Paper are documented in Enclosure 2 of the NRC letter to DOE, "NGNP-Assessment of Key Licensing Issues" [19]. Therein, NRC staff generally endorsed the approach to fuel qualification as proposed under the project. The staff identified one area of concern that may require a supplement to the currently planned fuel qualification program. Throughout the interactions, a key question remained regarding the extent to which irradiation testing in water-cooled materials test reactors, such as INL's Advanced Test Reactor (ATR), can provide an adequately prototypical environment for HTGR fuel. A concern existed the neutron spectrum in an HTGR is "harder" than in water-cooled reactors, and the composition of the test capsules irradiated in the program do not result in a prototypical number of plutonium fissions in the test fuel. This, in turn, caused the staff to question whether production of fission products (such as silver and palladium, both of which have higher fission yields from plutonium fission and can affect fuel particle performance) is high enough to ensure an understanding of their effects on fuel performance. Although the NGNP provided analyses information [20, 21] to support a position the proposed fuel irradiation program adequately addresses this



issue, NRC staff concerns remain. The issue could be addressed by conducting a proof test that includes post-irradiation safety testing of fuel from the production-scale fabrication of the initial core of the first reactor. NRC staff has indicated such a proof test would address uncertainties regarding the process of scaling up the fuel fabrication process from laboratory to engineering to production scale. The need for initial core fuel proof testing remains to be addressed by a future applicant.

- General agreement was expressed with the proposed NGNP performance standard concerning HTGR functional containment. The functional containment approach limits radionuclide releases to the environment by emphasizing retention of radionuclides at their source in the fuel rather than allowing significant fuel particle failures and relying upon other external barriers to provide compliance with identified top-level regulatory dose acceptance criteria.
- The licensing basis event identification and categorization process developed and proposed under NGNP included a frequency versus consequence approach for evaluating postulated event sequences against top-level regulatory criteria (primarily offsite dose). Initially, based on public meeting discussions and a draft feedback summary written by NRC staff, this approach appeared to be generally reasonable. Some members of the staff believed a supplement was probably necessary to the proposed set of design basis accidents. This proposed supplement would provide additional deterministically postulated accidents. NGNP personnel felt adding events from outside the proposed event selection process created significant uncertainty for the industry. The concept of a supplement was also subject to challenge by ACRS recommendations. This issue (and other related topics) was not addressed in the July 2014 NRC staff position report. The omission of this topic, as well as the overall licensing basis event identification and categorization process in general, was attributed to staff concerns issuing feedback on the topic at that time might be inconsistent with the concurrent NRC efforts related to post-Fukushima Near-Term Task Force (NTTF) Recommendation 1 and subsequent development of a risk management regulatory framework.
- The proposed mechanistic methodology for defining and evaluating source terms was deemed reasonable by NRC staff.
- The staff was receptive to future emergency planning proposals for a probabilistic risk assessment informed approach in sizing the emergency planning zone. Proposals might include the use of accident dose assessments when determining an appropriate emergency planning zone size. SECY-11-0152 contains a partial response to NGNP white paper proposals [22]. Clarification beyond SECY-11-0152 was not provided due to the need for NRC action on related policy issues. Further staff evaluation of the NGNP emergency planning approach was curtailed pending availability of more site and plant design information.

Certain key issues will require NRC policy determinations. The staff indicated general agreement with the systematic approaches proposed by the NGNP project staff and understood them to provide a reasonably sound basis for developing a license application. There are licensing issues that remain to be addressed by license applicants through direct NRC staff interaction. The status of these licensing activities is summarized in a 2014 INL report [23].

## **A.4 U.S. HTGR Precedents**

### **A.4.1 Peach Bottom**

A construction permit was issued to Philadelphia Electric Company for the Peach Bottom Unit 1 HTGR plant in 1962. This 40-MW(e) plant operated from 1967 to 1974 using BISO-based fuel. Although the fuel type used for this plant is not closely related to TRISO fuel, it was one of the original HTGR plants.

### **A.4.2 Fort St. Vrain**

The Fort St. Vrain (FSV) Nuclear Generating Station was a prismatic fuel HTGR that generated 842 MW(t) to achieve a net output of 330 MW(e). FSV operated from 1974 to 1989. Licensing interactions on FSV were based on HEU TRISO fuel.

### **A.4.3 Others**

During the last 25 years, the NRC has had two occasions to consider LEU TRISO fuel for HTGRs. These include the NRC review of the MHTGR that began in 1985 and resulted in the issuing of NUREG-1338 in 1995. Later in 2001, Exelon initiated pre-application interactions on the Pebble-Bed Modular Reactor (PBMR) design, which resulted in the NRC requesting additional information in June 2002. In late 2002, the NRC issued a closeout letter noticing the closure of the PBMR Project based on Exelon's request. The letter also stated the staff did not perform a detailed technical review of previous documents and was based on a limited screening review to ensure the issues, review status, and views and positions noted within the documents were consistent with the NRC's views and understanding.

## **A.5 References**

1. U.S. Code of Federal Regulations. *Domestic Licensing of Production and Utilization Facilities*. 10 CFR Part 50. [http://ecfr.gpoaccess.gov/cgi/t/text/text-idx?c=ecfr&tpl=/ecfrbrowse/Title10/10cfr50\\_main\\_02.tpl](http://ecfr.gpoaccess.gov/cgi/t/text/text-idx?c=ecfr&tpl=/ecfrbrowse/Title10/10cfr50_main_02.tpl)
2. U.S. Nuclear Regulatory Commission. *Guidance for Developing Principal Design Criteria for Non-Light-Water Reactors*. RG 1.232. Washington, D.C.: April 2018.
3. U.S. Nuclear Regulatory Commission. *Issues Pertaining to the Advanced Reactor (PRISM, MHTGR, and PIUS) and CANDU 3 Designs and Their Relationship to Current Regulatory Requirements*. SECY-93-092. Washington, D.C.: July 16, 1993.
4. U.S. Nuclear Regulatory Commission. *Draft Preapplication Safety Evaluation Report for the Modular High-Temperature Gas-Cooled Reactor*. NUREG 1338. Washington, D.C.: March 1989.
5. U.S. Nuclear Regulatory Commission. *Policy Issues Related to Licensing Non-Light-Water Reactor Designs*. SECY-03-0047. Washington, D.C.: March 28, 2003.

6. U.S. Nuclear Regulatory Commission. *Status of Response to the June 26, 2003, Staff Requirements Memorandum on Policy Issues Related to Licensing Non-Light-Water Reactor Designs*. SECY-04-0103, Washington, D.C.: June 23, 2004.
7. U.S. Nuclear Regulatory Commission. *Second Status Paper on the Staff's Proposed Regulatory Structure for New Plant Licensing and Update on Policy Issues Related to New Plant Licensing*. SECY-05-0006, Washington, D.C.: January 7, 2005.
8. U.S. Nuclear Regulatory Commission. *Draft SECY Paper—Functional Containment Performance Criteria for Non-Light Water Reactor Designs*. ADAMS Accession No. ML18031A721, Washington, D.C.: January 30, 2018.
9. U.S. Nuclear Regulatory Commission, Advisory Committee on Reactor Safeguards, Correspondence from M.L. Corradini to K.L. Svinicki, "Draft SECY Paper, Functional Containment Performance Criteria for Non-Light Water Reactor Designs," ADAMS Accession No. ML18108A404, Washington, D.C.: May 10, 2018.
10. U.S. Nuclear Regulatory Commission, Correspondence from V.M. McCree to M.L. Corradini, "Response to the Advisory Committee on Reactor Safeguards' Letter Regarding Draft SECY Paper—Functional Containment Performance Criteria for Non-Light Water Reactor Designs," ADAMS Accession No. ML18156A401, Washington, D.C.: June 27, 2018.
11. U.S. Nuclear Regulatory Commission. *Staff Requirements: Functional Containment Performance Criteria for Non-Lightwater Reactors*, SECY-18-0096, Washington, D.C.: December 4, 2018.
12. U.S. Nuclear Regulatory Commission. *Draft Preapplication Safety Evaluation Report for the Modular High-Temperature Gas-Cooled Reactor (MHTGR)*. NUREG-1338. Washington, D.C.: March 1989.
13. U.S. Nuclear Regulatory Commission. *Preapplication Safety Evaluation Report for the Modular High-Temperature Gas-Cooled Reactor (MHTGR)*, NUREG-1338. Washington, D.C.: December 1995.
14. U.S. Nuclear Regulatory Commission. *Evaluation of High-Temperature Gas-Cooled Reactor Fuel Particle Coating Failure Models and Data*. NUREG-0111. Washington, D.C.: November 1976.
15. U.S. Nuclear Regulatory Commission. *Standard Review Plan for the Review of Safety Analysis Reports for Nuclear Power Plants: LWR Edition*. NUREG-0800, Rev. 3, Washington, D.C.: March 2007.
16. U.S. Nuclear Regulatory Commission. *TRISO-Coated Particle Fuel Phenomena Identification and Ranking Tables (PIRTs) for Fission Product Transport Due to Manufacturing, Operations, and Accidents*. NUREG/CR-6844, Washington, D.C.: July 2004.
17. *NGNP Licensing Plan*. Idaho National Laboratory, Idaho Falls, ID: June 26, 2009. PLN-3202.

18. U.S. Nuclear Regulatory Commission. *Policy Statement on the Regulation of Advanced Reactors*, Federal Register 73 FR 60612, Washington, D.C.: October 14, 2008.
19. G.M. Tracy, Director, U.S. Nuclear Regulatory Commission, Office of New Reactors, Letter to Dr. J. Kelly, DOE Deputy Assistant Secretary for Nuclear Technologies, "NGNP—Assessment of Key Licensing Issues," ML14174A734, with Enclosure 1 ("Summary Feedback on Four Key Licensing Issues," ML14174A774) and Enclosure 2 ("Assessment of White Paper Submittals on Fuel Qualification and Mechanistic Source Terms," Rev.1, ML14174A845).
20. G. Gibbs, Idaho National Laboratory, letter to U.S. Nuclear Regulatory Commission, September 20, 2010, "Contract Number DE-AC07-05ID14517—Next Generation Nuclear Plant—Response to Questions about the Applicability of the Advanced Gas Reactor Testy Results to Next Generation Nuclear Plant—NRC Project No. 0748," CCN 222202; ML102770386.
21. D. Petti, Idaho National Laboratory, letter to U.S. Nuclear Regulatory Commission, September 20, 2013, "Contract Number DE-AC07-05ID14517—Next Generation Nuclear Plant Project Submittal—Additional Information on Selected Fuel Qualification/Mechanistic Source Terms Follow-Up Items—NRC Project No. 0748," CCN 228482; ML12268A031.
22. U.S. Nuclear Regulatory Commission. *Development of an Emergency Planning and Preparedness Framework for Small Modular Reactors*. SECY-11-0152. Washington, D.C.: October 28, 2011.
23. W. Moe. *NRC Licensing Status Summary Report for NGNP*. Idaho National Laboratory, Idaho Falls, ID: November 2014. INL/EXT-13-28205, Revision 1.

# B

## INTERNATIONAL COATED-PARTICLE DEVELOPMENT EXPERIENCE

---

### B.1 General Experience and Coated Particle Evolution

Coated particles start with a spherical kernel of fissile or fertile material that is surrounded by one or more refractory coatings. By the early 1960s, coated-particle fuel development for carbonaceous matrix-moderated helium-cooled HTGRs was well under way in the United Kingdom in support of the DRAGON research reactor [1], in the U.S. in support of the Peach Bottom Unit 1 prototype power reactor [2], and in Germany in support of the AVR research and power reactor [3]. Coated particle designs for these reactors varied considerably, as illustrated in Figure B-1 (the AVR fuel loadings evolved through many designs in the course of over two decades of plant operation, including the LEU TRISO design discussed in Section 4.2).

Coated-particle fuel development programs have also been conducted in France, Russia, Japan, China, South Africa, and South Korea. The development of coated-particle fuel technology for both the pebble-bed and prismatic designs has drawn from an extensive international background of coated-particle fuel fabrication and testing experience spanning more than 50 years and covering a broad range of parameters as summarized below:

- Kernel characteristics:
  - Diameter – 100 to 800  $\mu\text{m}$
  - Fissile/fertile materials – uranium, thorium, plutonium (mixed and unmixed)
  - Chemical forms – oxide, carbide, oxycarbide
  - Enrichment – ranging from natural to HEU and plutonium
- Coating characteristics:
  - BISO – variations in buffer and pyrocarbon (PyC) coating thicknesses and properties
  - TRISO – variations in buffer, PyC and SiC (or zirconium carbide) thicknesses and properties
- Fuel forms:
  - Spheres – multiple geometries and fabrication methods
  - Compacts – cylindrical and annular shapes with variations in particle packing fractions and fabrication methods

- Irradiation facilities:
  - Materials Test Reactors – HFR (Netherlands), FRJ 2 DIDO (Germany), IVV-2M (Russia), Siloe (France), R2 (Sweden), BR2 (Belgium), High-Flux Isotope Reactor (HFIR) and ATR (U.S.), with wide variations in neutron energy spectra and degree of irradiation acceleration
  - Research and Demonstration Reactors – DRAGON (United Kingdom), Peach Bottom I (United States), AVR (Germany), FSV (United States), Thorium High Temperature Reactor (THTR) (Germany), HTTR (Japan), and HTR-10 (China)
- Irradiation and testing conditions:
  - Burnup – ranging from below 1% to above 70% fissions per initial metal atom (FIMA)
  - Fast fluence – ranging from below  $1 \times 10^{21}$  to above  $10 \times 10^{21}$  n/cm<sup>2</sup>
  - Irradiation temperature – ranging from 600 to 1950°C
  - Accident simulation temperature – ranging from 1400 to 2500°C

This broad range of experience and data has supported the development of a detailed understanding of the parameters and phenomena of importance in the fabrication and performance of coated-particle fuel. Extensive bilateral and multilateral international information exchanges facilitated the incorporation of this broad experience base into the German and other modern coated-particle fuels. A detailed review of U.S. and German experience and the relationship to fuel performance and fuel performance modeling is documented in an Electric Power Research Institute (EPRI) report [4].

The evolution of the German fuel design, arriving at the LEU UO<sub>2</sub> TRISO pressed sphere selected as a basis for the pebble-bed reactor concept, is summarized in a section of a report on the AVR [3]. A broader range of international experience, focused mainly on LEU TRISO fuel, was addressed in an International Atomic Energy Agency (IAEA) coordinated research project conducted in the 1990s [5].

A more recent coordinated research project on TRISO-coated particle fuel was conducted in the early 2000s [6]. Two key parts of that project were: (1) an international quality control round robin test campaign for measuring important attributes of TRISO-coated particles; and (2) an international fuel performance benchmarking exercise to compare international codes that model TRISO-coated particle fuel under both normal operation and postulated accident conditions. In considering this experience and data, the international community has converged on common LEU TRISO particle designs, as discussed in Section 4.2, as having very similar coating thicknesses and properties with variations in kernel diameter, enrichment, and composition (UO<sub>2</sub> and UCO), depending on specific service conditions and requirements.

## B.2 LEU UO<sub>2</sub> Experience in Russia

Coated-particle fuel development in Russia was based on a spherical fuel element incorporating UO<sub>2</sub> coated particles similar to a German design, with reactor design enrichments ranging from 6.5 to 21% [5]. Fuel development and testing included both low and high-temperature isotropic pyrocarbon for the dense pyrocarbon<sup>20</sup> layers [7]. In support of these designs, the fuel fabrication, irradiation, and testing program was conducted from 1975 through 1990. As-manufactured particle defect fractions on the order of 10<sup>-5</sup> were achieved at both laboratory and semi-industrial scale. Russian coated-particle fuel fabrication development is described in several papers in the proceedings of an IAEA meeting on gas-cooled reactor fuel development [8].

The fuel irradiation program was conducted using enrichments higher than the reactor design values, ranging from 21 to 45%. The irradiations covered a wide range of conditions [9]:

- Temperatures: 400 to 1950°C
- Burnup: 1 to 41% FIMA
- Fast fluence: 0.1 to 2.7 × 10<sup>25</sup> n/m<sup>2</sup>, E > 32fJ.

The irradiation temperature and burnup ranges substantially exceeded typical design ranges for coated particles of design similar to the German fuel. Thus, the Russian program produced valuable irradiation data on the ultimate capability of the fuel and fuel behavior at conditions exceeding the nominal operating range. The investigation of the capability of a particle design similar to the German particle yielded the following conclusions [9]:

- Irradiation at 1000°C produced insignificant gaseous fission product release at burnups of 15–20% FIMA
- Irradiation at 1200°C produced depressurization of separate coated particles<sup>21</sup> at burnups of 10–15% FIMA
- Irradiation at 1400°C produced increased gaseous fission product release at burnups of 5–13% FIMA.

The results also indicated particles with low-temperature isotropic PyC layers achieved higher burnups prior to gas release than those with high-temperature isotropic layers.

The Russian program also investigated fuel (both loose particle and sphere forms) response to over-power conditions to explore failure limits. Power pulse experiments of 1 sec duration were carried out at power levels of ~30, 66, and 124 times the nominal maximum power level, with no indications of significant gaseous fission product release. Extended overpower tests at ~10 times the nominal maximum under adiabatic conditions for 5, 10, and 30 seconds showed no

---

<sup>20</sup> At temperatures between 1250 and 1350°C, a low-temperature isotropic coating is produced by chemical vapor deposition. In the range of 1800 to 2100°C, a different type of pyrocarbon, "high-temperature isotropic," is deposited. Both forms were investigated in early coated-particle fuel development, with the low-temperature isotropic form selected for further development.

<sup>21</sup> The phrase, "depressurization of separate coated particles," was taken from the referenced paper. It is interpreted to refer to individual failures of loose particles during irradiation.

indications of damage in the first two cases, but failure of the fuel sphere and a significant fraction of the particles in the last case [8]. These conditions are not achievable in a reactor because of negative temperature reactivity feedback and continued heat removal from the sphere, but the results are relevant to the ultimate capability of the fuel.

### **B.3 LEU UO<sub>2</sub> Experience in China**

The coated-particle fuel program in China was initially established to support the construction and operation of the Institute of Nuclear and newEnergy Technology (INET) HTR-10 reactor. The HTR-10 project was initiated in 1990, following an HTGR conceptual design and feasibility study [10]. Development of fuel fabrication methods was based on the German particle and spherical fuel element design using fuel fabrication equipment obtained from Germany. Fabrication of fuel for the first core of HTR-10 began in December 1999 [11] with the production of 11,700 fuel spheres by September 2000 sufficient to support initial criticality, which was achieved in December 2000 with a core containing a mixture of 16,890 fuel and carbonaceous matrix spheres.<sup>22</sup>

The low power level (10 MWth) combined with the replication of the German fuel design, which enabled the use of the German fuel performance data, supported the demonstration of large margins to fuel service condition limits. The fuel irradiation and testing program was conducted in parallel with the initial operation of HTR-10 [10]. Following initial criticality, a series of tests was completed at a power level of 3.44 MWth, supporting subsequent operation at 10 MWth, which was achieved in January 2003 [12].

The fuel quality, as indicated by the free-uranium content in the fuel spheres, improved by over an order of magnitude during the course of production for the HTR-10 core (a total of 25 batches of spheres). Free-uranium content (as measured by the burn-leach procedure) in the early batches was typically  $\sim 10^{-4}$ , while the last 15 batches were typically  $\sim 10^{-5}$  and lower [11]. To facilitate irradiation and testing of HTR-10 fuel as soon as possible, sphere samples were taken from the first and second batches [13]; thus, the as-manufactured quality of the tested spheres was representative of the lower quality early fuel production.

Irradiation of four fuel spheres taken from early in the first HTR-10 core production, as described above, began in the Russian IVV-2M reactor in July 2000 and was completed in February 2003 [13]. The irradiation rig contained five capsules—capsules 2 through 5 contained fuel spheres, while capsule 1 contained carbonaceous matrix specimens. The irradiations were conducted at  $\sim 1000^{\circ}\text{C}$ , with short-term increases to  $\sim 1200^{\circ}\text{C}$ , and to burnups ranging from 95 to 107 GWd/MTHM. In-pile gas release measurements indicated the presence of one or two exposed kernels in two of the irradiated spheres from the beginning, consistent with the as-manufactured free-uranium measurements for early production batches.

---

<sup>22</sup> The initial core loading for HTR-10 included both fuel and graphite spheres to achieve the desired core volume. As burnup proceeds, the fraction of graphite spheres is decreased to compensate for burnup in the approach to an equilibrium core.



One of the capsules failed during irradiation with loss of gas-release data, and post-irradiation examination (PIE) showed substantial damage to the sphere (in-pile gas-release measurements failed when the capsule failed). Another capsule was subjected to a high-temperature test at the end of the irradiation, resulting in temperatures well beyond the planned conditions (and a significant fraction of exposed kernels as determined in the PIE) when a control thermocouple (TC) failed. In-pile gas-release data indicated no failures occurred during irradiation when conditions remained within specified levels.

An additional irradiation of fuel spheres produced in China for the HTR-10 was conducted in the HFR Petten reactor in an experiment designated HFR-EU1 [14, 15]. The HFR-EU1 experiment included two spheres from China and three from the German program (from AVR 21-2, representative of the highest quality German fuel), with the two fuels placed in separate capsules, each with in-pile gas release measurement capability. A primary objective of the irradiation was to subject the spheres to high burnups (for example, 17% FIMA for Chinese spheres, 20% FIMA for German spheres) to investigate the ultimate capability of the coated-particle design developed in Germany. The experiment was performed in two campaigns from September 2006 to February 2008 and continued from October 2009 to February 2010. The surface temperature of pebble INET 2 during irradiation was approximately 940°C. At the end of irradiation, the experiment had accumulated 16 reactor cycles totaling 445 EFPD.

The calculated burnup was 9.3% FIMA (pebble INET 1) and 11.6% FIMA (pebble INET 2)—both somewhat lower than the originally planned value—and the maximum fast neutron fluence ( $E > 0.1$  MeV) was about  $4.95 \times 10^{25}$  n/m<sup>2</sup>. The <sup>85m</sup>Kr release-rate-to-birth-rate (R/B) ratio for the INET capsule was approximately  $8 \times 10^{-8}$ . Based on the Booth Model [16] and assuming a capsule-average temperature of 900°C, the calculated <sup>85m</sup>Kr release fraction from a single coated particle would be  $3.26 \times 10^{-3}$ , and from a single failed particle in the capsule with two INET fuel spheres (~16,600 particles)  $1.96 \times 10^{-7}$ , which is higher than the observed R/B. This indicates no complete particle failure occurred during the irradiation and the measured fission gas release originates from uranium and thorium impurities in the carbonaceous matrix of the pebbles and in the graphite cups used to hold the pebbles in place.

Development of fuel for the High-Temperature Reactor-Pebble-bed Modular (HTR-PM) reactor has been conducted at INET starting around 2004 and is based closely on the development of HTR-10 fuel technology. The manufacturing technology and facilities were enhanced to the industrial scale and a demonstration line was established with the capability to produce 100,000 pebbles per year. The HTR-PM fuel uses the same TRISO coated particle design as HTR-10, but the uranium loading increased from 5 to 7 g per pebble, corresponding to an increase in particles from 8,000 to 12,000 per pebble. At the same time, the free uranium fraction in the pebbles decreased from  $5 \times 10^{-4}$  to  $6 \times 10^{-5}$ . After establishing the technology, a batch of spheres was fabricated, with several being selected at random for an irradiation qualification test in HFR Petten.

Irradiation testing of five HTR-PM fuel spheres was performed in HFR Petten [17]. The irradiation was designed so the upper four pebbles would reach a burnup higher than 12.3% FIMA with center temperatures of 1050±50°C. The irradiation took 355 full-power irradiation days and was completed in December 2014. Based on neutronics calculations, the total fast fluence levels were between 3.79 and  $4.95 \times 10^{25}$  n/m<sup>2</sup> ( $E > 0.1$  MeV). Burn-up estimates are

11.1% FIMA for Pebble 5 and between 12.6 and 13.7% FIMA for the other pebbles. The central temperatures remained within the target boundaries of  $1050 \pm 50^\circ\text{C}$ . The calculated R/B from a single failed particle (out of 60,000 particles) at  $1050^\circ\text{C}$  is  $1.1 \times 10^{-7}$  for  $^{85\text{m}}\text{Kr}$ . Measured  $^{85\text{m}}\text{Kr}$  R/B values during the last cycle were between  $2.4$  and  $3.3 \times 10^{-9}$ , indicating no particle failure.

PIE of the HTR-PM irradiated fuel specimens has been performed at Petten and Karlsruhe separately. The initial PIE at Petten shows the dimensional shrinkage in all five pebbles is between 0.88% and 1.25%, and further PIE has been performed at the European Commission Joint Research Center in Karlsruhe. There, the irradiated fuel pebbles have been exposed to heating tests in pure helium in the KühlFinger-Apparatur (KüFA) facility, which simulates high-temperature accident conditions in the reactor. These final PIE results have not yet been published.

#### **B.4 LEU UO<sub>2</sub> Experience in Japan**

The Japanese high-temperature gas reactor program is centered on the HTTR, which has a thermal power of 30 MW and  $950^\circ\text{C}$  maximum coolant outlet temperature. The HTTR achieved criticality in November 1998 and has undergone a series of rise-to-power tests [18]. In December 2001, an outlet temperature of  $850^\circ\text{C}$  was achieved, and in April 2004, a temperature of  $950^\circ\text{C}$  was achieved. As of July 2004, the reactor had operated for 224 effective full-power days (EFPDs). The planned core life cycle is 660 EFPDs [19]. It is planned to couple a high-temperature process-heat application to the HTTR through its intermediate heat exchanger in the future.

The fuel elements are prismatic graphite pin-in-blocks with vertical bore holes containing fuel rods (graphite sleeves) with annular fuel compacts [20]. Each compact contains about 13,000 TRISO-coated fuel particles with a 600- $\mu\text{m}$ -diameter UO<sub>2</sub> kernel, a 60- $\mu\text{m}$ -thick buffer, and 30- $\mu\text{m}$ -thick inner pyrolytic carbon (IPyC), 25- $\mu\text{m}$ -thick SiC, and 45- $\mu\text{m}$ -thick outer pyrolytic carbon (OPyC) layers. Uranium enrichments vary in 12 stages, from 3.4 to 9.9%, and average 6%. The end-of-life core average burnup is designed to be 2.4% FIMA, and the design limit peak burnup is 3.6% FIMA. The fuel quality of the HTTR first core is a heavy-metal (HM) contamination of  $2.5 \times 10^{-6}$ , initial through-coating defects of  $2.5 \times 10^{-6}$ , and initial SiC defects of  $8 \times 10^{-5}$ . The measured R/B ratio of  $^{88}\text{Kr}$  at full power, a  $950^\circ\text{C}$  outlet temperature, and approximately 200 EFPDs of reactor operation was  $1.0 \times 10^{-8}$ , corresponding to gaseous diffusion from HM contamination and no significant in-reactor fuel particle failures. The high-temperature demonstration was maintained for about 5 days.

HTTR-type fuel was irradiated in the HRB-22 test in the HFIR to burnups in the range of 4.1 to 6.7% FIMA [20, 21]. Online gamma monitoring detected four fuel-particle failures out of 32,200 particles irradiated, or a failure fraction of  $1.2 \times 10^{-4}$ . PIE and safety tests were performed at temperatures ranging from 1600 to  $1800^\circ\text{C}$ . In one test at  $1600^\circ\text{C}$ , one failed particle was detected out of about 2,800 particles in 219.4 hours. Tests at 1700 and  $1800^\circ\text{C}$  revealed large variations in metallic fission-product releases from particle to particle, which could only be explained by the presence or absence of cracks in the SiC layer. A series of irradiations was carried out with HTTR fuels in Oarai Gas Loop-1 in the Japan Materials Testing Reactor. The results of three irradiations with particle numbers of about 65,000 in each experiment indicate through-wall failures were less than  $3 \times 10^{-4}$  at 95% confidence after burnups up to 3.7% FIMA [22].

A modified coated particle design was developed to allow burnups of approximately 10% FIMA in HTTR. Preliminary testing in materials test reactors (MTRs) at ~7 to 9% FIMA indicated good performance, albeit with several particle failures that were postulated to be due to as-fabricated SiC defects based on fuel performance models [23]. This fuel notably involved a change in the specification for kernel diameter (from 600 to ~550  $\mu\text{m}$ ), buffer layer thickness (from 60 to 90  $\mu\text{m}$ ), and SiC layer thickness (from 25 to 35  $\mu\text{m}$ ) compared to the initial HTTR fuel particles. Based on these results, additional modifications in the particle design were implemented with a specified kernel diameter of 500  $\mu\text{m}$  (9.9%  $^{235}\text{U}$  enrichment) and buffer thickness of 95  $\mu\text{m}$  [24], such that it closely resembled the standard TRISO particle design from the German program. This fuel was recently irradiated to >9% FIMA in the WWR-K reactor (Kazakhstan). A few exposed kernels were observed based on R/B data, but these were again postulated to be related to particles with as-fabricated SiC defects [25], indicating no in-pile particle failures occurred.

### **B.5 German High-Quality LEU- $\text{UO}_2$ Pebble-Fuel Experience**

Experience with coated particle fuel in Germany began in the early era of particle fuel development, and progressed through varying particle types employed in the AVR. The German LEU  $\text{UO}_2$  TRISO fuel design evolved from decades of international coated-particle fuel fabrication, irradiation, and PIE and safety testing experience covering a wide range of particle designs, fuel forms, and irradiation and testing conditions. Numerous international bilateral and multilateral data and analytical methods exchanges (such as those discussed in IAEA-IWGGCR/8 [8]) facilitated the effective incorporation of this experience into the definition and development of the German LEU  $\text{UO}_2$  TRISO fuel particle and sphere design that began in the late 1970s.

Fuel development in the 1980s demonstrated the high as-manufactured fuel quality and excellent in-pile performance that can be accomplished with LEU  $\text{UO}_2$  fuel. Efforts involved refinement of fuel fabrication and quality control capabilities, irradiation testing of fuel spheres both in MTRs and in AVR, and PIE and heating tests to assess performance in-pile and under accident conditions, and have been summarized in several publications [26-28]. The results demonstrated low as-manufactured particle defect fractions and low particle failure fractions during irradiation and during post-irradiation heating tests at postulated accident temperatures.

This effort culminated in the large-scale fabrication campaign of the so-called GLE-4/2 fuel for AVR (16.8%  $^{235}\text{U}$ ) and the small-scale fabrication of the proof test fuel for the HTR-Modul 200-MWt modular reactor design in 1988 (10.6%  $^{235}\text{U}$ ), both with very low defective particle fractions ( $\leq 2.0 \times 10^{-5}$  and  $\leq 5.3 \times 10^{-5}$ , respectively; representing the upper bound at 95% confidence) [27]. Fuel fabrication efforts ceased in 1988 concurrent with the shutdown of THTR, but irradiation testing in MTRs continued through 1994, finishing with the proof test fuel irradiations (designated HFR-K5 and HFR-K6) in HFR-Petten.

A large body of experimental data obtained by means of an irradiation and PIE program, covering a wide range of operating parameters, supports the German LEU  $\text{UO}_2$  TRISO fuel design. This database supports establishment of an operating envelope for this fuel design, covering normal operation as well as transient and accident conditions.

### B.5.1 Fabrication

The LEU TRISO fuel types manufactured and tested in Germany are summarized in Table B-1 and Table B-2. Fuel spheres intended for AVR operation were manufactured in large numbers for the purpose of bulk testing in a reactor environment. Fuel spheres manufactured for the German LEU Phase 1 irradiation test program and for the Proof Test for the HTR-Modul were manufactured in smaller numbers.

**Table B-1**  
**LEU UO<sub>2</sub> TRISO fuels manufactured and tested**

Characteristic	Pre-1985 Production			Post-1985 Production	
	1981	1981	1983	1985	1988
Year of Manufacture	1981	1981	1983	1985	1988
Designation	GLE 3	LEU Phase I	GLE 4	GLE 4/2	Proof Test Phase 2
Matrix Material	A3-27	A3-27	A3-27	A3-3	A3-3
Irradiation Test Designation	AVR 19	HFR-K3 FRJ2-K13 HFR-P4 SL-P1 FRJ2-P27	AVR 21-1 FRJ2-K15	AVR 21-2	HFR-K5 HFR-K6
Approximate number of fuel spheres manufactured	24,600	100	20,500	14,000	200

The symbols used in the 'Irradiation Test Designation' row have the following meanings:

- The first 2 to 4 characters describe the reactor in which the test was done:
  - AVR = *Arbeitsgemeinschaft Versuchsreaktor* in Jülich, Germany
  - HFR = High Flux Reactor in Petten
  - FRJ2 = DIDO reactor in Jülich
  - SL = Siloe reactor in Grenoble
- The next group of characters describes the irradiation sample type and test number. In the case of AVR irradiations, the reload number is used (that is, AVR 19), which means that the fuel spheres made up the 19th partial reload of the reactor. In other tests, the letter K designates a full-sized fuel sphere, the letter P designates coated particles in any other form (that is, small spheres, compacts, or coupons) and the number is the test number. Thus, FRJ2-P27 means irradiation test number 27 performed on coated particles in the DIDO reactor in Jülich.

The data indicate the pre-1985 and post-1985 fuel designs are nearly identical, except for enrichment and HM loading in the spheres. Although the enrichment and HM loading varied, the amount of  $^{235}\text{U}$  per sphere was kept at approximately 1 gram.

The delineation between pre-1985 and post-1985 is not based on the fuel design, but rather on two particular improvements in the manufacturing process. Coated particles are "overcoated" with matrix material<sup>23</sup> prior to mixing them with additional matrix material in preparation for pressing of the fuel sphere. For the pre-1985 category, the overcoating of the particles was done manually, whereas for the post-1985 category, overcoating was automated using a specially designed mixer operated by a robot. This change in the overcoating process and the introduction of vibration tables in three stages to remove odd shaped kernels, coated particles, and overcoated particles during particle manufacturing resulted in a significant improvement in the "free uranium" burn-leach test results for completed fuel spheres. The free uranium fraction decreased by about a factor of four from the average of the pre-1985 results to the average of the post-1985 results.

**Table B-2**  
Manufacturing detail for LEU  $\text{UO}_2$  TRISO fuel types

Characteristic	Pre-1985 Production			Post-1985 Production	
	GLE 3	LEU Phase I	GLE 4	GLE 4/2	Proof Test Phase 2
Designation					
Kernel Diameter ( $\mu\text{m}$ )	500	497	501	502	508
Kernel Density ( $\text{g}\cdot\text{cm}^{-3}$ )	10.80	10.81	10.85	10.87	10.72
Coating Thickness ( $\mu\text{m}$ )					
Buffer Layer	93	94	92	92	102
Inner PyC Layer	38	41	38	40	39
SiC Layer	35	36	33	35	36
Outer PyC Layer	40	40	41	40	38
Coating Density ( $\text{g}\cdot\text{cm}^{-3}$ )					
Buffer Layer	1.01	1.00	1.01	1.1	1.02
Inner PyC Layer	1.86	~1.9	1.9	1.9	1.92
SiC Layer	3.19	3.20	3.20	3.2	3.20
Outer PyC Layer	1.89	1.88	1.88	1.9	1.92
Fuel Sphere Loading					
Heavy Metal (g/FS)	10	10	6	6	9.4
Uranium-235 (g/FS)	1	1	1	1	1
Enrichment (% U-235)	9.82	9.82	16.76	16.76	10.6
Coated Particle per FS	16400	16400	9560	9560	14580
Free-Uranium Fraction ( $\times 10^{-6}$ )	50.7	35	43.2	7.8	13.5

<sup>23</sup> The matrix material consists of a mixture of natural and synthetic graphite powders and a resin binder.

Forty GLE 4/2 spheres and 10 Proof Test spheres, containing 528,200 coated particles, were subjected to the burn-leach test<sup>24</sup>. Test results indicated the free uranium in these 528,200 particles was equivalent to the uranium in six coated particles. Therefore, the sample mean defect fraction is  $1.1 \times 10^{-5}$  and the expected defect fraction (50% confidence that population fraction is no higher) due to manufacturing is  $1.3 \times 10^{-5}$ , with a 95% confidence maximum defect fraction of  $2.2 \times 10^{-5}$ . Note the substantial majority of the fuel irradiation and testing data summarized in this section was produced from the GLE 3 and LEU Phase 1 (that is, pre-1985 production) fuels.

Details of the German LEU UO<sub>2</sub> TRISO fuel fabrication processes for kernels, coated particles, and spherical fuel elements are beyond the scope of this report. Numerous sources provide additional information as an introduction to the subject, including IAEA TECDOC-978 [5] and Kania et al. 2015 [29].

### **B.5.2 Irradiation and Accident Safety Testing**

The German fuel irradiation experience includes both bulk fuel testing in the AVR and carefully controlled and monitored irradiations in MTRs in Germany, the Netherlands, and France. Results of this test program have been summarized in other publications (an excellent starting point is Kania et al. 2013 [27], and an analysis of the data with a focus on as-manufactured defects and in-pile particle failures has been presented previously in Section 3.3 and associated appendix of the NGNP Fuel Qualification White Paper [30]. Key results, observations, and conclusions from the German program with regard to fuel performance are summarized in this section.

A summary of in-pile fuel conditions (burnup, fast fluence, and temperature) for the irradiation results discussed in this section is shown in Figures B-1 and B-2. The AVR fast fluence values were determined by a correlation with burnup and individually adjusted to reflect the expected  $\pm 10\%$  variation based on different trajectories taken by individual spheres. Also included in Figure B-3 is an example operating envelope developed related to the NGNP pebble-bed design [30]. The aggregate envelope of the existing data on German LEU UO<sub>2</sub> TRISO fuel substantially exceeds this envelope in terms of burnup and fast fluence. The MTR data include known temperature histories and extremes in burnup and fluence and time at temperatures well beyond the expected service conditions of pebble-bed fuel. These data also provide insights that support interpretation of the AVR irradiation data, such as particles with exposed kernels present from the beginning of the irradiations.

---

<sup>24</sup> Since the manufacturing process change that delineates the two categories significantly impacts the determination of the free-uranium fraction, only the burn-leach test results from the post-1985 category were used in the calculation of the expected “coated-particle defect fraction” due to manufacturing defects.

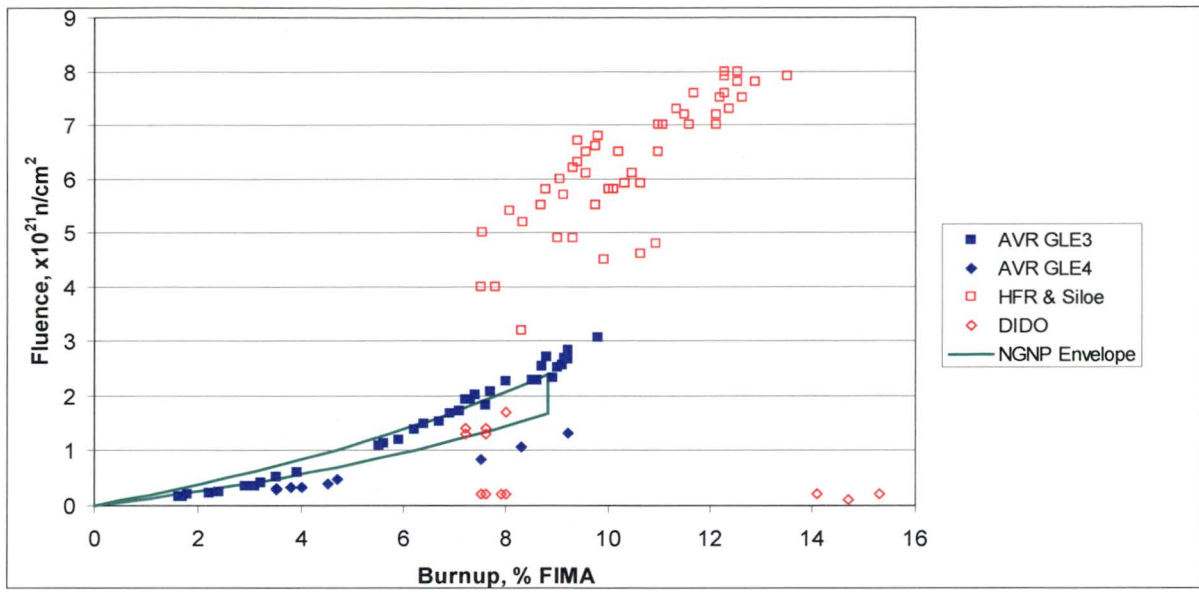


**Figure B-1**  
German LEU TRISO irradiation conditions, AVR and MTRs. The NNGP pebble-bed performance envelope is included for comparison [30]  
*Courtesy of Idaho National Laboratory and used with permission of Battelle Energy Alliance, LLC*

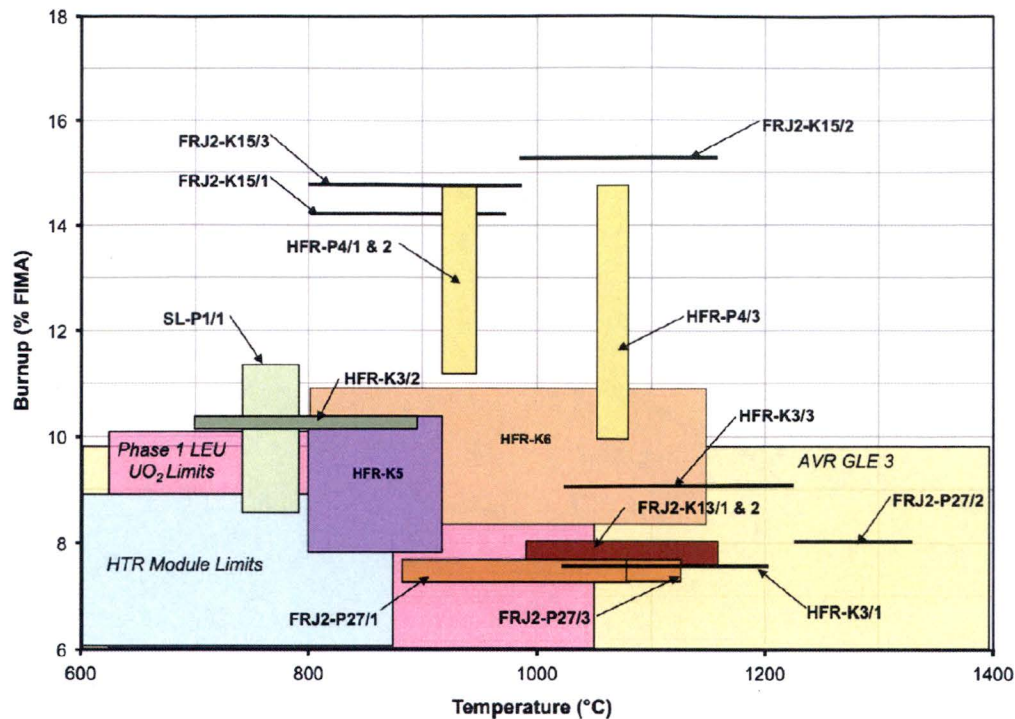


**Figure B-2**  
**Fuel burnup and mean operating temperature for German LEU UO<sub>2</sub> TRISO particles in accelerated irradiation tests conducted in European MTRs and in AVR prior to 2000**  
 Reprinted from *Journal of Nuclear Materials*, ©2003, with permission of Elsevier<sup>25</sup>

The two final proof test irradiations (HFR-K5 and HFR-K6) involved eight spheres at temperatures between 800 and 1140°C and peak burnup of about 11% FIMA with low fission gas release indicating no particle failure (<sup>85m</sup>Kr R/B ratios  $\leq 9.0 \times 10^{-7}$ ), giving a calculated particle failure fraction of  $\leq 2.6 \times 10^{-5}$  (upper bound at 95% confidence). Taken as a whole, German irradiation testing of 60-mm-diameter spherical fuel elements in MTRs (totaling approximately 277,000 particles and including Phase 1, GLE 3, and Proof Test fuel) resulted in no particle failures, which corresponds to a particle failure fraction of  $\leq 1.1 \times 10^{-5}$  at 95% confidence. Additional analysis, which includes data on exposed kernels in AVR spheres derived from post-irradiation heating test data in addition to the results from MTR irradiations indicates no failures out of approximately 477,000 particles.

<sup>25</sup> Reprinted from Kania et al., "Testing of HTR UO<sub>2</sub> TRISO fuels in AVR and in material test reactors," *J. Nucl. Mater.*, Vol. 441, 2013, pp. 545-562, Copyright 2003, with permission from Elsevier.



German fuel elements (including both standard spherical fuel elements as well as smaller cylindrical compacts containing ~1,600 particles in a central spherical fueled zone and indicated by the “P” nomenclature in the irradiation test designation in with burnup  $\leq 11\%$  FIMA also exhibited no failures during 1600°C isothermal accident tests in dry helium (based on  $^{85}\text{Kr}$  release fractions  $\leq 2 \times 10^{-6}$ )<sup>26</sup>, and cesium release fractions were below  $\leq 1 \times 10^{-4}$ , indicating intact, retentive SiC layers.

However, at reported burnups  $\geq 14\%$  FIMA<sup>27</sup> or temperatures  $\geq 1700^\circ\text{C}$  during post-irradiation heating tests, particle failures began to manifest as higher  $^{85}\text{Kr}$  releases. Cesium release also increased at the higher temperatures, with release fractions reaching  $\sim 10^{-2}$  to  $10^{-1}$  from fuel spheres at 1800°C (burnup  $< 11\%$  FIMA) and  $> 10^{-1}$  for fuel compacts (burnup 12% FIMA) [31]. Based on these results, it has been asserted, if the fuel is pushed to a burnup of  $\sim 15\%$  FIMA, accident temperatures should be limited to 1600°C, but for fuel with peak burnup of 11% FIMA the allowable accident temperature limit may be higher than 1600°C [27]. Additional post-irradiation heating under oxidizing conditions, performed on a more limited scale, demonstrated additional particle failure can occur after prolonged exposure (several hundred hours) in air above 1300°C, and 800°C exposure to steam can result in increased release of fission gas from exposed kernels.

Additional irradiation testing of German TRISO fuel was performed from 2004 to 2010 in HFR Petten using previously manufactured fuel spheres of the GLE-4/2 type and sponsored by the European Commission, with the intent of demonstrating the  $\text{UO}_2$  fuel performance at temperatures and burnup beyond the conventional fuel performance envelope for modular pebble-bed HTGRs [32-34]. Burnups achieved in these irradiations were approximately 11% and 14% FIMA in the EU1bis and EU1 irradiations, respectively (both falling somewhat short of the originally targeted values) [35], and some PIE results from the EU1bis experiment have been reported [36].

While the AVR spheres in the EU1 irradiation (sphere surface temperatures reported to be 950°C) exhibited relatively low fission gas R/B ratios indicating no failed particles [33], the higher-temperature EU1bis irradiation (sphere center temperatures were reportedly maintained at 1250°C [37]<sup>28</sup>) had  $^{85\text{m}}\text{Kr}$  R/B of  $4 \times 10^{-6}$ , indicating some particle failure occurred [34].

---

<sup>26</sup> Note that more recent heating tests on proof test spheres from the HFR-K5 and -K6 spheres has resulted in somewhat higher  $^{85}\text{Kr}$  release fractions, although still falling below  $1 \times 10^{-5}$ , indicating no particle failures (O. Seeger et al., *Nucl. Eng. Des.* Vol. 306, 2016, pp.59-69; D. Freis, *Accident Simulations and Post-Irradiation Investigations on Spherical Fuel Elements for High Temperature Reactors*, 2010 Doctoral dissertation, NRC translation 3806)

<sup>27</sup> Several methods were used to empirically measure the burnup of the fuel compacts; the reported values are the highest among the various methods, indicating the possibility that burnup could be overestimated by  $\sim 10\text{--}20\%$  (W. Schenk et al., *Performance of HTR Fuel Samples under High-Irradiation and Accident Simulation Conditions, with Emphasis on Test Capsules HFR-P4 and SL-P1*, Juel-3373, Research Center Jülich, 1994).

<sup>28</sup> Early in the irradiation, an operating error resulted in inadvertent introduction of pure neon, resulting in temperatures well above the target values. Post-irradiation thermal modeling of operation with pure neon indicated a temperature at the outer graphite shroud radius of 1350°C, which could result in sphere centerline temperatures approaching 1600°C for an extended period (S. de Groot, K. Bakker, A.I. van Heek, M.A. Fütterer, Modelling of the HFR-EU1BIS experiment and thermomechanical evaluation, *Nucl. Eng. Des.* 238 (2008) 3114-3120).

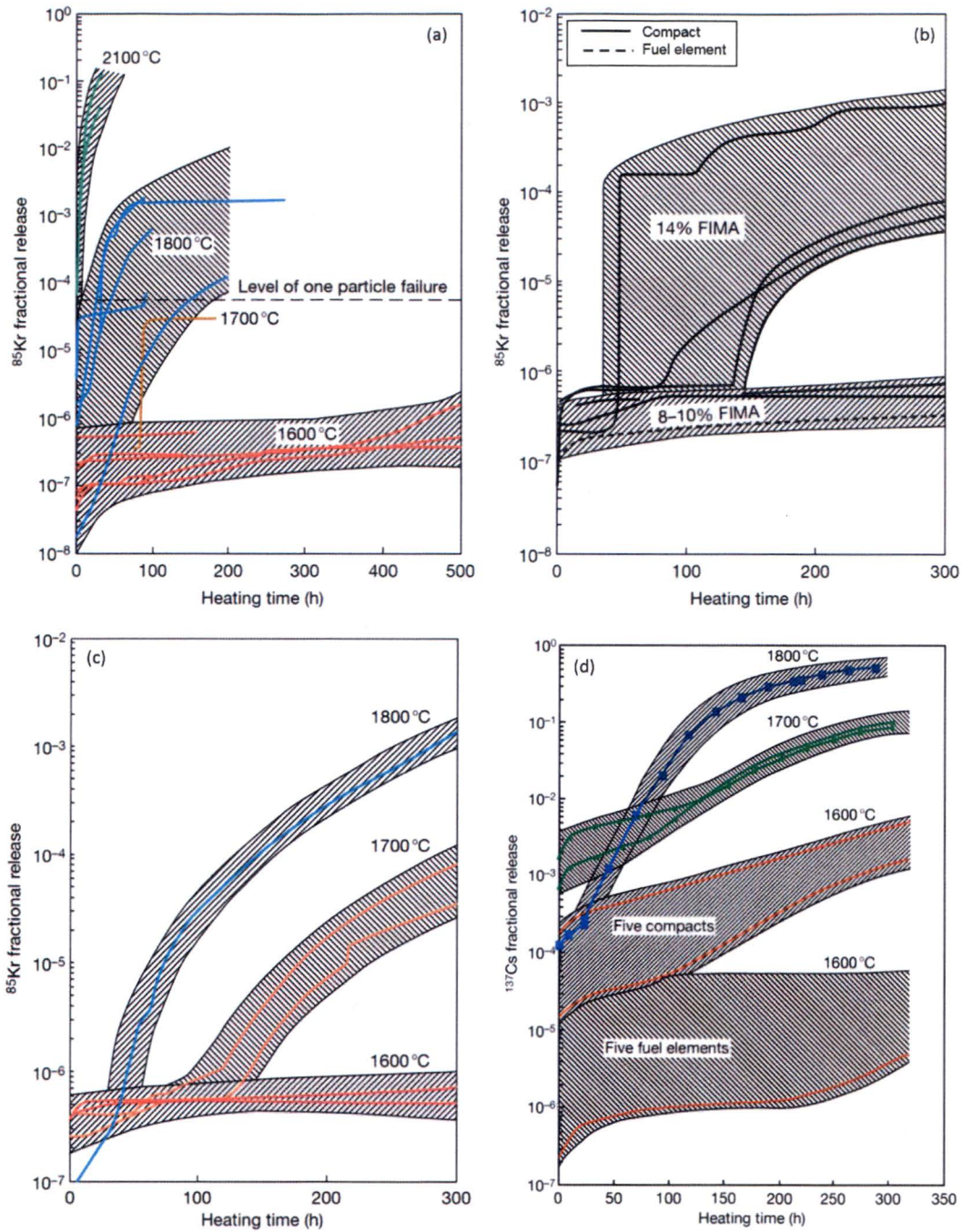


**Figure B-3**  
 Summaries of  $^{85}\text{Kr}$  and  $^{137}\text{Cs}$  release during German accident safety tests in helium. Note:  $^{85}\text{Kr}$  release results are for (a) spherical fuel elements at 1600–2100°C, (b) spherical fuel elements and cylindrical compacts with burnup 8–14% FIMA at 1600°C, (c) cylindrical compacts with burnup 10–12% FIMA at 1600–1800°C. (d)  $^{137}\text{Cs}$  release results for spherical fuel elements (1600°C) and cylindrical compacts (1600–1800°C)

Courtesy of Idaho National Laboratory and used with permission of Battelle Energy Alliance, LLC

Post-irradiation heating of several spheres from these irradiations resulted in low release of  $^{85}\text{Kr}$ , indicating no full TRISO coating failures. However,  $^{134}\text{Cs}$  fractional release at  $1600^\circ\text{C}$  reached  $1\text{--}2.5 \times 10^{-3}$  for EU1bis spheres<sup>29</sup> and  $6 \times 10^{-4}$  for an EU1 sphere, [38-40] all of which are significantly higher than observed in historic tests of German LEU  $\text{UO}_2$  TRISO fuel at similar temperatures, which indicates release through the SiC layer of the particles. This indicates the onset of degradation and/or layer failure. It appears these irradiation tests may have challenged an upper limit for acceptable performance for LEU  $\text{UO}_2$  fuel.

In a compilation of German irradiation and safety testing data, Kania et al. [27] have summarized the performance of spherical fuel elements during  $1600^\circ\text{C}$  isothermal heating tests and transient-temperature tests, which simulate the time-varying peak fuel temperature in the reactor during a depressurized loss of coolant flow accident with a maximum temperature of  $1620^\circ\text{C}$ . This includes spheres irradiated in AVR as well as fuel from proof test irradiations and the more recent EU irradiations. Based on five observed failures<sup>30</sup> out of 287,480 particles tested, the reported upper bound for the failure fraction at 95% confidence is  $\leq 3.7 \times 10^{-5}$ .

## B.6 References

1. R.A. Simon and P.D. Capp, 2002, "Operating experience with the Dragon high temperature reactor experiment," *Proceedings of the Conference on High Temperature Reactors (HTR-2002)*, Petten, the Netherlands, April 22-24, 2002. International Atomic Energy Agency, Vienna: 2002.
2. K.I. Kingrey. *Fuel Summary for Peach Bottom Unit 1 High-Temperature Gas Cooled Reactor Cores 1 and 2*. Idaho National Laboratory, Idaho Falls, ID: April 2003. INEEL/EXT-03-00103.
3. *AVR – Experimental High-Temperature Reactor, 21 Years of Successful Operation for a Future Energy Technology*. VDI-Verlag GmbH, Düsseldorf: June 1990.
4. *A Review of Radionuclide Release from HTGR Cores During Normal Operation*. Electric Power Research Institute, Palo Alto, CA: February 2004. 1009382.
5. *Fuel Performance and Fission Product Behaviour in Gas Cooled Reactors*. International Atomic Energy Agency, Vienna: November 1997. IAEA-TECDOC-978.
6. *Advances in High Temperature Gas Cooled Reactor Fuel Technology*. International Atomic Energy Agency, Vienna: June 2012. IAEA-TECDOC-1674.

---

<sup>29</sup> Subsequent analysis of the testing system by Seeger et al., indicates that the temperature of some of the EU1bis tests was most likely lower than originally reported by approximately  $100^\circ\text{C}$  (O. Seeger, "Evaluation of fission product releases obtained from Küfa safety tests in light of the setup's accuracy," *Proceedings of the 8th International Topical Meeting on High Temperature Reactor Technology (HTR 2016)*, Las Vegas, Nevada, November 6-10, 2016.)

<sup>30</sup> Note that all five failures included in the statistics occurred during transient-temperature tests in which the furnace temperature mimicked the peak fuel temperature during a depressurized loss of forced cooling accident, and were performed using spheres irradiated in AVR. Fuel-performance models would predict that the isothermal testing at  $\geq 1600^\circ\text{C}$  should be more challenging for the fuel. It is possible that these AVR spheres experienced exceptionally high temperatures during irradiation, resulting in elevated failure during post-irradiation heating and biasing the results.

7. G. Gibbs, Idaho National Laboratory, letter to U.S. Nuclear Regulatory Commission, September 20, 2010, "Contract Number DE-AC07-05ID14517—Next Generation Nuclear Plant — Response to Questions about the Applicability of the Advanced Gas Reactor Testy Results to Next Generation Nuclear Plant —NRC Project No. 0748," CCN 222202; ML102770386.
8. *Specialists' Meeting on Gas-Cooled Reactor Fuel Development and Spent Fuel Treatment*. International Atomic Energy Agency, Vienna: October 1983. IAEA-IWGGCR/8.
9. A. Chernikov and A. Deryugin. "Irradiation tests of HTGR Fuel under normal and accident conditions," *OECD Proceedings: The First Information Exchange Meeting on Survey on Basic Studies in the Field of High Temperature Engineering*. Paris, France, September 27-29, 1999. Organization for Economic Cooperation and Development, Paris: 2000.
10. D. Zhong and Z. Qin, "Overview of the 10 MW High Temperature Gas-Cooled Reactor Test Module," *Proceedings of the Seminar on HTGR Application and Development*. Beijing, China, March 19-21, 2001.
11. C. Tang et al., "Fabrication of the first loading fuel of 10 MW High Temperature Gas Cooled Reactor-Test Module (HTR-10)," *Proceedings of the Seminar on HTGR Application and Development*, Beijing, China, March 19-21, 2001.
12. X. Jing X., and Y. Yang, "Physical designs and calculations for the first full power operation of the 10 MW High Temperature Gas-Cooled Reactor – Test Module (HTR-10)," *Proceedings of the 2nd International Topical Meeting on High Temperature Reactor Technology (HTR-2004)*, Beijing, China, September 22-24, 2004.
13. C. Tang, X. Fu, J. Zhu, K.N. Koshceev, A.V. Kozlov, O.G. Karlov, Y.G. Degaltsev, and V.I. Vasiliev., "The behavior of HTR-10 fuel under irradiation," *Proceedings of the 2nd International Topical Meeting on High Temperature Reactor Technology (HTR-2004)*, Beijing, China, September 22-24, 2004.
14. Marmier, A., et al., 2008, "Preliminary results of the HFR-EU1 fuel irradiation of INET and AVR pebbles in the HFR Petten," *Proceedings of the 4th International Topical Meeting on High Temperature Reactor Technology (HTR-2008)*, Washington, D.C., September 28-October 1, 2008.
15. C. Tang, X. Fu, J. Zhu, H. Zhao, and Y. Tang, "Comparison of two irradiation testing results of HTR-10 fuel spheres," *Nuclear Engineering and Design*, Vol. 251, pp. 453–458 (2012).
16. A.H. Booth. *A Method of Calculating Fission Gas Release from UO<sub>2</sub> Fuel and Its Implication to the X-2-f Loop Test*. Atomic Energy of Canada Limited, Chalk River, Ontario, Canada: September 1957. Report AECL 496,
17. S. Knol, S. de Groot, R.V. Salama, J. Best, K. Bakker, I. Bobeldijk, J.R. Westlake, M.A. Fütterer, M. Laurie, C. Tang, R. Liu, B. Liu, and H. Zhao, "HTR-PM fuel pebble irradiation qualification in the high flux reactor in Petten," *Nuclear Engineering and Design*, Vol. 329, pp. 82–88 (2018).
18. S. Fujikawa, H. Hayashi, T. Nakazawa, K. Kawasaki, T. Iyoku, S. Nakagawa and N. Sakabas, "Achievement of reactor-outlet coolant temperature of 950°C in HTTR," *Journal of Nuclear Science and Technology*, Vol. 41, p. 1245 (2004).

19. K. Verfondern, J. Sumita, S. Ueta, and K. Sawa. *Modeling of Fuel Performance and Fission Product Release Behavior during HTTR Normal Operation (A Comparison of the FZJ and JAERI Modeling Approach)*. Japan Atomic Energy Research Institute, Tokai-Mura, Japan: March, 2001. JAERI-Research 2000-067.
20. K. Minato, K. Sawa, K. Fukuda, C.A. Baldwin, W.A. Gabbard, O.F. Kimball, C.M., et al., *HRB-22 Capsule Irradiation Test for HTGR Fuel (JAERI/USDOE Collaborative Irradiation Test)*, Japan Atomic Energy Research Institute, Tokai-Mura, Japan: March 1998. JAERI-Research 98-021.
21. K. Minato, K. Sawa, T. Koya, T. Tomita, A. Ishikawa, C.A. Baldwin, W.A. Gabbard, C.M. Malone, F.C. Montgomery, B.F. Myers, and N.H. Packan, "Fission product release behavior of individual coated fuel particles for high-temperature gas-cooled reactors," *Nuclear Technology*, Vol. 131, p. 36 (2000).
22. K. Hayashi, K. Sawa, T. Kitajima, T. Shiratori, H. Kikuchi, K. Fukuda, T. Itoh, H. Waragai. *Irradiation Experiments of the 13th–15th OGL-1 Fuel Assemblies*, Japan Atomic Energy Research Institute, Tokai-Mura, Japan: January 2000. JAERI-Research 2000-001.
23. K. Sawa and T. Tobita, "Investigation of irradiation behavior of SiC-coated fuel particle at extended burnup," *Nuclear Technology*, 142, pp. 250–259 (2003).
24. S. Ueta, J. Aihara, K. Sawa, A. Yasuda, M. Honda, N. Furihata, "Development of high temperature gas-cooled reactor (HTGR) fuel in Japan," *Progress in Nuclear Energy*, Vol. 53, pp. 788–793 (2011).
25. S. Ueta, J. Aihara, A. Shaimerdenov, D. Dyussambayev, S. Gizatulin, P. Chakrov, and N. Sakaba, "Irradiation test and post irradiation examination of the high burnup HTGR fuel," Paper 18491, *Proceedings of the 8th International Topical Meeting on High Temperature Reactor Technology (HTR 2016)*, Las Vegas, Nevada, November 6–10, 2016.
26. H. Nickel, H. Nabielek, G. Pott, and A.W. Mehner, "Long time experience with the development of HTR fuel elements in Germany," *Nuclear Engineering and Design*, Vol. 217, pp. 141–151 (2002).
27. M.J. Kania, H. Nabielek, K. Verfondern, and H.-J. Allelein, "Testing of HTR UO<sub>2</sub> TRISO fuels in AVR and in material test reactors," *Journal of Nuclear Materials*, Vol. 441, pp. 545–562 (2013).
28. A.W. Mehner, W. Heit, K. Röllig, H. Ragoss, and H. Müller, "Spherical fuel elements for advanced HTR manufacture and qualification by irradiation testing," *Journal of Nuclear Materials*, Vol. 171, pp. 9–18 (1990).
29. M.J. Kania, H. Nabielek, and H. Nickel, "Coated particle fuels for high-temperature reactors," in *Materials Science and Technology*. Wiley-VCH Verlag GmbH & Co., 2015.
30. *NGNP Fuel Qualification White Paper*. Idaho National Laboratory, Idaho Falls, ID: July 2010. INL/EXT-10-18610.
31. W. Schenk, G. Pott, and H. Nabielek, "Fuel accident performance testing for small HTRs," *Journal of Nuclear Materials*, Vol. 171, pp. 19–30 (1990).

32. M.A. Futterer, G. Berg, A. Marmier, E. Toscano, D. Freis, K. Bakker, and S. de Groot, "Results of AVR fuel pebble irradiation at increased temperature and burn-up in the HFR Petten," *Nuclear Engineering and Design*, Vol. 238 2008, pp. 2877–2885.
33. M. Laurie, A. Marmier, G. Berg, J.-M. Lapetite, M.A. Fütterer, and C. Tang, "Results of the HFR-EU1 fuel irradiation of INET and AVR pebbles in the HFR Petten," *Nuclear Engineering and Design*, Vol. 251, pp. 117–123 (2012).
34. K. Verfondern, A. Xhonneux, H. Nabielek, and H.-J. Allelein, "Computational analysis of modern HTGR fuel performance and fission product release during the HFR-EU1 irradiation experiment," *Nuclear Engineering and Design*, Vol. 273, 2014, pp. 85–97.
35. M. Phélip, "European programme on HTR fuel technology," Paper B06, *Proceedings of the 2nd International Topical Meeting on High Temperature Reactor Technology (HTR 2004)*, Beijing, China, September 22-24, 2004.
36. M. Barrachin, R. Dubourg, S. de Groot, M.P. Kissane, and K. Bakker, "Fission-product behavior in irradiated TRISO-coated particles: Results of the HFR-EU1bis experiment and their interpretation," *Journal of Nuclear Material*, Vol. 415, pp. 104–116 (2011).
37. S. de Groot, K. Bakker, A.I. van Heek, and M.A. Futterer, "Modelling of the HFR-EU1BIS experiment and thermomechanical evaluation," *Nuclear Engineering and Design*, Vol. 238, pp. 3114–3120 (2008).
38. O. Seeger, M. Laurie, A. El Abjani, J. Ejton, D. Boudaud, D. Freis, P. Carbol, V.V. Rondinella, M. Fütterer, and H.-J. Allelein, "KüFA safety testing of HTR fuel pebbles irradiated in the High Flux Reactor in Petten," *Nuclear Engineering and Design*, Vol. 306, pp. 59–69 (2016).
39. D. Freis, P.D.W. Bottomley, A.I. Kellerbauer, V.V. Rondinella, and P. Van Uffelen, "Accident testing of high-temperature reactor fuel elements from the HFR-EU1bis irradiation," *Nuclear Engineering and Design*, Vol. 241, pp. 2813–2821 (2011).
40. O. Seeger, K. Knebel, W. de Weerd, P. Carbol, P.D.W. Bottomley, V.V. Rondinella, and H.-J. Allelein, "Simulated accident testing of a fuel element from the HFR-EU1bis irradiation campaign," *Nuclear Engineering and Design*, Vol. 271, pp. 171–179 (2014).
41. D.A. Petti, P.A. Demkowicz, J.T. Maki, and R.R. Hobbins, "TRISO-coated particle fuel performance," in R.J.M. Konings(ed.): *Comprehensive Nuclear Materials*. Elsevier, Amsterdam, Vol. 3, pp. 151-213 (2012).



### **Export Control Restrictions**

Access to and use of this EPRI product is granted with the specific understanding and requirement that responsibility for ensuring full compliance with all applicable U.S. and foreign export laws and regulations is being undertaken by you and your company. This includes an obligation to ensure that any individual receiving access hereunder who is not a U.S. citizen or U.S. permanent resident is permitted access under applicable U.S. and foreign export laws and regulations.

In the event you are uncertain whether you or your company may lawfully obtain access to this EPRI product, you acknowledge that it is your obligation to consult with your company's legal counsel to determine whether this access is lawful. Although EPRI may make available on a case by case basis an informal assessment of the applicable U.S. export classification for specific EPRI products, you and your company acknowledge that this assessment is solely for informational purposes and not for reliance purposes.

Your obligations regarding U.S. export control requirements apply during and after you and your company's engagement with EPRI. To be clear, the obligations continue after your retirement or other departure from your company, and include any knowledge retained after gaining access to EPRI products.

You and your company understand and acknowledge your obligations to make a prompt report to EPRI and the appropriate authorities regarding any access to or use of this EPRI product hereunder that may be in violation of applicable U.S. or foreign export laws or regulations.

**The Electric Power Research Institute, Inc.** (EPRI, [www.epri.com](http://www.epri.com)) conducts research and development relating to the generation, delivery and use of electricity for the benefit of the public. An independent, nonprofit organization, EPRI brings together its scientists and engineers as well as experts from academia and industry to help address challenges in electricity, including reliability, efficiency, affordability, health, safety and the environment. EPRI members represent 90% of the electric utility revenue in the United States with international participation in 35 countries. EPRI's principal offices and laboratories are located in Palo Alto, Calif.; Charlotte, N.C.; Knoxville, Tenn.; and Lenox, Mass.

Together...Shaping the Future of Electricity

### **Programs:**

Nuclear Power

Advanced Nuclear Technology

© 2019 Electric Power Research Institute (EPRI), Inc. All rights reserved. Electric Power Research Institute, EPRI, and TOGETHER...SHAPING THE FUTURE OF ELECTRICITY are registered service marks of the Electric Power Research Institute, Inc.

3002015750

### **Electric Power Research Institute**

3420 Hillview Avenue, Palo Alto, California 94304-1338 • PO Box 10412, Palo Alto, California 94303-0813 USA  
800.313.3774 • 650.855.2121 • [askepri@epri.com](mailto:askepri@epri.com) • [www.epri.com](http://www.epri.com)